



Photochemical degradation and biodegradation of organic colloids in boreal waters

Olga Oleinikova

► To cite this version:

Olga Oleinikova. Photochemical degradation and biodegradation of organic colloids in boreal waters. Hydrology. Université Paul Sabatier - Toulouse III, 2018. English. NNT: 2018TOU30014 . tel-01903106v2

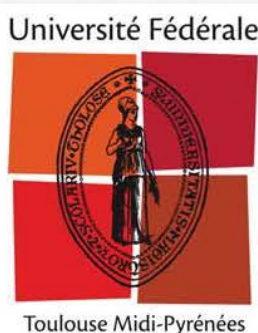
HAL Id: tel-01903106

<https://theses.hal.science/tel-01903106v2>

Submitted on 18 Feb 2019

HAL is a multi-disciplinary open access archive for the deposit and dissemination of scientific research documents, whether they are published or not. The documents may come from teaching and research institutions in France or abroad, or from public or private research centers.

L'archive ouverte pluridisciplinaire **HAL**, est destinée au dépôt et à la diffusion de documents scientifiques de niveau recherche, publiés ou non, émanant des établissements d'enseignement et de recherche français ou étrangers, des laboratoires publics ou privés.



THÈSE

En vue de l'obtention du

DOCTORAT DE L'UNIVERSITÉ DE TOULOUSE

Délivré par :

Université Toulouse 3 Paul Sabatier (UT3 Paul Sabatier)

Cotutelle internationale avec l'Université d'Etat de Moscou

Présentée et soutenue par :
Olga Oleinikova

le jeudi 1 février 2018

Titre :

Dégradation photochimique et biodégradation des colloïdes organiques dans les eaux de surface boréales

École doctorale et discipline ou spécialité :
ED SDU2E : Surfaces et interfaces continentales, Hydrologie

Unité de recherche :
GET - Géosciences Environnement Toulouse, UMR 5563 CNRS

Directeur/trice(s) de Thèse :
HDR, DR2 CNRS Oleg POKROVSKY (GET)
Pr. Andrey BYCHKOV (l'Université d'Etat de Moscou)

Jury :
M. Oleg POKROVSKY (Université de Toulouse 3) - Directeur de these
M. Andrey BYCHKOV (Université d'Etat de Moscou Lomonossov) - CoDirecteur de these
M. Marc BENEDETTI (Institut de Physique du Globe de Paris) - Rapporteur
Mme Aline DIA (Université Rennes I) - Rapporteur
M. Jerome VIERS (Université de Toulouse 3) - Examinateur
Mme Liudmila SHIROKOVA (Université de Toulouse 3) - Invitée

Remerciements

Je voudrais tout d'abord remercier deux mes directeur de thèse, Oleg Pokrovsky et Andrew Bychkov, pour tous leur conseils et encadrement scientifique.

Je voudrais remercier aussi les chercheurs de l'Université d'Etat de Moscou, Sergey Lapitskiy et Olga Drozdova, pour l'aide pendant les travaux de terrain et leur conseils précieux.

Je tenais à remercier Liudmila Shirokova pour son aide pendant la recherche microbiologique et son soutien moral.

Je remercie également Laurent Orgogozo pour sa gentillesse et ses conseils.

Je remercie aussi Carole Causserand, Aurélie Marquet, Franck Poitrasson , Manuel Henry, Jonathan Prunier, Jérôme Chmeleff, Frédéric Candaudap, Stéphanie Mounic, Stéphanie Balor, Pascale Bénézeth, Anastassia Borisova, pour leur aide et leurs conseils pendant mon travail au laboratoire GET.

Je voudrais remercier aussi les membres de jury pour leur temps et attention : Marc Benedetti, Aline Dia, Jerome Viers, Liudmila Shirokova.

Je tenais à remercier ma famille et mes amis pour leur soutien.

Je voudrais remercier Campus France et le Gouvernement Français pour ma bourse de doctorat en cotutelle de thèse franco-russe. Et aussi les projets de fondations scientifiques russes RSF № 14-50-00029, RFBR grants №№ 14-05-00430, 15-05-05000, 16-55-150002 pour le financement mes études de terrain et les expériences à conditions naturelles et en laboratoire en Russie.

Dégradation photochimique et biodégradation des colloïdes organiques dans les eaux de surface boréales

Résumé général

La matière organique dissoute (MOD) est un composant important des eaux naturelles, déterminant la forme des éléments et les émissions de gaz à effet de serre (CO_2 , CH_4), et influence la biodiversité des milieux des eaux. Les eaux boréales sont connues pour être généralement riches en fer, et cela est vrai en particulier pour les eaux de la région étudiée (Carélie du Nord, Russie). Le fer est associé aux MOD dans les complexes de bas poids moléculaire et les colloïdes organo-ferreux de haut poids moléculaire, qui agissent comme les principaux transporteurs d'éléments traces métalliques dans le continuum hydrologique typiques de cette région : sol - marais - rivière - lac. La transformation des colloïdes organo-ferreux se fait sous l'influence de deux facteurs principaux: la dégradation bactérienne et la dégradation photochimique. Cette étude est consacrée à l'analyse du comportement du carbone organique dissous (COD) et des éléments traces (ET) des eaux de surface en zone boréale sous l'influence de l'activité métabolique des bactéries hétérotrophes et de l'oxydation photolytique des MOD sous l'effet de la lumière du soleil. Dans les expériences, un lixiviat de tourbière, un échantillon d'eau de marais, un échantillons d'eau de ruisseaux, un échantillon de rivière, un échantillon d'eau de lac humique, un échantillon d'eau de lac oligotrophique et un pluvio-lessivat collecté sous un pin, échantillons dans lesquelles dominent les MOD de nature humique, ont été utilisés comme substrats.

Des expériences en laboratoire utilisant des communautés monosouches de bactéries aérobies hétérotrophes *Pseudomonas aureofaciens* et *Pseudomonas saponiphila* (prélevées sur le territoire de Carélie) ont permis d'établir que la MOD allochtone des milieux aquatiques en zone boréale possède une forte résistance à l'activité des bactéries étudiées. Le taux de minéralisation bactérienne du COD était de 0 à $4.3 \text{ mgC.L}^{-1}.\text{jour}^{-1}$ selon le substrat, et la fraction de faible poids moléculaire ($<1 \text{ kDa}$) de la MOD est plus susceptible de destruction que celle de poids moléculaire élevé (de 1 kDa à $0.22 \mu\text{m}$). L'interaction des bactéries avec divers substrats aqueux a montré pour une large gamme d'éléments (Al, Fe, Mn, Ni, Co, Cu, Cd, REE, U) une prédominance significative d'une adsorption rapide sur la surface cellulaire observée

lors de la première heure d'expérience ($t < 1\text{h}$) par rapport à une diminution lente observée lors de la suite de l'expérience ($1\text{h} < t < 96\text{h}$), diminution lente lié à l'assimilation intracellulaire des métaux et à la coprécipitation extracellulaire des éléments avec des hydroxydes de Fe et Al. L'analyse de divers substrats a montré une augmentation de l'adsorption des métaux avec le rapport DOC/Fe dans la solution initiale, ce qui peut être due à la compétition entre Fe et d'autres cations métalliques pour les sites d'adsorption anioniques des surfaces des cellules bactériennes. Le suivi des dynamiques d'élimination des métaux des solutions expérimentales pendant 96 heures n'a pas mis en évidence de lien entre l'élimination des métaux et le pH et les valeurs absolues de concentration de DOC et de Fe. Une relation a été établie entre la diminution lente (96 h) des éléments et le degré initial de sursaturation de la solution en oxydes et hydroxydes de fer et d'aluminium.

Des expériences en conditions naturelles avec des échantillons d'eau de rivière et de marais a montré que la destruction photolytique de la MOD est beaucoup plus efficace pour l'eau de marais. Le taux de minéralisation du COD était de $0.3 \text{ mgC.L}^{-1}.\text{jour}^{-1}$ dans la rivière et de $2.5 \text{ mgC.L}^{-1}.\text{jour}^{-1}$ dans l'eau de marais. Il existe trois processus principaux responsables de l'élimination et de la redistribution des microéléments entre les différentes fractions colloïdales dans les eaux de tourbières riches en MOD et en Fe sous l'action de la lumière du soleil: 1) la dégradation de la partie organique de la fraction colloïdale ($1 \text{ kD} - 0.22\mu\text{m}$) avec la formation de ligands organiques à faible poids moléculaire ($<1 \text{ kDa}$); 2) la coagulation et la précipitation des oxydes et des hydroxydes de Fe et Al avec les éléments-hydrolysat trivalents et tétravalents comme V, P, Cr et As, après l'élimination de la partie organique par rayonnement solaire; 3) libération de métaux alcalins et alcalino-terreux, Mn, Co, Ni, Zn et SO_4^{2-} à partir de complexes organiques avec les MOD. Ainsi, la dégradation des MOD en zone boréale provoquée par la lumière du soleil peut conduire à la formation des formes ioniques, donc potentiellement biodisponibles, d'éléments traces tels que K, V, Cr, Mn, Co, Ni, Zn, Ba; à une réduction de la concentration dans l'eau les éléments toxiques (Cr, As); et enfin à une diminution de la concentration de l'élément limitant le développement des microorganismes – le phosphore.

Mots clés: *carbone organique dissous, boréal, fer, éléments traces, biodégradation, adsorption, coagulation, photodégradation, complexation, fractionnement granulométrique*

General abstract

Dissolved organic matter (DOM) is an important component of natural waters, determining the form of elements and the emission of greenhouse gases (CO_2 , CH_4), as well as affecting water biodiversity. A feature of boreal waters, and in particular the study area waters (North. Karelia, Russia), is high concentration of Fe (III), associated with DOM in low-molecular complexes and in high-molecular organo-ferric colloids, which act as the main carriers of metallic trace elements in the most typical hydrological continuum soil – bog – river – lake. The transformation of organo-ferric colloids occurs under the influence of two main factors: bacterial and photochemical degradation. The present study is devoted to the analysis of dissolved organic carbon (DOC) and trace elements (TE) behavior in surface waters of the boreal zone under the influence of the heterotrophic bacteria metabolic activity and photolytic oxidation of DOM under sunlight exposure. For the purpose of experiments there were used substrates with predominate allochthonous DOM of humic nature, including peat leachate, pine crown throughfall, fen, humic lake, stream, river and oligotrophic lake.

An experiment carried out in laboratory conditions using monocultures of heterotrophic aerobic bacteria *Pseudomonas aureofaciens* and *Pseudomonas saponiphila* (isolated on the territory of Karelia) allowed to establish that allochthonous DOM of the boreal zone reservoirs possesses high resistance to the activity of the explored bacteria. The rate of bacterial mineralization of DOC was observed in range from 0 to $4.3 \text{ mgC L}^{-1}\text{day}^{-1}$, depending on the substrate, and the low molecular weight fraction ($<1 \text{ kDa}$) of DOM was found to be more prone to destruction than high molecular weight (from 1 kDa to $0.22 \mu\text{m}$). The interaction of bacteria with various aqueous substrates showed a significant predominance of short-term ($< 1 \text{ h}$) adsorption on the cell surface for a wide range of elements (Al, Fe, Mn, Ni, Co, Cu, Cd, REE, U) over a long term (1 h – 96 h) intracellular uptake of metals and extracellular coprecipitation of elements with Fe and Al hydroxides. Among different substrates, there was an increase in the adsorption with the increase of DOC/Fe ratio in solution, which can be linked to a competition between Fe and metal cations for anionic adsorption sites on cell surface. The long-term removal of dissolved metals did not show any link to pH, DOC, and Fe concentration. However, there was a consistency between long-term element removal and initial supersaturation degree with respect to main secondary phases (Fe and Al oxy(hydr)oxides).

An experiment in natural conditions with samples of river and bog water showed that photolytic destruction of DOM is much more effective for bog water. The rate of the DOC mineralization was $0.3 \text{ mgC L}^{-1}\text{day}^{-1}$ for the river and $2.5 \text{ mgC L}^{-1}\text{day}^{-1}$ for bog water respectively. Three major processes of dissolved load transformation under sunlight in natural waters include: (i) degradation of organic part of colloidal ($1 \text{ kDa} - 0.22 \mu\text{m}$) organic matter and production of low molecular weight ($< 1 \text{ kDa}$) organic ligands; (ii) coagulation and precipitation of Fe and Al-rich oxy(hydroxide) and incorporated trivalent and tetravalent hydrolysates, V, P, Cr and As, after the solar radiation-induced removal of stabilizing dissolved organic matter, and (iii) liberation of alkalis, alkaline-earth, Mn, Co, Ni, Zn and SO_4^{2-} from organic complexes. It follows that the sunlight-induced degradation of natural DOM in the boreal zone is capable of producing ionic (and thus potentially bioavailable) micro-nutrients such as K, V, Cr, Mn, Co, Ni, Zn, Ba, while scavenging sizeable amount of toxic trace elements (Cr, As) but also phosphorus – the life-limiting element for microorganisms.

Key words: *dissolved organic carbon, boreal, iron, trace elements, biodegradation, adsorption, coagulation, photodegradation, complexation, size fractionation*

Введение

Растворенное органическое вещество (РОВ) является важной составляющей природных вод, определяющей формы нахождения элементов и эмиссию парниковых газов (CO_2 , CH_4), а также влияющей на биоразнообразие водоемов. Особенностью бореальных вод, и в частности вод исследуемого региона (Сев. Карелия, Россия) являются высокие концентрации Fe (III), которое связано с РОВ в низкомолекулярных комплексах и высокомолекулярных железо-органических коллоидах, которые действуют как основные носители металлических микроэлементов в наиболее типичном гидрологическом ряду почва - болото - река – озеро. Преобразование железо-органических коллоидов происходит под действием двух основных факторов: бактериальной и фотохимической деструкции. Настоящее исследование посвящено рассмотрению поведения растворенного органического углерода (РОУ) и микроэлементов (МЭ) поверхностных вод бореальной зоны при воздействии метаболической активности гетеротрофных бактерий и фотолитическом окислении РОВ при солнечном свете. В экспериментах в качестве субстратов были использованы фильтраты болотной, речной и озерной вод, вытяжки из торфа, воды ручья и смыва с кроны сосны, в которых преобладает аллохтонное РОВ гумусовой природы.

Эксперимент в лабораторных условиях с использованием монокультур гетеротрофных аэробных бактерий *Pseudomonas aureofaciens* и *Pseudomonas saponiphila* (выделена на территории Карелии) позволил установить, что аллохтонное РОВ водоемов бореальной зоны обладает высокой устойчивостью к деятельности изученных бактерий. Скорость бактериальной минерализации РОУ составила от 0 до 4,3 мг С/л сут в зависимости от субстрата, причем низкомолекулярная фракция (<1 кДа) РОВ более подвержена деструкции, чем высокомолекулярная (от 1 кДа до 0,22 мкм). Взаимодействие бактерий с различными водными субстратами показало значительное преобладание процесса быстрой (<1 ч) адсорбции на поверхности клеток для широкого ряда элементов (Al, Fe, Mn, Ni, Co, Cu, Cd, REE, U) над долгострочной (1 ч - 96 ч) внутриклеточной ассимиляцией металлов и внеклеточным соосаждением элементов с гидроксидами Fe и Al. Анализ различных субстратов показал увеличение адсорбции металлов с увеличением отношения РОУ/Fe в исходном

растворе, которое может быть связано с конкуренцией катионов Fe и других металлов за анионные поверхности адсорбции бактериальных клеток. Динамика выведения металлов из экспериментальных растворов на протяжении 96 часов не показала связи с pH, концентрацией РОУ и Fe. Установлена связь между долгосрочным (96 ч) выведением элементов и начальной степенью пересыщения раствора оксидами и гидроксидами железа и алюминия.

Эксперимент в природных условиях с пробами речной и болотной воды показал, что фотолитическая деструкция РОВ значительно эффективнее для воды болота. Скорость минерализации РОУ составила 0,3 мг С/л сут в речной и 2,5 мг С/л сут в болотной воде. Можно выделить три основных процесса преобразования железо-органических коллоидов под действием солнечного света: 1) деградация органической части колloidной фракции (1 кДа - 0,22 мкм) с образованием органических лигандов с низкой молекулярной массой (<1 кДа); 2) коагуляция и осаждение окси- гидроксидов Fe и Al, захватывающих трехвалентные и четырехвалентные элементы-гидролизаты V, P, Cr и As, после удаления стабилизирующей органической части солнечным излучением; 3) высвобождение щелочных и щелочноземельных металлов, Mn, Co, Ni, Zn и SO_4^{2-} из органических комплексов с РОВ. Таким образом, вызванная солнечным светом деградация РОВ в boreальной зоне способна приводить к образованию ионных, следовательно потенциально биодоступных, форм микроэлементов, таких как K, V, Cr, Mn, Co, Ni, Zn, Ba ; уменьшению концентрации в воде токсичных микроэлементов (Cr, As) ; снижению концентрации лимитирующего жизнедеятельность микроорганизмов элемента – фосфора.

Ключевые слова: *растворенный органический углерод, boreальный, железо, микроэлементы, биодеструкция, адсорбция, коагуляция, фотодеструкция, комплексообразование, распределение по фракциям*

Table des matières

Résumé général	3
General abstract.....	5
Введение.....	7
Chapitre 1. Introduction général.....	12
1.1. Contexte de l'étude	12
1.1.1. <i>La matière organique dans les écosystèmes aquatiques continentaux</i>	12
1.1.2. <i>Les métaux dans les écosystèmes aquatiques continentaux</i>	13
1.1.3. <i>Transformation des colloïdes organo-minéraux par des bactéries hétérotrophes dans les eaux des zones boréales</i>	15
1.1.4. <i>Transformation de la matière organique sous l'action de la lumière du soleil dans les eaux naturelles</i>	18
1.2. Description de la région.....	21
1.2.1. <i>Climat</i>	21
1.2.2. <i>Rivières, lacs et marécages</i>	22
1.2.3. <i>Sol et végétation</i>	25
1.3. Objectifs de l'étude	27
1.4. Structure de la thèse.....	28
Chapitre 2. Transformation of organo-ferric peat colloids by a heterotrophic bacterium	30
2.1. Résumé	31
2.2. Abstract.....	32
2.3. Introduction	33
2.4. Materials and Methods	36
2.4.1. <i>Isolation and culturing of P. saponiphila</i>	36
2.4.2. <i>Peat leachate preparation</i>	37
2.4.3. <i>Experimental design</i>	37
2.4.4. <i>Analytical techniques</i>	39
2.4.5. <i>Modeling</i>	40
2.5. Results	41
2.5.1. <i>Removal of different colloidal fractions in the course of experiments</i>	41
2.5.2. <i>Partitioning of TE among different size fractions of peat leachate during its interaction with P. saponiphila</i>	49
2.5.3. <i>Control experiments of DOC and TE release from the biomass and metal adsorption on cell surfaces</i>	54
2.6. Discussion.....	59
2.6.1. <i>General features of DOC and TE biodegradability and adsorption on cell surfaces.</i>	59
2.6.2. <i>Response of organo-ferric colloids to the presence of bacterial cells</i>	61

2.6.3. Consequences for biogeochemistry of carbon and trace metals in peat-drained boreal waters	64
2.7. Conclusions	67
2.8. Acknowledgements	68
Chapitre 3. Low biodegradability of dissolved organic matter and trace metal from subarctic waters.....	69
3.1. Résumé	70
3.2 Abstract.....	71
3.3. Introduction	72
3.4. Materials and Methods	75
3.4.1. <i>Heterotrophic bacteria</i>	75
3.4.2. <i>Organic substrates of boreal surface waters</i>	76
3.4.3. <i>Experimental set-up</i>	78
3.4.4. <i>Analytical techniques</i>	78
3.4.5. <i>Statistical treatment and thermodynamic modeling</i>	79
3.5. Results	81
3.5.1. <i>Evolution of biomass, live cell number, pH, and dissolved carbon</i>	81
3.5.2. <i>Trace metal concentration change in the presence of bacteria</i>	81
3.5.3. <i>Metal speciation and saturation degree of solution</i>	92
3.6. Discussion.....	95
3.6.1. <i>DOC and trace element behavior during biodegradation: short-term adsorption and long-term removal via coagulation and assimilation</i>	95
3.6.2. <i>Heterotrophic bacteria control on carbon and trace metals in boreal organic-rich waters</i>	101
3.7. Conclusions	104
3.8. Acknowledgements	104
Chapitre 4. Dissolved organic matter degradation by sunlight coagulates organo-mineral colloids and produces low-molecular weight fraction of metals in boreal humic waters.....	105
4.1. Résumé	106
4.2. Abstract.....	108
4.3. Introduction	108
4.4. Sampling, materials and methods	111
4.4.1. <i>Environmental setting</i>	111
4.4.2. <i>Experimental setup</i>	112
4.4.3. <i>Sample analysis</i>	113
4.4.4. <i>Thermodynamic modeling and statistical treatment</i>	114
4.5. Results	115
4.5.1. <i>pH, DOC, SUVA, phosphorus and anions in <0.22 µm fraction</i>	115
4.5.2. <i>Fe, Al and trace element in 0.22 µm fraction during sunlight exposure</i>	120

<i>4.5.3. Elementary composition of colloids, DOC and TE size fractionation change in the course of photo-degradation</i>	124
4.6. Discussion.....	130
<i> 4.6.1. Change of concentration, optical properties and size fractionation of DOC during sunlight exposure.....</i>	130
<i> 4.6.2. Mechanisms of organo-mineral colloid transformation during irradiation of stream and bog waters</i>	132
<i> 4.6.3. Natural implications.....</i>	139
4.7. Concluding remarks.....	140
4.8. Acknowledgements	141
Chapitre 5. Conclusion général	142
Bibliographie	147

Chapitre 1. Introduction général

1.1. Contexte de l'étude

1.1.1. La matière organique dans les écosystèmes aquatiques continentaux

La matière organique (MO) des systèmes aquatiques a deux sources: la première est le lessivage de la terre, formant ainsi la MO allochtone; la deuxième est la production de bioplancton et d'algues directement dans la colonne d'eau, la MO autochtone. La MO des écosystèmes aquatiques se compose principalement d'atomes de carbone, mais ses constituants importants sont l'hydrogène, l'azote et le phosphore.

La matière allochtone des eaux de surface provient principalement du lessivage de sols et dans une moindre mesure de la litière végétale, puis transite par les marais et les petits cours d'eau, pour ensuite rejoindre les grandes rivières et se déverser dans les lacs (Hedges et al., 1986). La quantité de substances humiques compte en moyenne pour 89% de la teneur totale de la MO allochtone des zones boréales (Zobkova et al., 2015). La plus grande partie du carbone de la MO allochtone des zones boréales est présent sous forme de carbone organique dissous (COD) et une plus petite quantité est présente sous forme de carbone organique particulaire (COP) (Cole et al., 2007). Les zones boréales forestières sont caractérisées par la prédominance du COD sur le carbone inorganique, représenté par les bicarbonates (HCO_3^-) et le gaz carbonique dissous (CO_2), sauf pour les bassins versants de roches carbonatées (Cole et al., 2007, Finlay et al., 2009; Stets et al., 2009). Les proportions entre les différentes fractions de taille du carbone organique (moléculaire, colloïdale, particulaire) allochtone dépendent de la latitude géographique, des conditions climatiques et du type de sol (Meybeck 1993). Il existe deux fractions différentes de COD : une fraction dissoute stricto sensu (<1 nm) et une fraction colloïdale (de 1 nm à 0.4-0.45 µm). Le plus souvent, les formes de carbone organique sont isolées par filtration (Linnik et al., 2006, Pokrovsky et al., 2005, Vasyukova et al., 2010).

La matière organique autochtone est principalement constituée de composants labiles - produits facilement oxydables par voie biochimique (glucides libres, lipides, protéines, acides organiques volatils, etc.). Les sources de COD autochtones comprennent la libération métabolique du bioplancton, des algues et la lyse des cellules microbiennes (Stedmon et Markager, 2005). Contrairement aux lacs

oligotrophes et mésotrophe, les lacs eutrophes se caractérisent par une production élevée de MO autochtone. La production primaire de plancton dépend de la taille du lac, de la latitude, de l'insolation et de la disponibilité des éléments nutritifs (Tranvik et al., 2009). Avec l'augmentation saisonnière de l'approvisionnement en éléments traces des bassins versants, la production de COD autochtone augmente jusqu'à atteindre des valeurs comparables à celles du COD allochtone (Jansson et al., 2008).

Malgré la faible part des eaux de surface par rapport à la superficie des terres émergées, elles jouent un rôle important dans le cycle global du carbone (Dean et Gorham 1998, Cole et al., 2007, Battin et al., 2008) et affectent le climat à l'échelle régionale en échangeant de l'eau et de la chaleur avec l'atmosphère (Krinner, 2003). La consommation et la production de dioxyde de carbone, de méthane et d'oxydes d'azote par les microorganismes des hydrosystèmes continentaux régulent la concentration de ces gaz à effet de serre dans l'atmosphère. Les analyses modernes montrent que les lacs jouent un rôle important pour le stockage transitoire, la transformation, la séquestration et la minéralisation du carbone provenant des eaux de ruissellement de la terre (Tranvik et al., 2009).

Le carbone allochtone et autochtone suit trois grandes voies de conversion dans les lacs, en fonction desquelles l'écosystème aquatique sera une source ou un puit de CO₂ : 1) COD et COP sont transférés de la colonne d'eau au sédiment par floculation de MO ou bioabsorption et dépôt de matière organique sous forme particulaire ; (2) COD et COP sont détruites par des processus photochimiques et microbiens (minéralisation de MO avec formation de CH₄, CO et CO₂); (3) COD et COP migrent vers les eaux riveraines, souterraines et graduellement dans les eaux marines (Tranvik et al., 2009).

1.1.2. Les métaux dans les écosystèmes aquatiques continentaux

La présence de métaux a un effet significatif sur le développement et le fonctionnement des organismes aquatiques. Certains métaux sont nécessaires à la vie des micro-organismes: comme par exemple le fer, le magnésium, le cuivre, le zinc, le cobalt. Néanmoins à des concentrations trop élevées ils sont toxiques. D'autres métaux sont uniquement toxiques, typiquement Hg, Cd, Pb, Sn, Ni, Cr. Certains d'entre eux (Cr (VI) et Ni (II) par exemple) ont même des propriétés mutagènes et cancérogènes (Bailey et al., 2002).

La toxicité d'un métal n'est pas déterminée uniquement par sa concentration totale dans l'eau, mais dépend également de l'état dans lequel il se trouve et migre dans un milieu aqueux. La forme la plus毒ique d'un métal est celle qui se caractérise par une grande activité biologique et chimique. Pour la majorité des micro-éléments de l'eau, les ions libres (hydratés) sont les plus biologiquement disponibles pour les organismes (Florence et al., 1992). Pour des métaux tels que le mercure, le plomb, l'étain, ce sont leurs composés organométalliques qui sont les plus toxiques (Linnik, 2000a). Ceux-ci sont formés à la fois par des processus microbiologiques, et par les interactions chimique avec les substances humiques. Les composés organométalliques de ces métaux sont caractérisés par des liaisons covalentes métal-carbone. Ils ont une plus grande toxicité que les ions métalliques libres, car ils se dissolvent facilement dans les lipides qui constituent les cellules des organismes vivants et peuvent s'y accumuler. En revanche, dans la plupart des cas, les complexes métalliques contenant de la MO humique d'eau de surface sont des composés de coordination de type chélate. Ces complexes ont une faible toxicité, car la complexation avec la MO est associée à une diminution de l'activité chimique et biologique des métaux. Par exemple la complexation réduit la capacité des métaux à pénétrer dans les membranes cellulaires des hydrobiontes (Salomons et al., 1984). Il est probable que dans les réservoirs à haute teneur en MO humique, les métaux (Pb, Zn, Cd, Hg, Mo, Cr, Mn, Ni, Sn, Co, Ti, Cu, V) sont sous forme de complexes non toxiques (Florence et al., 1983, 1992 ; Förstner et al., 1983 ; Linnik, 2000b). De plus, non seulement les substances humiques mais aussi d'autres composés organiques comme par exemple les exométabolites du bioplancton (polyphénols, protéines, glucides, polypeptides, acides aminés, etc.) sont impliqués dans la formation de complexes, qui réduisent également la toxicité des métaux (Ferrarello et al., 2002). Plus la force de liaison du métal dans les complexes avec les MOD est élevée, plus la probabilité de réduire sa toxicité pour les organismes aquatiques est grande.

Les substances humiques, en raison de leurs propriétés réductrices, ont un effet significatif sur la transformation de formes coexistantes de métaux qui peuvent exister à plusieurs degrés d'oxydation. Dans les eaux de surface, les substances humiques provoquent la réduction de V (V), Cr (VI) et Mo (VI) en V (IV), Cr (III) et Mo (V) puis se complexent avec ces formes réduites (Linnik et al., 2007).

Parmi les facteurs contribuant à la diminution de la toxicité des métaux, outre la complexation, l'adsorption sur les particules en suspension et les sédiments de fond

est aussi importante. L'accumulation de métaux dans les sédiments de fond due à l'adsorption et à la sédimentation est l'un des principaux processus conduisant à leur élimination du cycle biologique. Dans les masses d'eau à haute teneur en MOD, la plus grande partie des métaux se présente sous la forme de composés complexes, ce qui augmente la capacité de migration des métaux. En effet La chélation des métaux adsorbée sur les particules et les sédiments permet leur remise en solution, ce qui peut entraîner une contamination secondaire de l'environnement aquatique (Samanidou et al., 1991). Effectuer des recherches pour comprendre la spéciation et les formes des métaux dans les eaux naturelles, qui sont des systèmes biochimiquement complexes, est primordial pour surveiller l'état écologique des masses d'eau et la migration des éléments chimiques dans les eaux de surface.

1.1.3. Transformation des colloïdes organo-minéraux par des bactéries hétérotrophes dans les eaux des zones boréales

Une quantité significative de CO₂ est émise par les eaux continentales vers l'atmosphère en raison de la dégradation bactérienne de la matière organique dissoute (MOD) (Battin et al., 2009; Tranvik et al., 2009). Dans les rivières et les lacs boréaux, on sait que la MOD allochtone (issue des plantes, des sols et des tourbe) est la principale source de nutriments pour le métabolisme du bactérioplancton aérobie hétérotrophe (Tranvik, 1998a, b, Tranvik et al., 2009, Wilkinson et al. 2013). De nombreuses études sur l'interaction des sols et des eaux avec des consortiums microbiens indigènes en présence de nutriments ajoutés artificiellement ont démontré qu'entre 10% et 40% du carbone organique dissous (COD) est généralement disponible pour la consommation bactérienne pendant plusieurs semaines (Berggren et al., 2007, 2009, 2010). Cette échelle de temps est comparable au temps de résidence dans les lacs et les rivières. La biodégradabilité des MOD lessivés des sols (y compris des pergélisol) a été examinée par Vonk et al. (2015 a, b) qui ont conclu qu'en moyenne de 5 à 20% du COD sont dégradés dans les petits cours d'eau (<250 km²) et que de 10 à 30% du COD des lixiviat du sol sont biodégradables après 7 jours en présence des bactéries. D'autres travaux récents étudient les interactions entre espèces microbiennes natives issues de divers milieux aquatiques et les eaux de ces mêmes milieux ont démontré que les sources de petits cours d'eau et les lixiviat du sol sont riches en MOD biodégradables comparativement aux eaux des rivières et des lacs.

(Van Heees et al., 2005, Mann et al 2015, Larouche et al., 2015, Spencer et al., 2015, Vonk et al., 2015b).

Les approches traditionnelles pour la quantification de la minéralisation bactérienne de la MOD dans échantillons d'eau naturelle avec ou sans substrats nutritifs ajoutés sont basées sur le suivi des concentrations en CO₂/O₂ (Roehm et al., 2009; Berggren et al., 2012 et leurs références). Des études expérimentales récentes basées sur la biodégradation des MOD par des cultures bactériennes mono-souches issues des milieux naturels illustrent le potentiel de cette technique pour révéler les mécanismes qui contrôlent la dynamique du carbone organique et des métaux traces dans les sols (Fertzsche et al., 2012, Drozdova et al., 2014, 2015), les eaux (Bonneville et al., 2006, Shirokova et al., 2015) et les systèmes minéraux (Wu et al., 2007, 2008, Stockman et al., 2012).

La source principale des MOD allochtones sont les tourbières, les sols et les végétaux réagissant avec les eaux de surface alors que la source principale des MOD autochtones est la dégradation du périphyton, du plancton et des plantes aquatiques ainsi que de leurs exométabolites (Chupakov et al., 2017). Bien entendu dans l'essentiel des eaux des surfaces continentales on a une combinaison de MOD provenant de diverses sources terrestres et aquatiques. On sait que la contribution des composantes allochtones varie selon les saisons et l'espace (Lloyd et al., 2012, Scheibe et Gleixner, 2014) et que les bactéries aquatiques reçoivent différents substrats biodégradables au cours de l'année. Pour caractériser la capacité des bactéries hétérotrophes à minéraliser divers substrats organiques, des expériences avec des souches individuelles et des substrats naturels sont une méthode efficace.

L'intérêt pour la dynamique des métaux dans les environnements aquatiques boréaux est double. D'une part, Fe, Mn, Zn, Ni, Co, Cu, Mn sont des micronutriments potentiellement limitants pour le plancton dans les lacs, les rivières, la zone côtière et surtout l'océan Arctique. D'autre part, la migration des métaux toxiques (Cd, Pb, Hg, U) et métalloïdes (As, Sb, Se) de la terre à l'océan est susceptible d'augmenter à mesure que les pergélisol dégèlent, la période active (non gelée) de la l'année s'allongeant et le débit des rivières augmentant. La caractéristique spécifique de toutes les eaux boréales soumises aux changements climatiques est la prédominance des colloïdes organiques et organo-ferriques allochtones qui agissent comme transporteurs principaux de ces oligo-éléments et toxiques métalliques et métalloïdes (Ingri et al., 2000; Andersson et al., 2001, 2006; Dahlqvist et al., 2004 2007, Neubauer et al., 2013,

Vasyukova et al., 2010, Stolpe et al., 2005, 2013, Catrouillet et al., 2016). Par conséquent, les eaux des rivières boréales et subarctiques et des tourbières ont des concentrations en éléments faiblement solubles (Fe, Al, hydrolysats trivalents et tétravalents) plus élevées que les valeurs moyennes mondiales observées dans les eaux de rivière, comme on l'a observé en Europe du Nord (Andersson et al. 2006, Dahlqvist et al., 2007, Vasyukova et al., 2010, Ilina et al., 2016), en Alaska (Stolpe et al., 2013) et en Sibérie (Pokrovsky et al., 2016a, b).

Bien que l'interaction des bactéries hétérotrophes avec les composés organo-ferriques solides du sol et des sédiments soit assez bien étudiée (Huang et al., 2005, Bosch et al., 2010, Jackson et al., 2011, Sivan et al., 1998, 2011, 2014, Wu et al., 2014, Liu et al., 2015), les facteurs contrôlant le comportement des métaux traces au cours de la minéralisation des colloïdes organo-ferriques par des bactéries hétérotrophes sont mal identifiés et non caractérisés. De tels facteurs peuvent être par exemple le pH, la conductivité spécifique et la concentration du COD en solution; la nature des MOD (en fonction de leur origine : rivière, lac, sol, tourbière, marais), le rapport du carbone organique au Fe dans la fraction dissoute, la durée de l'interaction et les souches des bactéries hétérotrophes présentes.

Une étude récente sur lixiviat de tourbe et de mousse en zone de pergélisol a démontré que durant la consommation de MOD par les bactéries hétérotrophes terrestres et aquatiques (*P. reactans* et *P. aureofaciens*) les éléments traces (ET) sont soumis à une adsorption sur la surface cellulaire et à une incorporation dans les cellules vivantes via une captation active ou passive (Shirokova et al., 2017). D'une manière analogue à la transformation des colloïdes pendant la photodégradation (Kopáček et al., 2006, 2008, Porcal et al., 2009, 2013, 2015), une partie des ET sous formes de complexes organiques peut être libérée et précipiter sous la forme d'oxydes et hydroxydes ou rester en solution sous la forme d'ions libres ou faiblement complexés et de molécules neutres. Cela peut être accompagné par une restructuration des MOD de la fraction colloïdale (1 kDa – 0.45 µm) en (i) élément de la fraction de bas poids moléculaire (<1 kDa) pouvant former des complexes stables d'ET, et (ii) en élément de la fraction de particules (> 0.45 µm) qui peuvent piéger les métaux dissous de la colonne d'eau dans les sédiments.

Les études de thermokarsts (Pokrovsky et al., 2013a) et de lacs boréaux humiques (Pokrovsky et Shirokova, 2013; Shirokova et al., 2013b, 2016) ont mis en évidence une telle transformation des colloïdes aquatiques liée au réchauffement

prolongé des eaux de surface riches en matières organiques et à l'activité hétérotrophe accrue du bactérioplancton. D'autre part, la fraction de bas poids moléculaire des MOD et des ET devrait être plus biodisponible et sensible à la transformation microbienne que les colloïdes de haut poids moléculaire. Cette suggestion est cohérente avec les résultats expérimentaux relatifs aux interactions entre bactéries et colloïdes naturels provenant de différentes sources terrestres et aquatiques (Roehm et al., 2009, Yang et al., 2016). De même la consommation par le plancton marin de Fe colloïdal est de 6 à 30 fois plus faible que celle de Fe de bas poids moléculaire, et le Fe lié à de colloïdes de petites tailles (1-10 kDa) est consommé à un taux plus élevé que le Fe lié avec de colloïdes de plus grandes tailles (10 kDa – 0.2 µm), pour des concentrations de carbone colloïdal similaires (Chen et Wang, 2001). La fraction de faible poids moléculaire potentiellement biodisponible est probablement présente dans les lixiviats de végétation fraîche et les eaux des petits cours d'eau drainant la tourbe et les sols podzoliques (Ilina et al., 2016). En revanche, les eaux des tourbières ombrotrophes et marécageuses et les eaux de lacs humiques peuvent avoir des MOD plus réfractaires, qui sont moins biodisponibles pour les microorganismes aquatiques. Les bactéries du sol sont susceptibles de dégrader la matière organique provenant du sol alors que les bactéries hétérotrophes aquatiques devraient métaboliser plus efficacement la MOD aquagène. On peut donc supposer d'une part que la biodisponibilité des formes de faible poids moléculaire du carbone organique et des métaux sera plus élevée que celle des métaux colloïdaux, et d'autre part que plus la concentration de COD allochtone est élevée, plus l'impact des bactéries aquatiques sur la concentration des métaux en solution est faible.

1.1.4. Transformation de la matière organique sous l'action de la lumière du soleil dans les eaux naturelles

La minéralisation photochimique du carbone organique dissous (COD), de l'azote et du phosphore est un processus important du cycle biogéochimique des nutriments, modifiant notamment leur biodisponibilité (Cotner et Heath, 1990, de Haan, 1993, Miller et Zepp, 1995, Bushaw et al. .., 1996, Zepp et al., 1998, Wetzel et al., 1995, Tarr et al., 2001, Vähäalto et al., 2003, Kopácek et al., 2003, Vähäalto et Wetzel, 2004). Cette minéralisation contribue aux émissions de CO₂ des eaux de surface vers l'atmosphère (Cory et al., 2013, 2014). La mise en évidence du fait que l'oxydation photochimique de la matière organique dissoute (MOD) dépasse

significativement la respiration bactérienne dans les eaux arctiques et subarctiques (Cory et al., 2007, 2014, 2015) a conduit à un intérêt grandissant pour la caractérisation des propriétés chimiques et structurales des produits de photodégradation de la MOD (Gonsior et al., 2013, Ward et Cory, 2016). Dans le même temps, le devenir des éléments majeurs et des éléments traces (ET) liés aux MOD sous forme de colloïdes lors de l'exposition solaire des eaux de surface reste peu connu, à l'exception de plusieurs études en laboratoire sur la transformation du Fe en interaction avec des eaux de rivières de climat tempéré, avec des solutions de fulvates et d'humates du sol (Garg et al., 2013a, b, Porcal et al., 2009a, b, 2013a, b, 2015), et avec des eaux estuariennes (Blazevic et al., 2016). La seule étude portant sur la concentration et la spéciation de divers ET, en plus du Fe, pendant la photo-oxydation de MOD est celle de Shiller et al. (2006) sur des rivières tempérées, qui sont relativement pauvres en MOD et en Fe (COD = 7 mg / L, Fe = 140 µg / L).

Au cours de la dernière décennie, des progrès substantiels ont été réalisés dans la caractérisation du transport colloïdal de COD et d'éléments majeurs et traces dans les eaux riches en substances humiques des milieux subarctiques en fonction de la lithologie (Vasyukova et al., 2010), de la latitude (Pokrovsky et Schott 2002) et de la saison. (Ingri et al., 2000, Andersson et al., 2001, 2006, Dahlqvist et al., 2004, 2007, Shiller, 2010, Lyvén et al., 2003, Pokrovsky et al., 2010, Bagard et al., 2011, Stolpe et al., 2013a, b). L'état colloïdal des ET est particulièrement important pour les eaux de surface riches en MOD et en Fe, ce qui est typique des tourbières et des cours d'eau qui drainent la taïga et la toundra à haute latitude. Une étude récente (Ilina et al., 2016) a quantifié la transformation des colloïdes dans leurs milieux d'origine (dans les solutions de sol et les eaux de tourbières), lors de leur transit (dans les rivières et les cours d'eau) et dans les zones réceptrices (les lacs). Un tel continuum hydrologique (sol - tourbière - rivière - lac) est typique des régions boréales européennes (Kothawala et al., 2006, Laudon et al., 2011, Lidman et al., 2012, 2014). En accord avec des études antérieures de ce continuum hydrologique arctique et subarctique (Lapierre et del Giorgio, 2014; Vonk et al., 2015a, b), nous avons émis l'hypothèse que les deux principaux processus responsables de la transformation des colloïdes en milieux marécageux et rivulaires sont la biodégradation et photodégradation de la matière organique dissoute (Ilina et al., 2013, 2014, 2016).

Pour distinguer la biotransformation et la phototransformation et évaluer les vitesses et les mécanismes de photodégradation, des expériences d'incubation

contrôlées sont nécessaires, et un certain nombre d'études expérimentales ont permis de caractériser l'efficacité de la photo-dégradation des MOD dans l'Arctique (Cory et al., 2014; Ward et Cory, 2016, Stubbins et al., 2016), la zone boréale (Salonen et Vähäalto, 1994, Lindell et al., 2000, Tranvik et Bertilsson, 2001, Köhler et al., 2002, Porcal et al., 2014, Groenveld et al., 2016), la zone tempéré (Xu et Jiang, 2013) et la zone tropical (Suhett et al., 2007, Stubbins et al., 2010, Spencer et al., 2009). La grande majorité de ces études ont analysé les concentrations et les propriétés moléculaires des MOD et seulement quelques travaux ont abordé la photo-oxydation et la photo-réduction du Fe et d'autres composants inorganiques dans des eaux pauvres en MOD, dans des eaux de lacs acides et dans l'eau de mer (Waite et Morel, 1984, Collienne, 1983, Anderson et Morel, 1982, Porcal et al., 2004) ou dans des eaux des marais subtropicaux (Helms et al., 2013). Quelques travaux sur des eaux acides riches en Fe et Al et des solutions artificielles riches en MOD ont mis en évidence la possibilité d'une coagulation colloïdale et d'une précipitation d'hydroxyde de Fe et Al après photodégradation de complexes de MOD avec des métaux (Helms et al., 2013, Kopacek et al. , 2005, 2006). Dans le cas d'une rivière tempérée, la photo-oxydation des MOD entraîne d'une manière analogue une diminution du Fe dissous ($<0,02 \mu\text{m}$) et des ET associé au Fe et aux colloïdes organiques tels que Co, Ni, Cu, Cr, V, Ce, Pb, U (Shiller et al., 2006).

1.2. Description de la région

La zone boréale est partagée par les pays les plus au Nord de notre planète, tels que la Russie, la Suède, la Finlande, la Norvège, le Canada, les Etats-Unis, du nord du Kazakhstan et du Japon. La forêt boréale est le plus grand biome terrestre du monde s'étendant sur toutes les latitudes moyennes et hautes (de 55°N jusqu'au cercle polaire nord) (Sayre, 1994). La zone boréale a un rôle majeur comme réservoir de carbone. Les sites d'étude se trouvent en zone boréale dans la région de Carélie du Nord (66°N, 31°E) en Russie, aux abords de la frontière finlandaise (Fig. 1.1).

Le lieu choisi pour prélever des échantillons d'eau utilisés dans des expériences est le parc national « Paanajarvi ». Sur le territoire du parc, l'activité économique de l'homme est limitée et l'industrie est absente.



Fig. 1.1. Carte de la zone boréale européenne avec la zone d'étude de Carélie du Nord (1).

Source: EEA. UNEP/GRID Warsaw final map production

1.2.1. Climat

Le climat de la zone d'étude est subarctique (climat tempéré froid sans saison sèche avec aucun mois chaud – i.e. avec plus de 22°C de température moyenne - Dfc dans la classification de Köppen), avec une influence océanique. Des masses d'air venaient de l'Atlantique Nord tout au long de l'année et apportent de l'air humide et des températures modérées. Dans les mois d'été, les masses d'air de l'océan Arctique arrivent, ce qui limite les chaleurs estivales.

La température annuelle moyenne dans la zone étudiée est d'environ 0°C, il y a ici de longs hivers et de courtes périodes estivales sans gel. Le mois le plus chaud de l'année est le mois de juillet, avec une température moyenne de 15°C, la période la plus froide est en janvier et février, lorsque la température moyenne est de -13°C. Les températures minimales en hiver peuvent être inférieures à -45°C, et les températures maximales en été montent à +35°C. La moyenne annuelle des précipitations est estimée entre 450 et 550 mm, avec une couverture neigeuse de 70 à 80 cm durant 7 à 8 mois, d'octobre à avril-mai.

1.2.2. Rivières, lacs et marécages

Les principaux réservoirs du parc « Paanajarvi » sont le lac Paanajarvi avec le réseau de lacs et de rivières associés et les fleuves Olanga et Nuris qui se jettent dans le lac Pyaozero. La Carélie du Nord est une contrée très humide, où il y a une forte densité de rivières, de ruisseaux, de lacs et de marais. Les rivières sont de plutôt de type montagneux, avec des rapides et des cascades, mais aussi avec des tronçons en pente douce. Le débit de ces rivières est alimenté par la pluie et la fonte des neiges, et elles sont en relations avec les nombreuses zones humides marécageuses et les nappes d'eaux souterraines.

Les eaux des lacs de taille petite (jusqu'à 10 km²) à moyenne (jusqu'à 100 km²) sont légèrement minéralisées, souvent de teinte brune en raison des apports d'eaux de marais (riches en matières organiques) amenés par les ruisseaux. En été, la température des eaux des lacs de petites tailles peut monter jusqu'à 22-25°C.

Les marais de cette région de Carélie représentent de 10 à 20% de la surface du territoire. Un grand nombre de marais est trouvé leur origine dans le relief fluvioglaciaire et le climat subarctique. Les petits marécages ayant des surfaces variant de 0.03 – 0.05 km² à 0.3 - 0.5 km² sont très répandus. Ce sont soit des marécages eutrophes dont les tourbes sont constituées d'herbes et de mousse soit des marécages colonisés presque exclusivement par des sphaignes.

Les eaux choisies pour les expériences de photodestruction et de biodégradation des colloïdes organiques sont des eaux provenant de la rivière Palojoki, du lac oligotrophique Tsipringa, du ruisseau Vostochniy, du lac humique à la source de celui ci, d'un marais du bassin versant du lac Tsipringa, d'un lixiviat de tourbière

voisine de ce marais et de pluvio-lessivats collectés sous un pin (l'essence la plus répandu dans cette région) aux abords du lac Tsipringa.



Fig. 1.2. La rivière Palojoki

La rivière Palojoki (fig. 1.2) sort du lac Kivakalampi, contourne le massif rocheux de Kivakki par le sud et se jette dans le lac Pyaozero. La rivière Palojoki, longue d'approximativement 9 km, est caractérisée par un courant rapide, avec un dénivellé de 150 m. Les roches du bassin versant sont des granites, des granosyénites, des syénites et des syénites-diorites du Paléoprotérozoïque ; des gneiss de granite à biotite, des biotites, des biotites-amphibolites, des gneiss amphibolites et des amphibolites du Paléoarchéen ; et enfin des dépôts glaciaires quaternaires.

Le lac Tsipringa (fig. 1.3), d'une superficie de 20 km², a été formé lors de la construction en 1966 de la centrale hydroélectrique de Kuma dans la région de Louhi sur les rivières Kuma, Kundozerka et Sofjana. Les massifs forestiers du territoire n'ont pas été abattus et ont été inondés lors de la formation de la retenue d'eau de Kuma associée à ce barrage, retenue constituée d'un système lacustre dont fait partie le lac Tsipringa. Les eaux du lac oligotrophique Tsipringa, qui draine un bassin versant de

86 km², sont d'une grande propreté, répondant par exemple à tous les standards de potabilité.

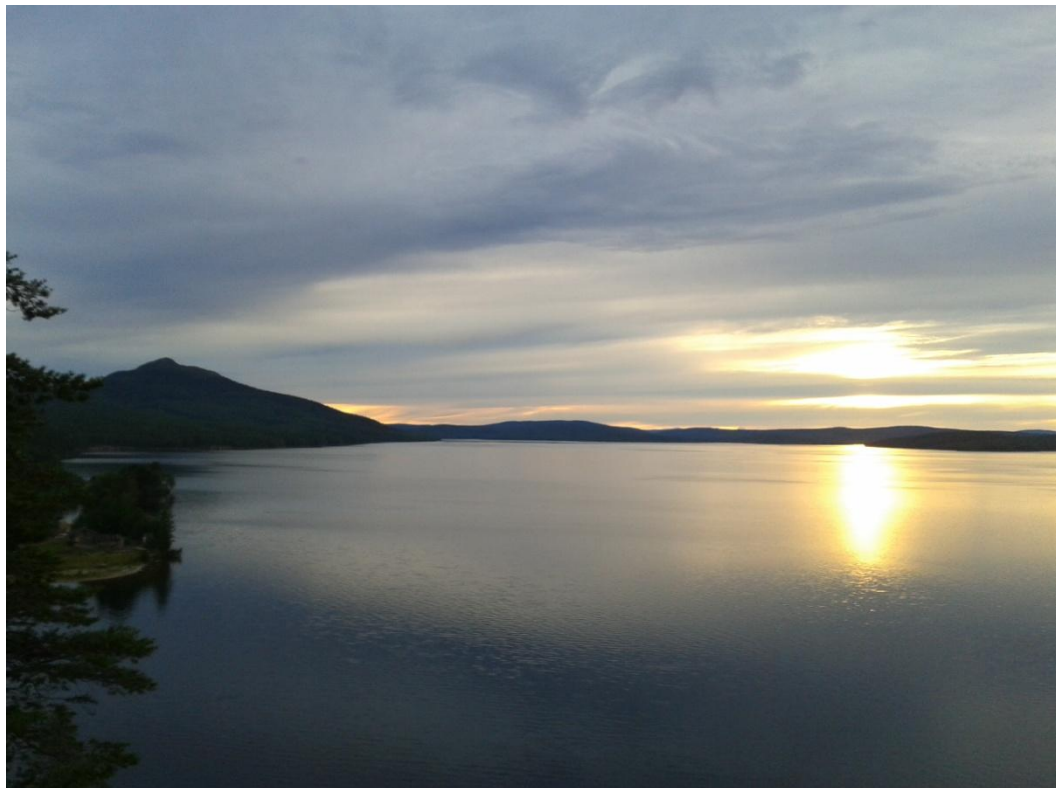


Fig. 1.3. Le lac Tsipringa



Fig. 1.4. Le ruisseau Vostochniy

Le ruisseau Vostochniy (fig. 1.4) coule d'ouest en est et se jette lui aussi dans le lac Tsipringa. Sa longueur est d'environ 1 km pour un dénivellé de 50 m et un bassin versant d'environ 0.95 km^2 . Les roches du bassin versant sont des gabbroïdes amphibolites des intrusions du Paléoprotérozoïque. Le lac humique qui est la source du ruisseau Vostochni est un petit lac avec des eaux brunes dues aux substances organiques dissoutes.



Fig. 1.5. Le marais dans le bassin versant du lac Tsipringa

Le marais échantillonné (fig. 1.5) est également situé dans le bassin versant du lac Tsipringa. La zone couverte par les tourbières est d'environ 1.19 km^2 . Les roches du bassin versant sont constituées de granitogneisses à biotites et d'amphibolites du Paléoarchéen. La tourbe qui a servi à la production de lixiviat pour les expérimentations a été collectée sur le territoire de ce marais.

1.2.3. Sol et végétation

La couverture du sol de la zone d'étude a été formée relativement récemment, elle est souvent absente sur les pentes abruptes et les affleurements rocheux. Les températures basses combinées à un hydromorphisme prononcé engendrent une faible activité de dégradation et par conséquent une accumulation de matière organique. La majorité des sols décrits sont donc des podzosols, avec une forte accumulation de

matière organique dans les horizons supérieurs. Le pH des podzols est fortement acide, les horizons supérieurs contiennent peu d'espèces chimiques basiques.

La végétation est constituée par des forêts de conifères, les principaux types d'arbres représentés étant le pin et l'épicéa (fig. 1.5). Il y a également une petite proportion d'arbres à feuilles caduques, bouleau, aulne et tremble. Sorbier des oiseleurs et genévrier constituent un sous-bois clairsemé. Les myrtilles et les canneberges prédominent dans la strate arbustive et les mousses vertes dans la strate muscinale. Les plantes herbacées sont très peu représentées. Sur les pentes des montagnes seule la strate cryptogamique et muscinale est présente, avec des mousses vertes, des lichens (dont du lichen des rennes), de la bruyère, de l'airelle rouge et de la busserole.



Fig. 1.6. Les forêts de conifères au nord de la Carélie

1.3. Objectifs de l'étude

Ce travail est consacré à l'étude de deux des principaux processus de transformation de la matière organique dissoute dans les eaux de surface en zone boréale : l'oxydation photochimique et l'action bactérienne. Les observations portent principalement sur le comportement du carbone organique dissous (COD) et des éléments traces (ET) de l'eau sous l'influence de la lumière du soleil et de l'activité métabolique des bactéries hétérotrophes.

Les principaux objectifs de l'étude sont:

1. Caractériser l'adsorption rapide (0-1 h d'expérience) et la diminution lente (1-93 h d'expérience) du COD et des ET dans la fraction dissoute stricto sensu (poids moléculaire faible, <3 kDa) et les fractions colloïdales d'eau riches en substances humiques sous l'action de bactéries hétérotrophes (Chapitre 2).
2. Évaluer les facteurs influençant l'adsorption rapide (0-1 h d'expérience) et la diminution lente (1-93 h d'expérience) des éléments dans les eaux riches en substances organiques dissoutes sous l'influence des cultures aquatiques et du sol de bactéries hétérotrophes (Chapitre 2, 3).
3. Identifier les modèles de comportement du COD et des ET dans diverses eaux d'un continuum hydrologique typique de région subarctique (sol-marais-rivière-lac) en relation avec l'activité métabolique des bactéries hétérotrophes (Chapitre 3).
4. Dans le cas de milieux marécageux et rivulaires boréaux, étudier la transformation des colloïdes organo-minéraux lors de la destruction photochimique de la matière organique (Chapitre 4), en fonction des paramètres suivants :
 - caractéristiques quantitatives des changements dans les concentrations de COD, de fer et des ET ;
 - nature des éléments chimiques qui se lient aux colloïdes organiques et aux oxydes et hydroxydes de fer en fonction du rapport COD/ET et COD/Fe ;
 - caractéristique de l'évolution de la composition élémentaire d'une fraction colloïdale de 1 kDa - 0,22 µm ;

De plus, il s'agit de vérifier la possibilité de former des complexes organométalliques de faible poids moléculaire dans le processus d'irradiation des eaux naturelles avec la lumière du soleil.

1.4. Structure de la thèse

Cette thèse est basée sur trois articles acceptés pour publication, qui constituent les principaux chapitres (Chapitres 2, 3, 4). Le chapitre 5 présente les conclusions générales de l'étude. A la fin du manuscrit il y a une liste bibliographique commune à tous les chapitres.

Chapitres 2. Oleinikova O.V., Shirokova L.S., Gérard E., Drozdova O.Yu, Lapitskiy S.A., Bychkov A.Yu, Pokrovsky O.S. Transformation of organo-ferric peat colloids by a heterotrophic bacterium. *Geochimica et Cosmochimica Acta*, 2017, **205**, 313-330.

Ce chapitre décrit la principale méthode expérimentale utilisée dans ce travail pour caractériser le processus de transformation de la matière organique dissoute et le comportement des éléments traces des eaux naturelles sous l'influence de l'activité métabolique d'une monoculture de bactérie hétérotrophe. Une souche de bactérie hétérotrophe *Pseudomonas saponiphila* a été extraite d'un ruisseau du nord-ouest de la Carélie (Russie) et une monoculture de cette souche bactérienne a été mis en présence d'un lixiviat de tourbe sans ajout de nutriment. Les transformations (adsorption, assimilation, dégradation, ...) des colloïdes organo-ferriques a été observée dans trois fractions (0.45 µm, 50 kDa et 3 kDa) pendant 4 journées d'expérience. Par ailleurs, différentes expériences complémentaires ont été menées pour étudier l'effet du pH sur le taux d'adsorption et la cinétique d'adsorption des éléments traces sur la surface cellulaire.

Chapitres 3. Oleinikova O.V., Shirokova L.S., Drozdova O. Yu., Lapitskiy S. A., Pokrovsky O.S. Low biodegradability of dissolved organic matter and trace metals from subarctic waters. *Science of the Total Environment*, 2017, article accepted for publication (31 Oct 2017).

Ce chapitre poursuit l'étude expérimentale de la transformation de la matière organique dissoute et du comportement des éléments traces sous l'influence des bactéries entamée au chapitre précédent. Nous avons étudié les interactions de souches bactériennes cultivables extraites d'eaux (*Pseudomonas saponiphila*) et de sols (*Pseudomonas aureofaciens*) naturels avec 7 substrats constitués par des échantillons d'eaux caractéristiques de différents microenvironnements d'une région subarctique (Carélie du Nord). Parmi ces substrats figurent un lixiviat de tourbière, un échantillon

d'eau de marais, un échantillon d'eau de ruisseaux, un échantillon de rivière, un échantillon d'eau de lac humique, un échantillon d'eau de lac oligotrophique, et un pluvio-lessivat collecté sous un pin (l'essence la plus répandu dans cette région). Ces substrats sont caractérisés par des concentrations en carbone organique dissous (COD) très variable (de 4 à 60 mg/L).

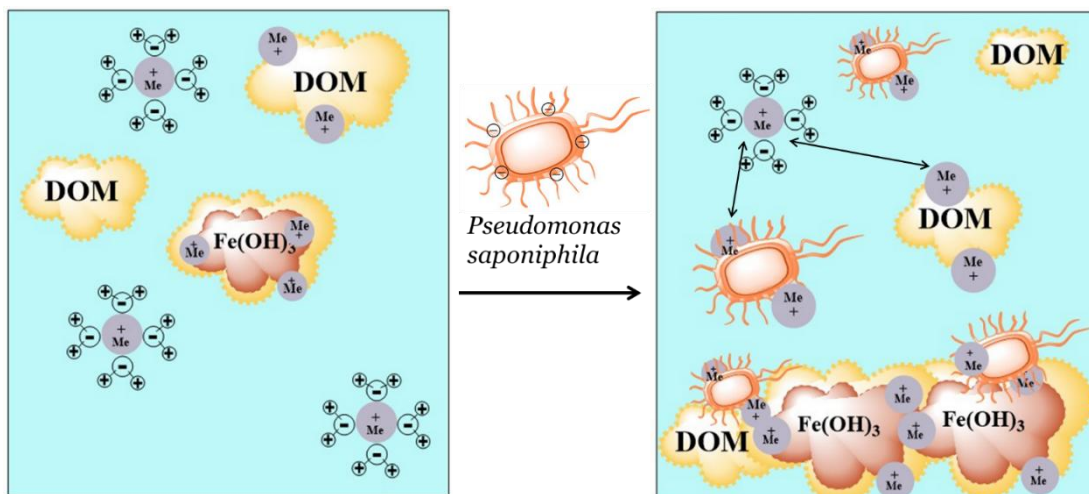
Chapitres 4. Oleinikova O.V., Drozdova O.Yu., Lapitskiy S.A., Demin V.V., Bychkov A.Yu, Pokrovsky O.S. Dissolved organic matter degradation by sunlight coagulates organo-mineral colloids and produces low-molecular weight fraction of metals in boreal humic waters. *Geochimica et Cosmochimica Acta*, 2017, **211**, 97-114.

Ce chapitre présente une étude expérimentale de la transformation des colloïdes organo-minéraux d'eaux naturelles de zone boréale sous l'influence de la lumière solaire. Pour mieux comprendre les évolutions des concentrations, des répartitions entre les différentes fractions colloïdales et dissoutes, des spéciations des microéléments dans des eaux boréales soumises au rayonnement solaire, nous avons effectué des expériences de photo-dégradation *in situ* sur des eaux de rivière et de tourbière d'un site vierge de tout activité humaine de la Carélie du Nord. La transformation des colloïdes organo-minéraux a été observée dans trois fractions (0.22 µm, 10 kDa et 1 kDa) pendant 10 journées d'exposition.

Chapitre 2. Transformation of organo-ferric peat colloids by a heterotrophic bacterium

Transformation des colloïdes organo-ferriques en présence de bactérie hétérotrophe

Geochimica Cosmochimica Acta 205 (2017), 313–330



Cartoon of peat colloid transformation in the presence of live *P. saponiphila* and dissolved (< 0.45 μm) metals ($\text{Me}(\text{aq})$) interaction with bacteria.

Transformation of organo-ferric peat colloids by a heterotrophic bacterium

Olga V. Oleinikova^{1,2}, Liudmila S. Shirokova^{1,3}, Emmanuele Gérard⁴, Olga Yu. Drozdova², Sergey A. Lapitskiy², Andrey Yu. Bychkov², Oleg S. Pokrovsky^{1,5*}

¹ GET (Geosciences and Environment Toulouse) UMR 5563 CNRS, University Paul Sabatier, 14 Avenue Edouard Belin, 31400 Toulouse, France

² Geological Faculty, Moscow State University, 1 Leninskie Gory, 119234 Moscow, Russia

³ Federal Center for Integrated Arctic Research; IEPS, 23 Nab. Severnoi Dviny, 163000 Arkhangelsk, Russia

⁴ IPGP - Institut de Physique du Globe de Paris, 1 Rue de Jussieu, Paris, France

⁵ BIO-GEO-CLIM Laboratory, Tomsk State University, 36 Lenina av., 634050 Tomsk, Russia

2.1. Résumé

La minéralisation bactérienne de matière organique dissoute (MOD) allochtone dans les eaux boréales est reconnue comme une source significative de CO₂ vers l'atmosphère et un des termes les plus importants du bilan du carbone aux hautes latitudes. En outre, en comparaison du grand nombres de travaux expérimentaux et d'études de terrain consacrés à la transformation de MOD de diverses origines, le comportement des métaux liés aux colloïdes organiques pendant la biodégradation est mal compris. Une souche de bactérie hétérotrophe *Pseudomonas saponiphila* a été extraite d'un ruisseau du nord-ouest de la Carélie (Russie) et une monoculture de cette souche bactérienne a été mis en présence d'un lixiviat de tourbe riche en Fe avec une composition colloïdale (3 kDa – 0.45 µm) approximative C₁₀₀₀Fe₁₂Al_{3.3}Mg₂Ca_{3.7}P_{1.2}Mn_{0.1}Ba_{0.5}, sans ajout de nutriment. La transformation (adsorption, assimilation, dégradation, ...) des colloïdes a été observée dans trois fractions (0.45 µm, 50 kDa et 3 kDa) pendant 4 journées d'expérience.

Une diminution relative de 5 % de la concentration du carbone organique dissout (COD) a été observée en fin d'expérience (93 heures) pour toutes les fractions à l'exception de celle de plus faible poids moléculaire (fraction < 3 kDa), pour laquelle une diminution relative de 16% a été observée. Ce comportement différencié de la fraction dissoute est probablement lié à l'assimilation biologique lente et/ou à la flocculation. Les éléments les plus affectés par la présence bactérienne étaient Al, Mn, Ni, Cu, Ga, REE, Y, U, du fait de l'adsorption à la surface cellulaire au cours de la première heure de l'expérience, et Fe, Ti, Zr et Nb, qui étaient eux l'objet à la fois de l'adsorption rapide et de l'assimilation lente ou coagulation / coprécipitation avec des hydroxydes de Fe. Il y avait une diminution du ratio Fe sur COD dans toutes les fractions au cours de l'interaction du lixiviat de tourbe avec *Pseudomonas saponiphila*. Les ratios de concentration entre la fraction dissoute (< 3 kDa) et la fraction colloïdale fine (50 kDa – 3 kDa) de quelques éléments (COD, Al, Ti, Cr, Fe, Co, Ni, Pb, et U) ont présenté une légère baisse (<10%), du probablement à de la flocculation. Le résultat important est que les quantités d'éléments extraits du fait de la présence de bactéries (adsorption ou assimilation) des fractions colloïdales (<0.45 µm et <50 kDa) sont deux à cinq fois plus importantes (suivants l'élément considéré) que celles qui sont extraites de la fraction dissoute (<3 kDa).

L'accélération de l'activité bactérienne hétérotrophe induite par le changement climatique dans les eaux boréales et subarctiques peut entraîner une élimination préférentielle du Fe par rapport au COD et la diminution des concentrations du COD et de quelques éléments (Al, Ti, Cr, Fe, Co, Ni, Pb, et U) dans la fraction de poids moléculaire faible <3 kDa, conjuguée à leurs augmentation dans la fraction colloïdale. La minéralisation améliorée des colloïdes organo-ferriques par les bactéries hétérotrophes dans le scénario de réchauffement climatique pourrait compenser le « brunissement » des eaux de surface.

Mots clés: *carbone organique, COD, Fe, Al, éléments traces, biodégradation, adsorption, coagulation, précipitation, boréale, eau*

2.2. Abstract

Bacterial mineralization of allochthonous (soil) dissolved organic matter (DOM) in boreal waters governs the CO₂ flux from the lakes and rivers to the atmosphere, which is one of the main factor of carbon balance in high latitudes.

However, the fate of colloidal trace element (TE) during bacterial processing of DOM remains poorly constrained. We separated monoculture of *Pseudomonas saponiphila* from a boreal creek and allowed it to react with boreal Fe-rich peat leachate of approximate colloidal ($3 \text{ kDa} - 0.45 \mu\text{m}$) composition $\text{C}_{1000}\text{Fe}_{12}\text{Al}_{3.3}\text{Mg}_2\text{Ca}_{3.7}\text{P}_{1.2}\text{Mn}_{0.1}\text{Ba}_{0.5}$ in nutrient-free media. The total net decrease of Dissolved Organic Carbon (DOC) concentration over 4 day of exposure was within 5% of the initial value, whereas the low molecular weight fraction of C_{org} ($\text{LMW}_{< 3 \text{ kDa}}$) yielded a 16%-decrease due to long-term bio-uptake or coagulation. There was a relative depletion in Fe over C_{org} of $0.45 \mu\text{m}$, colloidal and LMW fraction in the course of peat leachate interaction with *P. saponiphila*. Al, Mn, Ni, Cu, Ga, REEs, Y, U were mostly affected by bacterial presence and exhibited essentially the adsorption at the cell surface over first hours of reaction, in contrast to Fe, Ti, Zr, and Nb that showed both short-term adsorption and long-term removal by physical coagulation/coprecipitation with Fe hydroxide. The low molecular weight fraction ($\text{LMW}_{< 3 \text{ kDa}}$) of most TE was a factor of 2 to 5 less affected by microbial presence via adsorption or removal than the high molecular weight (HMW) colloidal fractions ($< 0.45 \mu\text{m}$ and $< 50 \text{ kDa}$). The climate change-induced acceleration of heterotrophic bacterial activity in boreal and subarctic waters may lead to preferential removal of Fe over DOC from conventionally dissolved fraction and the decrease of the proportion of $\text{LMW}_{< 3 \text{ kDa}}$ fraction and the increase of HMW colloids. Enhanced heterotrophic mineralization of organo-ferric colloids under climate warming scenario may compensate for on-going “browning” of surface waters.

Key words: *organic carbon, DOC, Fe, Al, trace element, biodegradation, adsorption, coagulation, precipitation, boreal, water*

2.3. Introduction

Significant amount of CO_2 is emitted by inland waters to the atmosphere due to bacterial degradation of dissolved organic matter (DOM) (Battin et al., 2009; Tranvik et al., 2009). In boreal rivers and lakes, allochthonous (plant, soil and peat-originated) DOM is known to be the main driver of the metabolism of heterotrophic aerobic bacterioplankton (Tranvik, 1998a, b; Tranvik et al., 2009; Wilkinson et al., 2013). Numerous laboratory and field studies demonstrated that about 10% of the dissolved

organic carbon (DOC) is generally available for bacterial uptake (i.e., Berggren et al., 2007, 2009, 2010), whereas the bioavailability of different molecular weight organic matter ranges from 20 to 60% (Roehm et al., 2009). The biodegradability of DOM leached from permafrost and non-permafrost soils was reviewed by Vonk et al. (2015), and many recent studies addressed the soil leachate DOM lability in small headwater streams (Van Hees et al., 2005; Mann et al. 2015; Larouche et al., 2015; Spencer et al., 2015). In contrast to traditional approaches for evaluating the bacterioplankton mineralization of DOM via on-site monitoring CO_2/O_2 in isolated volumes of natural water with or without the addition of microbial substrates (Roehm et al., 2009; Berggren et al., 2012 and references therein), experimental studies of biodegradation of DOM by pure bacterial cultures separated from natural settings may reveal the mechanisms that control both organic carbon and trace metal dynamics in soils (i.e., Fritzsche et al., 2012; Drozdova et al., 2014, 2015), waters (Bonneville et al., 2006; Shirokova et al., 2015) and mineral systems (Wu et al., 2007, 2008; Stockman et al., 2012). Here, we used an experimental approach to characterize the short-term and long-term interaction of organo-trace element complexes with cultivable aquatic aerobic *Pseudomonas* bacteria.

The interest to metal dynamics in boreal aquatic environments is double. From the one hand, Fe, Mn, Zn, Ni, Co, Cu, Mn are potentially limiting micronutrients for plankton in lakes, rivers, the coastal zone and especially the Arctic Ocean. From the other hand, the delivery of toxic metals (Cd, Pb, Hg, U) and metalloids (As, Sb, Se) from the land to the ocean may increase as the frozen soil thaws, the active (unfrozen) period of the year lengthens and the river discharge increases. Specific feature of all boreal waters subjected to on-going climate change is the dominance of allochthonous organic and organo-mineral colloids that act as main carriers of these metal micronutrients and toxicants (Ingri et al., 2000; Andersson et al., 2001, 2006; Dahlqvist et al., 2004 2007; Neubauer et al., 2013; Vasyukova et al., 2010; Stolpe et al., 2005, 2013). Although the interaction of heterotrophic bacteria with solid organo-ferric compounds from soil and sediments is fairly well studied (Huang et al., 2005; Bosch et al., 2010; Jackson et al., 2011; Sivan et al., 1998, 2011, 2014; Wu et al., 2014; Liu et al., 2015), the partitioning of trace metals between colloidal and low molecular weight fraction and between colloids of different size is still poorly known. In a recent study of peat and moss leachate from permafrost zone, we demonstrated that during consumption of DOM by soil and aquatic heterotrophs (*P. reactans* and *P.*

aureofaciens), the trace elements (TE) are subjected to adsorption on the cell surface and incorporation within the live cells via active or passive uptake (Shirokova et al., 2017). Similar to colloid transformation during photo-degradation (Kopáček et al., 2006, 2008; Porcal et al., 2009, 2013, 2015), a part of TE can be liberated from organic complexes and either precipitate in the form of oxy(hydr)oxides or remain in solution in the form of free or weakly complexed ions and neutral molecules. This can be accompanied by a restructuring of DOM from colloidal (1 kDa - 0.45 µm) to (i) low molecular weight ($\text{LMW}_{< 1 \text{ kDa}}$) fraction which may lead to the formation of stable LMW complexes of TE, and (ii) particulate ($> 0.45 \mu\text{m}$) fraction which may scavenge dissolved metals from the water column to the sediments. Such a transformation of aquatic colloids, linked to prolonged heating of organic-rich surface waters and enhanced heterotrophic activity of bacterioplankton, has been evidenced in thermokarst (Pokrovsky et al., 2013a) and boreal humic (Pokrovsky and Shirokova, 2013; Shirokova et al., 2013b, 2016) lakes. From the other hand, the low molecular weight fraction of DOM and TE is expected to be more bioavailable and susceptible to microbial transformation than the high molecular weight colloids. This suggestion is consistent with results of microbial processing of natural colloids from different terrestrial and aquatic sources (cf., Roehm et al., 2009; Yang et al., 2016). To address this controversy, we performed an experimental characterization of DOC and TE fractionation between different fractions of colloids from well-defined substrate in the presence of bacterial monoculture using a size-separation technique.

The aims of this work were to quantify the OC and TE distribution between main colloidal pools of peat leachate in response to metabolic activity of heterotrophic bacteria and to distinguish between rapid surface adsorption and bacterially-induced coagulation/precipitation of different size peat colloids. We anticipate that quantifying the impact of microbial activity on colloid stability will help to predict potential bioavailability of colloidal, organic-bound trace metals for other aquatic microorganisms along the trophic chain in boreal waters affected by leaching of surrounding peat.

2.4. Materials and Methods

2.4.1. Isolation and culturing of *P. saponiphila*

The soil/aquatic aerobic gram-negative bacterium *Pseudomonas saponiphila* was isolated from the stream Vostochnyi (66.3°N, 30.7°E) of Northern Karelia, NW Russia using cultures on nutrient agar plates. The phylogenetic affiliation of cultivable strain was performed by DNA extracting (UltraClean® Microbial DNA Isolation Kit MO BIO) and 16S rRNA gene amplifying (bacterial specific primers 27F (5'-AGAGTTGATCCTGGCTCAG-3') and prokaryote-specific reverse primers 1492R (5'-GGTTACCTTGTACGACTT-3'), see Gérard et al., 2009 for the condition of PCR amplification) and sequencing (GATC biotech). The sequence shared 99% identity with JN033556 *Pseudomonas saponiphila* strain ME BHU9 (Gammaproteobacteria, Pseudomonadales), Genbank ID GQ258636. Cells were cultured to a stationary stage during 5 days on a shaker at 25°C in darkness using a 10% nutrient bouillon (NB) with the following composition: 0.1 g L⁻¹ glucose, 1.5 g L⁻¹ peptone, 0.6 g L⁻¹ NaCl and 0.3 g L⁻¹ yeast extract.

The live cell number during the experiment was assessed via culturing on agar plates. The active bacteria number count (colony forming-units, CFU mL⁻¹) was performed using Petri dish inoculation on nutrient agar (0.1, 0.2 and 0.5 mL of the sampled solution in triplicate with an estimated uncertainty between 30 and 50 %) in a laminar hood box. Inoculation of blanks was routinely performed to ensure the absence of contamination from the external environment. The total biomass of the bacteria was also quantified by measuring humid (centrifuged 15 min at 8000× g) and dry (lyophilized) weight and optical density at 600 nm (OD_{600 nm}) following the standard procedures of bacterial biomass preparation for metal adsorption experiments (Fein et al., 1997, 2001; Gonzalez et al., 2010; Pokrovsky et al., 2013b). Before the inoculation of the peat leachate, the cells were rinsed twice in sterile 0.01 M NaNO₃ solution using centrifugation at 7000× g (~ 500 mL of solution for 1 g of wet biomass) to remove as much of the adsorbed metals and cell exudates from the surface as possible.

2.4.2. Peat leachate preparation

Because the watershed of the Vostochnyi stream and surrounding bog-forest zone of Northern Karelia contain abundant peat deposits within the ombrotrophic bogs and minerotrophic fens (see Ilina et al., 2014, 2016 for site description), the experimental leachate was prepared by reacting intact peat soil (sampled from 15 to 30 cm depth within the Vostochnyi stream watershed) with distilled water ($10 \text{ g}_{\text{dry}} \text{ L}^{-1}$) in an atmosphere-saturated environment at 25°C on a shaker. After 48 h of reaction, the solution was centrifuged at $4000\times g$ for 10 min, filtered through a $0.45 \mu\text{m}$ sterile disposable Nalgene filtration unit and used as the substrate in the bacterial experiment. Prior the experiments, the sterile leachates were stored during 5 days at room temperature and filtered ($< 0.45 \mu\text{m}$) second time to provide the maximal stability of peat leachate to physico-chemical coagulation. The sterility of peat leachate was verified by inoculation on nutrient agar. All manipulations were performed in a sterile laminar hood box. The peat leachate thus prepared was rich in colloidal Fe which was 4 times more abundant than Al and 1-2 orders of magnitude higher than other trace elements (see section 3.2 below).

2.4.3. Experimental design

A conceptual scheme of conducted experiments is presented in **Fig. 2.1**. Freshly-collected bacteria at the stationary growth stage were rinsed in 0.85% NaCl and allowed to starve in nutrient-free 0.85% NaCl solution during 5 days. The starvation period was necessary to evacuate all the intracellular nutrient resources, notably the organic acids. After 5 days in NaCl solution, the cells remained fully viable as followed from live cell count: within $\pm 30\%$, there was no change in the number of colony-forming units (CFU) before and after the storage. The cells were rinsed again 3 times before the experiment, concentrated in a mother suspension and added to sterile peat leachate (typically 2 mL of bacterial suspension to 200 mL of leachate) to provide the wet biomass concentration of $1 \text{ g}_{\text{wet}} \text{ L}^{-1}$. The polypropylene flasks were shaken on a ping-pong thermostatic shaker at $25\pm 0.5^\circ\text{C}$ and aerated via Biosilico® ventilation porous caps during 4 days. Aliquots of homogeneous suspension were sampled 1, 20, 47, 68 and 93 h after the addition of bacteria and processed for $0.45 \mu\text{m}$, 3 kDa and 50 kDa filtration/ultrafiltration as described below. All the experiments were run in duplicates.

Four control experiments, also run in duplicates, included studying of: (C1) Stability of cell-free peat leachate as a function of time and solution pH; (C2) DOC and TE release from cells in peat-free aqueous solution; (C3) Kinetics of DOC and TE adsorption onto cells, and (C4) pH-edge adsorption of DOC and TE onto cells. Note that these kinetic and abiotic control experiments encompassed larger span of time and chemical composition than the biotic experiments. They were conducted under conditions when the biodegradation of organo-ferric colloids by *P. saponiphila* could not occur.

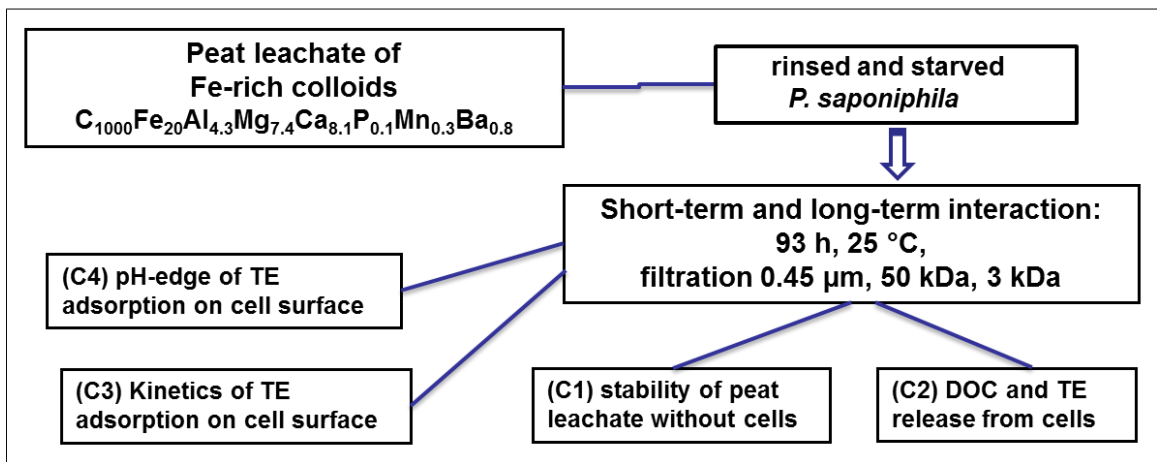


Fig. 2.1. Scheme of the experiments, which were all run in duplicate. Natural peat sampled in boreal subarctic zone and *P. saponiphila* extracted from adjacent creek were used for experiments. The main biotic experiments included sterile peat leachate (25 mg/L of DOC, 1 mg/L of Fe) that interacted with nutrient-free *P. saponiphila* (1 g_{wet}/L). Control experiments included one abiotic (C1) control of the peat leachate stability and three biotic ones: the DOC and TE release from cells (C2), the kinetics of DOC and TE adsorption on cell surfaces at fixed pH (C3) and the pH-dependent adsorption edge of leachate components on cell surfaces (C4).

The first “stability control” experiment (C1) was sterile filtered (< 0.45 µm) biomass-free peat leachate at variable pH and it was processed exactly as bacterial sample, i.e., filtered and ultrafiltered after various exposure time. The ”DOC and TE release control” (C2) was wet biomass of *P. saponiphila* in MilliQ water without peat leachate, used only for 0.45 µm filtration. The “adsorption kinetic” control (C3) of peat leachate constituents adsorption onto bacterial biomass included the monitoring of major and trace element concentration (< 0.45 µm) in bacterial suspension over 3 h of reaction via sampling after 1, 15, 30, 60, 90, 120 and 180 minutes. Finally, because the live bacteria are capable modifying the pH of surrounding medium, the “pH adsorption” control (C4) included short-term adsorption of peat leachate constituents

(< 0.45 µm) on cell surfaces in a wide range of pH (from 4 to 10), studied over 1 h of exposure on a shaker at 20°C.

Aliquots of homogeneous suspension (20 mL) were sampled daily from the reactors using sterile pipette in a sterile laminar hood box. During sampling, the reactor was vigorously mixed by magnet stir bar thus producing highly homogeneous cell suspension. Therefore, although half of initial suspension was removed in the course of experiment, the total biomass and live cell concentration were not affected by sampling. The optical density and pH were measured in suspension subsamples, while 0.1 to 0.5 mL was used for inoculation of the nutrient agar plates in triplicate for viable cell counts after dilution by a factor of 10,000.

The sampled aliquot was centrifuged at 7000x g and separated into three fractions which were used for: *i*) conventional filtration through disposable 0.45 µm acetate cellulose filters and *ii*) ultrafiltration through 3 and 50 kDa using centrifugal filters Amicon Ultracel® . These disposable 50-mL polypropylene vials fitted with 3,000 or 50,000 NMWL regenerated cellulose filters were first treated by 1% HNO₃, and rinsed 3 times via passing between 50 and 100 mL of MilliQ water through the membrane. The DOC and metal blanks were a factor of 3 to 10 lower than the minimal concentrations of these components in experimental fluids. The first 15-mL portion of sample supernatant that passed through 3 and 50 kDa membranes was rejected. Each fraction of filtrate was sub-devised into non-acidified and acidified portions, for carbon/UV/pH and trace element measurements, respectively.

2.4.4. Analytical techniques

The DOC was analyzed using a Shimadzu TOC-V_{CSN} Total Carbon Analyzer with an uncertainty of 3% and a detection limit of 0.1 mg L⁻¹. The pH was measured with an accuracy of ± 0.01 pH units. The UV absorbance of the filtered samples was measured at 280 nm using quartz 10-mm cuvette on a Cary-50 spectrophotometer. The specific UV-absorbency (SUVA₂₈₀, L mg⁻¹m⁻¹) is used as a proxy for aromatic C, molecular weight and source of DOM (Uyguner and Bekbolet, 2005; Weishaar et al., 2003; Ilina et al., 2014 and references therein). Filtered solutions for the cation and trace element analyses were acidified (pH = 2) with HNO₃ and stored in polystyrene vials that had been previously washed with 0.1 M HCl and rinsed with ultrapure MilliQ deionized water. The sampling vials were prepared in a clean bench room class A 10,000. Major and trace elements (TEs) were determined with an ICP-MS Agilent

7500 ce that is used in GET laboratory (Toulouse) for the analysis of organic-rich rivers and lakes (cf. Pokrovsky et al., 2016a, b). The uncertainty of element concentration measurements ranged from 5 to 10% at $[TE] > 1 \mu\text{g L}^{-1}$, 10 to 20% at $0.01 < [TE] < 1 \mu\text{g L}^{-1}$, and from 20 to 30% at $[TE] < 0.01 \mu\text{g L}^{-1}$. The international geostandard SLRS-5 was analyzed every 20 samples to check the validity and reproducibility of the analyses (Yeghicheyan et al., 2014). Good agreements were found between the replicated measurements of SLRS-5 and the certified values (relative difference $< 20\%$ SD on the repeated measurements) of all major and trace elements discussed in this study.

2.4.5. Modeling

Statistical treatment of experimental data included the calculation of errors and confidence intervals for the measured values of pH, O.D., cell number, DOC, major and TE concentrations, and of biotic and chemical parameters of the experimental solution among different duplicates, bacteria and substrates over the full duration of the experiment. A value of $P < 0.05$ indicated that the differences in the overall concentration – time trend are important and are statistically significant compared with internal variations between replicates.

To characterize the degree of metal complexation with organic ligands in various size fraction of peat leachate in the course of experiment, we used Visual MINTEQ (Gustafsson, 2011, version 3.1, October 2014) for Windows in conjunction with a database and the NICA-Donnan humic ion binding model (Benedetti et al., 1995; Milne et al., 2003) and Stockholm Humic Model (SHM). The input parameters of the model were pH, DIC, anions, cations, total TE and DOC concentrations and the output file yielded the speciation of Ba, Ca, Cd, Co, Cu, K, Mg, Mn, Na, Ni, Pb, Sr, Zn, Al, Fe^{III}, Th^{IV} and U^{VI}O₂. The model also predicted the saturation state of solution with respect to dominant secondary minerals and amorphous phases, and the percentage of metal complexed with organic ligands relative to the total dissolved metal.

2.5. Results

2.5.1. Removal of different colloidal fractions in the course of experiments

The number of live bacteria remained fairly stable over 4 days of experiment, although there was some increase of CFU at the beginning of experiment (**Fig. 2.2 A**). Given the uncertainty of live cell count after a series of dilution (ca. 30 to 50 %), this increase cannot be interpreted as an increase in overall biomass. The latter remained essentially constant or decreased from 1 g_{wet}/L to 0.89 g_{wet}/L following the optical density evolution (**Fig. 2.2 B**).

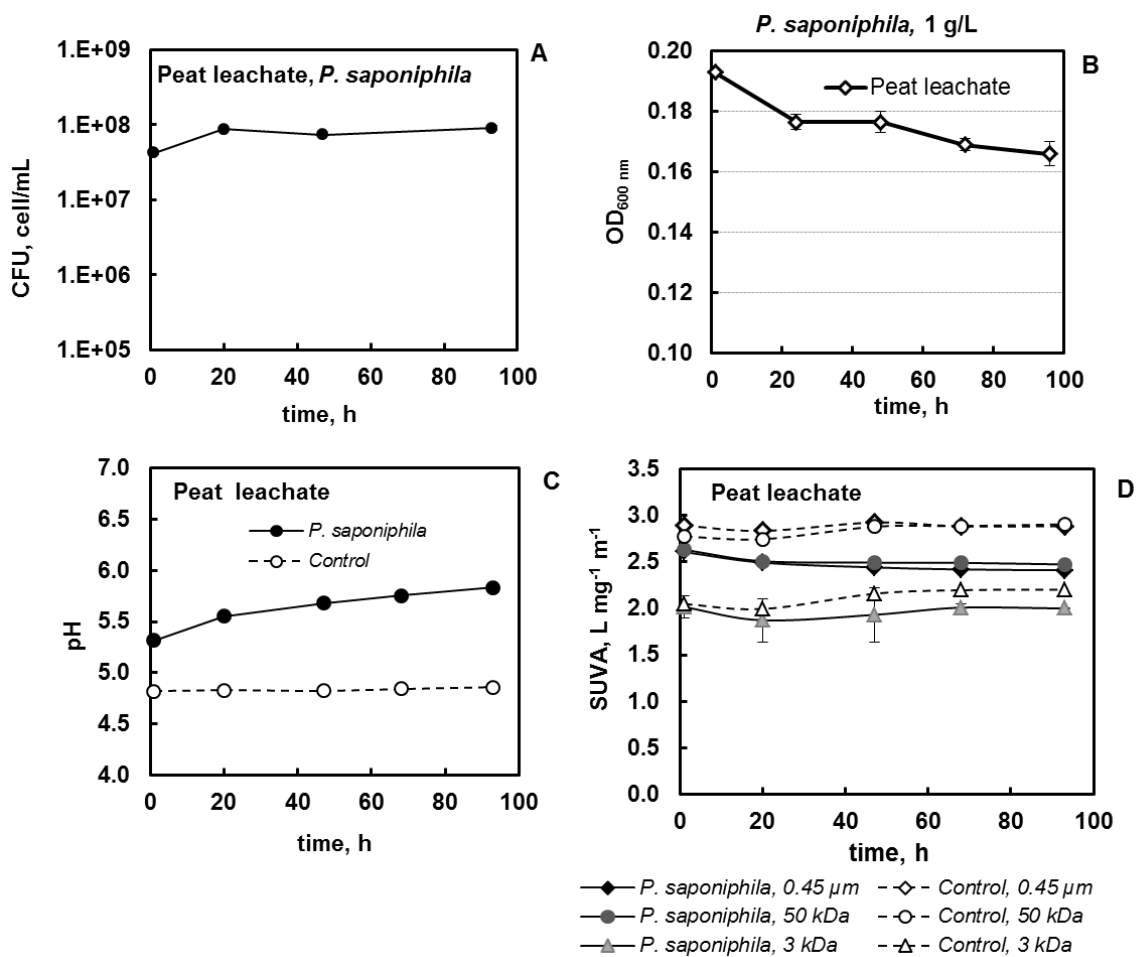


Fig. 2.2. Live cell number expressed as colony forming units (CFU, cell/mL), A; cell biomass measured as optical density (B); pH (C) and specific UV-absorbency at 280 nm (SUVA₂₈₀, D) evolution in the course of experiments. The live cell number is estimated with $\pm 30\text{--}50\%$ uncertainty. The uncertainty on the biomass (OD_{600 nm}), pH and SUVA are within the symbol size unless shown explicitly.

The pH slightly increased from 5.3 to 5.8 (**Fig. 2.2 C**). Over 4 days of exposure, the concentration of organic carbon (OC) remained constant and quite

similar to bacteria-free control for all three filtered fractions (**Fig. 2.3 A**). The decrease of OC concentration in the experiment relative to control was between 1 and 1.5 mg/L over 93 h for 0.45 μm and 50 kDa fractions which constituted 5.5 \pm 1.0% of the initial OC concentration. The 3 kDa fraction yielded 15.8 \pm 0.3% relative decrease in OC after 93 h of exposure. The specific UV absorbency at 280 nm (SUVA₂₈₀) remained generally stable for all size fractions (5 \pm 3% of the initial value), with 30% lower value in LMW_{< 3 kDa} fraction ($2.02\pm0.12 \text{ L mg}^{-1} \text{ m}^{-1}$) compared to 0.45 μm fraction ($2.61\pm0.02 \text{ L mg}^{-1} \text{ m}^{-1}$, see **Fig. 2.2 D** of the Supplement). The decrease of the 0.45 μm fraction of SUVA₂₈₀ over 93 h of exposure, from 2.61 ± 0.02 to $2.41\pm0.01 \text{ L mg m}^{-1}$ was significant ($p < 0.05$).

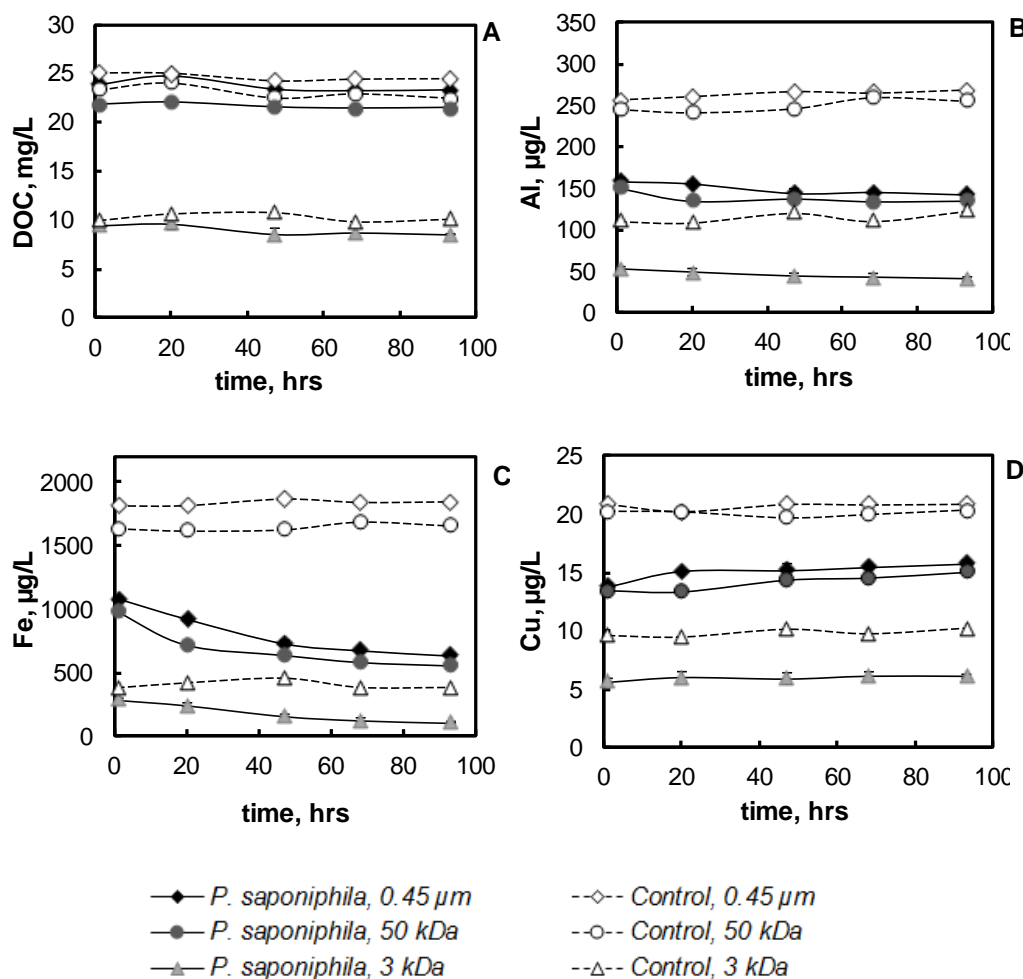


Fig. 2.3. Organic carbon (A), Al (B), Fe(C) and Cu (D) concentration over time in 3 fraction of peat leachate in the presence of *P. saponiphila*. Here and in figures below, solid diamonds, squares and triangles with solid lines correspond to 0.45 μm , 50 kDa and 3 kDa fraction of biotic experiment. The open symbols with dashed lines are for corresponding bacteria-free peat leachate (C1). The standard deviation of the duplicate samples is within the symbol size unless shown explicitly.

The majority of trace metals exhibited a weak decrease of concentration relative to the control in the period between 20 and 93 h of exposure. In contrast, the initial adsorption after 1 h of reaction was clearly pronounced for Al, Fe, and Cu as it is seen from the difference between peat leachate control and bacterial suspension at the beginning of experiment (**Fig. 2.3 B, C and D**, respectively). The integral values of fast adsorption (0-1 h) and assimilation/coagulation (20-93 h) for all size fractions are listed in **Table 2.1**, whereas the apparent rates of assimilation/coagulation for elements affected by this process are listed in **Table 2.2**. Examples of elements that exhibited adsorption over the first hour of exposure are shown in figures **2.4** and **2.5** and include divalent metals such as Mn, Co, Ni and Cd (**Fig. 2.4 A, B, C and D**, respectively), and trivalent and tetravalent hydrolysates (Ti, Zr, Y, La, Th) and U (**Fig. 2.5 A-F**).

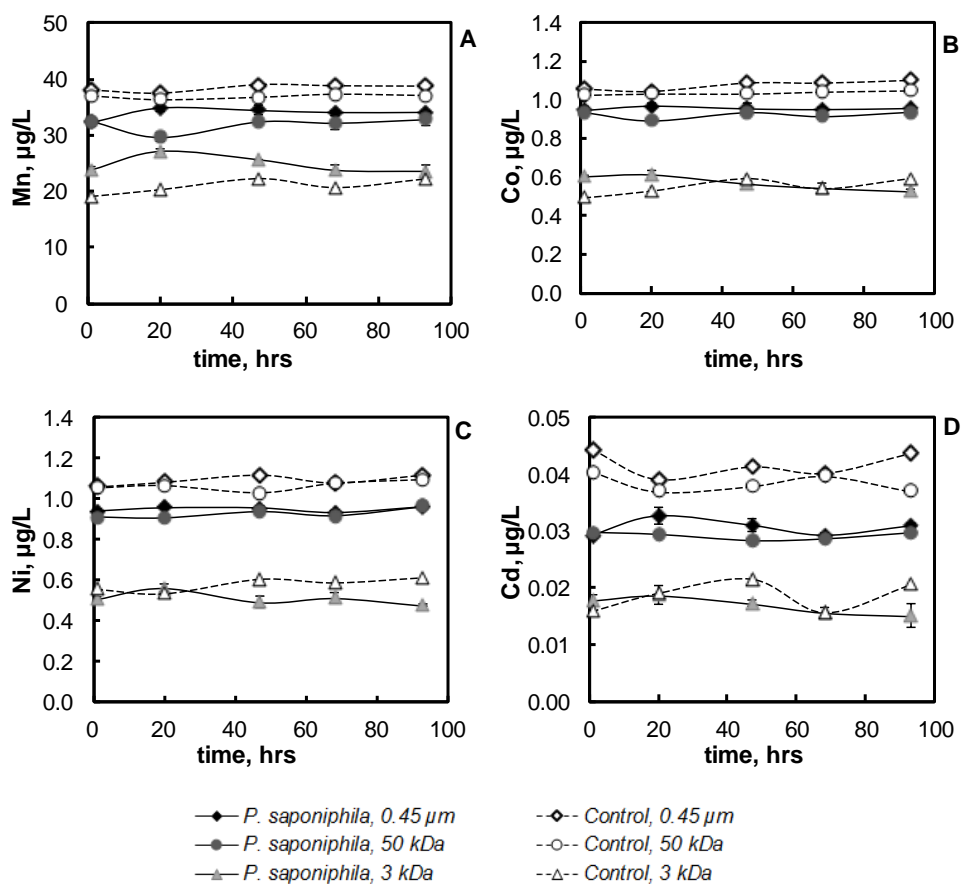


Fig. 2.4. Mn (A), Co (B), Ni (C) and Cd (D) concentration change over time in 3 fractions of peat leachate in the presence of 1 g_{wet}/L of *P. saponiphila*.

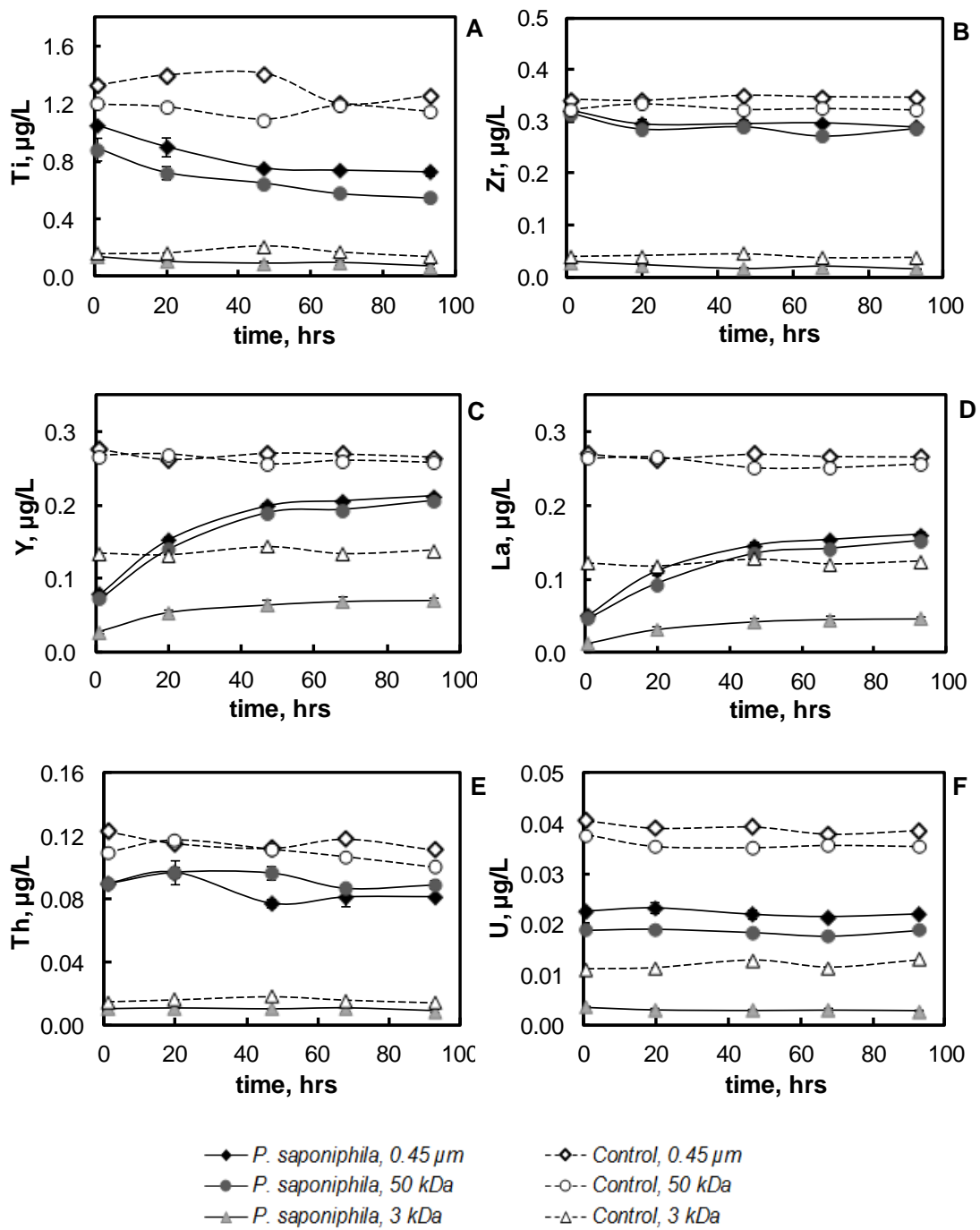


Fig. 2.5. Ti (A), Zr (B), Y (C), La (D), Th (E) and U (F) concentration change over time in 3 fractions of peat leachate in the presence of 1 g_{wet}/L of *P. saponiphila*.

Oxyanions and neutral species were poorly affected by both short-term adsorption and assimilation/coagulation as their concentrations remained stable over full duration of experiment as shown for Cr, As, Mo and Sb in **Fig. 2.6 A, B, C and D**, respectively. The increase of Mo concentration in all fractions in the course of experiment could be due to the release of this micronutrient from the cells via efflux or desorption as it is known for live bacteria (e.g., Shirokova et al., 2015).

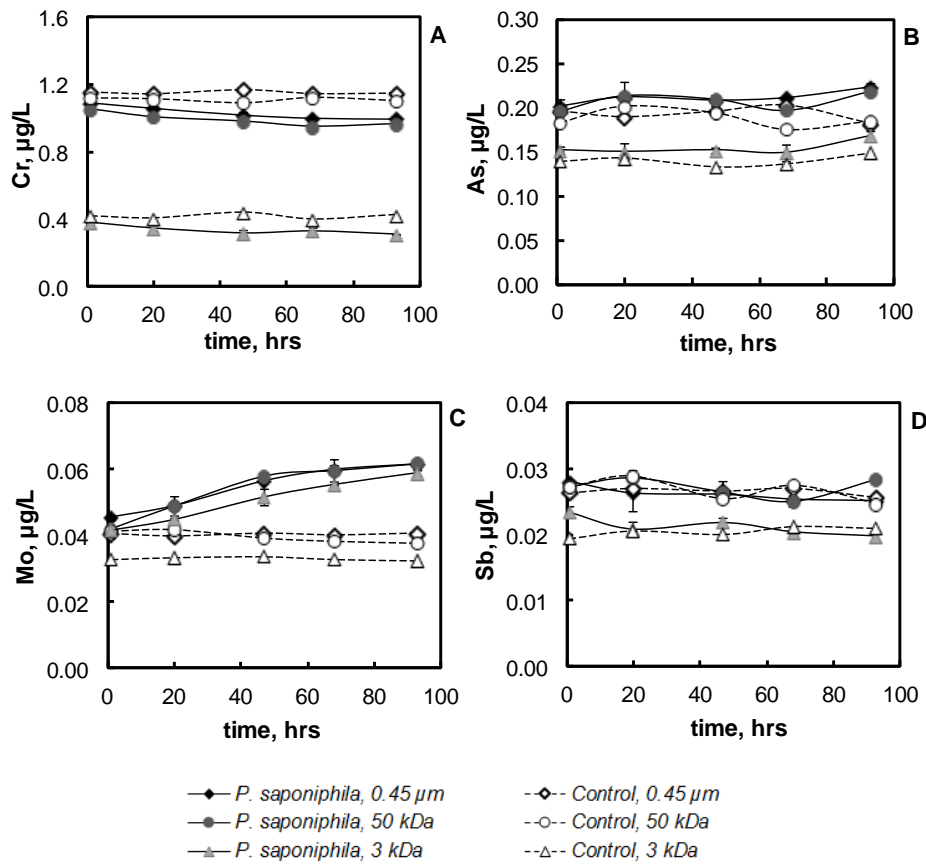


Fig. 2.6. Cr (A), As (B), Mo (C) and Sb (D) concentration change over time in 3 fractions of peat leachate reacting with *P. saponiphila*.

The ratio of the amount of short-term (0–1 h) adsorbed to long-term (20–93 h) incorporated / coagulated trace element systematically decreased from 0.45 µm to 3 kDa fraction following the order “0.45 µm > 50 kDa > 3 kDa”. This ratio was significantly higher than 1 for Al and decreased by a factor of 1.5 from 0.45 µm to 3 kDa fraction ($6.14 \rightarrow 6.30 \rightarrow 4.75$). It also decreased between 0.45 µm and 3 kDa fractions by a factor of ~3 for Fe ($1.65 \rightarrow 1.54 \rightarrow 0.53$) and Ti ($0.88 \rightarrow 0.93 \rightarrow 0.26$). This clearly indicates that the precipitation/assimilation over 4 days dominated over fast adsorption for the $\text{LMW}_{< 3 \text{ kDa}}$ smallest fraction of Fe and Ti, whereas for all other metals (Al, V, Mn, Co, Ni, Cu, Ga, Y, Cd, REE, Hf, Th, U) the adsorption strongly dominated over assimilation as listed in **Table 2.3**.

Based on measured long-term removal rates of TE in the presence of bacteria ($R_{20-93 \text{ h}}$, $\mu\text{g L}^{-1} \text{ d}^{-1}$) and element concentration in the control ([TE], $\mu\text{g L}^{-1}$), a half-life time of peat leachate constituents can be calculated as $0.5 \times R_{20-93 \text{ h}} / [\text{TE}]$ (**Table 2.4**). The elements affected by long-term bacterial removal from the peat leachate, notably Fe, demonstrate a two-fold decrease of the half-life time from $\text{HMW}_{0.45\mu\text{m}-50 \text{ kDa}}$ colloids to $\text{LMW}_{50 \text{ kDa}-3 \text{ kDa}}$ colloids and further to $\text{LMW}_{< 3 \text{ kDa}}$ fraction.

Table 2.1. Integral values of fast adsorption on the cell walls and slow assimilation/removal of peat leachate components in the presence of 1 g_{wet} L⁻¹ of *Pseudomonas saponiphila*. Not listed are Mg, Si, As, Sb and Cs showing neither adsorption nor assimilation in the course of experiment

Element	Long-term (1-93 h) assimilation or coagulation/precipitation, µg/g _{wet}			Short-term (0-1 h) adsorption, µg/g _{wet}		
	< 0.45 µm	< 50 kDa	< 3 kDa	< 0.45 µm	< 50 kDa	< 3 kDa
DOC	540 ± 170	330 ± 140	950 ± 410	1150 ± 170	1530 ± 140	520 ± 410
B	no effect	no effect	no effect	11.8 ± 2.5	62 ± 31	no effect
Al	16.0 ± 2.9	15.1 ± 1.7	12.2 ± 3.7	98.3 ± 2.9	95.2 ± 1.7	58.0 ± 3.7
Ca	no effect	no effect	36.6 ± 5.9	no effect	no effect	no effect
Ti	0.321 ± 0.024	0.338 ± 0.033	0.070 ± 0.015	0.282 ± 0.024	0.314 ± 0.033	0.018 ± 0.015
V	no effect	no effect	no effect	0.238 ± 0.015	0.218 ± 0.007	0.059 ± 0.01
Cr	0.09 ± 0.01	0.09 ± 0.01	0.07 ± 0.02	0.07 ± 0.01	0.07 ± 0.01	0.04 ± 0.02
Mn	no effect	no effect	no effect	5.7 ± 0.5	4.5 ± 0.7	no effect
Fe	441 ± 13	424 ± 8	180 ± 11	732 ± 13	653 ± 8	96 ± 11
Co	no effect	no effect	0.075 ± 0.014	0.108 ± 0.014	0.091 ± 0.010	no effect
Ni	no effect	no effect	0.031 ± 0.017	0.123 ± 0.08	0.142 ± 0.006	0.050 ± 0.017
Cu	no effect	no effect	no effect	7.1 ± 0.2	6.8 ± 0.1	3.9 ± 0.4
Ga	no effect	no effect	no effect	0.026 ± 0.001	0.015 ± 0.001	0.009 ± 0.001
Rb	no effect	0.34 ± 0.16	no effect	no effect	no effect	no effect
Y	no effect	no effect	no effect	0.199 ± 0.002	0.196 ± 0.001	0.108 ± 0.005
Zr	0.032 ± 0.005	0.028 ± 0.004	0.013 ± 0.003	0.020 ± 0.005	0.009 ± 0.004	0.010 ± 0.003
Nb	0.0013 ± 0.0001	0.0015 ± 0.0001	no effect	0.0019 ± 0.0001	0.0011 ± 0.0001	no effect
Cd	no effect	no effect	0.003 ± 0.001	0.015 ± 0.001	0.011 ± 0.002	no effect
La	no effect	no effect	no effect	0.220 ± 0.003	0.218 ± 0.002	0.109 ± 0.003
Ce	no effect	no effect	no effect	0.483 ± 0.006	0.482 ± 0.003	0.243 ± 0.008
Pr	no effect	no effect	no effect	0.054 ± 0.001	0.055 ± 0.001	0.029 ± 0.001
Nd	no effect	no effect	no effect	0.212 ± 0.002	0.215 ± 0.003	0.116 ± 0.005
Sm	no effect	no effect	no effect	0.042 ± 0.001	0.043 ± 0.001	0.022 ± 0.001
Eu	no effect	no effect	no effect	0.0090 ± 0.0004	0.0104 ± 0.0003	0.0038 ± 0.0002
Tb	no effect	no effect	no effect	0.0061 ± 0.0001	0.0063 ± 0.0001	0.0032 ± 0.0001

Table 2.1, continued

Element	Long-term (1-93 h) assimilation or coagulation/precipitation, $\mu\text{g/g}_{\text{wet}}$			Short-term (0-1 h) adsorption, $\mu\text{g/g}_{\text{wet}}$		
	< 0.45 μm	< 50 kDa	< 3 kDa	< 0.45 μm	< 50 kDa	< 3 kDa
Gd	no effect	no effect	no effect	0.0410 \pm 0.0005	0.0418 \pm 0.0005	0.021 \pm 0.001
Dy	no effect	no effect	no effect	0.0372 \pm 0.0006	0.0387 \pm 0.0002	0.020 \pm 0.001
Ho	no effect	no effect	no effect	0.0075 \pm 0.0002	0.0072 \pm 0.0001	0.0041 \pm 0.0002
Er	no effect	no effect	no effect	0.0208 \pm 0.0003	0.0201 \pm 0.0002	0.0116 \pm 0.0005
Tm	no effect	no effect	no effect	0.0028 \pm 0.0001	0.0027 \pm 0.0001	0.0015 \pm 0.0001
Yb	no effect	no effect	no effect	0.0133 \pm 0.0003	0.0145 \pm 0.0003	0.0085 \pm 0.0005
Lu	no effect	no effect	no effect	0.0019 \pm 0.0001	0.0013 \pm 0.0001	0.0010 \pm 0.0001
Hf	0.0012 \pm 0.0002	no effect	no effect	0.0004 \pm 0.0002	0.0012 \pm 0.0002	0.0005 \pm 0.0003
Pb	0.04 \pm 0.01	0.04 \pm 0.01	no effect	no effect	no effect	no effect
Th	no effect	no effect	no effect	0.033 \pm 0.004	0.020 \pm 0.003	0.004 \pm 0.001
U	no effect	no effect	no effect	0.0179 \pm 0.0006	0.0188 \pm 0.0002	0.0075 \pm 0.0003

Table 2.2. Biomass-normalized rates of slow (1 – 93 h) gradual intracellular assimilation or extracellular coagulation in bacterial experiments. Only elements showing statistically significant effects are listed.

Element	Slow assimilation or coagulation, $\mu\text{g g}_{\text{wet}}^{-1} \text{ day}^{-1}$		
	< 0.45 μm	< 50 kDa	< 3 kDa
DOC	140 \pm 43	87 \pm 37	250 \pm 130
Al	4.2 \pm 0.8	4 \pm 0.4	3.2 \pm 1
Ti	0.084 \pm 0.006	0.089 \pm 0.009	0.018 \pm 0.004
Cr	0.024 \pm 0.003	0.023 \pm 0.001	0.018 \pm 0.004
Fe	116 \pm 3	111 \pm 2	47 \pm 3
Zr	0.009 \pm 0.001	0.007 \pm 0.001	0.003 \pm 0.001
Nb	0.0004 \pm 0.00003	0.0004 \pm 0.00003	no effect
Cd	no effect	no effect	0.001 \pm 0.0003
Hf	0.0003 \pm 0.00006	no effect	no effect
Pb	0.01 \pm 0.003	0.011 \pm 0.003	no effect

Table 2.3. The relative change of element concentration (compared to the control) during long-term assimilation/coagulation and short-term adsorption. B, Si, Ca, As, Rb, Mo, Sb and Cs did not show any measurable effect and not listed in this table

Element	Slow assimilation or coagulation/precipitation, % (1 – 93 h)			Element	Fast adsorption, % (0 – 1 h)		
	< 0.45 µm	< 50 kDa	< 3 kDa		< 0.45 µm	< 50 kDa	< 3 kDa
DOC	2 ± 1	2 ± 1	10 ± 4	DOC	5 ± 2	7 ± 1	5 ± 1
Al	10 ± 2	10 ± 1	23 ± 8	Al	38 ± 2	39 ± 1	53 ± 8
Ti	31 ± 3	38 ± 5	48 ± 14	Ti	21 ± 3	26 ± 5	no effect
V	no effect	no effect	no effect	V	16 ± 1	16 ± 1	6 ± 1
Cr	8 ± 1	8 ± 1	18 ± 4	Cr	6 ± 1	6 ± 1	9 ± 4
Mn	no effect	no effect	no effect	Mn	15 ± 2	12 ± 2	no effect
Fe	41 ± 2	43 ± 1	63 ± 6	Fe	40 ± 2	40 ± 1	25 ± 6
Co	no effect	no effect	no effect	Co	10 ± 1	9 ± 1	no effect
Ni	no effect	no effect	no effect	Ni	12 ± 1	13 ± 1	no effect
Cu	no effect	no effect	no effect	Cu	34 ± 1	34 ± 1	41 ± 6
Ga	no effect	no effect	no effect	Ga	66 ± 5	53 ± 4	61 ± 10
Y	no effect	no effect	no effect	Y	72 ± 1	73 ± 1	80 ± 8
Zr	10 ± 2	9 ± 1	45 ± 12	Zr	6 ± 2	3 ± 1	26 ± 12
Nb	15 ± 2	19 ± 2	no effect	Nb	18 ± 2	12 ± 2	no effect
Cd	no effect	no effect	15 ± 7	Cd	34 ± 3	26 ± 6	no effect
La	no effect	no effect	no effect	La	81 ± 3	83 ± 2	89 ± 9
Ce	no effect	no effect	no effect	Ce	78 ± 2	80 ± 1	87 ± 9
Pr	no effect	no effect	no effect	Pr	75 ± 2	76 ± 2	85 ± 9
Nd	no effect	no effect	no effect	Nd	72 ± 1	74 ± 2	82 ± 9
Sm	no effect	no effect	no effect	Sm	73 ± 2	74 ± 1	81 ± 9
Eu	no effect	no effect	no effect	Eu	57 ± 4	66 ± 3	51 ± 4
Tb	no effect	no effect	no effect	Tb	72 ± 2	74 ± 1	83 ± 8
Gd	no effect	no effect	no effect	Gd	74 ± 2	76 ± 2	83 ± 9
Dy	no effect	no effect	no effect	Dy	70 ± 2	73 ± 1	81 ± 10
Ho	no effect	no effect	no effect	Ho	68 ± 3	69 ± 2	79 ± 8
Er	no effect	no effect	no effect	Er	63 ± 1	64 ± 1	75 ± 7
Tm	no effect	no effect	no effect	Tm	59 ± 2	60 ± 3	69 ± 8
Yb	no effect	no effect	no effect	Yb	47 ± 1	51 ± 1	62 ± 6
Lu	no effect	no effect	no effect	Lu	44 ± 2	37 ± 3	51 ± 8
Hf	11 ± 2	no effect	no effect	Hf	4 ± 2	10 ± 2	24 ± 18
Pb	10 ± 3	11 ± 3	no effect	Pb	no effect	no effect	no effect
Th	no effect	no effect	no effect	Th	27 ± 5	18 ± 3	30 ± 8
U	no effect	no effect	no effect	U	44 ± 3	50 ± 1	68 ± 9

Table 2.4. Half-life time of elements in peat leachate in the presence of 1 g_{wet} L⁻¹ of live *P. saponiphila*.

Element	Half-life time of elements, days		
	0.45 µm - 50 kDa	50 kDa - 3 kDa	< 3 kDa
DOC	no effect	no effect	21 ± 11
Al	no effect	no effect	17 ± 5
Ti	no effect	7.4 ± 1	4.5 ± 1
Cr	no effect	no effect	11.6 ± 2.5
Fe	19 ± 15	9.8 ± 0.3	4.1 ± 0.3
Co	no effect	no effect	12 ± 6
Ni	no effect	no effect	35 ± 22
Zr	no effect	36 ± 9	6.5 ± 2.2
Nb	no effect	10.7 ± 2.7	no effect
Cd	no effect	no effect	11 ± 5
Hf	no effect	50 ± 20	no effect
Pb	no effect	13 ± 3	no effect

2.5.2. Partitioning of TE among different size fractions of peat leachate during its interaction with *P. saponiphila*

The restructuring of colloids during biodegradation is illustrated in the form of bar plots of size distribution between two main colloidal (0.45 µm – 50 kDa and 50 kDa – 3 kDa) and one LMW (< 3 kDa) pools at the beginning and at the end of experiments. These diagrams are constructed for the main colloid constituents (DOC, Al, Ti and Fe) in **Fig. 2.7 A, B, C and D**, respectively, divalent metals (**Fig. 2.8 A, B, C and D** for Mn, Cu, Ni and Pb, respectively) and other colloidal-affected trace elements (**Fig. 2.9 A, B, C and D** for Y, La, Th and U, respectively). The first main result is that the relative change of element pool in the course of bacterial exposure never exceeded 10%. However, for a number of element linked to colloids this change was statistically significant ($p < 0.05$) and exceeded the uncertainty of duplicates. Thus, there was a net removal of 5±3 % of DOC, Al, Cr, Ni from the LMW_{< 3 kDa} pool to LMW_{50 kDa-3kDa} colloidal pool (**Fig. 2.7A**). After 93 h of interaction between peat leachate and bacteria, Ti, Fe and Zr were partially removed from “truly dissolved” LMW_{< 3 kDa} pool into colloidal LMW_{50 kDa-3kDa} and HMW_{0.45µm-50 kDa} pools. In contrast, the distribution of Si, Mn, Cu, Ga, As, Cd, Y, Zr, REEs, Hf, Pb, Th, U among 3 main fractions was not affected by bacterial activity since there was no statistically significant shift ($p > 0.05$) of these element size fractionation pattern in the course of experiment.

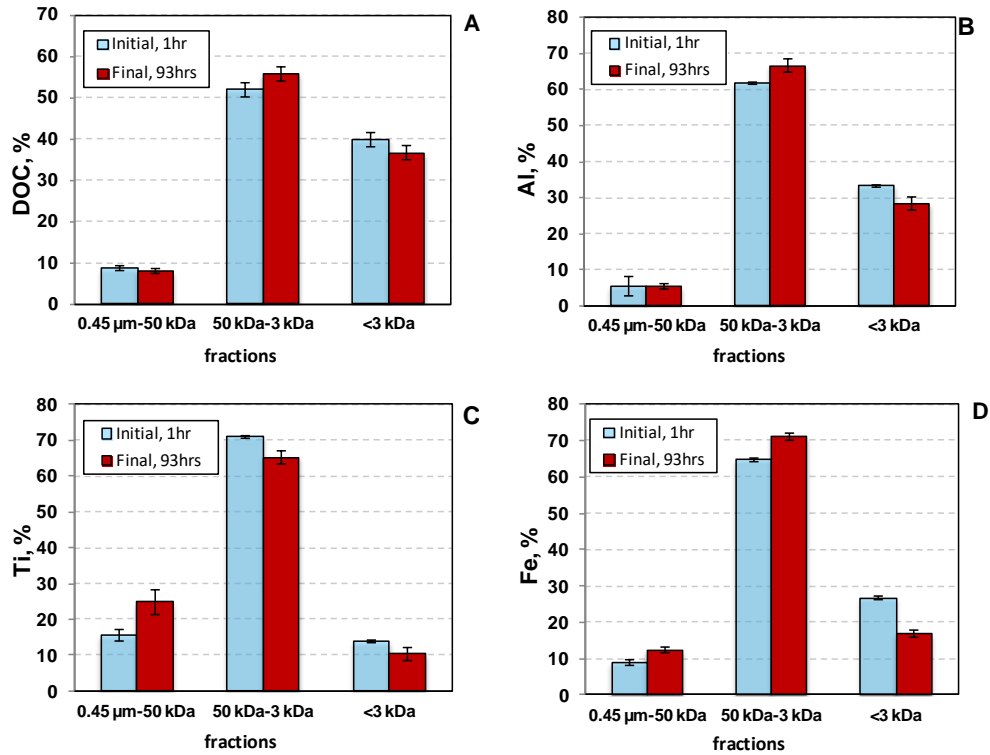


Fig. 2.7. DOC (A), Al (B), Ti (C) and Fe (D) distribution between 2 colloidal (0.45 μm – 50 kDa, 50 kDa – 3 kDa) and “truly” dissolved LMW_{< 3 kDa} pools at the beginning and the end of biodegradation experiment.

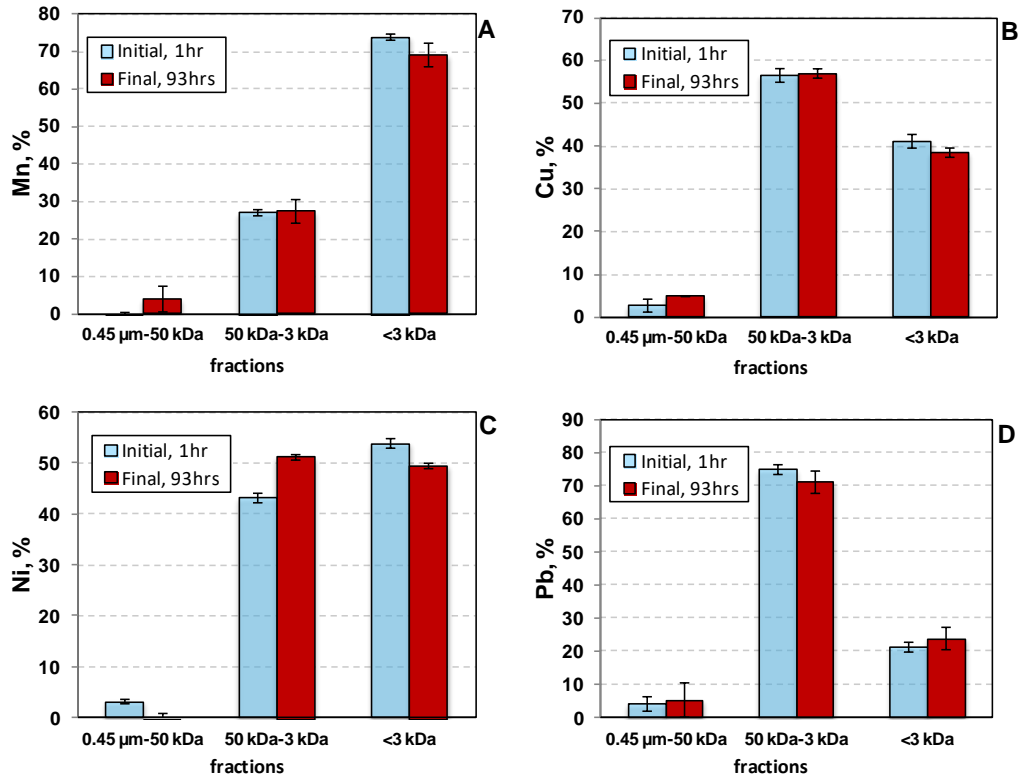


Fig. 2.8. Mn (A), Cu (B), Ni (C) and Pb (D) distribution between 2 colloidal (0.45 μm – 50 kDa, 50 kDa – 3 kDa) and “truly” dissolved LMW_{< 3 kDa} pools in the course of biodegradation experiment.

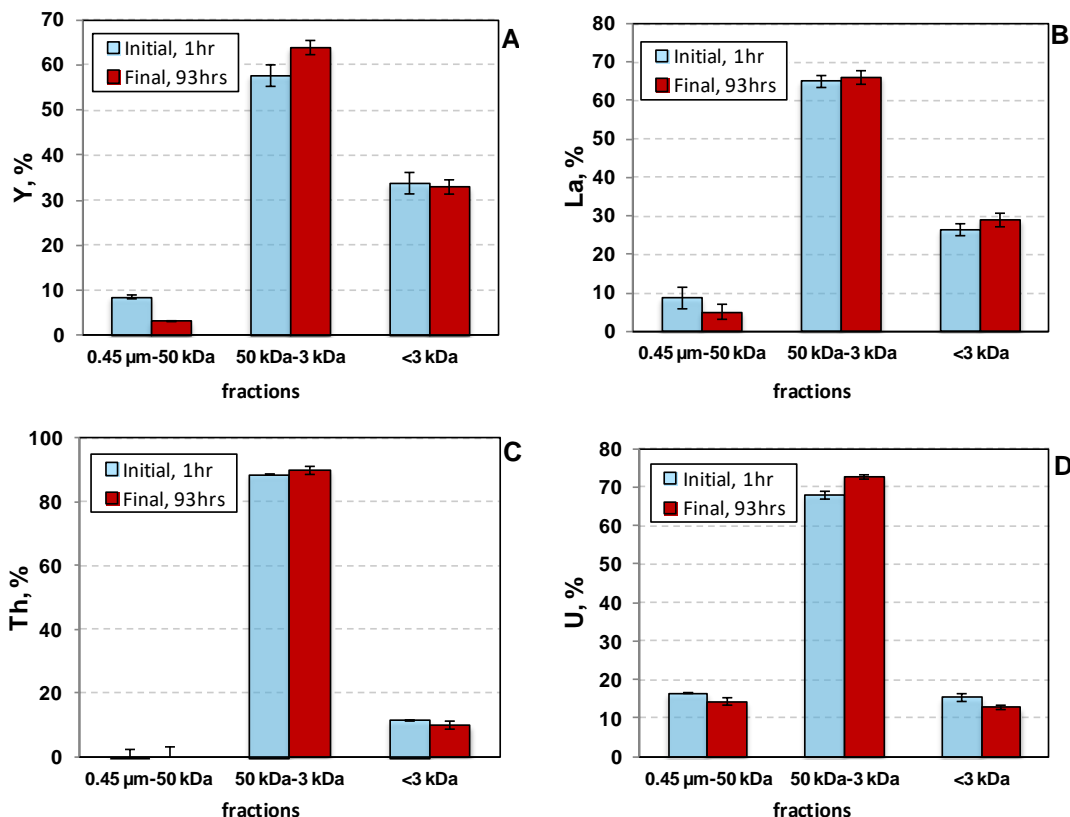


Fig. 2.9. Y (A), La (B), Th (C) and U (D) distribution between 2 colloidal ($0.45 \mu\text{m} - 50 \text{kDa}$, $50 \text{kDa} - 3 \text{kDa}$) and “truly” dissolved $\text{LMW}_{<3 \text{kDa}}$ pools in the course of biodegradation experiment.

The rate of decrease of $\text{LMW}_{<3 \text{kDa}}$ fraction integrated over 93 hr of experiment for DOC, Al, Ti, Cr, Fe, Co, Ni and Zr was equal to 250 ± 130 , 3.2 ± 1.0 , 0.018 ± 0.004 , 0.018 ± 0.004 , 47 ± 3 , 0.02 ± 0.01 , 0.008 ± 0.005 , and $0.003 \pm 0.001 \mu\text{g L}^{-1} \text{ day}^{-1}$ (Table 2.5). The $\text{LMW}_{50 \text{kDa}-3 \text{kDa}}$ colloidal pool of Ti and Fe increased with a rate of 0.07 ± 0.01 and $64 \pm 2 \mu\text{g L}^{-1} \text{ day}^{-1}$, respectively. The rate of $\text{HMW}_{0.45\mu\text{m}-50 \text{kDa}}$ colloidal pool change during long-term interaction could not be quantified.

Analysis of molar ratio of organic carbon to TE in colloids allowed assessing the transformation of colloidal chemical composition of colloids in the course of bacterial experiment. The initial peat leachate colloids ($3 \text{kDa} - 0.45 \mu\text{m}$) contained ca. 4 times more Fe than Al and exhibited approximate chemical composition of $\text{C}_{1000}\text{Fe}_{12}\text{Al}_{3.3}\text{Mg}_{2}\text{Ca}_{3.7}\text{P}_{1.2}\text{Mn}_{0.1}\text{Ba}_{0.5}$. After 47 to 68 h of experiment, the stoichiometry changed only slightly yielding always a Fe-dominating colloids $\text{C}_{1000}\text{Fe}_{7.7}\text{Al}_{3.1}\text{Mg}_{2.5}\text{Ca}_{4.5}\text{P}_{2.4}\text{Mn}_{0.2}\text{Ba}_{0.7}$. The molar ratio of C_{org} to Fe in colloids plotted as a function of exposure time allowed distinguishing three main pattern of elementary composition evolution over 93 h of peat leachate reaction with bacteria:

- (i) some adsorption at the beginning of experiment and slow removal of TE relative to DOC (Fe, Ti, V, Th shown in Figs 2.10 A, B, C and 2.11 A)
- (ii) initial adsorption of element relative to DOC followed by gradual release of TE (Mg, Ca, Mn, Co, REE, illustrated for Ca in Fig. 2.11 B)
- (iii) a lack of any significant (> 10%) change of (DOC/TE) in the course of biotic experiment with only initial adsorption of Al (Fig. 2.10 D), Cu (Fig. 2.10 E), U (Fig. 2.11 C) or without adsorption at all (Ni (Fig. 2.11 D), Zr, Pb (not shown)).

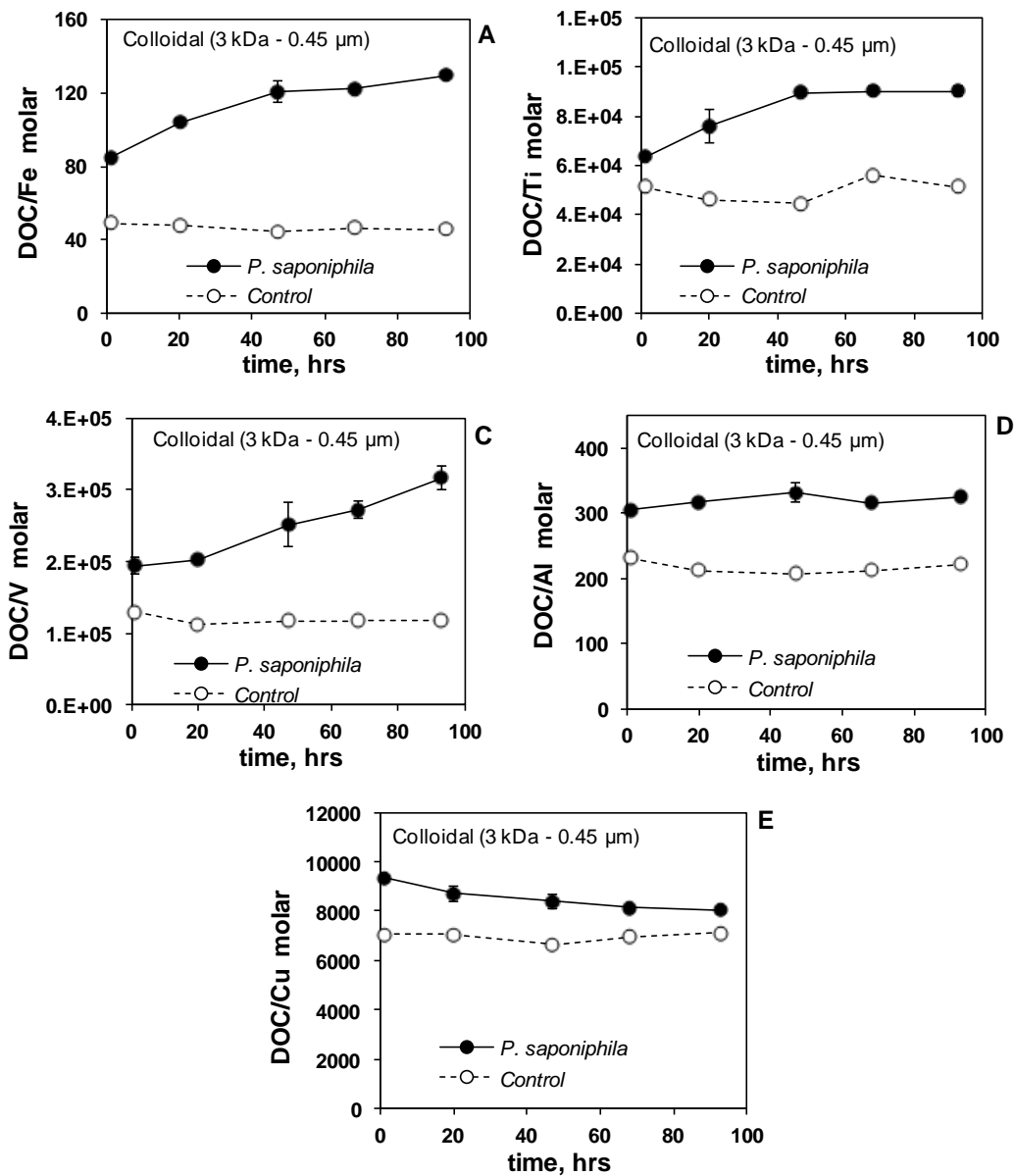


Fig. 2.10. Evolution of DOC/TE ratio in colloids (3 kDa – 0.45 μm) in the course of experiment with *P. saponiphila* (solid circles, solid line) and in control experiment (open circles, dashed line) of sterile peat leachate.

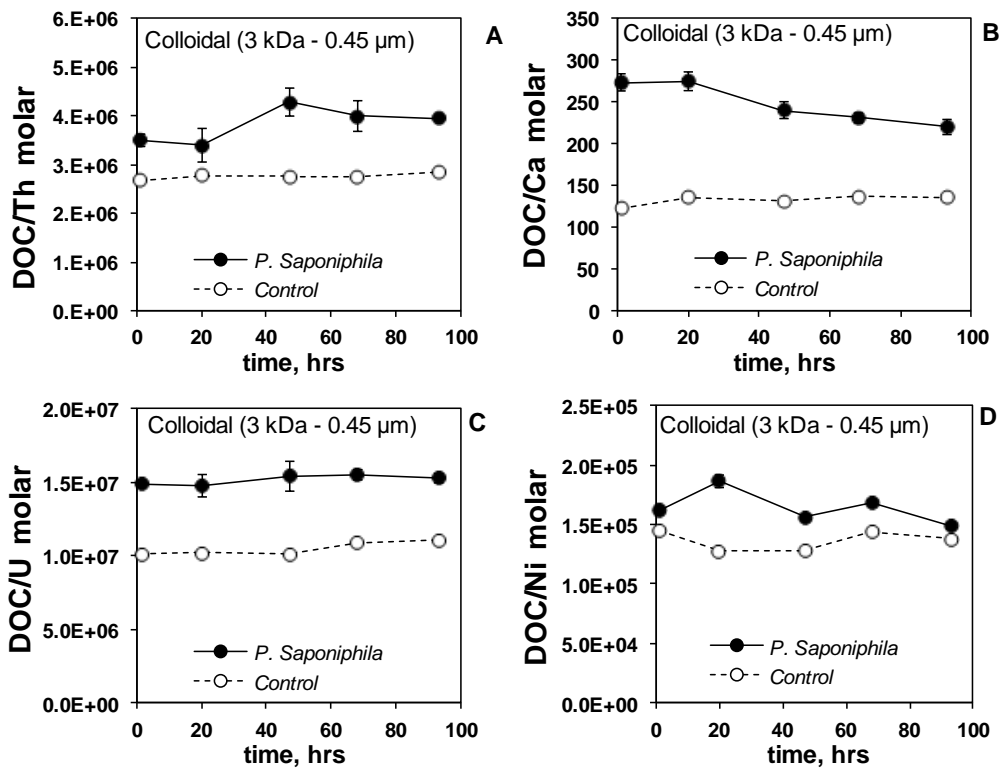


Fig. 2.11. Evolution of molar DOC/TE ratio in colloids (3 kDa – 0.45 μm) in the course of experiment with *P. saponiphila* (solid circles) and control experiment (open circles) of sterile peat leachate for Th (A), Ca (B), U (C) and Ni (D).

Table 2.5. The rate of element concentration decrease in two colloidal (0.45 μm – 50 kDa and 50 kDa – 3 kDa) and “truly dissolved” LMW_{<3 kDa} pools, integrated between 1 and 93 h of experiment. B, Mg, Si, Ca, V, Mn, Cu, Ga, As, Rb, Sr, Y, Mo, Sb, Cs, REEs, Th and U did not show any measurable effect of bacterial presence on long-term stability of their concentrations in peat leachate.

Element	Slow assimilation or coagulation, $\mu\text{g g}_{\text{wet}}^{-1} \text{day}^{-1}$ (1-93 h)		
	0.45 μm - 50 kDa	50 kDa - 3 kDa	< 3 kDa
DOC	no effect	no effect	250 ± 130
Al	no effect	no effect	3.2 ± 1.0
Ti	no effect	0.07 ± 0.01	0.018 ± 0.004
Cr	no effect	no effect	0.018 ± 0.004
Fe	4.4 ± 3.4	64 ± 2	47 ± 3
Co	no effect	no effect	0.02 ± 0.01
Ni	no effect	no effect	0.008 ± 0.005
Zr	no effect	0.004 ± 0.001	0.003 ± 0.001
Nb	no effect	0.0004 ± 0.0001	no effect
Cd	no effect	no effect	0.0007 ± 0.0003
Hf	no effect	0.0001 ± 0.00004	no effect
Pb	no effect	0.011 ± 0.003	no effect

2.5.3. Control experiments of DOC and TE release from the biomass and metal adsorption on cell surfaces

The 1st “stability control” experiment (C1) was designed to test the possibility of abiotic coagulation of peat leachate constituents in response to pH variation in the course of experiment. For this, the sterile, bacteria-free peat leachate was amended with different amount of acid or base, shaken 24 h at 20°C, and sampled for TE and pH measurements. Examples of high stability of leachate component over wide range of pH are given in **Fig. 2.12 A-F** for DOC, Ti, Cr, Ce and U. The results of this test indicated that even several unit variation of peat water pH cannot appreciably coagulate TE or remove them via adsorption on the walls of reactor.

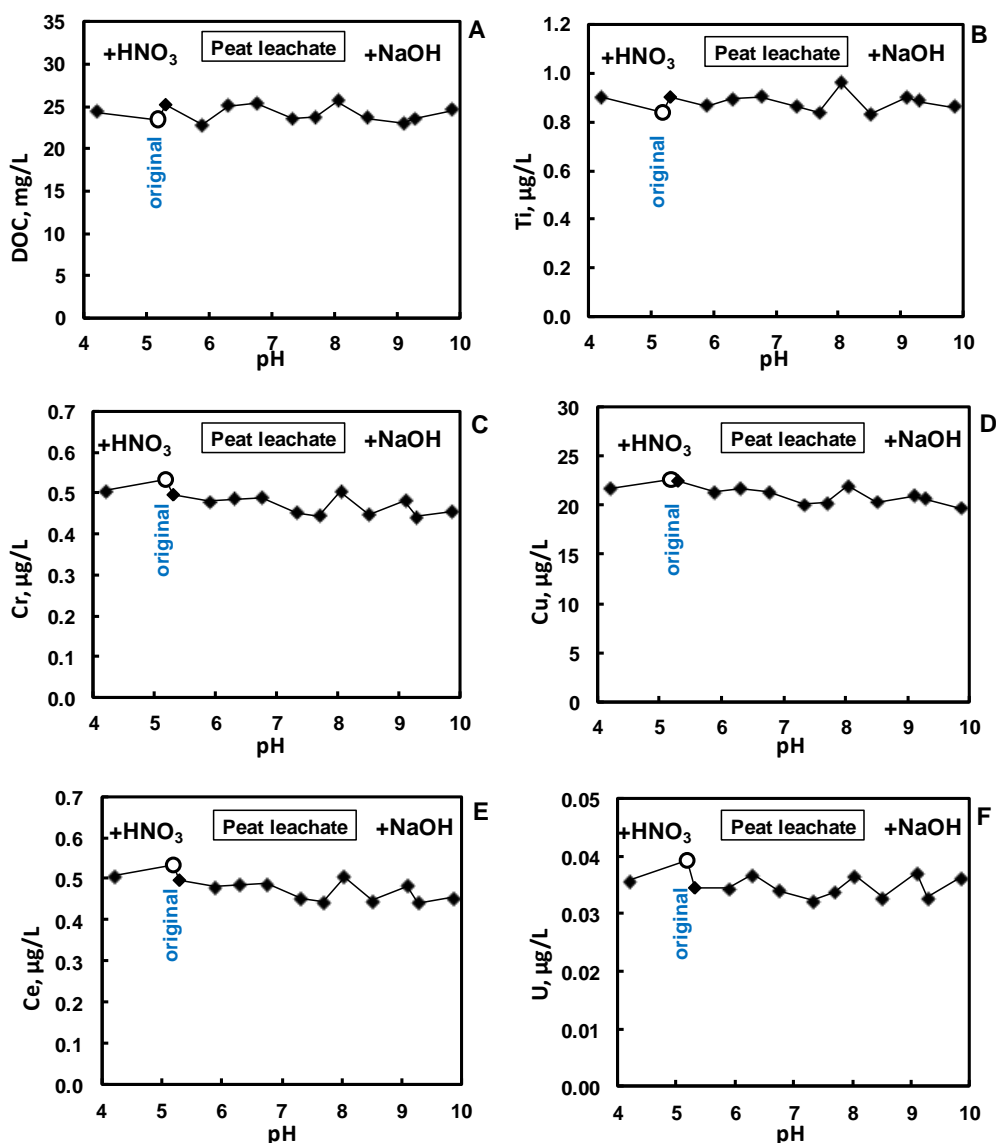


Fig. 2.12. C1 control experiment: the test of stability of peat leachate to the coagulation as a function of pH (0.45 µm fraction, bacteria-free). The open symbol represents the metal concentration in the initial peat leachate before the addition of acid or base.

Because several biologically-important elements can be released from viable cells over their life cycle, the 2nd “release control” experiment (C2) with 1 g_{wet}/L biomass of *P. saponiphila* in the distilled water was run at pH = 5.65±0.05, as a function of time between 1 and 100 hrs. Examples of temporal pattern of DOC and several TEs are presented in **Fig. 2.13**. The release of most TE (B, Al, Si, Ti, V, Mn, Fe, Co, Ni, Cu, Ga, Ge, As, Rb, Y, Zr, Nb, Cd, Sb, Cs, REEs, Hf, W, Pb, Th and U) in C2 experiment was very weak and did not exceed 10% of the magnitude of their concentration change in bacteria + peat leachate experiment. Therefore, the transformation of these elements in peat leachate by *P. saponiphila* can be studied without interferences of the desorption/efflux from live cells. However, P, K, Zn, Mo, Sr, Ba and Cr were released from live cells in the amount that exceeded or was comparable with the magnitude of their concentration change during bacterial-peat leachate experiments. Therefore, the behavior of < 0.45 µm fraction of these elements in biotic experiments with peat leachate could not be interpreted.

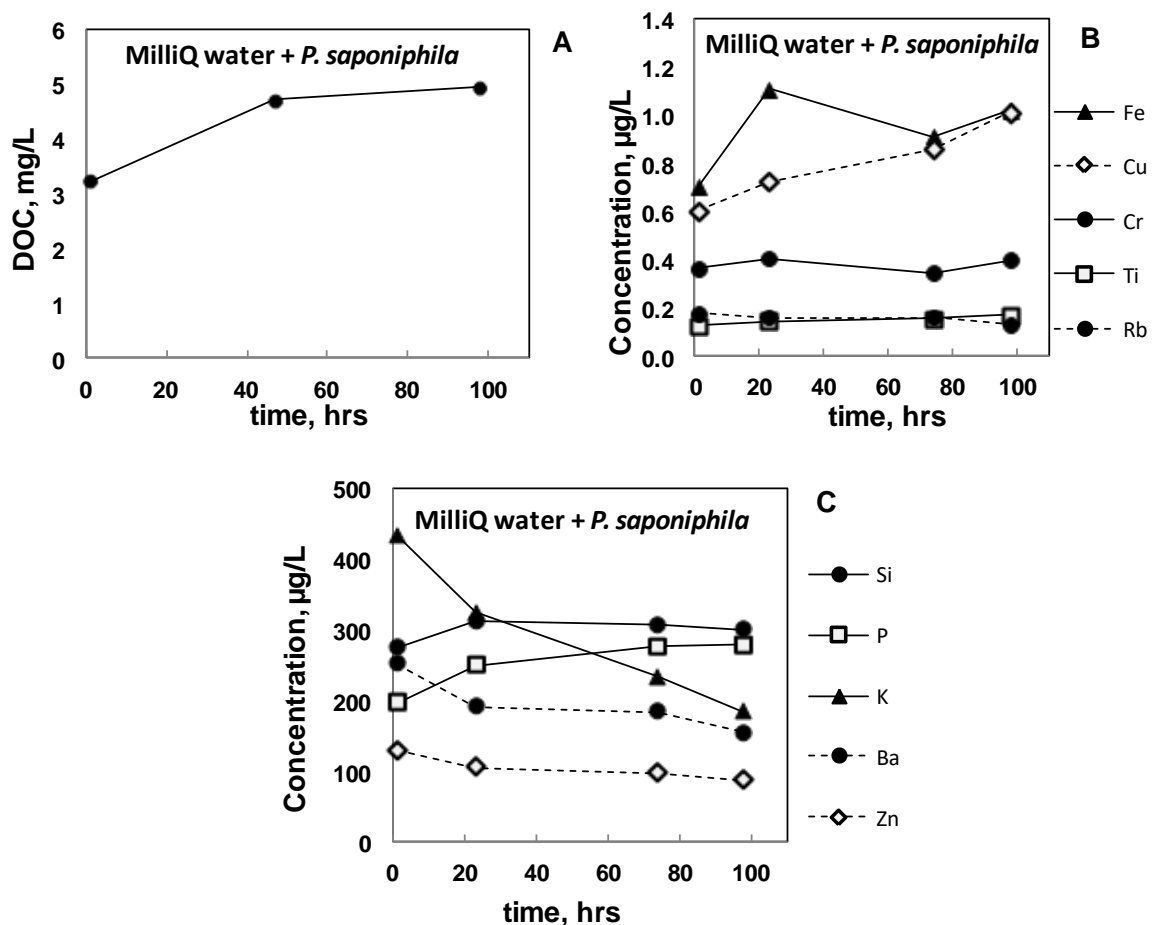


Fig. 2.13. C2 control experiment: the DOC (A), metals (B) and nutrients (C) release from *P. saponiphila* suspension (1 g_{wet} L⁻¹) in MilliQ water at pH = 5.6 to 5.7.

The kinetics of adsorption of peat leachate components on *P. saponiphila* wet biomass over 0-180 min was studied at $\text{pH} = 5.55 \pm 0.05$, in the 3rd series of control experiments (C3). During the first 10 minutes, $30 \pm 20\%$ of Al, Fe, Cu, Sr, Y, REEs, Th and U was removed, followed by quite stable concentration of an element as illustrated for Al, Fe, Cu and Ni in **Fig 2.14 A, B, C and D**, respectively. The initial adsorption was also clearly pronounced for Y, La, Th and U (**Fig. 2.15 A-D**). All other elements including DOC did not exhibit any short-term adsorption and the change of their concentration in these control experiments was typically $5 \pm 5\%$.

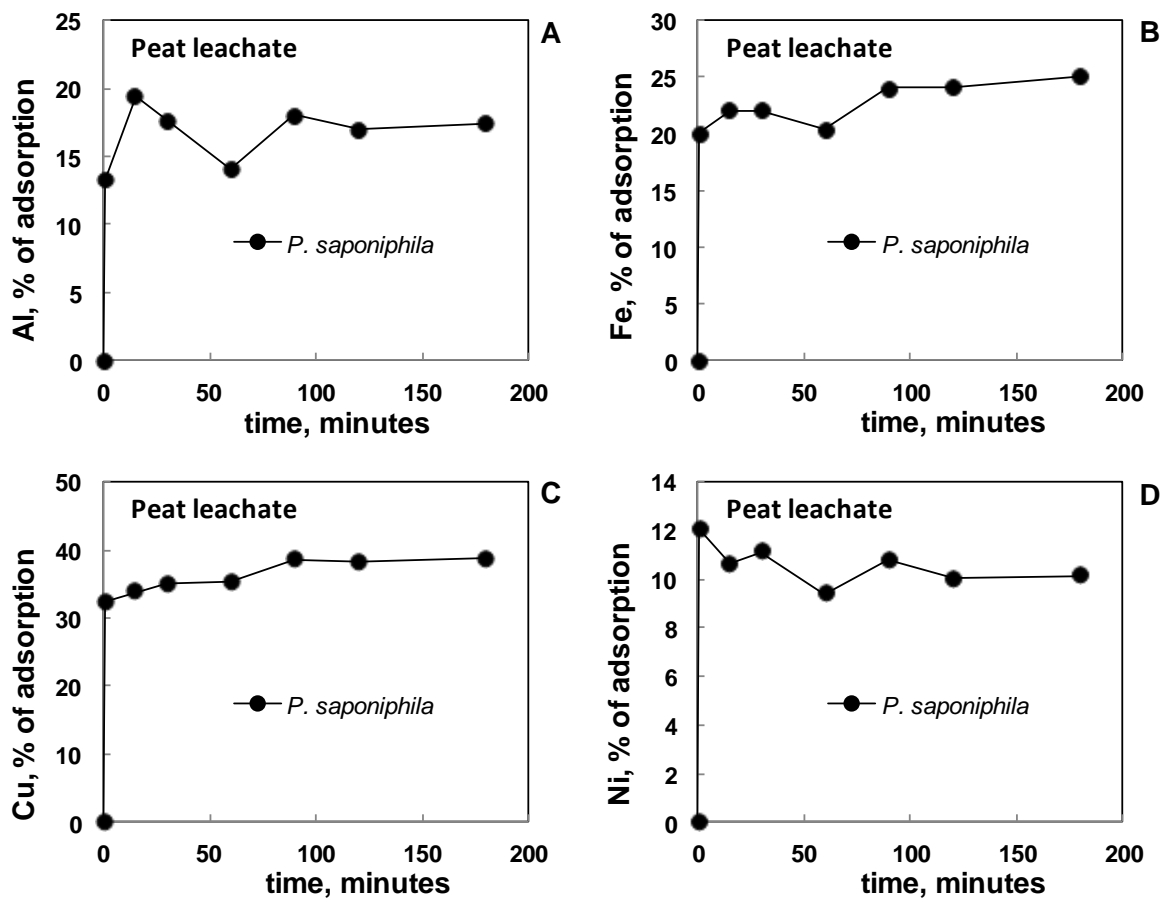


Fig. 2.14. Kinetics of peat constituents adsorption on *P. saponiphila* over 3 h of reaction represented by % of adsorbed Al (A), Fe (B), Cu (C) and Ni (D), as a function of time.

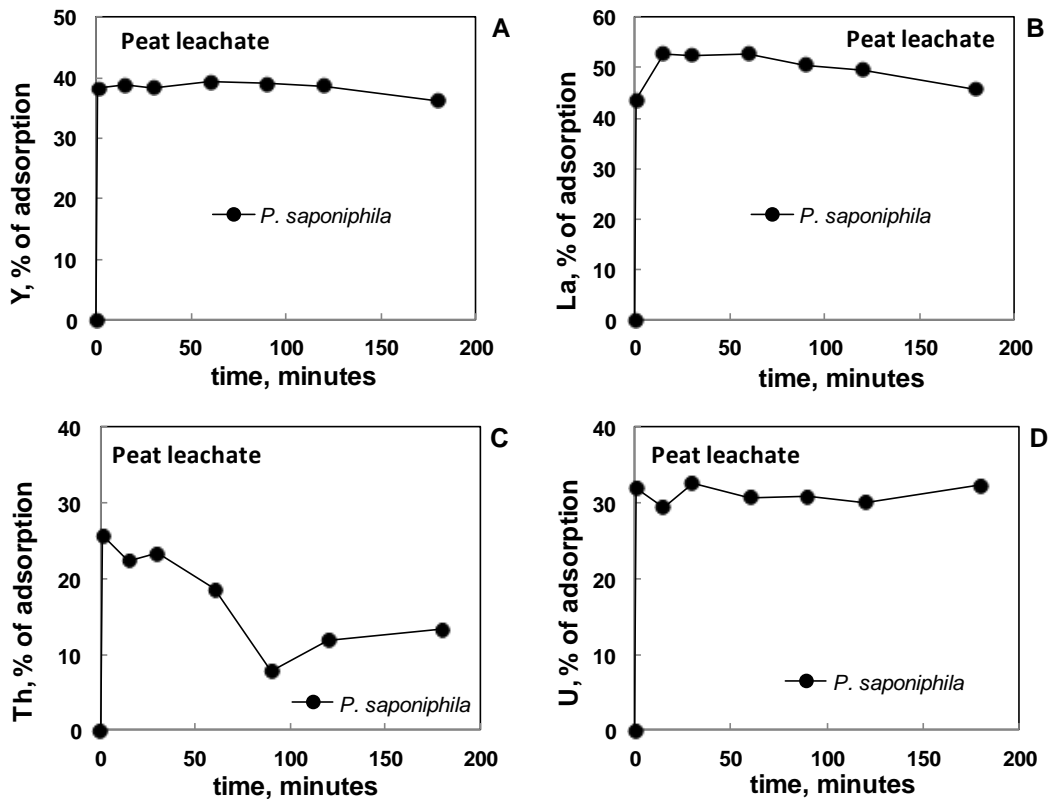


Fig 2.15. C3 control experiment: the kinetics of peat constituents adsorption on *P. saponiphila* after 3 h of reaction: Y (A), La (B), Th (C) and U (D).

In 4th series of control experiments (C4), the short-term adsorption of 0.45 μm -peat leachate components on 1 g_{wet}/L of live biomass *P. saponiphila* was studied as a function of pH. The [DOC] remained quite stable at $4 < \text{pH} < 7$ and it increased two-fold at $\text{pH} > 10$ (**Fig. 2.16 A**). Al and Fe demonstrated a decrease of concentration above pH 5.6 followed by an increase at $\text{pH} > 7$ (**Fig. 2.16 B, C**, respectively). V exhibited similar behavior (**Fig. 2.17 A**) whereas divalent metals like Ni, Mn, Cu, Cd demonstrated clear adsorption on the cell surface above pH 6 as their concentrations strongly decreased in alkaline relative to neutral aqueous solutions (**Figs. 2.16 D**, and **Fig. 2.17 B, C, D**, respectively). The concentrations of many other trace elements (Si, Cr, As, Y, Zr, Nb, Hf, Pb, U) were not significantly sensitive to the pH change between 4 and 9 (not shown). These experiments allowed evaluation of the effect of pH change during biotic experiment (**Fig. 2.2 C**) on short-term element adsorption: in most cases, these effects were within the experimental reproducibility or $\leq 10\%$. We therefore conclude that the observed TE concentration change in biotic experiment had minimal number of artifacts and essentially reflected dissolved metal and colloid interaction with live bacterial cells.

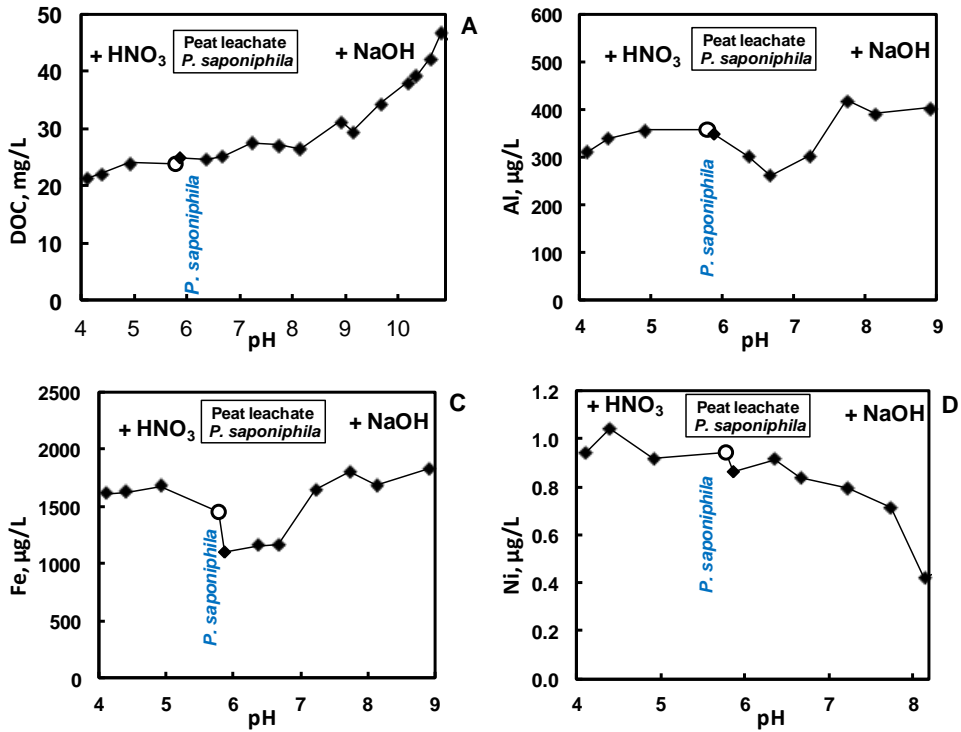


Fig. 2.16. Adsorption of peat leachate constituents onto *P. saponiphila* biomass as a function of pH, reflected by a decrease of aqueous concentration of metal in the presence of bacteria (control C4). The concentration of element in the presence of bacteria before acid or base addition is shown by open circle. The increase of DOC concentration in alkaline solutions (A) is due to leaching of soluble cell constituents. Experimental conditions: 1 g_{wet}/L of biomass, 1 h of exposure, 20°C.

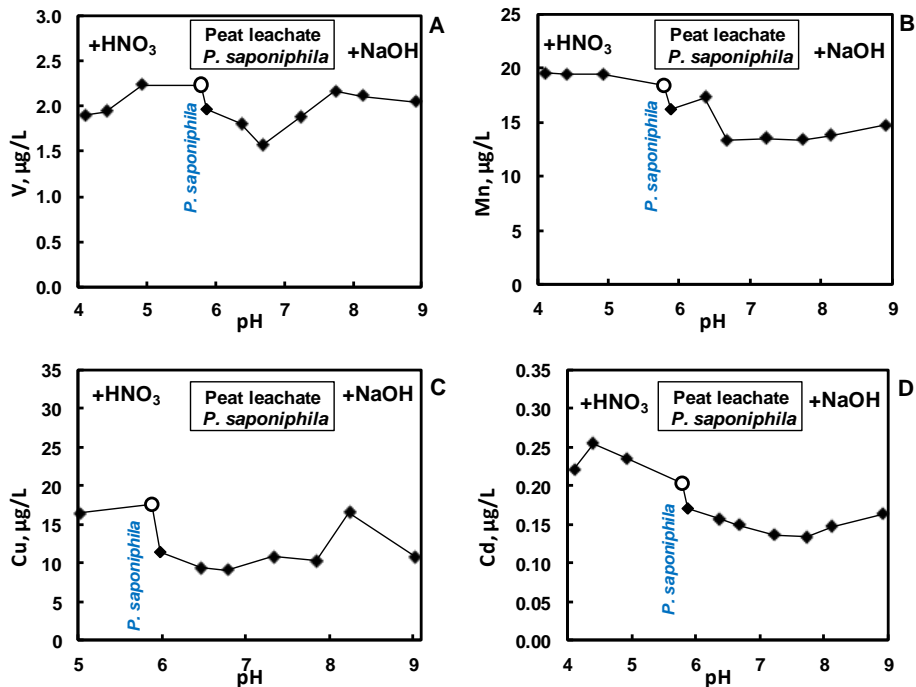


Fig. 2.17. C4 control experiment: the adsorption of peat leachate constituents onto *P. saponiphila* biomass as a function of pH. V (A), Mn (B), Cu (C) and Cd (D).

2.6. Discussion

2.6.1. General features of DOC and TE biodegradability and adsorption on cell surfaces.

The experimental reproducibility was quite high for all three size fraction of peat leachate, which allowed tracing the evolution of element concentration in the course of experiment. The observed changes of element concentration could be interpreted in terms of main physico-chemical and metabolic processes that occur in the aqueous solution – organic colloids – bacteria system.

The first unexpected result of this work was quite low bio-degradability of DOC over 4 days of experiment. The $5\pm0.5\%$ of initial DOC removal in $0.45\text{ }\mu\text{m}$ fraction (or 1 to $1.5\text{ mg/g}_{\text{wet}}$ bacteria) over 93 h is significantly smaller than 10 to 30 $\text{mg DOC/g}_{\text{wet}}$ over 10 days reported in previous experiments with soil and groundwater bacteria and Siberian permafrost peat and moss leachate (i.e., Shirokova et al., 2017). Moreover, the majority of $\text{DOC}_{<0.45\text{ }\mu\text{m}}$ was removed over the first hour of adsorption reaction rather than consumed by bacterial activity during subsequent 4 days. Presumably, the difference in the nature of peat from Siberian permafrost and permafrost-free boreal region of NW Russia as well as different metabolic activity of *P. saponiphila* of this study and *P. aureofaciens* / *P. reactans* used in our previous work, may be responsible for this contrasting behavior in the course of biodegradation.

In accord with former studies on metal adsorption onto heterotrophic bacteria (Pokrovsky et al., 2012a, 2013b; Gonzalez et al., 2014; Shirokova et al., 2017), we postulated that a significant ($p < 0.05$) difference between the control and the bacterial experiment after 1 h of exposure corresponded to initial adsorption of trace element onto the cell surface. A gradual and slow decrease of element concentration after first 12 h of reaction was interpreted as either intracellular incorporation (assimilation) or extracellular removal via colloid coagulation and metal oxyhydroxide formation. Note that a long-term ($> 1\text{ h}$) incorporation of metals inside the cells, so called “internalization flux” frequently occurs for non-growing but viable bacteria (i.e., Smiejan et al., 2003). The quantification of long-term carbon or metal removal in the biotic system required that *i*) the concentration of these components in the control remained constant within at least $\pm10\%$ of the initial value and *ii*) the difference between two consecutive sampling was statistically greater (at $p < 0.05$) than the

variation between the replicates. Note however that in most cases we could not distinguish between long-term intracellular incorporation and physical coagulation/precipitation of metals, because both process leading to slow removal of TE from solution.

In contrast to rather stable DOC pattern, there was a clear decrease of many TE concentration over 4 days of bacterial activity. This decrease could be linked to liberation by heterotrophic bacteria of the elements that were bound to organic colloids, thus leading to coagulation of metal hydroxides and a decrease of the concentration of dissolved ($< 0.45 \mu\text{m}$) metal. In particular, this could involve the Fe hydroxide coagulation and precipitation linked to bacterial degradation of organic matter that stabilized large Al and Fe hydroxide colloids in the initial peat leachate. The removal of aqueous Fe via formation of insoluble Fe hydroxide precipitates on bacterial surfaces in the form of Fe coating has been recently evidenced in the experiments with *Caulobacter*-dominated bacterial communities grown on Fe- and nutrient-enriched humic boreal water (Xiao et al., 2016). The elements that could be affected by hydroxide removal were trivalent and tetravalent hydrolysates such as Ga, Y, REEs, Ti, Zr, Hf and Th. These elements are known to be associated with colloidal Fe oxyhydroxides in boreal waters of NW Russia (cf. Vasyukova et al., 2010; Ilina et al., 2016). The differential removal of DOC and metals is evidenced from the plot of DOC to TE ratio in the colloidal fraction (3 kDa – $0.45 \mu\text{m}$) for the elements clearly increasing this ratio in the course of the experiment relative to control (Fe, Ti, V, Th, **Fig. 2.10**).

Fast adsorption of TE onto bacterial surfaces was observed during the first hour of bacterial biomass addition to peat leachate, and it affected mostly Al, Ti, V, Fe, Mn, Co, Ni, Cu, Ga, Y, Cd, REEs, Th and U. This observation is consistent with results of permafrost peat leachate interaction with soil and groundwater heterotrophic bacteria (*P. aureofaciens* and *P. reactans*, respectively, Shirokova et al., 2017). Presumably, the pH-dependent adsorption edge of divalent metal (Mn, Co, Ni, Cu, Cd) on the bacterial surface (i.e., Fein et al., 1997, 2001; Gonzalez et al., 2010; Pokrovsky et al., 2012a) coincides with the range of pH values in the biodegradation experiments.

Many other elements present essentially in the form of organic and organo-ferric colloids demonstrated significant adsorption of both $\text{LMW}_{3 \text{ kDa} - 50 \text{ kDa}}$ and $\text{HMW}_{50 \text{ kDa} - 0.45 \mu\text{m}}$ colloidal fractions (Al, Ti, Fe, Cu, REEs, U). According to vMinteq calculation, these elements are fully complexed with DOM in the peat leachate. A

pronounced adsorption of DOM colloids on negatively-charged surfaces of *Pseudomonas* strain (e.g., Gonzalez et al., 2010) implies positive charge of organo-ferric colloids. These colloids may have Fe oxy(hydr)oxides as main surface moieties, dominated by $>\text{FeOH}_2^+$ groups at pH < 6 (Stumm, 1992). Such an affinity of colloidal form of trace metals to the surfaces of heterotrophic bacteria is rather unexpected result. It suggests potentially high reactivity of colloidal trace metals to other negatively-charged organic surfaces present in soil and river system such as plant litter, peryphytic biofilm or submerged vegetation and requires further experimental assessment.

Finally, elements which are not associated with DOM but also do not adsorb because of their weak interaction with cell surfaces include anions and neutral molecules, such as B, Si, Mo, As, and Sb. Although some of these elements may potentially be beneficial for bacterial metabolism (e.g., B, V, Mo), their concentrations are likely not limited for heterotrophic bacterium under experimental conditions of this study.

2.6.2. Response of organo-ferric colloids to the presence of bacterial cells

A schematic cartoon of peat colloid transformation in the presence of *P. saponiphila* is shown in **Fig. 2.18**. The low molecular weight fraction of OC (< 3 kDa) was found to be most susceptible to biodegradation over 93 h of exposure as the decrease of $\text{OC}_{< 3 \text{ kDa}}$ concentration in the biotic experiment relative to the control was a factor of 1.5 higher than that for < 0.45 μm and < 50 kDa fractions. This is consistent with generally higher bioavailability of LMW fraction of DOC because the LMW carbon compounds of terrestrial origin are known to be highly beneficial for bacterial growth in boreal lakes (i.e., Berggren et al., 2010; Roehm et al., 2009) as well as in organic-rich permafrost soil leachates (Ward and Cory, 2015; Drake et al., 2015). The lower molecular weight species were more susceptible to biological degradation in a temperate stream than higher molecular weight species (Sleighter et al., 2014). It is therefore expected that the LMW fraction of C_{org} is more bioavailable and susceptible to microbial transformation than the high molecular weight colloids (50 kDa – 0.45 μm). This hypothesis is based on the similarity of pore sizes and transport channels of live cells (10–30 Å in bacteria, 35–50 Å in plant cells, Carpita et al., 1979; Trias et al., 1992) and the minimal conventional pore sizes used in colloid separation (1 to 3 kDa, 1.5–2 nm, Guo and Santchi, 2007), and it is also consistent with results of

microbial processing of natural colloids from different terrestrial and aquatic sources (cf., Roehm et al., 2009; Yang et al., 2016). In this study, the $15.8 \pm 0.3\%$ of initial $\text{OC}_{< 3 \text{ kDa}}$ was consumed after 93 h of reaction corresponding to the rate of biodegradation of $0.4 \text{ mg L}^{-1} \text{ g}_{\text{wet}}^{-1} \text{ d}^{-1}$. This rate, however, cannot be extrapolated to natural environment, because *i*) the concentration of heterotrophic bacteria in the experiments is about 2 orders of magnitude higher than that in the field, and *ii*) we could not confirm or dismiss a linear response of the DOC consumption rate to the biomass concentration. However, at chosen experimental conditions the half life time of peat carbon $\text{LMW}_{< 3 \text{ kDa}}$ is equal to 21 ± 11 days, which is comparable with water residence time in peat-affected humic lakes of the study site (from first days to first weeks, Ilina et al., 2014). The half-life time of $\text{LMW}_{< 3 \text{ kDa}}$ fraction of metals affected by long-term removal (Al, Ti, Cr, Fe, Co, Ni, Zr, Cd) ranges from several days to several weeks (**Table 2.4**) and thus also suggests high reactivity of this fraction in natural settings. In contrast, HMW colloidal fraction is weakly affected by the presence of bacteria and may persist over the open water period in boreal aquatic environments.

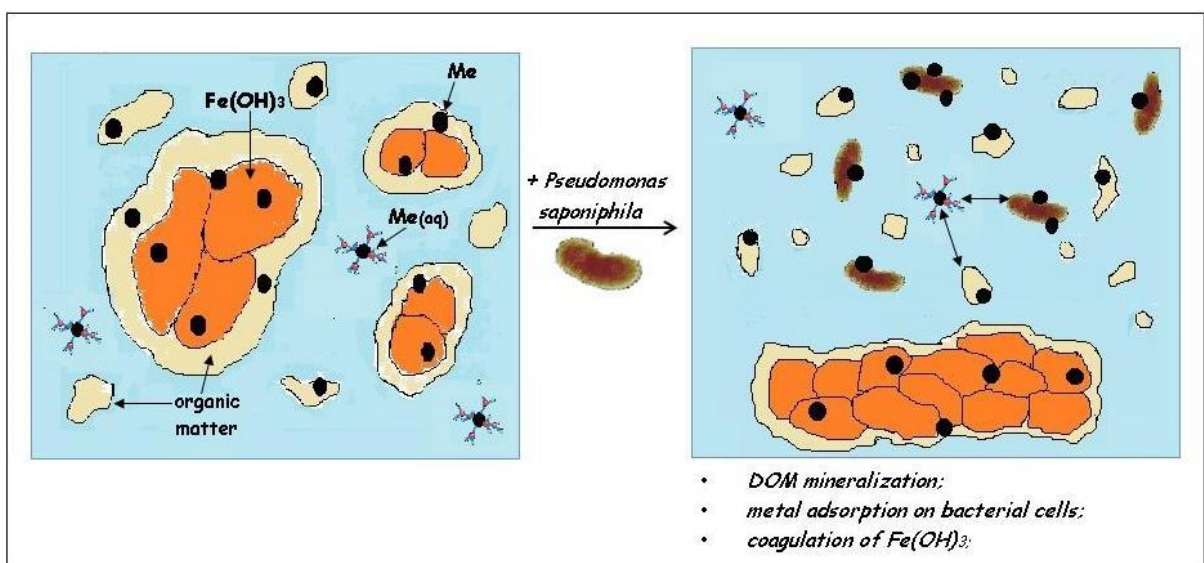


Fig. 2.18. A cartoon of peat colloid transformation in the presence of live *P. saponiphila* and dissolved ($< 0.45 \mu\text{m}$) metals (Me(aq)) interaction with bacteria. Bacterial activity preferentially removes Fe over DOC from organo-mineral colloids; trace metals coprecipitate with coagulating Fe oxy(hydr)oxide. The heterotrophic bacterium processes colloids ($3 \text{ kDa} - 0.45 \mu\text{m}$) from peat leachate essentially via short-term adsorption on cell surface (Al, Mn, Ni, Cu, Ga, Y, REE, U) and extracellular coagulation in the form of Fe hydroxides (Ti, Zr, Nb).

The speciation calculation using vMinteq demonstrated that all trivalent and tetravalent hydrolysates and U^{VI} are fully complexed with DOM. Alkaline earth

elements (Ca, Mg, Sr, Ba), Mn and Zn are complexed by 85-90% to fulvic acids, whereas Ni, Cu, Cd and Pb are present as organic complexes with only 0-5% of metal in the ionic form. The 0.45 μm fraction was supersaturated with respect to soil aluminum hydroxide ($\Omega = 2.3$), gibbsite ($\Omega = 8.0$) and kaolinite ($\Omega = 7.3$) and strongly under saturated ($\Omega < 0.1$) with respect to Fe hydroxides. The $\text{LMW}_{< 3 \text{ kDa}}$ fraction was also strongly undersaturated with respect to Fe hydroxides and twice less saturated with respect to Al phases compared to $< 0.45 \mu\text{m}$ fraction. Therefore, the removal of Fe in the form of particulate Fe hydroxide could be only due to liberation of part of Fe from organic complexes after bacterial degradation of colloidal DOM that stabilized Fe(III) polymers in solutions. Unfortunately, straightforward confirmation of Fe hydroxide formation was not possible without microscopic/spectroscopic analyses of the cell biomass and inorganic precipitates at the end of experiment.

In the course of biotic experiments, we observed a preferential depletion of solution in colloidal Fe and an enrichment in colloidal Al because the ratio $(\text{Fe}/\text{Al})_{\text{molar}}$ in the 1 kDa – 0.45 μm fraction decreased from 3.6 ± 0.1 after 1 h of reaction to 2.5 ± 0.1 after 93 h. This suggests higher reactivity of Fe component of colloids compared to Al one. At first glance, this contradicts to the fact that the 0.45 μm fraction was supersaturated with respect to Al-bearing phases but undersaturated with respect to Fe oxy(hydr)oxides. However, the ratio of adsorbed to accumulated/coagulated metal in $< 0.45 \mu\text{m}$ fraction was a factor of 4 higher for Al relative to Fe. Thus, significant amount of Al was removed at the very beginning of peat leachate interaction with bacterial suspension, and further transformation of colloids was mainly due to Fe (III) removal.

To the best of our knowledge, no quantitative information on colloidal size fractionation of TE in the presence of heterotrophic bacteria is available in the literature. The results of the present study demonstrate that only a few trace metals present in the form of organic and organo-ferric colloids changed their conventionally dissolved ($< 0.45 \mu\text{m}$) concentration in the presence of live *P. saponiphila*. The metals most affected by long-term removal rather than fast adsorption on the cells surfaces are Cr, Fe, Al, Ti, and Zr. These elements also demonstrate a weak ($\leq 10\%$) but statistically significant ($p < 0.05$) net impoverishment in the $\text{LMW}_{< 3 \text{ kDa}}$ “truly” dissolved fraction and the enrichment in the $\text{LMW}_{50 \text{ kDa} - 3 \text{ kDa}}$ and $\text{HMW}_{0.45 \mu\text{m} - 50 \text{ kDa}}$ colloidal fractions (see **Fig. 2.7**).

In the course of bacterial experiment, the pH of peat leachate increased by ca. 0.5 units from 1st hour to 93 h of reaction (**Fig. 2.2 C**). Such an increase is not negligible and it is capable to increase the proportion of colloidal forms of C_{org}, Al, Fe, Ni, Y, REE and U as reported in the laboratory study of colloidal fractionation in Fe- and organic-rich boreal surface waters as a function of pH (Vasyukova et al., 2012). This early observation is fully consistent with the results of the present study. Presumably, the bacteria induce the coagulation of truly dissolved organic forms into colloids of higher molecular weight which finally are transformed into particles subjected to precipitation (**Fig. 2.18**). This scheme is in accord with general understanding of bacterially-controlled colloid transformation in surface waters (Tranvik, 1998a; Berggren et al., 2010; Amon and Benner, 1996) as a main driver of autochthonous change of DOC and TE speciation in boreal lakes and rivers (Pokrovsky et al., 2013a; Shirokova et al., 2013b; Ilina et al., 2014). Although the colloidal coagulation deduced from the increase in the molecular size of DOC and related metals observed in our experiments does not exceed 10% of the initial concentration of peat leachate constituents, the rates of transformation of conventionally dissolved <0.45 µm fraction (DOC, 140 µg g_{wet}⁻¹ day⁻¹; Fe, 116 µg g_{wet}⁻¹ day⁻¹) are high enough and suggest that biodegradation is capable removing 50% of initial DOC and > 99% of initial Fe over 3 summer months of open water period in the subarctic zone.

2.6.3. Consequences for biogeochemistry of carbon and trace metals in peat-drained boreal waters

The heterotrophic bacterioplankton is known to efficiently mineralize allochthonous DOM in organic-rich waters (Tranvik, 1998a, b; Tranvik and Jorgensen, 1995; Kritzberg et al., 2004; Jansson et al., 2000, 2007; Ask et al., 2008). In boreal rivers and lakes approximately 10% of DOC can be consumed by heterotrophic bacteria on the time scale of 5 to 14 days (Berggren et al., 2007, 2010), whereas between 4 and 46% of DOC in Alaskan Arctic streams was biodegradable over 40 days (Larouche et al., 2015). Note similar order of magnitude of the degree of DOC removal in the bacterial experiments with *P. saponiphila* monoculture conducted in this study (5±0.5 %). Typical values of bacterial respiration in surface continental waters are on the order of 0.1 mg C L⁻¹ day⁻¹ (Berggren et al., 2007) although the value as high as 8.6 mg C L⁻¹ day⁻¹ was reported for a temperate creek. Heterotrophic

bacteria from the European permafrost zone consumed lake water DOC over first 48 h with a rate of $0.09 \text{ mg L}^{-1} \text{ d}^{-1}$, whereas the DOC consumption from adjacent peat soil was five times higher (Roehm et al., 2009). Humic lakes of Siberian thermokarst zone located entirely within frozen peat substrate exhibited bacterial mineralization rate of 0.3 to $0.4 \text{ mg C L}^{-1} \text{ day}^{-1}$ (Shirokova et al., 2013a). Over 4 days of exposure in this study, the DOC concentration decreased at a rate of $0.14 \pm 0.04 \text{ mg C L}^{-1} \text{ day}^{-1}$, in fair agreement with natural observations. Moreover, the half-life time of elements affected by long-term removal in the presence of *P. saponiphila* (1 week to 1 month, Table 3) is comparable with water residence time in small organic-rich surface water bodies of N. Karelia (Ilina et al., 2014, 2016) and other boreal regions (Ågren et al., 2014; Manasypov et al., 2015).

These similarities are remarkable given *i*) 2 order of magnitude higher bacterioplankton concentrations in the experiments compared to natural sites and *ii*) the fresh, undecomposed nature of the organic substrate from experimental peat leachate compared to more refractory DOM which was already bio-and photo-processed DOM in streams and lakes. At these conditions, one would expect much stronger biodegradation in the experimental solutions compared to natural settings. Two reasons may be responsible for observed inconsistency between the relatively low biodegradation of DOC and high bacteria concentration in our experiments. First, it is possible that the strain of *P. saponiphila* extracted from a boreal stream is not capable efficiently decompose dissolved organic matter released from the peat. Thus, *Caulobacter*, not Gammaproteobacteria, dominated bacterial communities grown on P and Fe-enriched humic lake water (Xiao et al., 2016). Second, the peat leachate may not contain sufficient amount of biologically-labile substances. For example, dissolved P and N limitation is known for boreal lake plankton (Arvola et al., 1996; Vidal et al., 2011; Chupakov et al., 2017). Note here that the soil and peat DOM is generally much less biodegradable than the aquagenic DOM (Nguyen and Hur, 2011), although the degradation in the water column is known to preferentially remove the oxidized, aromatic compounds, whereas the aliphatic and N-containing compounds are either resistant to degradation or tightly cycled and thus persist in aquatic systems (Kellerman et al., 2015).

With the acceleration of heterotrophic bacterial activity in boreal and subarctic waters, linked to rising the temperature (Porcal et al., 2013) and the increase of the availability of organic substrates (Drake et al., 2015), the chemical composition of

surface waters affected by peat leaching will be subjected to transformation by bacterial processes. The colloidal restructuring may include the decrease of the proportion of LMW_{< 3 kDa} fraction and the increase of HMW colloids. The interaction of *P. saponiphila* with peat leachate yielded progressive enrichment of colloids in OC relative to Fe. At the end of experiment, this enrichment achieved a factor of 3 relative to the bacteria-free control of peat leachate (**Fig. 2.10 A**), together with the increase of the proportion of HMW Fe colloids (**Fig. 2.7 D**). Such an increase strongly suggests the removal of Fe via preferential adsorption of Fe-rich colloidal components on bacterial surfaces, intracellular uptake, and/or coagulation in the form of hydroxide. These processes are consistent with natural observations that the heterotrophic respiration of allochthonous OM should lead to coagulation and sedimentation of OM-poor, Fe-rich particles in lakes of both permafrost (Audry et al., 2011; Shirokova et al., 2013a) and non-permafrost peatlands (Shirokova et al., 2013b).

In this regard, heterotrophic mineralization of organo-ferric colloids by *P. saponiphila* and, presumably, by other heterotrophic bacteria, may alleviate some consequences of ongoing climate change in boreal and temperate surface waters. Thus, due to rising the water and soil temperature, both DOC and Fe concentrations are reported to increase causing so-called “browning” of surface waters (Kritzberg and Ekstrom, 2012; Porcal et al., 2013; Weyhenmeyer et al., 2014). In peatland-affected boreal and permafrost waters, Fe concentration rise is expected to be strongly pronounced (Sarkkola et al., 2013; Pokrovsky et al., 2016b). Preferential removal of colloidal and conventionally dissolved Fe over C_{org} by heterotrophic bacterioplankton discovered in this study may compensate this possible rise, given that the heterotrophic metabolism accelerates with temperature (cf., Cabaniss et al., 2005).

2.7. Conclusions

Experimental study of the impact of heterotrophic bacteria *Pseudomonas saponiphila* on colloidal size distribution of organic carbon and trace metal in peat leachate allowed distinguishing adsorption and assimilation/coagulation of trace elements. The colloidal composition of peat leachate was dominated by Fe which was 4 times more abundant than Al and 1-2 orders of magnitude higher than other trace elements. Low molecular weight fraction of DOC (< 3 kDa) was preferentially processed by live bacteria as its concentration decreased by $15.8 \pm 0.3\%$ over 4 days of exposure. Fe was strongly affected by bacterial activity demonstrating a 40% increase of DOC/Fe ratio in the colloidal fraction over 4 days of experiment. V, Ti and Th followed the behavior of Fe demonstrating a gradual removal over time. In contrast, divalent metals micronutrients (Mn, Ni, Cu) and toxicants (Cd, Pb) demonstrated only adsorption on bacterial surfaces over first hour of reaction with minimal long-term impact by cell metabolism.

A short-term (3 h) adsorption of peat leachate constituents on *P. saponiphila* biomass revealed that $30 \pm 20\%$ of Al, Fe, Cu, Sr, Y, REEs, Th and U adsorb over first 10 h whereas DOC and all other TE did not adsorb (< 5-10% of the initial amount). In response to pH rise from 5 to 7 due to microbial metabolism, Al, V, Mn, Fe, Ni, Cu, Cd decreased their concentration by ca. 30-60% suggesting some adsorption of colloidal metals. Overall, short term adsorption on the cell surfaces turned out to be more important than the slow intracellular uptake or physical removal as coagulation/coprecipitation. Only a few low-soluble element bound to colloids (Al, Ti, Fe, Zr, Nb, Hf, Pb, and Th) were affected by long-term removal, presumably via coprecipitation with coagulated Fe oxy(hydr)oxides. A small (< 10%) but statistically significant partitioning of DOC and TE between various size fraction consisted in 5 to 10% shift from “truly dissolved” LMW_{< 3 kDa} fraction to LMW_{50 kDa–3 kDa} and HMW_{0.45 μm–50 kDa} colloidal pools.

The rate of DOC mineralization in the experiment ($0.14 \pm 0.04 \text{ mg C L}^{-1} \text{ day}^{-1}$) was comparable with that reported in natural peatland waters, despite that the experimental concentration of live bacteria was 2 orders of magnitude higher than the natural one. However, the half-life time of colloidal metals in the presence of *P. saponiphila* was comparable with water residence time in boreal organic-rich surface waters. Preferential removal of Fe over DOC from dissolved+colloidal fraction by

heterotrophic bacterial metabolism can be a possible mechanism against the “browning” of boreal waters occurring in response to water and soil warming.

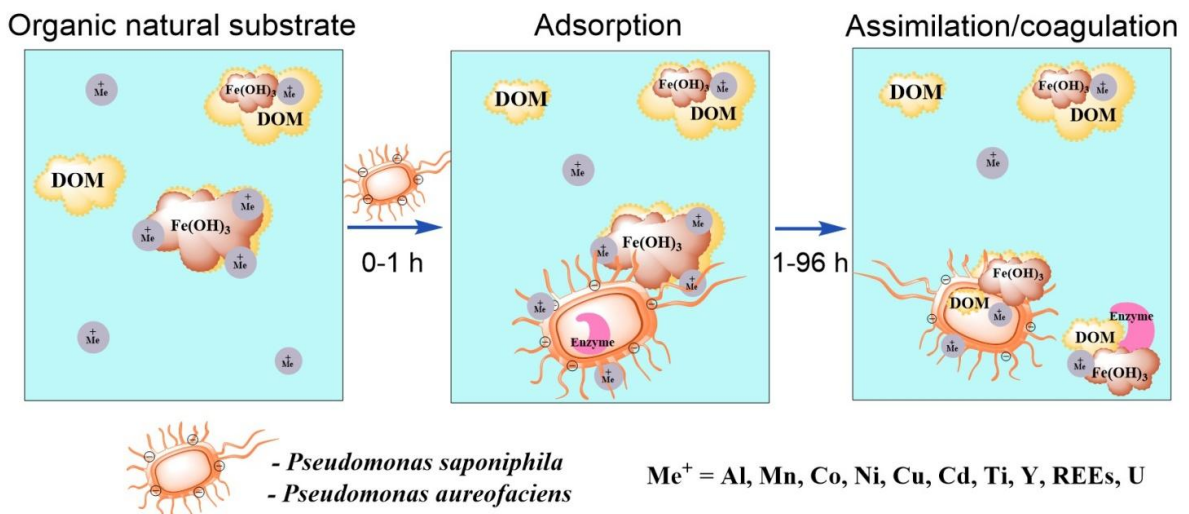
2.8. Acknowledgements

We acknowledge the main support from RSCF (RNF) grant No 15-17-10009 “Evolution of thermokarst lake ecosystems” (experiments, analysis) and RFBR grants №№ 14-05-00430, 15-05-05000, 16-55-150002 (field sampling). Additional support was from RSF № 14-50-00029 (bacterial separation, modeling). OP was partially funded from BIO-GEO-CLIM grant No 14.B25.31.0001 of the Russian Ministry of Science and Education and Tomsk State University.

Chapitre 3. Low biodegradability of dissolved organic matter and trace metal from subarctic waters

Haute résistance de la matière organique dissoute et des micro-éléments métalliques des eaux continentales subarctiques à la biodégradation

Science of the Total Environment, 2017, article accepted for publication (31 Oct 2017)



Low biodegradability of dissolved organic matter and trace metals from subarctic waters

Olga V. Oleinikova^{1,2}, Liudmila S. Shirokova^{1,3},

Olga Yu. Drozdova², Sergey A. Lapitskiy², Oleg S. Pokrovsky^{1*}

¹ GET (*Geosciences and Environment Toulouse*) UMR 5563 CNRS, University Paul Sabatier,
14 Avenue Edouard Belin, 31400 Toulouse, France

² Geological Faculty, Moscow State University, 1 Leninskie Gory, 119234 Moscow, Russia

³ N. Laverov Federal Center for Integrated Arctic Research; IEPS, 23 Nab. Severnoi Dviny,
163000 Arkhangelsk, Russia

3.1. Résumé

Afin de caractériser la variabilité des processus de minéralisation par des bactéries hétérotrophes de la matière organique dissoute (MOD) des eaux continentales boréales, processus qui sont connus pour contrôler les flux de CO₂ depuis ces eaux continentales vers l'atmosphère, nous avons étudié les interactions de souches bactériennes cultivables d'eau (*Pseudomonas saponiphila*) et de sol (*Pseudomonas aureofaciens*) avec sept substrats constitués par des échantillons d'eaux caractéristiques de différents micro-environnements d'une région subarctique (Carélie du Nord). Parmi ces substrats figurent un lixiviat de tourbière, un échantillon d'eau de marais, un échantillon d'eau de ruisseaux, un échantillon de rivière, un échantillon d'eau de lac humique, un échantillon d'eau de lac oligotrophique, et un pluvio-lessivat collecté sous un pin (l'essence la plus répandu dans cette région). Ces substrats sont caractérisés par des concentration en carbone organique dissous (COD) très variable (de 4 à 60 mg/L). La plus forte diminution de concentration en COD après 4 jours de réaction (33±5%, 43±3% et 53±7% de la concentration initiale dans les eaux de marais, dans les eaux de ruisseau et dans les eaux de lac humique, respectivement) est observée en présence de *P. aureofaciens*. La bactérie hétérotrophe aquatique *P. saponiphila* a dégradé environ 5% du COD dans le lixiviat de tourbe, et n'a pas eu d'effet notable sur les COD des autres substrats.

Le comportement des éléments en traces est principalement contrôlé par l'adsorption rapide (0-1 h d'expérience) sur les surfaces des cellules, indépendamment

de la nature de l'échantillon d'eaux et de la souches bactérienne considérée. Les taux d'adsorptions observés varient entre 20% et 60% pour le fer (Fe^{3+}), 15 et 55% pour l'aluminium (Al), 10 et 60% pour le manganèse (Mn), 10 et 70% pour le nickel (Ni), 20 et 70% pour le cuivre (Cu), 10 et 60% pour l'yttrium (Y), 30 et 80% pour les éléments des terres rares (REE), 15 et 50% pour l'uranium (U). L'étude expérimentale en laboratoire de la dynamique des processus d'adsorption des colloïdes organiques et organo-minéraux d'échantillons d'eaux naturelles sur les surfaces des cellules bactériennes est nouvelle, et elle montre que ces processus sont potentiellement importants pour comprendre les compositions en micro-éléments des eaux boréales. Les diminutions lentes du Fe et de l'Al dissous sont généralement cohérentes avec les sursaturations des solutions considérées par rapport aux hydroxides de ces élément, sursaturations calculées par modélisation thermodynamique (visual Minteq). La stabilité des matières organiques et des éléments en traces relevée dans cette étude dans les différents échantillons d'eaux continentales boréales considérées en présence de hautes concentrations (1 g/L, ce qui est plusieurs ordres de grandeurs au dessus des concentrations en milieux naturels) de bactéries hétérotrophes cultivables suggère que la biodegradation efficace des matières organiques dissoutes observées in situ dans les eaux de surfaces des milieux subarctiques pourrait être due à l'activité de consortiums bactériens plutôt qu'à l'activité de souches isolées.

Mots clés: *carbone organique dissous, boréal, éléments traces, biodégradation, adsorption, coagulation*

3.2 Abstract

The heterotrophic mineralization of dissolved organic matter (DOM) controls the CO_2 flux from the inland waters to the atmosphere, especially in the boreal waters, although the mechanisms of this process and the fate of trace metals associated with DOM remain poorly understood. We studied the interaction of culturable aquatic (*Pseudomonas saponiphila*) and soil (*Pseudomonas aureofaciens*) Gammaproteobacteria with seven different organic substrates collected in subarctic settings. These included peat leachate, pine crown throughfall, fen, humic lake, stream, river, and oligotrophic lake with variable dissolved organic carbon (DOC) concentrations (from 4 to 60 mg L⁻¹). The highest removal of DOC over 4 days of reaction was observed in the presence of *P. aureofaciens* (33±5%, 43±3% and 53±7%

of the initial amount in fen water, humic lake and stream, respectively). *P. saponiphila* degraded only 5% of DOC in fen water but did not affect all other substrates. Trace elements (TE) were essentially controlled by short-term (0 – 1 h) adsorption on the surface of cells. Regardless of the nature of organic substrate and the identity of bacteria, the degree of adsorption ranged from 20 to 60 % for iron (Fe^{3+}), 15 to 55% for aluminium (Al), 10 to 60% for manganese (Mn), 10 to 70% for nickel (Ni), 20 to 70% for copper (Cu), 10 to 60% for yttrium (Y), 30 to 80% for rare earth elements (REE), and 15 to 50% for uranium (U^{VI}). Rapid adsorption of organic and organo-mineral colloids on bacterial cell surfaces is novel and potentially important process, which deserves special investigation. The long-term removal of dissolved Fe and Al was generally consistent with solution supersaturation degree with respect to Fe and Al hydroxides, calculated by visual Minteq model. Overall, the biomass-normalized biodegradability of various allochthonous substrates by culturable bacteria is much lower than that of boreal DOM by natural microbial consortia.

Key words: *dissolved organic carbon, boreal, trace elements, biodegradation, adsorption, coagulation*

3.3. Introduction

Bacterial processing of dissolved organic matter (DOM) in organic-rich continental waters is one of the main factors responsible for net heterotrophic status (CO_2 emission to the atmosphere) of inland waters (Battin et al., 2009; Tranvik et al., 2009). This is especially true for boreal and subarctic waters where large amounts of plant, soil, and peat-originated DOM drive the metabolism of heterotrophic aerobic bacterioplankton (Tranvik, 1998a, b; Wilkinson et al., 2013). Numerous laboratory and field studies incubated soils and waters with native microbial consortia in the presence of added nutrients and demonstrated that between 10% and 40% of the dissolved organic carbon (DOC) is generally available for bacterial uptake over a time frame of several weeks, comparable with the water residence time in lakes and rivers (i.e., Berggren et al., 2007, 2009, 2010). The biodegradability of DOC leached from permafrost and non-permafrost soils was reviewed by Vonk et al. (2015b) who concluded that in average 5 to 20% of DOC is lost in small streams ($< 250 \text{ km}^2$) and 10 to 30% of DOC from soil leachate is biodegradable over 7 day incubation. Based on incubation of natural waters containing native microbial associates, it was shown that the small headwater streams and soil leachate contain most biodegradable DOM

(Van Heees et al., 2005; Mann et al. 2015; Larouche et al., 2015; Spencer et al., 2015; Vonk et al., 2015b). However, the use of complex natural organic substrates with microbial consortia does not allow quantification of the degree of specific substrate vulnerability and does not identify the factors controlling the rate of DOM mineralization. In contrast, experimental microcosm studies of DOM biodegradation by culturable bacterial strains demonstrated their capacity to reveal the mechanisms that control both organic carbon and metal dynamics in soils (i.e., Fritzsche et al., 2012; Drozdova et al., 2014, 2015), waters (Bonneville et al., 2006; Shirokova et al., 2015, 2017; Oleinikova et al., 2017) and mineral systems (Wu et al., 2007, 2008; Feng et al., 2011; Stockman et al., 2012).

Natural waters of the boreal zone typically contain two types of dissolved organic matter – allochthonous, originated from bog, soil, and vegetation reaction with surface waters, and autochthonous, which stems from degradation of periphyton, plankton and aquatic plants as well as their exometabolites (Chupakov et al., 2017). It is obvious that for any given inland water body, a combination of DOM from various terrestrial and aquatic sources is likely. The contribution of allochthonous components (bog, soil, litter leachates) is known to vary seasonally and spatially (Lloyd et al., 2012; Scheibe and Gleixner, 2014) and therefore, the aquatic bacteria receive different biodegradable substrates simultaneously in the course of the year. To untangle the ability of heterotrophic bacteria to mineralize various organic substrates, experiments with individual strains and natural substrates are more efficient.

Specific feature of all boreal waters is the presence of organic and organo-mineral colloids that act as main carriers of metal micronutrients and toxicants (Ingri et al., 2000; Andersson et al., 2001, 2006; Dahlqvist et al., 2004 2007; Neubauer et al., 2013; Vasyukova et al., 2010; Stolpe et al., 2005, 2013). Unlike other surface waters of the world, boreal waters subjected to the influence of mires contain significant amount of dissolved Fe(III), which is linked to DOM and other trace metals via low molecular complexes or large-size organo-ferric colloids. As a result, boreal and subarctic rivers and bog waters are an order of magnitude richer in many low-soluble elements (Fe, Al, trivalent and tetravalent hydrolysates) compared to the world river average as it is known from northern Europe (Andersson et al., 2006; Dahlqvist et al., 2007; Vasyukova et al., 2010; Ilina et al., 2016), Alaska (Stolpe et al., 2013), and Siberia (Pokrovsky et al., 2016a, b). Although the interaction of heterotrophic bacteria with solid organo-ferric compounds from soil and sediments is fairly well studied

(Huang et al., 2005; Bosch et al., 2010; Jackson et al., 2011; Sivan et al., 2011, 2014; Wu et al., 2014; Liu et al., 2015), the factors controlling the behavior of trace metals during mineralization of organo-ferric colloids by heterotrophic bacteria are poorly identified and not quantified. Such possible factors may be the pH, specific conductivity, and DOC concentration in solution; the nature of the DOM (river, lake, soil, bog, peat or litter lessivates), the ratio of organic carbon (C_{org}) to Fe in the dissolved fraction, the duration of interaction and the identity of heterotrophic bacteria. Recently, pure heterotrophic bacteria culture interaction with peat and moss leachate from the permafrost-bearing peatlands (Shirokova et al., 2015, 2017b) and bog water (Oleinikova et al., 2017) were characterized to assess the role of bacteria in colloid transformation of boreal waters and to quantitatively distinguish short-term surface adsorption and long-term intracellular assimilation of DOC and metals. However, a systematic comparison of different substrates for the same bacterial species has never been attempted.

Generally, the low molecular weight fraction of DOM and nutrients is expected to be more bioavailable and susceptible to microbial transformation than the high molecular weight colloids. This suggestion is consistent with results of microbial processing of natural colloids from different terrestrial and aquatic sources (cf., Roehm et al., 2009; Yang et al., 2016). As a corollary to these observations, from studies with marine plankton it is known that the uptake of colloidal-bound Fe is 6 to 30 times lower than the uptake of low molecular weight (LMW) Fe and that Fe linked to small colloids (1-10 kDa) is taken up at a higher rate than Fe bound with large colloids (10 kDa – 0.2 μ m) at otherwise similar colloidal C concentration (Chen and Wang, 2001). The LMW potentially bioavailable fraction is likely to be present in fresh vegetation leachates and small-size streams draining peat and podzol soil (Ilina et al., 2016). In contrast, the bog/ fen and humic lake waters may have more refractory DOM, which is less suitable for aquatic microorganisms. The soil bacteria are likely to degrade soil-derived organic matter whereas the aquatic heterotrophs should be more akin to aquagenic DOM. It thus can be hypothesized that the bioavailability of LMW forms of C_{org} and metals will be higher than that of colloidal metals, and the higher the allochthonous DOC concentration, the lower the impact of aquatic bacteria on metal concentration in solution.

To test these hypotheses, we performed a comparative study of two bacterial species interacting with various dissolved organic substrates available in boreal peat

soil, mire, stream, river, and lake. The aims of this work were to quantify the DOC and trace element (TE) removal under metabolic activity of heterotrophic bacteria and to distinguish between rapid surface adsorption and bacterially-induced coagulation/precipitation of different size peat colloids. We anticipate that quantifying the impact of microbial activity on OC and TE concentration will help to predict potential bioavailability of organic-bound trace metals in boreal waters along the hydrological continuum from the peat soil to the lake via streams.

3.4. Materials and Methods

3.4.1. Heterotrophic bacteria

The soil aerobic gram-negative bacterium *Pseudomonas aureofaciens* CNMN PsB-03 is known for its ability to produce large amounts of gel-forming extracellular polymeric substances (EPS) on a sucrose-peptone (SP) medium (Emnova et al., 2007; Gonzalez et al., 2010). For biomass accumulation, the strain was cultured in SP medium (40 g L^{-1} sucrose, 15 g L^{-1} peptone, 5 g L^{-1} NaCl and 1 g L^{-1} Na_2HPO_4) for 5 days at $25\text{ }^{\circ}\text{C}$ and harvested at the beginning of the stationary phase. The aquatic aerobic gram-negative bacterium *Pseudomonas saponiphila* was isolated from the stream Vostochnyi ($66.3\text{ }^{\circ}\text{N}$, $30.7\text{ }^{\circ}\text{E}$) of Northern Karelia, NW Russia using cultures on nutrient agar plates (Oleinikova et al., 2017). Cells were cultured to a stationary stage during 5 days on a shaker at $25\text{ }^{\circ}\text{C}$ in darkness using a nutrient bouillon (NB) containing 5.0 g L^{-1} peptone and 3.0 g L^{-1} protein extract. Unlike previous experiments that were conducted with the addition of nutrients (N, P) required for heterotrophic bacterioplankton (e.g., Haukka et al., 2005; Holmes et al., 2008; Mann et al., 2014), in the present study, the bacteria were allowed to starve during 2 days in nutrient-free NaCl solution prior the addition of organic substrates. This “NaCl-starvation” strategy allowed testing the bioavailability of mostly naturally relevant substrates for bacterial cultures with minimal interferences from intracellular resources of nutrients.

An active bacteria number count (colony forming-units, CFU mL^{-1}) was performed using Petri dish inoculation on nutrient agar (0.1, 0.2, and 0.5 mL of the sampled solution in triplicate with an uncertainty of 10-20%) in a laminar hood box. The inoculation of blanks was routinely performed to ensure the absence of contamination from the external environment. The total biomass of the bacteria was measured using humid (centrifuged during 15 min at $8000\times g$) and dry (lyophilized)

weight following the standard procedures of bacterial biomass preparation for metal adsorption experiments (Fein et al., 1997, 2001; Gonzalez et al., 2010; Pokrovsky et al., 2013). Optical density at 600 nm ($OD_{600\text{ nm}}$) was also used for estimating the total biomass of heterotrophic bacteria in the reactor (Shirokova et al., 2012). Before the inoculation of natural substrates, the cells were rinsed 3 times in sterile NaCl (14 mM) to condition the cells in inert electrolyte solution, similar in ionic strength to the growth media. Final rinsing was with sterile 0.01 M NaNO₃ solution using centrifugation at 7000× g (~ 500 mL of solution for 1 g of wet biomass) to remove as much of the adsorbed metals and cell exudates from the surface as possible and to avoid complexation of Cl⁻ with trace metals. The cell integrity after centrifugation was verified by optical immersion microscopy, and 100% cell viability was confirmed by inoculation on nutrient agar. In addition, Transmission Electron Microscopy (TEM) was used to characterize cell status before and after incubation. For this, aliquots of untreated live bacterial cells suspensions in the substrates were examined with a JEOL JEM-1400 HC at 120 kV. The bacterial cells (*P. aureofaciens*) reacted with bog water were centrifuged 5 min at 7000 g and isolated biomass was slightly diluted with MilliQ water. A droplet of obtained suspension was placed on the TEM grid coated with a carbon film and dried for several minutes at room temperature. Images were taken using Gatan Orius SC1000B 11 Megapixels camera.

3.4.2. Organic substrates of boreal surface waters

To cover contrasting and representative sources of DOM from the boreal zone, we sampled subarctic catchments of Northern Karelia, 40-60 km south from the Arctic Circle. The Palojoki River has a watershed area of 32 km², it flows out of Kivakkalampi lake, and drains the basic intrusive Kivakka. The Vostochniy Stream with a catchment area of 0.95 km² originates from the system of interconnected humic lakes located within the ombrotrophic bog zone and empties into large oligotrophic Lake Tsipringa. The stream was sampled in the mouth reach, several meters above its mixing with the Tsipringa Lake. The minerotrophic fen water was collected at the lakeshore. Detailed description of Northern Karelia landscape context of sampled waters can be found elsewhere (Ilina et al., 2014, 2016). The peat leachate was prepared by reacting intact peat soil (sampled from 15 to 30 cm depth within the Lake Tsipringa watershed) with distilled water (10 g_{dry} L⁻¹) in an atmosphere-saturated environment at 25°C on a shaker. The pine crown throughfall was collected during

rain event in July 2015 on the pre-washed polyethylene film (9 m^2 area) placed at the floor level under pine crown of two isolated pine trees. First portion of the rainwater (10 L) was transferred from polyethylene film into clean collectors following by further filtration through $0.22\text{ }\mu\text{m}$ filter. Prior the experiments, all samples were again sterile – filtered ($0.22\text{ }\mu\text{m}$ Nalgene sterile filter unit). The sterility of thus filtered natural waters was verified by their inoculation on nutrient agar; no visible colonies were detected both on eutrophic and oligotrophic agar media. Chemical composition of collected waters is given in **Table 3.1**. The studied waters presented strong contrast in pH, DOC, and Fe concentration.

Table 3.1. Chemical composition of collected waters used as substrates in bacterial experiments.

Element, $\mu\text{g L}^{-1}$	Humic lake	Vostochniy Stream	Fen water	Peat leachate	Palojoki River	Pine crown throughfall	Tsipringa Lake
pH	6.9	6.9	5.1	4.9	6.6	5.1	7.5
DOC	20100	15800	47800	23800	12400	24400	3850
DIC	1800	2950	1150	1100	4300	12200	26200
Cl ⁻	1035	470	635	965	490	1295	630
SO ₄ ²⁻	865	1260	175	570	505	960	2110
Na	2480	2230	3660	1890	945	1400	1970
Mg	404	703	1304	357	648	159	1452
Al	54	116	173	197	79	90	2.8
Si	1415	3030	2740	378	2240	430	1460
K	254	257	400	1710	175	4110	129
Ca	2380	2780	2240	606	2360	392	5160
Mn	3.6	3.1	70	24.1	4.8	53	0.61
Fe	65	94	1600	1370	180	12	11
Co	0.065	0.057	1.16	0.65	0.038	0.097	0.017
Ni	1.41	0.59	1.76	0.69	0.19	1.72	0.32
Cu	26.2	25.5	13.9	41.9	49.8	17.7	3.5
Zn	112	185	290	270	5.4	315	94
Sr	14.94	15.34	0.36	1.93	12.98	5.72	14.07
Ba	290	261	297	258	3.2	284	367
La	0.051	0.264	0.269	0.192	0.145	0.057	0.018
Pb	0.38	0.07	0.70	0.25	0.05	0.25	0.02
U	0.003	0.008	0.022	0.031	0.009	0.003	0.010

3.4.3. Experimental set-up

Experiments with *P. aureofaciens* included the Vostochnyi Stream, the Palojoki River, humic lake, fen water and peat leachate. Cells of *P. saponiphila* reacted with stream water and humic lake, the terminal oligotrophic lake (Tsipringa), the peat leachate, the fen water, and the pine crown throughfall.

After rinsing, 0.2 g of wet cells were added to 200 mL of sterile-filtered (0.22 µm) substrates to provide the wet biomass concentration of 1 g_{wet} L⁻¹. The polypropylene flasks were shaken on a ping-pong thermostatic shaker at 25±0.5°C and aerated via Biosilico® ventilation porous caps during 4 days. All the experiments were run in duplicates. The control (bacteria-free) experiments were performed for each sterile substrate, which was shaken and sampled in parallel to biotic experiments. Aliquots of homogeneous suspension (20 mL) were sterile sampled 1, 24, 48, 72, and 96 h after the addition of bacteria. During sampling, the reactor was vigorously shaken thus producing homogeneous cell suspension. The optical density and pH were measured in suspension subsamples, while 0.1 to 0.5 mL was used for inoculation of the nutrient agar plates in triplicate for viable cell counts after dilution by a factor of 10,000.

The sampled aliquot was centrifuged at 7000 rpm and used for filtration through 0.22 µm acetate cellulose filters. The DOC and metal blanks were a factor of 3 to 10 lower than the minimal concentrations of these components in experimental fluids. The filtrates were sub-divided into non-acidified and acidified portions, for carbon/UV/pH and trace elements measurements, respectively.

3.4.4. Analytical techniques

The DOC was analyzed using a Shimadzu TOC-V_{CSN} Total Carbon Analyzer with an uncertainty of 3% and a detection limit of 0.1 mg L⁻¹. The pH was measured using a glass combination electrode with an accuracy of ± 0.01 pH units. The UV absorbance of the filtered samples was measured at 254 nm using quartz 10-mm cuvette on Cary-50 spectrophotometer. The specific UV-absorbency (SUVA₂₅₄, L mg⁻¹m⁻¹) is used as a proxy for aromatic C, molecular weight and source of DOM (Uyguner and Bekbolet, 2005; Weishaar et al., 2003; Ilina et al., 2014 and references therein). Filtered solutions for the cation and trace element analyses were acidified (pH = 2) with double distilled ultrapure HNO₃ and stored in polystyrene vials that had been previously washed with 0.1 M HCl and rinsed with ultrapure MilliQ deionized

water. The sampling vials were prepared in a clean bench room class A 10,000. Major and trace elements (TEs) were determined with an ICP-MS Agilent 7500 ce that is used in GET laboratory (Toulouse) for the analysis of organic-rich rivers and lakes (cf. Pokrovsky et al., 2016a, b). The uncertainty of element concentration measurements ranged from 5 to 10% at $> 1 \mu\text{g L}^{-1}$ and from 20 to 30% at $< 0.01 \mu\text{g L}^{-1}$. The international geostandard SLRS-5 was analyzed every 20 samples to check the validity and reproducibility of the analyses (Yeghicheyan et al., 2014). Good agreements were found between the replicated measurements of SLRS-5 and the certified values (relative difference $< 20\%$ SD on the repeated measurements) of all major and trace elements discussed in this study.

3.4.5. Statistical treatment and thermodynamic modeling

For the treatment of experimental data, we postulated that a significant ($p < 0.05$) difference between the control and the bacterial experiment after 1 h of exposure corresponded to initial adsorption (0 – 1 h) of trace element onto the cell surface. This was in accord with other studies on metal adsorption onto heterotrophic bacteria (Pokrovsky et al., 2012, 2013; Gonzalez et al., 2014a; Shirokova et al., 2017). Slow decrease of element concentration between 1 and 96 h of incubation was interpreted as either intracellular assimilation or extracellular removal (1 – 96 h) via colloid coagulation and metal oxyhydroxide formation. In this regard, we could not distinguish between intracellular incorporation and co-precipitation of trace metals together with Al and Fe hydroxides.

Statistical treatment of experimental data included calculation of errors and confidence intervals for the measured values of pH, $\text{OD}_{600 \text{ nm}}$, cell number, DOC, major and TE concentrations of the experimental solution among different duplicates, bacteria, and substrates over the full duration of the experiment. We used ANOVA to test the differences in the biotic and chemical parameters of the experimental solution among different replicates, bacteria, and substrates. A value of $p < 0.05$ indicated that the differences in the overall concentration and time trend are important and statistically significant compared with internal variations between replicates.

The metal complexation with organic ligands and solution saturation degree with respect to secondary Fe and Al hydroxide and aluminosilicates in the course of experiment were calculated using Visual MINTEQ (Gustafsson, 2011, version 3.1, October 2014) for Windows in conjunction with a database and the NICA-Donnan

humic ion binding model (Benedetti et al., 1995; Milne et al., 2003) and Stockholm Humic Model (SHM). The input parameters of the model were pH, DIC, anions, cations, total TE and DOC concentrations, and the model provided the saturation state of solution with respect to Al(OH)_3 , Fe(OH)_3 , halloysite, imogolite and kaolinite and the percentage of metal complexes with DOM.

3.5. Results

3.5.1. Evolution of biomass, live cell number, pH, and dissolved carbon

The live cell number remained constant for all substrates and both bacterial species (**Fig. 3.1 A, B**). The typical decrease of total cell concentration was 10% over 3 days of exposure, with the exception of *P. aureofaciens* in humic lake and Vostochnyi stream (50% over 3 days). Note that no detectable cell growth was observed, as the CFU value at the end of the experiment was equal, within 10%, to that of the initial suspension. Cell biomass, which was measured as optical density (OD_{600 nm}), decreased in the course of incubation (**Fig. 3.1 C, D**). After 4 days of exposure, the cells remained intact and non-deformed; however, in some cases newly formed dense material was detected in the vicinity of cells, probably corresponding to a coagulation of Fe-rich colloids (**Fig. 3.1 E**).

The pH value generally increased by 0.1 to 1 unit over 4 days of reaction (**Fig. 3.2**). The increase was much stronger in *P. saponiphila* (peat leachate, fen water, and pine throughfall) compared to *P. aureofaciens* (only humic lake, the Vostochnyi Stream and the Palojoki River). There was no sizeable DOC decrease over the first 1 h of reaction (**Fig. 3.3**). The long-term removal (1 – 96 h) of DOC by *P. aureofaciens* was high in humic lake and stream (53±7 and 43±3%, respectively) and in the fen water (33±5%). No decrease of DOC was detected in other substrates in the presence of this bacterium. *P. saponiphila* did not produce any significant (> 5% relative to control) long-term DOC decrease in all 6 tested substrates. The SUVA_{254 nm} (and, thus, the aromaticity of substrates) increased in stream and fen waters (**Fig. 3.4**) consistent with the DOC decrease in the presence of *P. aureofaciens* (**Fig. 3.3**). A weak decrease of SUVA_{254 nm} (≤ 13%) was detected in humic lake and stream waters with *P. saponiphila*.

3.5.2. Trace metal concentration change in the presence of bacteria

The bacterial presence exerted notable effect on a number of dissolved trace metals. Between 16 and 30% of initially present Al was adsorbed over first hour on both bacteria surfaces in the stream, humic lake, fen waters and peat leachate (**Fig. 3.5 A, B**). The adsorption from the Palojoki River water and pine throughfall was almost two times greater (55%). The slow removal of Al was much weaker, with maximal decrease in concentration by 10 to 20% in humic lake and the stream in the presence of both bacteria (**Fig. 3.5 A, B**). Iron concentration responded most actively to the

presence of bacteria as it decreased in all studied substrates during short-term adsorption (20 to 60%, **Fig. 3.6 A-D**). The long-term Fe removal (1 – 96 h) was also observed in all substrates for both bacteria and ranged from 10 to 40%.

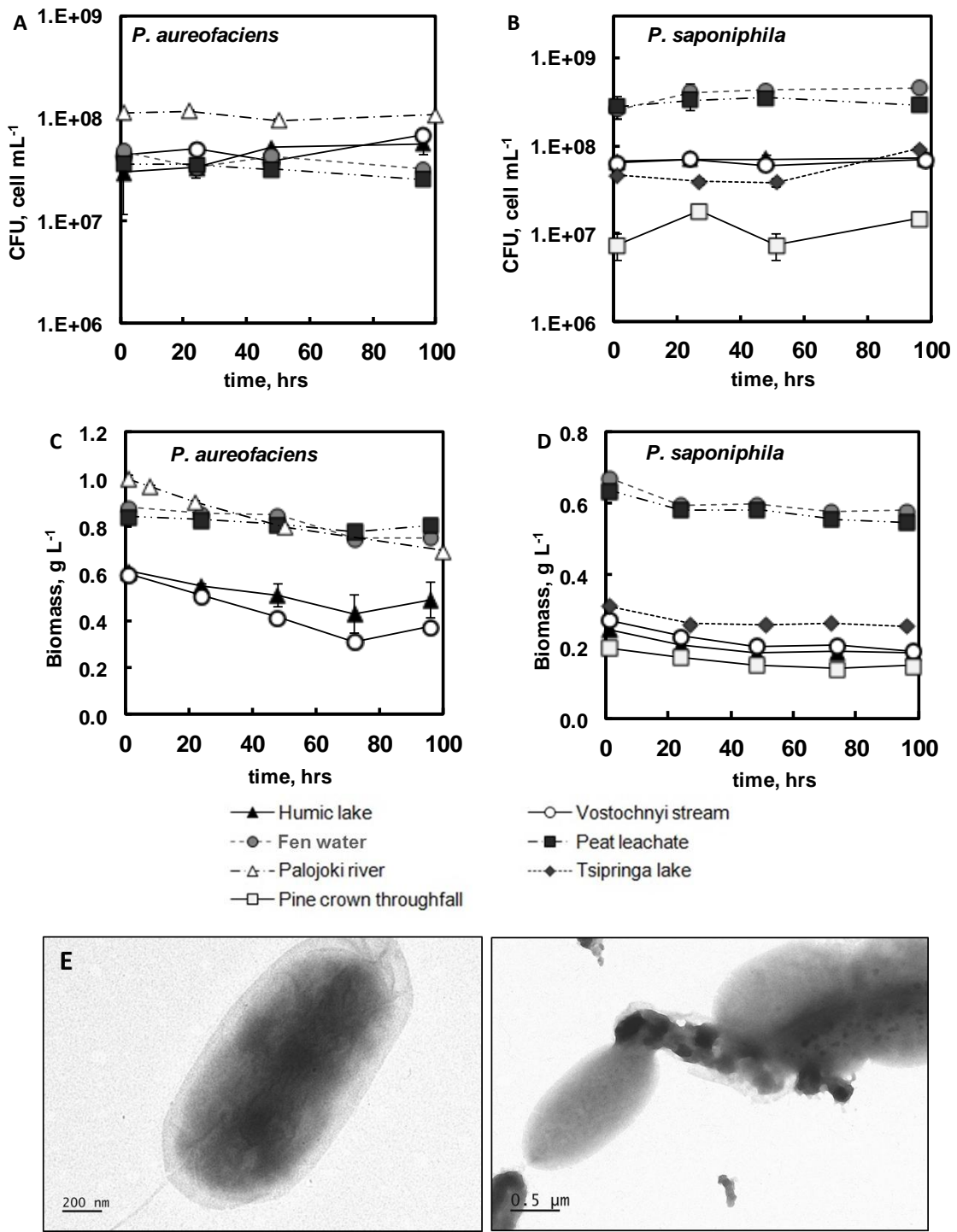


Fig. 3.1. Live cell number expressed as colony forming units (CFU, cell/mL), (A, B) and cell biomass measured as optical density (C, D) evolution in the course of experiments. The uncertainty on the CFU and biomass ($OD_{600\text{ nm}}$) are within the symbol size unless shown explicitly. (E): Transmission Electron Spectroscopy (TEM) images of *P. aureofaciens* after 4 days reaction in bog water.

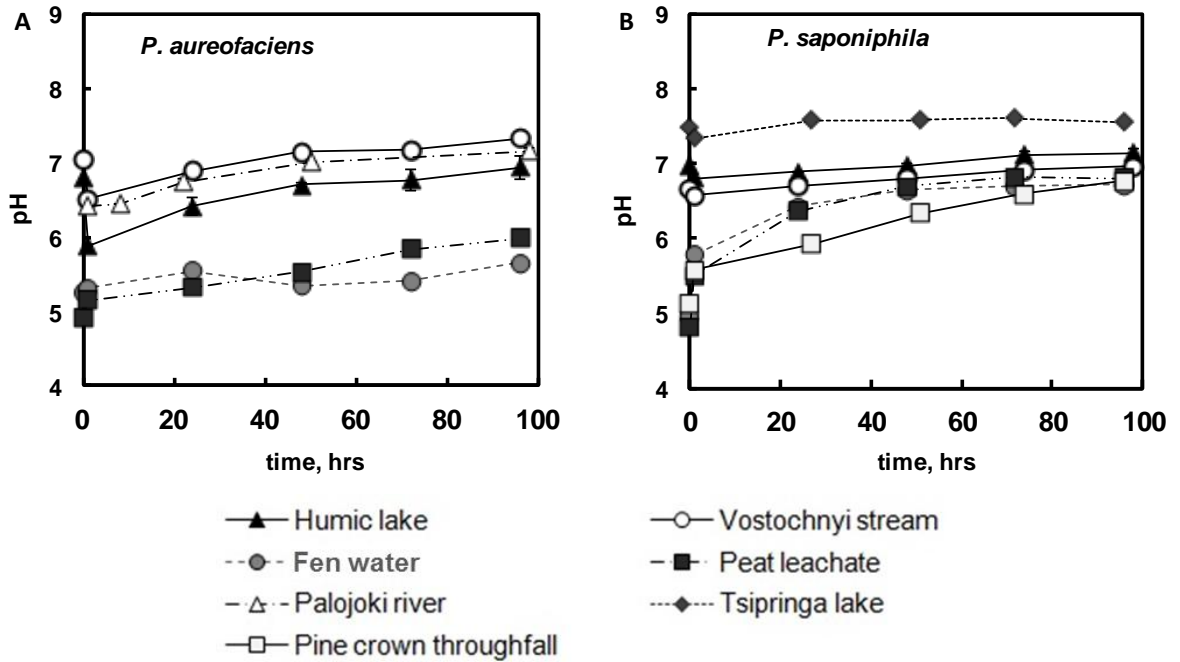


Fig. 3.2. pH value evolution in the course of experiments with *P. aureofaciens* (A) and *P. saponiphila* (B).

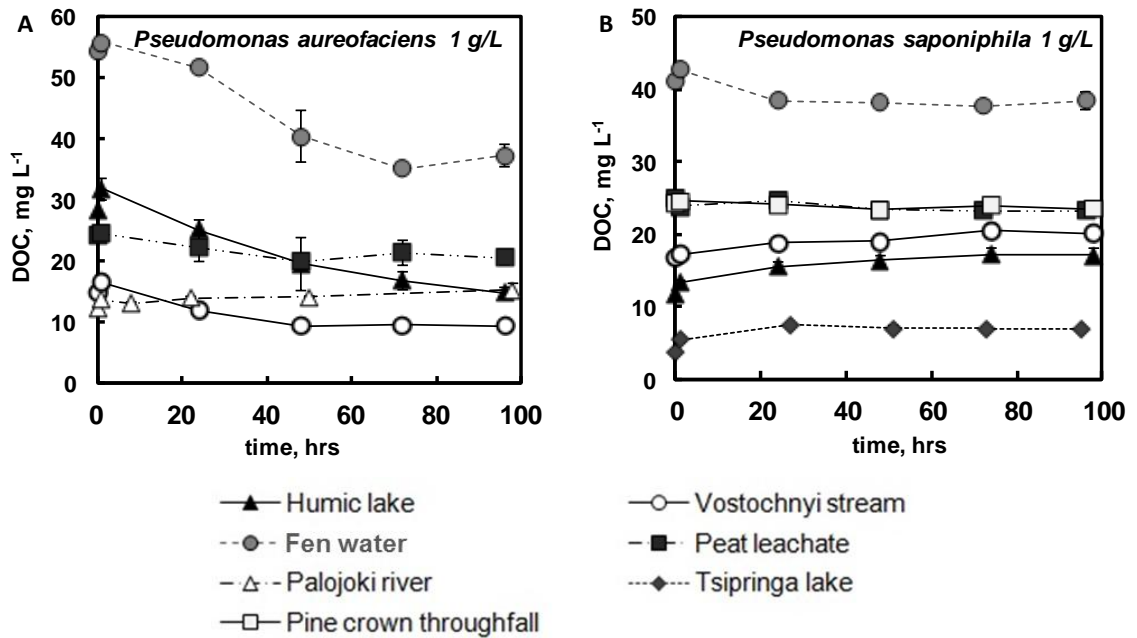


Fig. 3.3. Evolution of DOC concentration in various substrates in the presence of *P. aureofaciens* (A) and *P. saponiphila* (B). The standard deviation of the duplicate samples is within the symbol size unless shown explicitly.

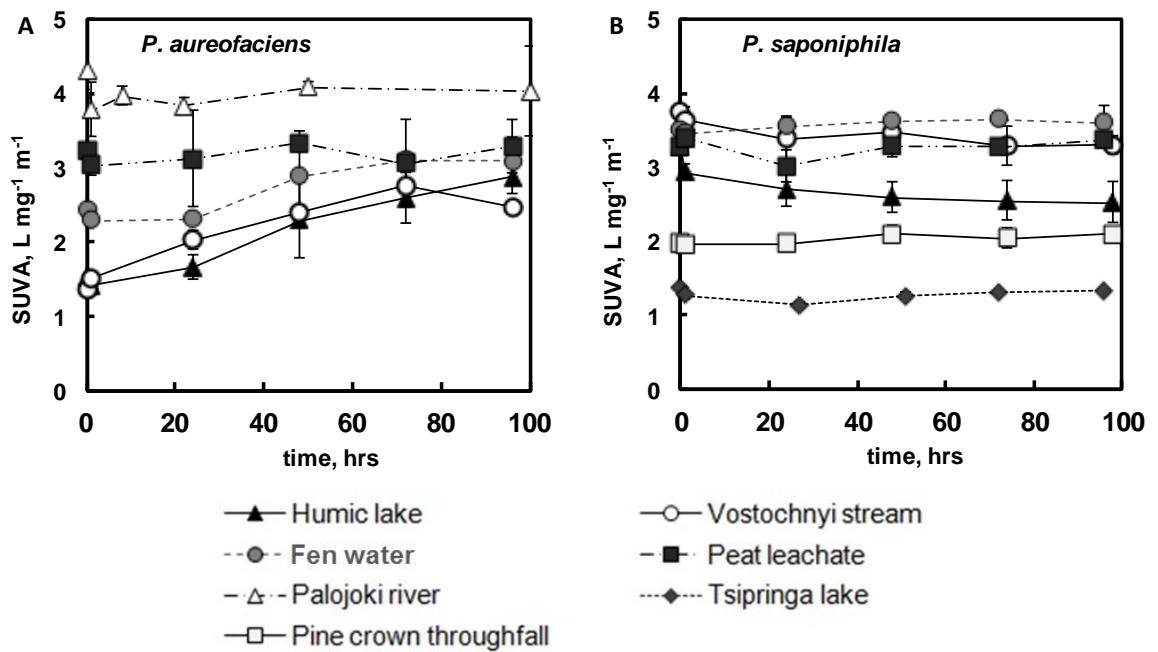


Fig. 3.4. SUVA₂₅₄ nm evolution in the course of experiments with *P. aureofaciens* (A) and *P. saponiphila* (B).

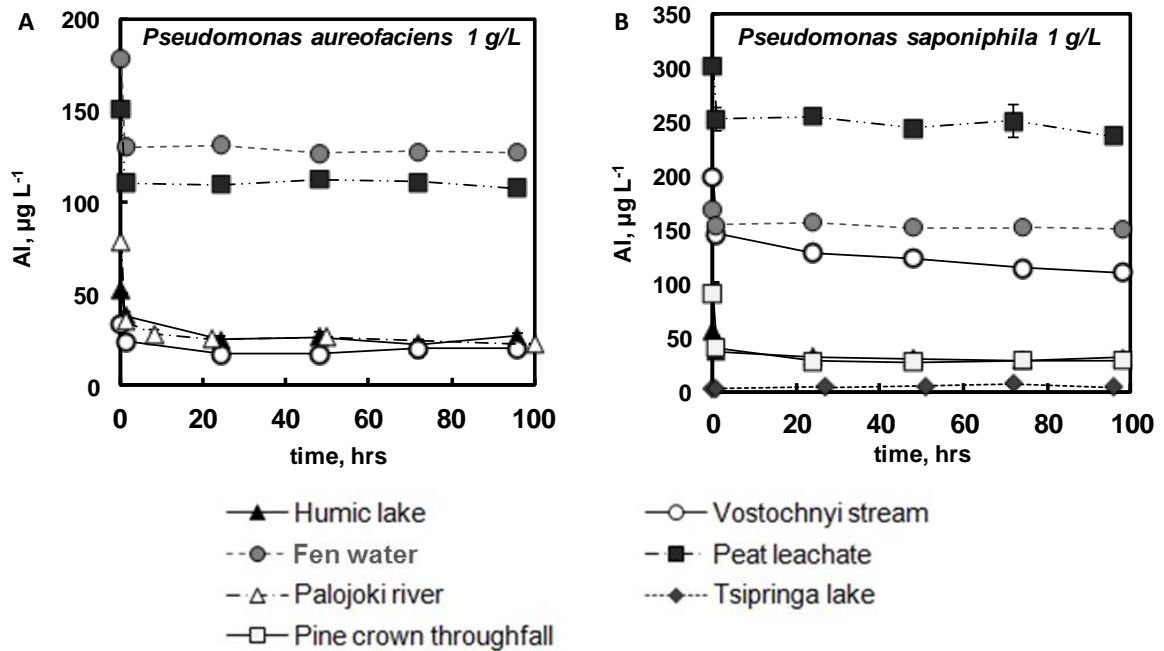


Fig. 3.5. Evolution of Al concentration in various substrates in the presence of *P. aureofaciens* (A) and *P. saponiphila* (B). The standard deviation of the duplicate samples is within the symbol size unless shown explicitly.

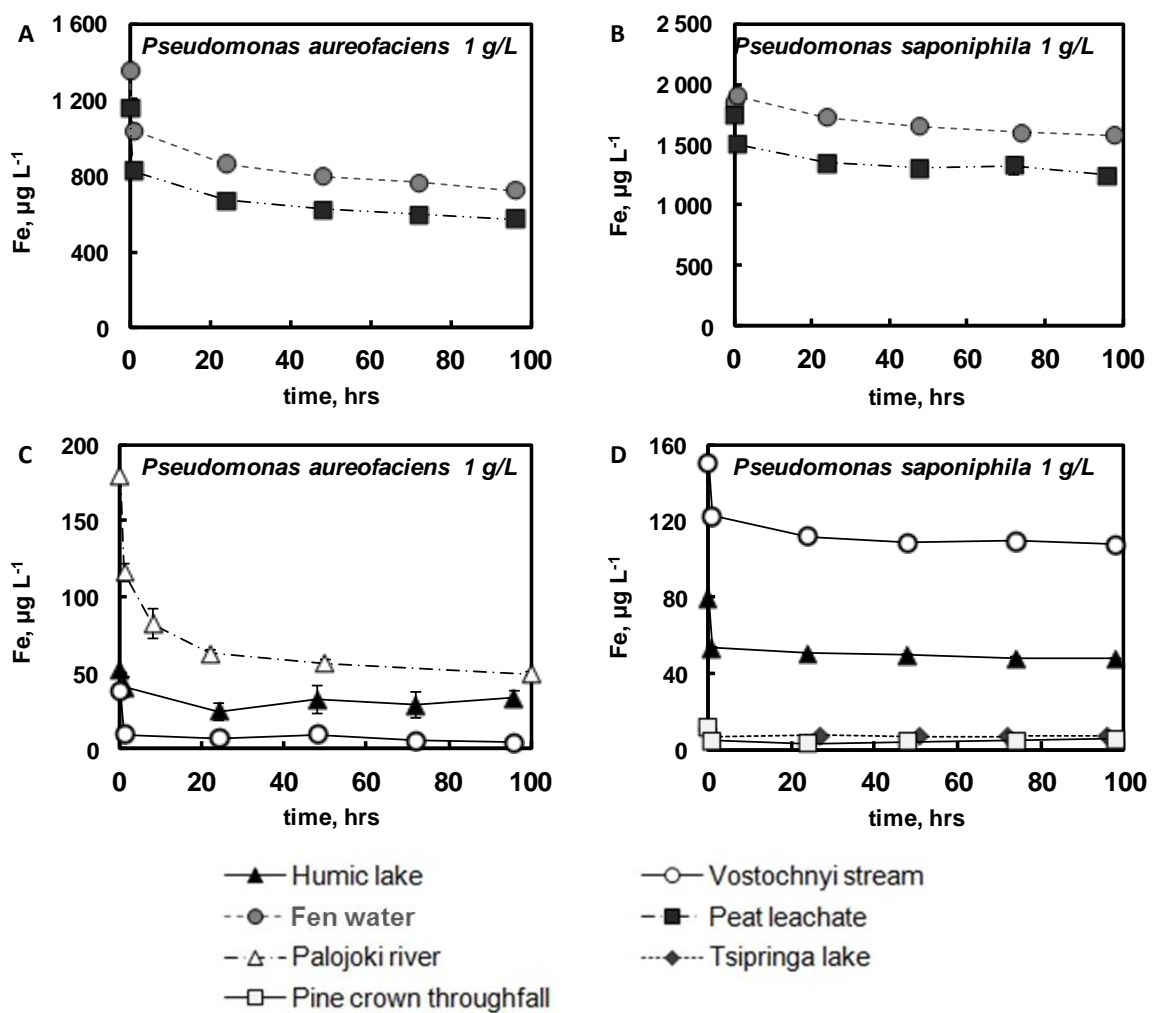


Fig. 3.6. Evolution of Fe concentration in various substrates in the presence of *P. aureofaciens* (A, C) and *P. saponiphila* (B, D). The standard deviation of the duplicate samples is within the symbol size unless shown explicitly.

For all other metals, only short-term (0–1 h) adsorption was detected at the experimental conditions of this study. Cu was always affected by adsorption within first hour of reaction (20 to 70%, **Fig. 3.7 A, B**). Over longer exposure period, no systematic variation in Cu concentration was observed, or these variations were $\leq 20\%$ of the starting value. Ni was subjected to fast removal from humic lake, fen water, peat leachate and pine throughfall in the presence of both bacteria (**Fig. 3.7 C, D**). A weak long-term removal of Cu occurred only in fen water and peat leachate in the presence of *P. aureofaciens*.

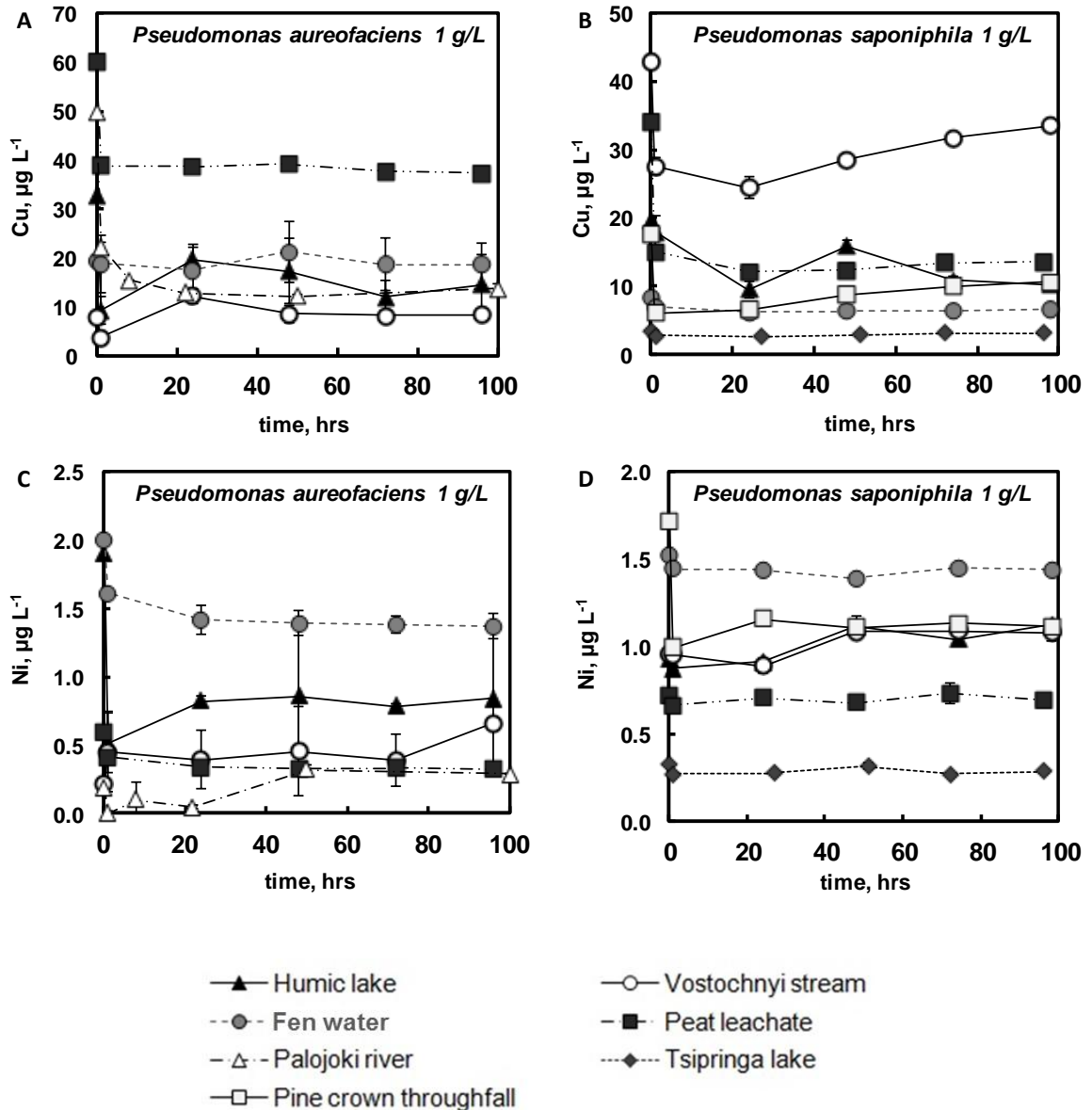


Fig. 3.7. Evolution of Cu (A, B) and Ni (C, D) concentration in various substrates in the presence of *P. aureofaciens* (A, C) and *P. saponiphila* (B, D). The standard deviation of the duplicate samples is within the symbol size unless shown explicitly.

The short-term adsorption was also clearly seen for Y and light rare earth elements (La, Ce, Pr, Nd, 30 to 70%, illustrated in Fig. 3.8-3.9), Cd (10 to 50%, Fig. 3.10) and U (10 to 30% in most substrates, Fig. 3.11). The long-term removal of these elements in the presence of *P. saponiphila* was weak except for Cd in humic lake (35%), fen water (34%) and peat leachate (47%) and for rare earth elements (REE) which exhibited 20 to 50% removal from humic lake, Vostochnyi stream and pine throughfall. Note that among all studied substrates, pine throughfall demonstrated maximal short-term adsorption of trace metals but relatively low long-term removal.

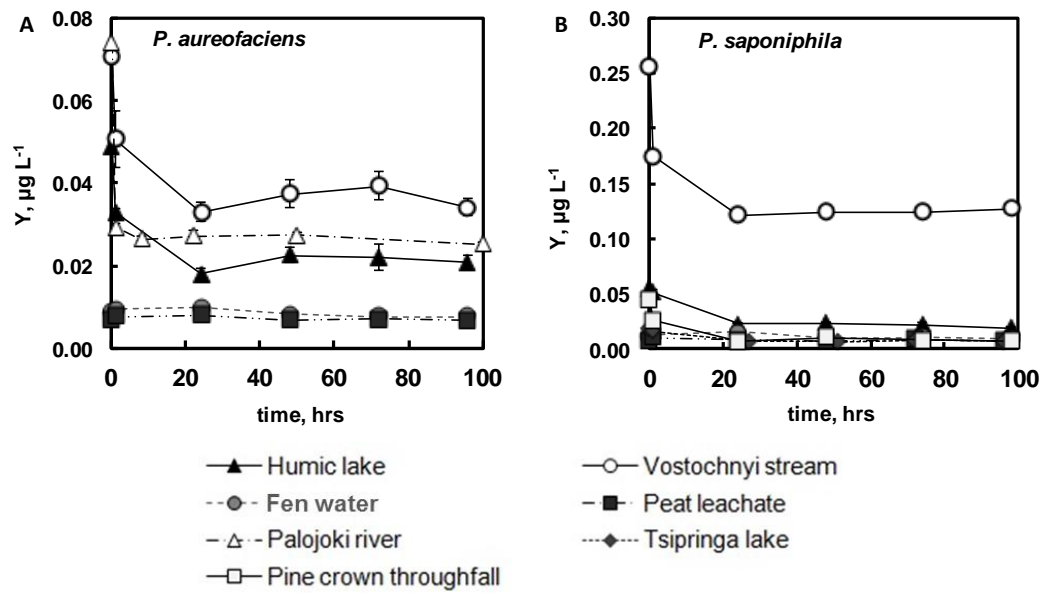


Fig. 3.8. Y concentration evolution in the course of experiments with *P. aureofaciens* (A) and *P. saponiphila* (B).

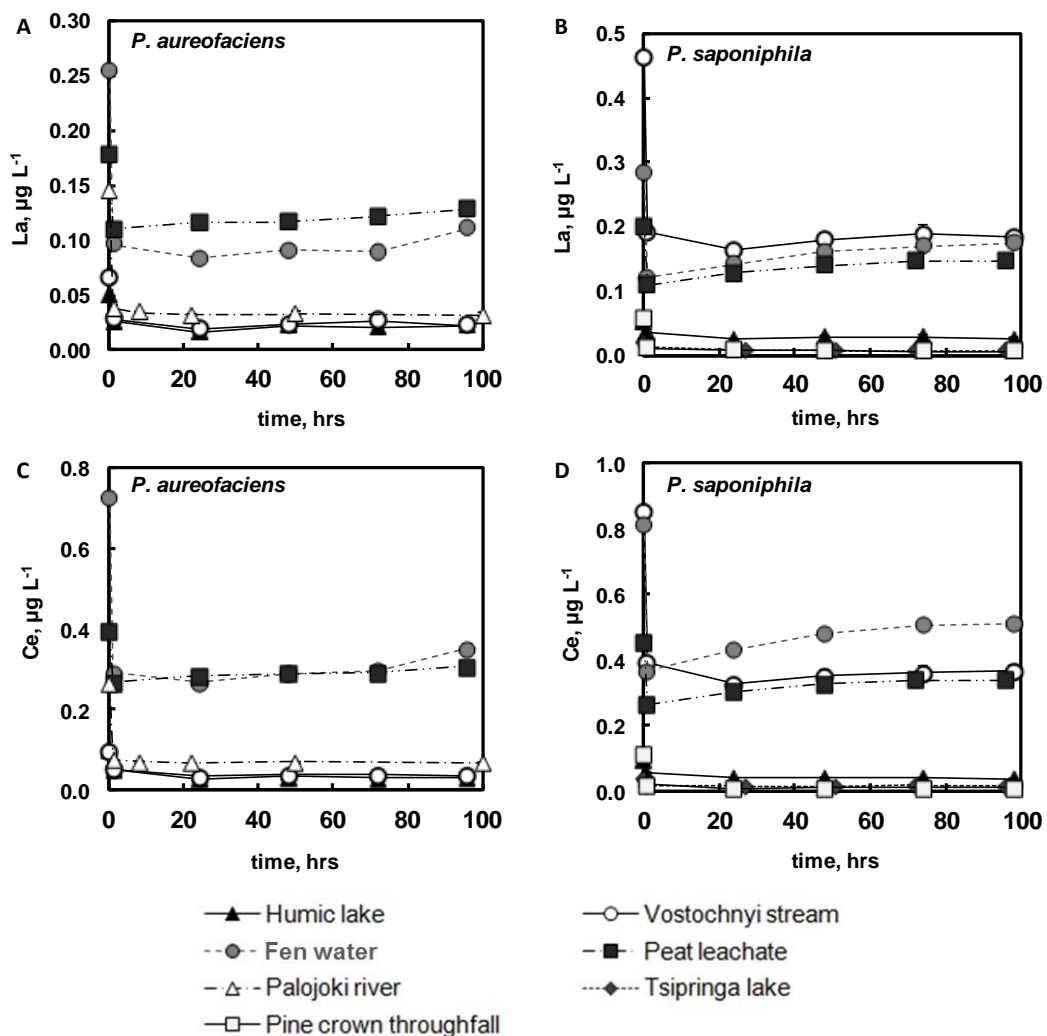


Fig. 3.9. La (A, B) and Ce (C, D) evolution in the course of experiments with *P. aureofaciens* (A, C) and *P. saponiphila* (B, D).

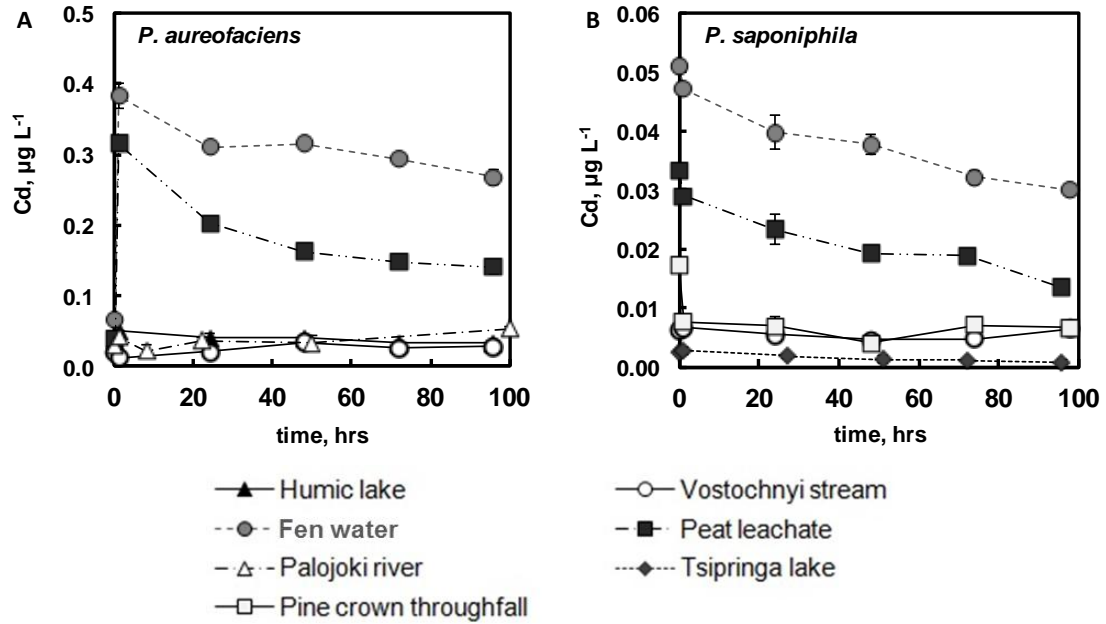


Fig. 3.10. Cd concentration evolution in the course of experiments with *P. aureofaciens* (A) and *P. saponiphila* (B).

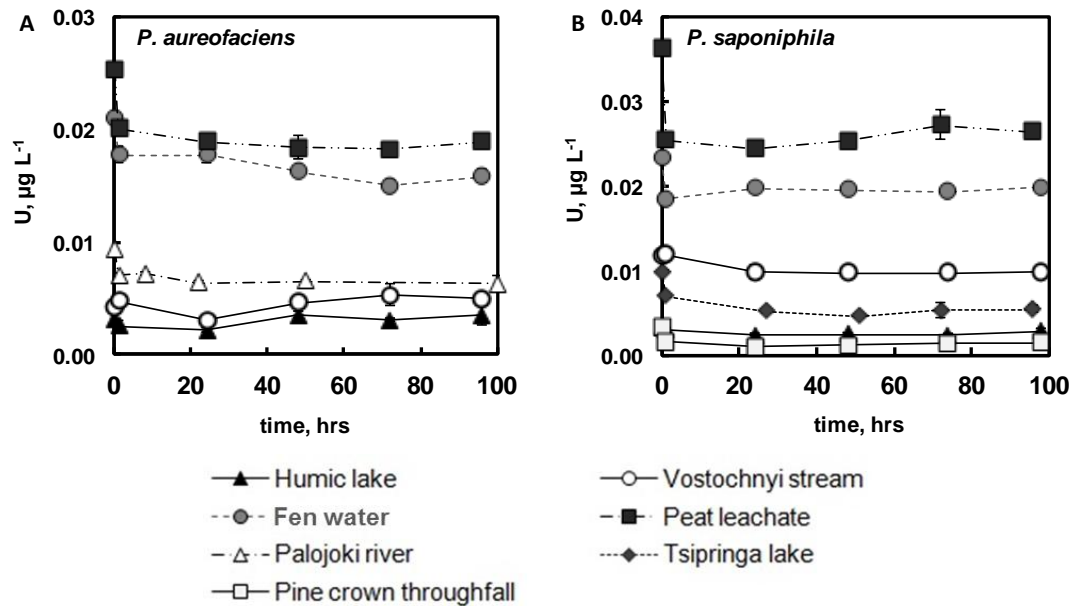


Fig. 3.11. U^{VI} concentration evolution in the course of experiments with *P. aureofaciens* (A) and *P. saponiphila* (B).

The element concentration patterns in the presence of bacteria and all substrates are summarized in **Fig. 3.12**. In experiments with *P. aureofaciens*, the short adsorption was significant ($p < 0.05$) in all substrates for Al, Mn, Fe, Cu, Y, REEs, and U, for Ti in bog water and peat leachate and Co and Ni. This bacterium produced slow removal of Fe (all substrates), Al, Y, Cd (humic lake and stream), Co, Ni, Mn (fen water and peat leachate). The presence of *P. saponiphila* yielded clear adsorption of Al, Fe, Mn, Cu, Cd, REEs and U and slow decrease of Fe, Mn, Al and Cd (in some substrates).

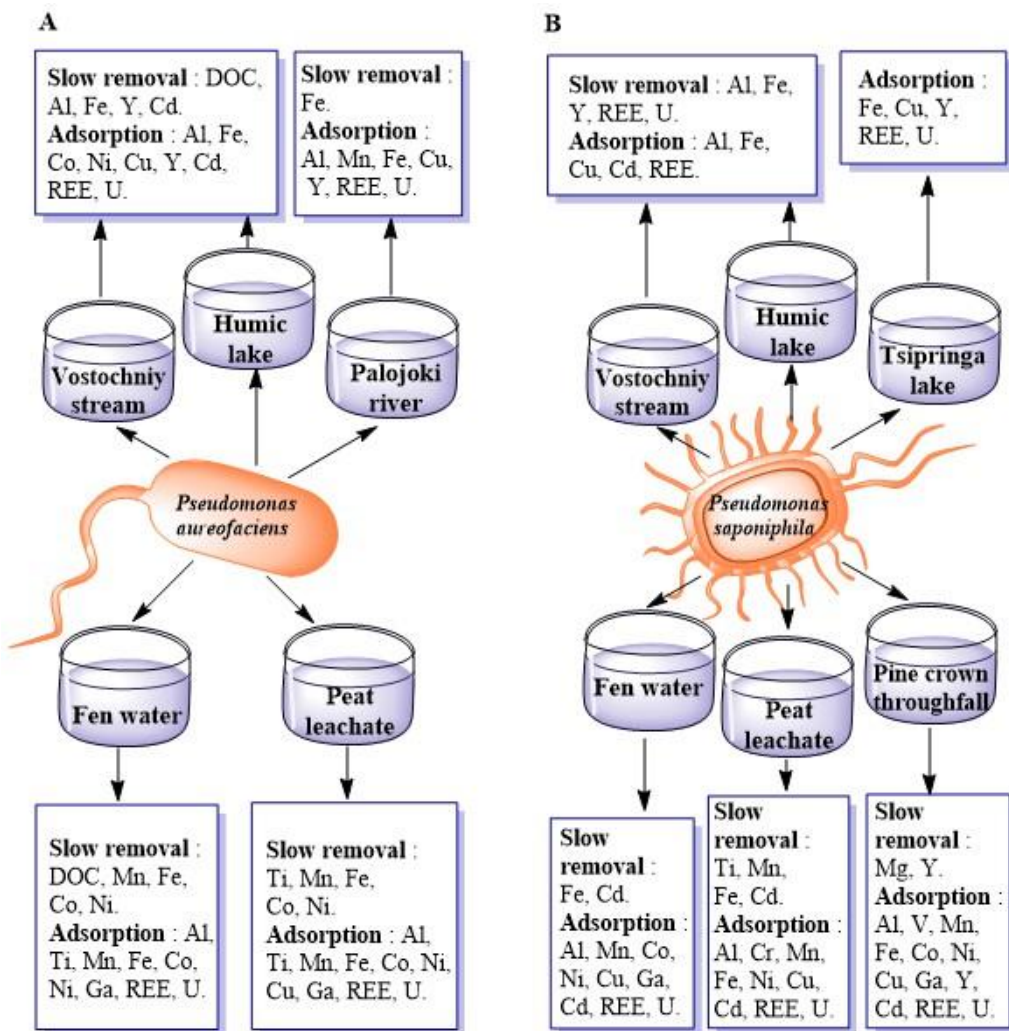


Fig. 3.12. Summary of *P. aureofaciens* (A) and *P. saponiphila* (B) heterotrophic bacterial effect on element concentration in various organic substrates of boreal waters.

Because trace metals are essentially present as organic complexes and organo-ferric, organo-aluminum colloids (see section 3.5.3 below), we attempted to relate the fast adsorption and slow removal of trace metal to the main constituents of organo-mineral colloids of substrates. For this, we used DOC, Fe concentration, (DOC/Fe) molar ratio, and the pH of organic substrate. There was no statistically significant link ($R^2 < 0.44$) between the percentage of adsorbed element and DOC concentration as illustrated for Al, Mn, Fe, Ni, Cu, and La in **Fig. 3.13**. The long-term removal of Al and Fe increased with DOC increase, which was not however visible for Mn and Cd (**Fig. 3.14**). We observed a decrease of fast adsorption with the increase of initial Fe concentration in the substrates, shown in **Fig. 3.15** for Al, Mn, Ni and Ce. Note that the relative amount of assimilated/coagulated TE was not correlated with dissolved Fe concentration in the substrates ($R < 0.5$, not shown). Using the ratio DOC to Fe in the

initial substrate allowed seeing the cumulative effect of bulk solution chemistry on TE adsorption. Thus, there was a significant increase in the adsorbed fraction of Al, Cu, Mn, Ni, Cd, Ce with the increase in $(\text{DOC}/\text{Fe})_{\text{molar}}$ of the initial solution (**Fig. 3.16**) with $0.46 \leq R \leq 0.65$. In contrast, there was no relationship between the fraction of slowly removed TE and the DOC to Fe ratio ($R < 0.5$, not shown). The percentage of initial fast adsorption was found to be independent on the pH of organic substrate ($R < 0.5$ as shown in **Fig. 3.17** for Al, Mn, Fe, Co, Cu, Y, Cd, Ce and U).

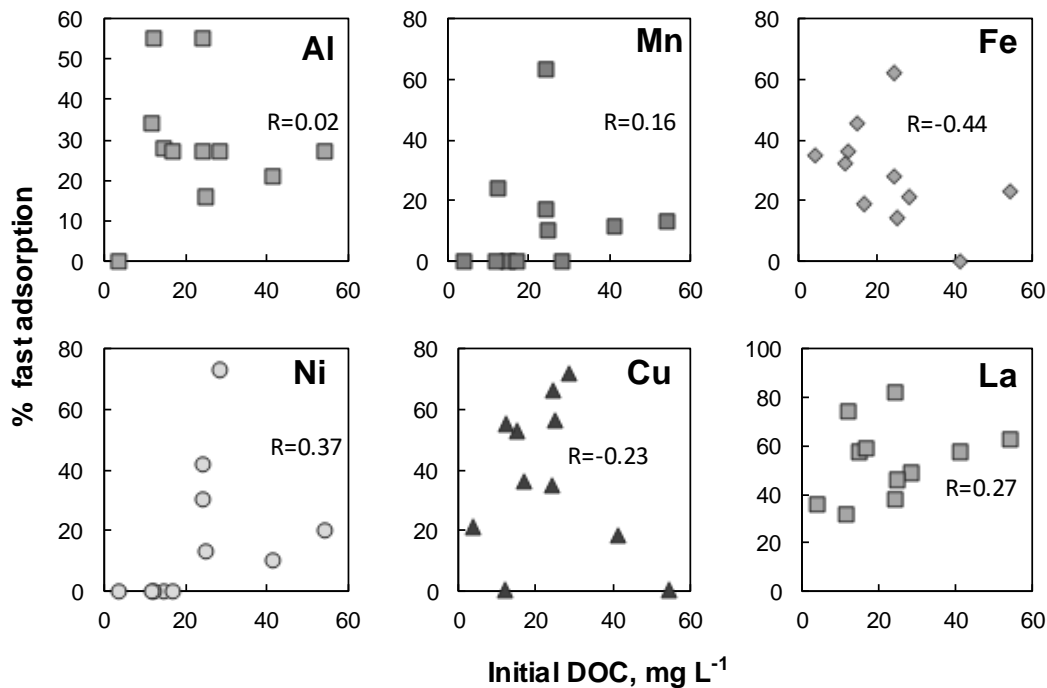


Fig. 3.13. Percentage of initial adsorption (< 1 h) of Al, Mn, Fe, Ni, Cu, and La as a function of DOC concentration in all substrates for *P. aureofaciens* and *P. saponiphila*. R is for Pearson correlation coefficient.

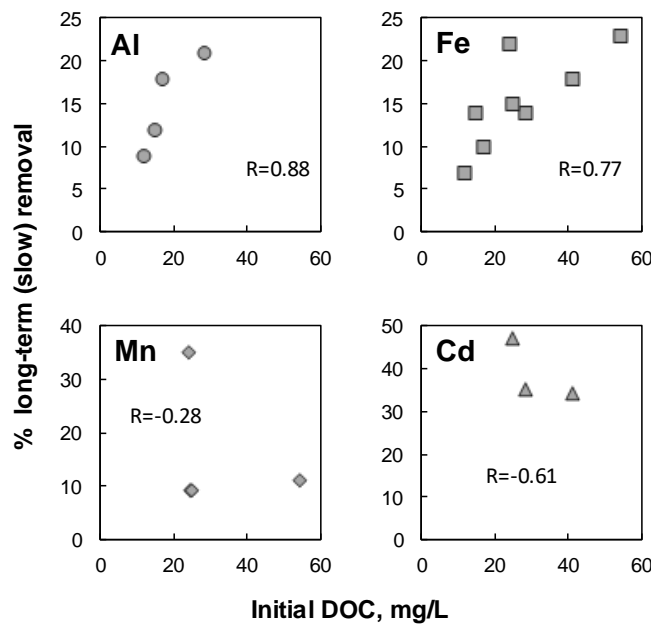


Fig. 3.14. Percentage of slow removal of Al, Fe, Mn, and Cd as a function of DOC concentration in all substrates for *P. aureofaciens* and *P. saponiphila*. R is for Pearson correlation coefficient.

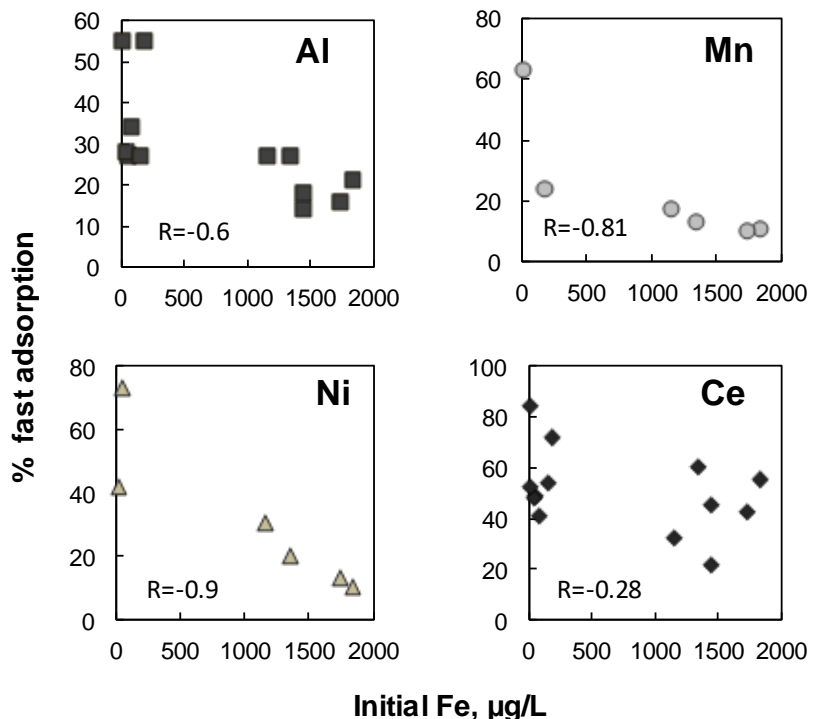


Fig. 3.15. Percentage of initial adsorption (< 1 h) of Al, Mn, Fe, Ni, Cu, and La as a function of DOC concentration in all substrates for *P. aureofaciens* and *P. saponiphila*. R is for Pearson correlation coefficient.

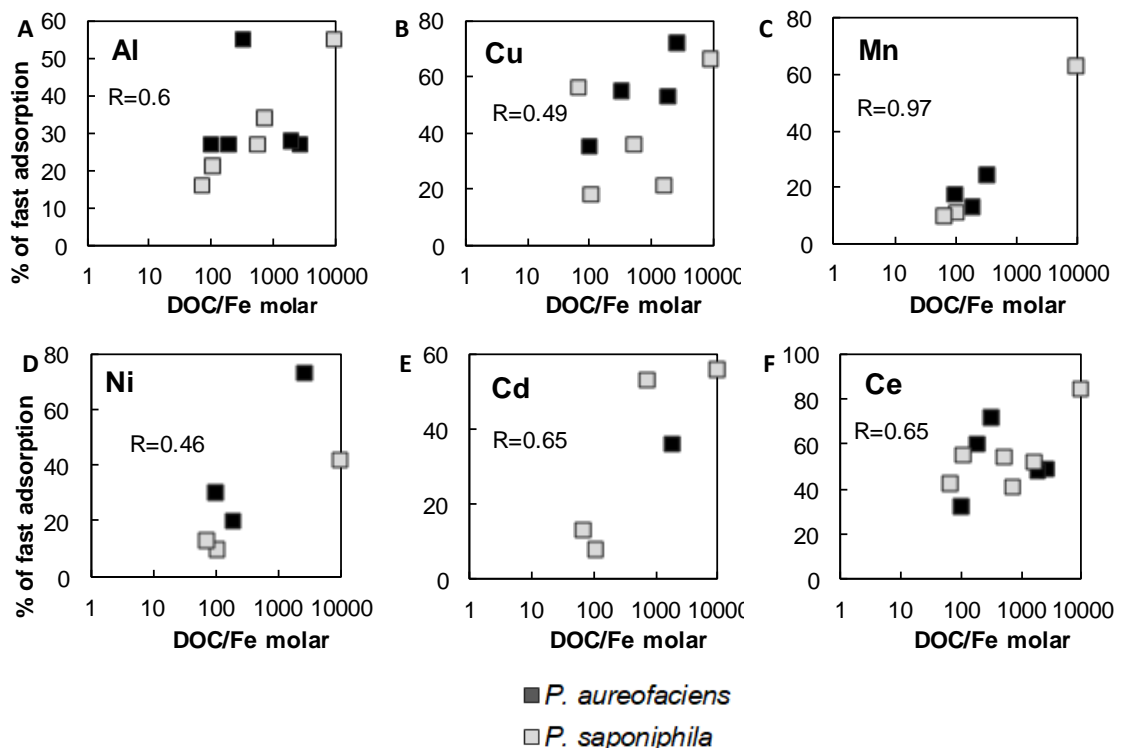


Fig. 3.16. Impact of DOC/Fe ratio in the initial substrate on the percentage of element removal during short-term adsorption (< 1 h) of Al (A), Cu (B), Mn (C), Ni

(D), Cd (E), and Ce (F) in all studied substrates (listed in Table 1). R is for Pearson correlation coefficient. Black and grey squares represent *P. aureofaciens* and *P. saponiphila*, respectively.

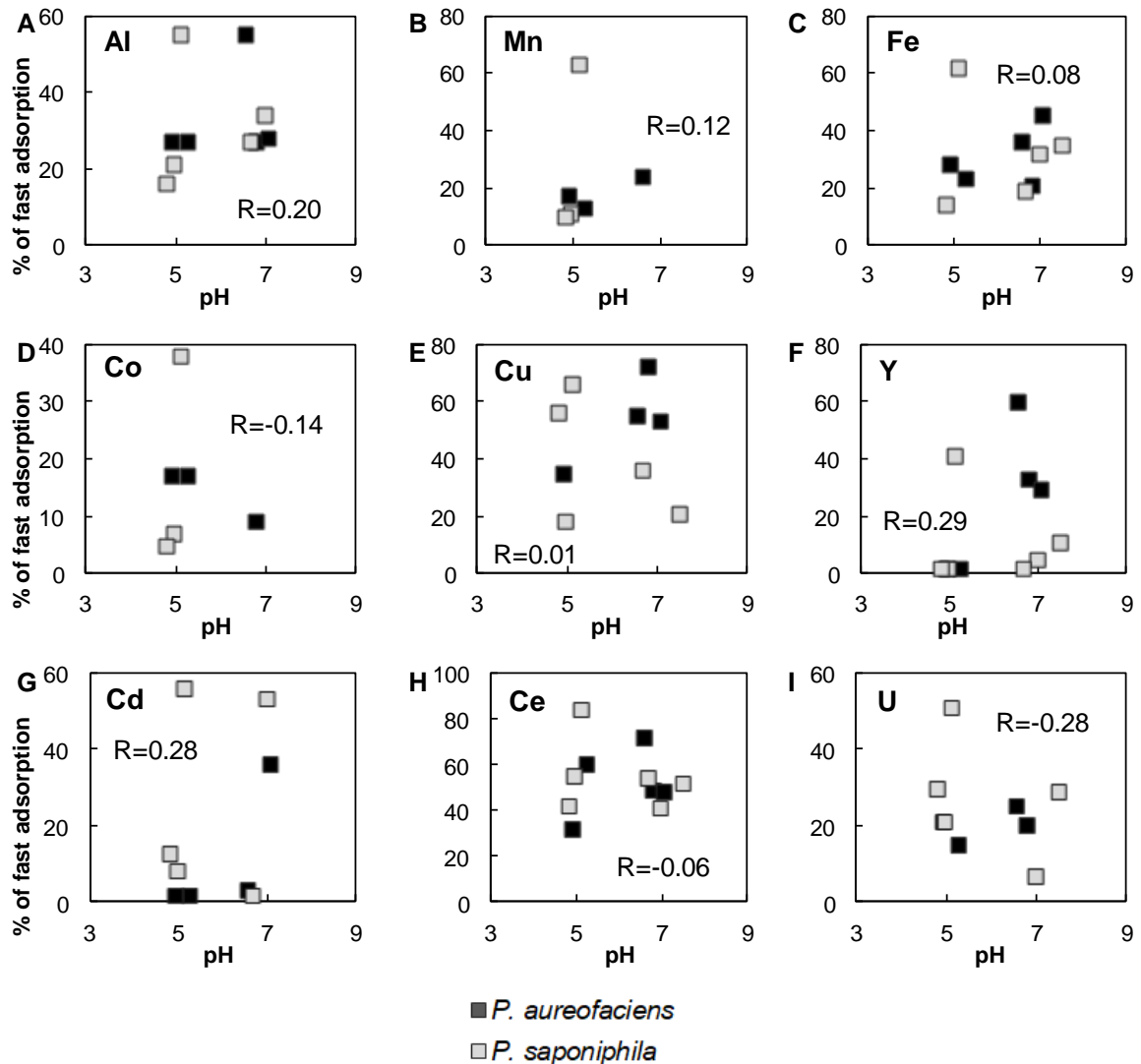


Fig. 3.17. The lack of pH impact on the percentage of element removal during short-term adsorption (< 1 h) of Al (A), Mn (B), Fe (C), Co (D), Cu (E), Y (F), Cd (G), Ce (H) and U (I) in all studied substrates (listed in Table 1). R is for Pearson correlation coefficient. Black and grey squares represent *P. aureofaciens* and *P. saponiphila*, respectively.

3.5.3. Metal speciation and saturation degree of solution

The SHM and NICA-Donnan models yielded similar (within $\pm 10\%$) degree of metal complexation with NOM. This difference between SHM and NICA-Donnan was within the dispersity of experimental measurements and thus only the results of NICA-Donnan are used for discussion. The speciation calculation using vMinteq demonstrated that all trivalent and tetravalent hydrolysates, Cu^{2+} , Pb^{2+} and U^{VI} (except

in oligotrophic Tsipringa lake) are fully complexed with DOM as > 98% of these TE are in the form of complexes with fulvic acids (**Table 3.2**). Alkaline earth elements (Ca, Mg, Sr, Ba), Zn, Mn, Ni and Cd are complexed by 40 to 80% to fulvic acids. Overall, the highest degree of metal complexation with organic ligands is predicted in pine throughfall (> 60% of organic complexes for all TE except alkali) and the lowest in the oligotrophic lake. For divalent micronutrients (Mn, Zn, Ni, Co, Cd), the following order of metal complexation is observed: oligotrophic lake ≤ peat leachate < fen water ~ Vostochnyi stream < humic lake < pine throughfall.

Table 3.2. Element speciation calculation using vMinteq

Component	% organic complexes					
	Tsipringa Lake	Pine crown throughfall	Peat leachate	Fen water	Vostochnyi Stream	Humic lake
Al ³⁺	36.7	99.9	98.8	99.6	96.1	98.8
Ba ²⁺	3.2	63.8	32.6	38.2	25.9	45.2
Ca ²⁺	6.1	65.3	34.5	42.7	37.0	56.5
Cd ²⁺	45.3	78.7	44.4	61.9	77.2	89.4
Ce ³⁺	99.9	99.9	98.7	99.4	100.0	100.0
Co ²⁺	25.2	74.3	41.1	56.3	68.1	83.1
Cu ²⁺	99.8	99.6	85.2	95.4	99.9	100.0
Fe ³⁺	100.0	100.0	99.4	99.9	100.0	100.0
K ⁺	0.1	1.0	0.5	1.0	0.5	0.9
La ³⁺	100.0	99.9	98.7	99.3	100.0	100.0
Mg ²⁺	5.4	64.9	34.0	41.7	34.7	54.3
Mn ²⁺	5.9	65.3	34.5	42.7	36.9	56.5
Na ⁺	0.1	1.0	0.5	1.0	0.5	0.9
Ni ²⁺	59.5	88.7	60.0	79.3	90.4	95.6
Pb ²⁺	98.5	97.0	86.0	95.0	99.5	99.8
Sr ²⁺	3.6	64.0	32.9	38.9	27.7	47.2
Th ⁴⁺	0.0	98.5	90.3	65.1	0.0	0.0
UO ₂ ²⁺	16.3	100.0	99.5	99.8	98.1	99.7
Zn ²⁺	49.0	74.9	43.7	60.2	74.7	87.7

The supersaturation degree of substrates with respect to main possible secondary phases is listed in **Table 3.3**. The oligotrophic lake and pine throughfall were undersaturated with respect to Al-, Si- and Fe-bearing phases, which was consistent with the lack of slow removal of Fe, Al and related metals during interaction with bacteria. The fen water and peat leachate were initially undersaturated with respect to Al hydroxides (S.I. < 0) but oversaturated with respect to ferrihydrite, goethite and lepidocrocite (S.I. = 0.5-1.0, 3.0±0.3 and 1.84, respectively). This was

consistent with the lack of long-term removal of Al but clear removal of Fe (**Figs 3.5 and 3.6**). Finally, humic lake and stream were supersaturated with respect to Al hydroxide and gibbsite as well as lepidocrocite and goethite. In these samples, Al and Fe demonstrated slow decrease of concentration over 4 days of reaction.

Table 3.3. The supersaturation degree of substrates with respect to main possible secondary phases

Mineral	Saturation Index					
	Tsipringa Lake	Pine crown throughfall	Peat leachate	Fen water	Vostochnyi Stream	Humic lake
Al(OH) ₃ (Soil)	< 0	< 0	< 0	< 0	0.90	0.06
Boehmite	< 0	< 0	< 0	< 0	0.62	< 0
Diaspore	1.40	< 0	0.39	0.28	2.32	1.47
Gibbsite	0.54	< 0	< 0	< 0	1.45	0.61
Ferrihydrite	< 0	< 0	0.56	0.01	< 0	< 0
Ferrihydrite (aged)	0.12	< 0	1.07	0.52	0.30	< 0
Lepidocrocite	1.44	< 0	2.39	1.84	1.61	0.56
Goethite	2.32	< 0	3.27	2.72	2.49	1.44
Halloysite	< 0	< 0	< 0	< 0	0.88	< 0
Imogolite	< 0	< 0	< 0	< 0	1.42	< 0
Kaolinite	0.55	< 0	< 0	< 0	3.02	0.66
Quartz	< 0	< 0	< 0	< 0	0.03	< 0

3.6. Discussion

3.6.1. DOC and trace element behavior during biodegradation: short-term adsorption and long-term removal via coagulation and assimilation

The experimental reproducibility of duplicates allowed resolving the fine features of element concentration evolution in the course of experiment. The observed changes in element concentrations are interpreted in terms of main physico-chemical and metabolic processes that may occur in the aqueous solution – organic colloids – bacteria system. Overall, we observed low bio-degradability of DOC over 4 days of experiment. The aquatic bacterium *P. saponiphila* was not capable of producing any measurable DOC decrease in all substrates, and only peat leachate yielded 5±3% decrease in DOC between 1 and 96 h of incubation (**Table 3.4**). In the presence of soil bacterium *P. aureofaciens*, less than 5% of initial DOC was consumed during first hour of exposure. Only humic lake, the stream and fen water produced sizeable decrease in DOC over 4 days of exposure (53, 43 and 33%, see **Table 3.4**). At the same time, the viability of both bacteria remained quite high and the number of live cells did not appreciably decrease over 4 days of experiments. Therefore, the DOM biodegradability by *Pseudomonas* assessed in this study represents the maximal possible rate at already high ($1 \text{ g}_{\text{wet}} \text{ L}^{-1}$) biomass concentration. The maximal values of biodegradability in peat leachate, humic lake and fen water (1, 3 and 4 mg DOC/g_{wet}/day, respectively) are, however, comparable with the range 1 to 3 mg DOC g_{wet}⁻¹ day⁻¹ reported in previous experiments with soil and groundwater bacteria and Siberian permafrost peat and moss leachate (i.e., Shirokova et al., 2017a).

Fast adsorption of TE onto bacterial surfaces was observed during the first hour after the addition of bacterial biomass to filtered substrates, and it affected mostly Al, Fe, Mn, Co, Ni, Cu, Ga, Y, Cd, REEs and U. The pH is expected to be the major controlling factor of cation adsorption on heterotrophic bacterial surfaces (Fein et al., 1997; Gonzalez et al., 2010, 2012; Drozdova et al., 2014), since the deprotonation of amphoteric surface sites increases with the increase in pH. However, the initial fast adsorption was found to be independent on the pH of organic substrate as shown for Al, Fe, Mn, Cu, Co, Cd, Y, and Ce (**Fig. 3.17**). This result is remarkable given that the divalent cations are present as both organic and free complexes and thus should exhibit strong difference in the dependence of their adsorption on pH. It is possible that, at relatively low concentration of free cations in natural DOM-rich substrates, the pH-dependent adsorption edge of these TE is located at pH < 5 (Gonzalez et al., 2010,

2014b; Pokrovsky et al., 2012, 2013b; Oleinikova et al., 2017). Another explanation is that most TEs are > 98% complexed with DOM and thus their free concentration is very low. At high DOC concentration in solution, the organic complexes of metals act as main adsorbates of bacterial surfaces. Besides, Fe-rich colloids may also adsorb onto cell surfaces, and the competition with dissolved Fe(III) may determine the overall adsorption pattern. Only U^{VI} demonstrated some decrease in adsorption with the increase in pH ($R_{Pearson} = -0.28$, **Fig. 3.17 I**) which could be due to the appearance of negatively charged uranyl-carbonate complexes (Ilina et al., 2016; Pokrovsky et al., 2016a) that desorbed U^{VI} at pH ≥ 6.5.

The lack of relationship between the percentage of adsorbed Al, Fe, Cu, Mn, Ni, and La and DOC concentration (**Fig. 3.13**) suggests that the organic complexes of Fe and Al impeded the formation of insoluble Fe and Al hydroxides whereas the divalent metals adsorbed onto the cells in the form of organic complexes. Moreover, a decrease in fast adsorption of Al, Mn, Ni and REE with the increase in Fe concentration in the substrate (**Fig. 3.15**) can be explained by a competition between divalent or trivalent metals and Fe³⁺ and Fe(III) hydroxocomplexes for surface sites. Indeed, the increase in Al, Cu, Mn, Ni, Cd, Ce with the increase in (DOC/Fe)_{molar} of the initial solution (**Fig. 3.16**) clearly indicates that there is a competition of TE with Fe for the adsorption sites on bacterial surfaces whereas DOM does not impede the adsorption of metals. Interestingly that this trend was similar for elements partially (40 to 80%) complexed with organic ligands (Mn, Ni, Co, Cd) and those present as entirely (> 98%) organic complexes (Al, Cu, REEs).

According to vMinteq calculation, Al, Ti, Fe, Cu, and REEs are fully complexed with DOM in all substrates. The ionic charge of organic complexes of these metals should be negative and thus their adsorption onto negatively charged bacterial cells (e.g., Gonzalez et al., 2010) is not expected. However, there was noticeable adsorption of these TE on negatively charged surfaces of *Pseudomonas* strains that implies positive charge of organo-ferric colloids binding TE. These colloids may have Fe oxy(hydr)oxides as main surface moieties, dominated by >FeOH₂⁺ groups at pH < 7 (Stumm, 1992). Such an affinity of colloidal form of trace metals to the surfaces of heterotrophic bacteria was recently demonstrated for *P. saponiphila* on peat leachate and fen water (Oleinikova et al., 2017). A broader significance of the discovered adsorption of organic and organo-Fe colloids is that many other organic surfaces present in soil and river systems such as plant litter, peryphytic biofilms, or submerged vegetation may exhibit high reactivity with respect to colloidal trace metals.

Table 3.4. Integral values (average and standard deviation of the percentage of initial amount) of fast adsorption on the cell walls and slow assimilation/removal of substrate components in the presence of 1 g_{wet} L⁻¹ of *Pseudomonas saponiphila* and *Pseudomonas aureofaciens*. Not listed are Li, B, Si, P, As, Sr, Sb, Hf, Pb, Th showing neither adsorption nor assimilation in the course of experiment. The change in elements concentration which was less than 5% of the initial value was considered as negligible, i.e., within the experimental reproducibility ($\pm 5\%$).

Element	Fast adsorption, % of initial amount										
	<i>Pseudomonas aureofaciens</i>					<i>Pseudomonas saponiphila</i>					
	Humic lake	Vostoch. Stream	Fen water	Peat leachate	Palojoki River	Humic lake	Vostoch. stream	Fen water	Peat leachate	Pine through-fall	Tsipringa Lake
DOC	<5	<5	<5	<5	<5	<5	<5	<5	<5	<5	<5
Al	27±8	28±9	27±2	27±2	55±2	34±2	27±2	21±1	16±2	55±2	<5
Ti	<5	<5	17±4	15±4	<5	<5	<5	<5	<5	<5	<5
V	<5	<5	<5	<5	<5	<5	<5	<5	<5	70±11	<5
Cr	<5	<5	9±2	<5	<5	<5	<5	<5	24±2	<5	<5
Mn	<5	<5	13±2	17±1	24±3	<5	<5	11±1	10±2	63±2	<5
Fe	21±10	45±11	23±2	28±1	36±3	32±2	19±2	<5	14±2	62±4	35±3
Co	9±2	<5	17±1	17±2	<5	<5	<5	7±1	5±3	38±2	<5
Ni	73±32	<5	20±4	30±3	<5	<5	<5	10±1	13±3	42±2	<5
Cu	72±30	53±10	<5	35±2	55±2	<5	36±3	18±2	56±2	66±3	21±9
Ga	<5	<5	45±4	43±3	<5	<5	<5	28±6	<5	21±4	<5
Y	33±8	29±11	<5	<5	60±2	<5	<5	<5	<5	41±2	11±4
Zr	<5	<5	<5	<5	<5	<5	9±2	<5	<5	26±3	<5
Cd	<5	36±22	<5	<5	<5	53±2	<5	8±3	13±3	56±3	<5
La	49±9	57±11	62±2	38±2	74±2	31±2	59±2	57±2	46±2	82±3	36±5
Ce	49±8	48±10	60±2	32±2	72±1	41±2	54±3	55±2	42±4	84±2	52±2
Pr	53±4	49±11	57±2	28±2	71±1	38±2	50±2	52±2	37±3	74±2	43±4
Nd	43±5	52±11	54±2	22±2	81±5	38±3	47±3	12±5	<5	68±3	14±9
Sm	40±19	<5	56±3	21±3	61±2	<5	37±3	50±2	35±5	20±5	46±8
Eu	<5	<5	<5	<5	63±3	<5	<5	<5	<5	<5	32±10
Gd	22±11	29±19	58±3	19±2	66±2	<5	38±3	55±2	42±4	42±8	45±5
Tb	39±21	17±11	55±2	25±4	66	<5	41±2	55±2	14±5	48±4	31±6
Dy	43±8	22±10	51±2	20±2	52±3	<5	32±4	50±2	35±2	45±5	22±10
Ho	32±12	36±11	47±2	13±3	51±3	<5	27±5	47±2	14±4	32±2	<5
Er	27±14	45±14	42±2	17±2	54±4	<5	20±5	40±2	23±3	55±3	<5
Tm	<5	<5	<5	<5	44±5	<5	22±5	34±3	<5	37±8	<5
Yb	<5	28±16	31±2	<5	38±5	<5	13±7	25±2	<5	53±4	<5
Lu	<5	<5	25±5	<5	46±2	<5	<5	26±2	<5	40±4	<5
U	20±10	<5	15±2	21±2	25±3	7±5	<5	21±2	30±3	51±2	29±4

Table 3.4, continued.

Slow assimilation/removal, % of initial amount											
Element	<i>Pseudomonas aureofaciens</i>					<i>Pseudomonas saponiphila</i>					
	Humic lake	Vostoch. stream	Fen water	Peat leachate	Palojoki river	Humic lake	Vostoch. stream	Fen water	Peat leachate	Pine through-fall	Tsipringa lake
DOC	53±7	43±3	33±5	<5	<5	<5	<5	<5	5±3	<5	<5
Al	21±8	12±9	<5	<5	<5	9±2	18±4	<5	<5	<5	<5
Ti	<5	<5	<5	10±5	<5	<5	<5	<5	10±3	<5	<5
V	<5	<5	<5	<5	<5	<5	<5	<5	<5	<5	<5
Cr	<5	<5	<5	<5	<5	<5	<5	<5	<5	<5	<5
Mn	<5	<5	11±2	35±2	<5	<5	<5	<5	9±2	9±2	<5
Fe	14±10	14±10	23±2	22±2	37±3	7±1	10±2	18±2	15±2	<5	<5
Co	<5	<5	12±2	26±3	<5	<5	<5	<5	<5	<5	<5
Ni	<5	<5	12±5	16±2	<5	<5	<5	<5	<5	<5	<5
Cu	<5	<5	<5	<5	<5	<5	<5	<5	<5	<5	<5
Ga	<5	<5	<5	<5	<5	<5	<5	<5	<5	<5	<5
Y	25±8	23±11	<5	<5	<5	<5	19±4	<5	<5	42±2	<5
Zr	<5	<5	<5	<5	23±8	<5	<5	<5	<5	<5	<5
Cd	35±7	<5	<5	<5	<5	<5	<5	34±3	47±3	<5	<5
La	<5	<5	<5	<5	<5	20±5	<5	<5	<5	<5	29±5
Ce	<5	<5	<5	<5	<5	21±6	<5	<5	<5	<5	<5
Pr	<5	<5	<5	<5	<5	31±5	<5	<5	<5	<5	<5
Nd	<5	<5	<5	<5	<5	27±3	7±3	<5	<5	<5	36±9
Sm	<5	<5	<5	<5	<5	49±4	17±3	<5	<5	54±5	<5
Eu	<5	<5	<5	<5	<5	<5	<5	<5	<5	<5	<5
Gd	<5	<5	<5	<5	<5	47±9	16±3	<5	<5	29±8	<5
Tb	<5	<5	<5	<5	<5	67±4	10±3	<5	<5	37±4	<5
Dy	<5	<5	<5	<5	<5	52±6	15±4	<5	<5	41±5	45±10
Ho	<5	<5	<5	<5	<5	55±8	17±5	<5	<5	<5	<5
Er	<5	<5	<5	<5	<5	61±4	16±5	<5	<5	<5	42±5
Tm	<5	<5	<5	<5	<5	51±5	21±5	<5	<5	<5	<5
Yb	<5	<5	<5	<5	<5	40±6	27±6	<5	<5	<5	<5
Lu	<5	<5	<5	<5	<5	44±7	32±7	<5	<5	<5	<5
U	<5	<5	<5	<5	<5	<5	<5	<5	<5	<5	<5

A long-term (1 – 96 h) decrease of TE concentration could be linked to consumption of DOM by heterotrophic bacteria and releasing the elements that were bound to organic colloids. Such a release could coagulate metal hydroxides thus decreasing the concentration of dissolved TE. Note that the removal of aqueous Fe via formation of insoluble Fe hydroxide on bacterial surfaces has been recently evidenced in the experiments with *Caulobacter*-dominated bacterial communities grown on Fe- and nutrient-enriched humic boreal water (Xiao et al., 2016). The removal of Fe and Al in the form of particulate Fe or Al hydroxide could occur as a result of (i) precipitation of Fe or Al hydroxides from initially supersaturated solutions, triggered by bacterial cells that could serve as nuclei and (ii) liberation of part of Fe from organic complexes after bacterial degradation of DOM that stabilized Fe(III) polymers in solutions. Although we observed some secondary precipitates near the cells after reaction (**Fig. 3.1 E**), a confirmation of Fe hydroxide formation was not possible without in-situ elementary analyses of cell biomass and inorganic precipitates in the course of experiment.

The elements that could be affected by long-term removal in the form of hydroxide were trivalent and tetravalent hydrolysates such as Al, Y, REEs, Ti (only in peat leachate), and Zr (only in the Palojoki River). These elements can coprecipitate with Fe oxyhydroxides in boreal waters (Vasyukova et al., 2010; Ilina et al., 2016). The DOM is capable to efficiently stabilize Fe(III) hydroxide in aqueous solution and prevent coagulation of colloidal Fe hydroxide. The EPS which are produced by heterotrophic bacteria are also capable to stabilize the metals in the vicinity of the cells (i.e., Tourney and Ngwenya, 2014). Former studies of Fe (II, III) interaction with heterotrophs demonstrated that, in the presence of surface organic ligands not screened by EPS layers, the polymerization of Fe(III) ions and formation of Fe-oxy(hydr)oxides is partially inhibited (Gonzalez et al., 2014b, Fakih et al., 2008). As a result, the adsorbed Fe(III) remains on the cell surface in the form of individual Fe atoms attached to organic moieties, conferring several advantages to the cells (Châtellier et al., 2004; Chan et al., 2009). The decrease of Fe(III) polymerization due to complexation with ligands was also demonstrated by EXAFS spectroscopy for Fe(III) interaction with soil organic functional groups (Karlsson et al., 2008).

A cartoon of *Pseudomonas* interaction with DOM and Fe hydroxide colloids is shown in **Fig. 3.18**. The adsorption of organo-ferric colloids is driven by electrostatic interaction between negatively charged bacterial cells and positively charged Fe-rich

colloids (**Fig. 3.18 A**). The higher the ratio of Fe/DOC in the initial substrate, the stronger the positive charge of colloids and thus the coverage of cell surface by adsorbed Fe. Since anionic sites of the cell surface may be screened by DOM-stabilized Fe hydroxides, the adsorption of trace metals competes with that of Fe and thus there is an increase in TE adsorption with an increase in DOC/Fe. At the highest values of DOC/Fe such as those in pine throughfall, the cell surfaces are not «screened» by abundant colloids and thus the interaction of divalent and trivalent cations with *Pseudomonas* cells is considerable. The adsorption of trace metals is minimal at low DOC/Fe in aqueous solution, when the cell surfaces are surrounded by positively charged organo-ferric colloids.

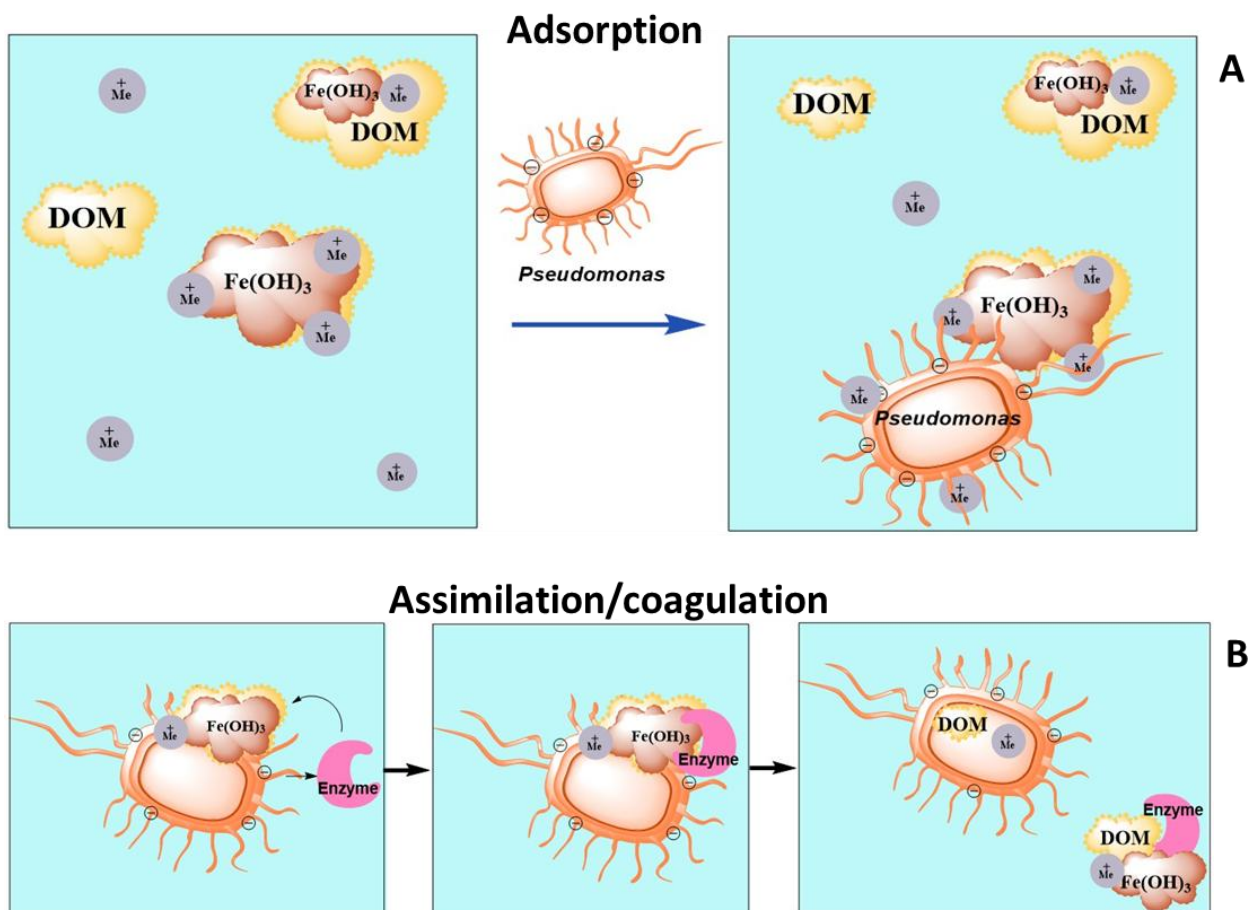


Figure 3.18. Cartoon of interaction between Fe-rich colloids and live *Pseudomonas* and dissolved ($< 0.45 \mu\text{m}$) metals ($\text{Me}^+(\text{aq})$) interaction with bacteria via adsorption (A) and assimilation/coagulation (B). Bacterial activity preferentially removed Fe over DOC from organo-mineral colloids; trace metals coprecipitated with coagulating Fe oxy(hydr)oxide. The heterotrophic bacterium processed colloids essentially via short-term adsorption of on cell surface (Al, Mn, Ni, Cu, Ga, Y, REE, U) and extracellular coagulation in the form of Fe hydroxides (Ti, Zr, Nb).

The maximal decrease of DOC concentration in the course of experiment was ca. 17 mg L⁻¹, which occurred over 96 h in fen water. During this period, the biomass of *P. aureofaciens* remained at 0.86±0.06 g_{wet} L⁻¹. Thus, the maximal possible biomass decrease of 0.06 g_{wet} L⁻¹ was equivalent to 3.75 mg L⁻¹ DOC (assuming humid/dry ratio of 8 and 50% of biomass composed of C). This value is much smaller than the overall DOC concentration decrease and thus the majority of DOC was presumably converted into CO₂ and DIC rather than into bacterial biomass. Similarly, for trace metal, active intracellular assimilation is less likely than the extracellular precipitation in the form of Al and Fe hydroxides. Specifically, the mechanism of long-term C_{org} and TE removal depicted in **Fig. 3.18 B** may include the production of enzymes by heterotrophic bacteria that interact with substrate (organic and organo-mineral colloids). This lead to dissociation of organic matter and Fe (III) and subsequent coagulation of Fe(III) hydroxides.

3.6.2. Heterotrophic bacteria control on carbon and trace metals in boreal organic-rich waters

The present study aimed at testing, using a suite of various contrasting organic substrates, the existing paradigm that the heterotrophic bacterioplankton efficiently mineralizes allochthonous DOM in organic-rich waters (Tranvik, 1998a, b; Tranvik and Jorgensen, 1995; Kritzberg et al., 2004; Jansson et al., 2000, 2007; Ask et al., 2008). In boreal rivers and lakes, heterotrophic bacteria can consume approximately 10% of DOC on the time scale of 5 to 14 days (Berggren et al., 2007, 2010). In Alaskan Arctic streams, between 4 and 46% of DOC was biodegraded over 40 days (Larouche et al., 2015) whereas in the Yukon River, 13 to 21% of the DOC was biodegradable on an annual basis (Wickland et al., 2012). For peat-covered catchments in Finland, from 4 to 8% of DOC was biodegradable over < 2 months (Hulatt et al., 2014; Asmala et al., 2014a). In Scottish moorland stream, less than 19% of DOM was biodegradable during 41-days incubation (Stutter et al., 2013). These numbers are generally higher than the degree of DOC removal in the bacterial experiments with *P. saponiphila* monocultures conducted in this study (5±5 %) over 4 days.

The absolute rates of C processing via bacterial respiration in high-latitude inland waters are more variable and range from 0.1 mg C L⁻¹ day⁻¹ to as high as 8.6 mg C L⁻¹ day⁻¹ in a temperate creek (Berggren et al., 2007). Heterotrophic bacteria from a subarctic lake consumed lake water DOC over first 48 h with a rate of 0.09 mg C L⁻¹

d^{-1} , whereas the DOC consumption from adjacent peat soil was five times higher (Roehm et al., 2009). Finally, humic lakes of Siberian thermokarst zone located entirely within frozen peat substrate exhibited bacterial mineralization rate of 0.3 to 0.4 mg C L $^{-1}$ day $^{-1}$ (Shirokova et al., 2013a).

Over 4 days of exposure of various organic substrates to soil and aquatic bacteria in this study, the DOC concentration decreased at a maximal rate of 4.3 ± 0.3 mg C L $^{-1}$ day $^{-1}$ in fen water with *P. aureofaciens*, whereas the other studied substrates yielded an order of magnitude lower biodegradation rates. However, we used about 3 order of magnitude higher bacterioplankton concentrations in the experiments compared to that reported in natural sites. Presumably, the intensity of bacterial degradation of DOM during several days in the experimental reactors is not directly proportional to the concentration of either aquatic or soil heterotrophic bacteria. Taken together, the studied organic substrates, which contained essentially allochthonous DOM, were quite weakly impacted by heterotrophic bacterial activity. The increase in the aromaticity of DOM in the course of experiment (see section 3.1) suggests preferential utilization of non-aromatic, aliphatic carbon compounds of low molecular weight. This is consistent with well-known observation that the soil and peat DOM are much less biodegradable than the aquagenic DOM (Nguyen and Hur, 2011). The substrates (streams, rivers, humic lake, peat leachate and pine throughfall) were presumably quite poor in freely bioavailable nutrients and organic acids. The low ability of heterotrophic bacteria to process allochthonous carbon is due to its recalcitrant aromatic and reduced nature (Hessen and Tranvik, 1998). For this reason, the ability of native bacteria to process allochthonous carbon is taxonomically limited (Jones et al., 2009). In particular, the dominant phylotypes in the bacterioplankton communities of boreal humic lake were *Actinobacteria* and *Verrucomicrobia* whereas the addition of plant litter leachate induced the dominance of *Proteobacteria* (Haukka et al., 2005). Recently, it has been shown that in boreal subarctic rivers, which were very similar to the environmental context of this study, the low molecular weight carbon was available to all bacterial communities for utilization, whereas the ability to degrade high molecular weight carbon was limited to a few taxa (Logue et al., 2016). It is thus possible that allochthonous (terrestrial) organic compounds studied in this work are quite poor substrates for heterotrophic *Pseudomonas* Gammaproteobacteria. As such, efficient biodegradation of natural refractory DOM from peat bog and soil litter occurs at microbial concentrations that are orders of magnitude lower than those

in the present study. Most likely, the biodegradation in natural settings requires the metabolic action of bacterial consortia. Compared to aquatic *P. saponiphila*, soil heterotrophs *P. aureofaciens* were efficient in degradation of DOM from larger amount of substrates, probably due to their higher metabolic versatility, acquired under variable soil micro-environments.

The degradability of dissolved trace metals by culturable heterotrophs was even lower than that of DOM. The majority of metals were removed during short-term surface adsorption rather than long-term metabolic assimilation or coagulation. In natural settings, the role of surface adsorption in metal removal by heterotrophic bacteria should be negligible because the typical concentration of bacteria in boreal waters is 2 to 3 orders of magnitude lower than that used in this study. Only Fe demonstrated non-negligible ($\geq 10\%$) long-term assimilation by cells or metabolically induced precipitation of Fe(III) hydroxide. An important natural consequence of this experimental result is that heterotrophic bacterial activity may decrease the magnitude of boreal waters browning, i.e., increase in Fe concentration in natural waters over past decades (Kritzberg and Ekstrom, 2012; Weyhenmeyer et al., 2014). Some insoluble trivalent (Al, Y, REE) and tetravalent (Ti, Zr) elements may be partially removed together with Fe, whereas the rise in concentration of other trace metals, reported in boreal waters over decadal scale of observation (Huser et al., 2011) is unlikely to be attenuated by heterotrophic bacterial metabolism. Another interesting consequence of obtained results is that there could be a decoupling between DOC and metal concentration rise in subarctic river. Due to higher resistivity of metals to in-stream microbial transformation processes, the surface waters may become progressively enriched in metals relative to DOC.

3.7. Conclusions

All 7 natural organic substrates from subarctic landscape containing essentially allochthonous DOM were weakly impacted by heterotrophic bacterial activity. Only 3 substrates (humic lake, stream and fen water) were sizably biodegraded over 4 days of incubation in the presence of soil heterotroph *P. aureofaciens*. Aquatic heterotroph *P. saponiphila* degraded $\leq 5\%$ of DOC in peat leachate without sizeable ($> 5\%$) effect on other substrates. During interaction between heterotrophic bacteria and various aquatic substrates from the subarctic zone, the short-term (< 1 h) adsorption on the cell surfaces of Al, Fe, Mn, Ni, Co, Cu, Cd, REEE, U^{VI} strongly dominated over long term (1 h – 96 h) removal. Only a few elements (DOC, Al, Mn, Fe, Co, Ni, Cd and in a lesser degree, Ti, Y and REEs) exhibited a 10 to 40% long-term removal (1 – 96 h of exposure) linked to either intracellular assimilation or extracellular precipitation in the form of iron hydroxide. This removal occurred in the fen water, humic lake, stream water, and peat leachate. The removal of Ca, Mg, Y, and REEs from pine throughfall ranged from 30 to 40%. Among different substrates, there was an increase in the adsorption with the increase of DOC/Fe ratio in solution, which can be linked to a competition between Fe and metal cations for anionic adsorption sites on cell surface. The long-term removal of dissolved metals did not show any link to pH, DOC, and Fe concentration. However, there was a consistency between long-term element removal and initial supersaturation degree with respect to main secondary phases (Fe and Al oxy(hydr)oxides).

The rate of long-term DOC mineralization in the experiment (0 to 4.3 mg C L⁻¹ day⁻¹ depending on substrates) was comparable to or lower than that reported in natural peatland waters, despite that the experimental concentration of live bacteria was several orders of magnitude higher than the natural one. This confirms quite low degradability of allochthonous boreal DOM by studied heterotrophic bacteria.

3.8. Acknowledgements

We acknowledge the main support from RSF (RNF) grant No 15-17-10009 “Evolution of thermokarst lake ecosystems” (experiments, analysis) and RFBR grants No 15-05-05000_a, 16-55-150002_a, 16-05-00542_a, and 17-05-00342_a. Additional support was from RSF № 14-50-00029 (bacterial separation, modeling). Liza Ruiz is thanked for help on bacterial culturing.

**Chapitre 4. Dissolved organic matter degradation by
sunlight coagulates organo-mineral colloids and
produces low-molecular weight fraction of metals in
boreal humic waters**

**Transformation des colloïdes organo-minéraux sous la
lumière du soleil dans les eaux humiques boréales : le
devenir du carbone organique et des microéléments**

Geochimica et Cosmochimica Acta, 2017, **211**, 97-114



Dissolved organic matter degradation by sunlight coagulates organo-mineral colloids and produces low-molecular weight fraction of metals in boreal humic waters

Olga V. OLEINIKOVA^{1,2}, Olga Yu. DROZDOVA², Sergey A. LAPITSKIY²,
Vladimir V. DEMIN³, Andrew Yu. BYCHKOV² and Oleg S. POKROVSKY^{1,4,5*}

¹ GET (*Geosciences and Environment Toulouse*) UMR 5563 CNRS, 14 Avenue
Edouard Belin, 31400 Toulouse, France

² Geological Faculty of Moscow State University, 1 Leninskie Gory, 119234 Moscow,
Russia

³ Institute of Soil Science MSU-RAS, 1 Vorobievy Gory, 119234 Moscow, Russia

⁴ N. Laverov Federal Center for Integrated Arctic Research, Russian Academy of
Science, Arkhangelsk, Russia

⁵ BIO-GEO-CLIM Laboratory, Tomsk State University, 36 Lenina av., 634050 Tomsk,
Russia

4.1. Résumé

La dégradation photochimique de la matière organique dissoute (MOD), au même titre la minéralisation bactérienne, est reconnue comme une source significative des émissions de CO₂ depuis les eaux de surface des hautes latitudes vers l'atmosphère. Les travaux sur l'oxydation photochimique de MOD sont nombreux et l'étude de la chimie du carbone organique dissout (COD) et de son devenir se développe rapidement, cependant le comportement des microéléments pendant la photodégradation de MOD reste pratiquement inconnu. Cette information est particulièrement importante vu que la plupart des microéléments dans les eaux boréales sont contenus dans les colloïdes organiques et organo-minéraux. Pour mieux comprendre les évolutions des concentrations, des répartitions entre les différentes fractions colloïdales et dissoutes, des spéciations des microéléments dans les eaux boréales soumises au rayonnement solaire, nous avons effectué des expériences de photo-dégradation in situ sur des eaux de rivière et de tourbière d'un site vierge de tout activité humaine de la Carélie du Nord (subarctique russe).

Après 5 jours d'exposition, la photodégradation de la MOD de la rivière était beaucoup moins importante que celle dans l'eau de tourbière, avec respectivement 25% et 60% de baisse relative de concentration en COD.

La concentration du Fe et de l'Al ne diminuent au cours de l'expérience de photodégradation que dans l'eau de la tourbière (90% et 50% respectivement, au 5ème jour de d'expérience), alors qu'aucune diminution détectable de la concentration d'Al et de Fe (<0.22 µm) n'a été observée dans l'eau de la rivière boréal. Un certain nombre de microéléments faiblement solubles liés à des colloïdes organo-ferriques ont le même comportement que Fe pendant l'exposition de l'eau de tourbière à la lumière solaire: Al, P, Ti, V, Cr, As, Y, Zr, Nb, REE, Hf, Th, Pb et U. Un deuxième groupe d'éléments (Li, B, Mg, Ca, Sr, Ba, Na, K, Rb, Si, Mn, Ni, Cu, Co, Cd, Sb) était indifférent à la photodégradation de MOD, certains présentant des fluctuations erratiques (\pm 10-15% du témoin) au cours de l'exposition à la lumière.

L'évolution des répartitions des éléments entre les différentes fractions colloïdales et dissoute pendant la photo-dégradation a été évaluée par ultrafiltration à travers des membranes de 10 et 1 kDa d'Amicon au début de l'expérience, ainsi qu'après 100 h et 193 h d'exposition. Au cours de l'exposition au soleil, la fraction dissoute stricto sensu (poids moléculaire faible <1 kDa) et les fractions colloïdales fine et grossière (1 à 10 kDa et 10 kDa à 0.22 µm)) de l'eau de la rivière ont présenté une stabilité élevée.

En revanche, l'insolation de l'eau de la tourbière produisait une quantité significative de COD, Al, Fe, U, Mg, Ca, Mn, Co, Ni, Sr, Cd and Ba sous forme dissoute, avec des augmentations de concentrations dans la fraction <1 kDa d'un facteur 3 ± 1 suivant les éléments. Il y avait un enrichissement préférentiel de la fraction dissoute <1 kDa en Fe, Al, Ca, Mg et d'autres métaux divalents par rapport au COD.

Le réchauffement climatique conduisant à l'élévation de la température de l'eau dans la zone boréale conduira à une intensification des processus de flocculation / sédimentation des hydroxydes de Fe et d'Al, ainsi qu'à une augmentation des productions de matière organique de dissoute stricto sensu (<1 kDa) et de complexes organo-métalliques.

Mots clés: *photodégradation, Arctique, fer, carbone organique, éléments traces, complexation, fractionnement granulométrique*

4.2. Abstract

Photochemical degradation of dissolved organic matter (DOM) is recognized as the major driver of CO₂ emission to the atmosphere from the inland waters of high latitudes. In contrast to numerous studies of photo-induced DOM transformation, the behavior of trace element (TE) during photodegradation of boreal DOM remains virtually unknown. Towards a better understanding of concentration, size fractionation and speciation change of DOM and TE in boreal waters subjected to solar radiation, we conducted on-site photo-degradation experiments in stream and bog water collected from a pristine zone of the Northern Karelia (Russian subarctic). The removal of Fe and Al occurred only in the bog water (90 % and 50% respectively, over 5 days of reaction), whereas no detectable decrease of dissolved (< 0.22 µm) Al and Fe concentration was observed in the boreal stream. A number of low-soluble TE linked to Fe-rich organo-mineral colloids followed the behavior of Fe during bog water exposure to sunlight: Al, P, Ti, V, Cr, As, Y, Zr, REEs, Hf, Th, Pb and U. The second group of elements (Li, B, Mg, Ca, Sr, Ba, Na, K, Rb, Si, Mn, Ni, Cu, Co, Cd, Sb) was indifferent to photodegradation of DOM and exhibited a non-systematic variation ($\pm 10\text{-}15\%$ from the control) of < 0.22 µm fraction in the course of sunlight exposure. The bog water insolation yielded a factor of 3 ± 1 increase of low molecular weight (LMW < 1 kDa) fraction of organic carbon, Al, Fe, U, Mg, Ca, Mn, Co, Ni, Sr, Cd and Ba after 200 h of sunlight exposure compared to the dark control. The LMW < 1 kDa fraction was preferentially enriched in Fe, Al, Ca, Mg and other divalent metals relative to C_{org}. The climate warming leading to water temperature rise in the boreal zone will intensify the Fe and Al hydroxide coagulation while increasing the production of LMW organic ligands and free metals and metal - organic complexes.

Key words: photodegradation, Arctic, iron, organic carbon, trace element, complexation, size fractionation

4.3. Introduction

Photochemical mineralization of dissolved organic carbon (DOC), nitrogen and phosphorus greatly regulates biogeochemical cycle of nutrients via changing their bioavailability (Cotner and Heath, 1990; de Haan, 1993; Miller and Zepp, 1995; Moran and Zepp, 1995; Bushaw et al., 1996; Zepp et al., 1998; Wetzel et al., 1995;

Tarr et al., 2001; Vähäalto et al., 2003; Kopácek et al., 2003; Vähäalto and Wetzel, 2004) which in turn contributes to the intensity of CO₂ emission from the inland waters to the atmosphere (Cory et al., 2013, 2014). A growing understanding that photochemical oxidation of dissolved organic matter (DOM) significantly exceeds the bacterial respiration in the Arctic and subarctic waters (Cory et al., 2007, 2014, 2015) greatly stimulated the progress in characterization of chemical and structural properties of DOM photoproducts (Gonsior et al., 2013; Ward and Cory, 2016). At the same time, the fate of major and trace element (TE), linked to DOM in the form of colloids, during sunlight exposure of inland waters remains poorly unknown, except several laboratory studies of Fe transformation in temperate stream and soil fulvates and humates (Garg et al., 2013a, b; Porcal et al., 2009a, b, 2013a, b, 2015) and estuarine zones (Blazevic et al., 2016). The only study which addressed the concentration and speciation of various TE, in addition to Fe, during photo-oxidation of DOM is that of Shiller et al. (2006) on relatively organic- and Fe-poor (DOC = 7 mg/L, Fe = 140 µg/L) temperate river.

Over past decade, substantial progress has been achieved in characterizing colloidal transport of DOC, major and trace element in humic-rich waters of the subarctic as a function of lithology (Vasyukova et al. 2010), latitude (Pokrovsky and Schott 2002) and season (Ingri et al., 2000; Andersson et al., 2001, 2006; Dahlqvist et al., 2004, 2007; Shiller, 2010; Lyvén et al., 2003; Pokrovsky et al. 2010; Bagard et al. 2011; Stolpe et al. 2013a, b). Colloidal status of TE is especially important for DOC- and Fe-rich surface waters, typical for bogs and streams dominating high latitude taiga and tundra zone. A recent study of our group (Ilina et al., 2016) quantified the transformation of colloids between their sources (soil solutions and bog waters), the transporters (rivers and streams) and the receptor zones (lakes). Such a hydrological continuum (soil – bog – river – lake) is most typical for European boreal regions (e.g., Kothawala et al., 2006; Laudon et al., 2011; Lidman et al., 2012, 2014). In accord with previous studies of landscape continuum in the artic and subarctic zone (Lapierre and del Giorgio, 2014; Vonk et al., 2015a, b), we hypothesized that the two main processes responsible for transformation of colloids during water travel from the soil or bog to the river are bio- and photo-degradation of dissolved organic matter (Ilina et al., 2013, 2014, 2016).

For distinguishing bio- and photo-transformation and assessing the rates and mechanisms of photo-degradation, controlled incubation experiments are necessary,

and a number of experimental studies elucidated the efficiency of DOM photo-degradation in the Arctic (Cory et al., 2014; Ward and Cory, 2016; Stubbins et al., 2016), boreal (Salonen and Vähäalto, 1994; Lindell et al., 2000; Tranvik and Bertilsson, 2001; Köhler et al., 2002; Porcal et al., 2014; Groenveld et al., 2016), temperate (Xu and Jiang, 2013) and tropical (Suhett et al., 2007; Stubbins et al., 2010; Spencer et al., 2009) settings. The overwhelming majority of these studies analyzed concentrations and molecular properties of DOM and only a few works in DOM-poor waters addressed photo-oxidation and photo-reduction of Fe and other inorganic components in natural waters, such as DOM-poor acidic lakes and seawater (Waite and Morel, 1984; Collienne, 1983; Anderson and Morel, 1982; Porcal et al., 2004) or the subtropical swamp water (Helms et al., 2013). Few works on Fe-and Al-rich acidic waters and artificial DOM-rich solutions demonstrated the possibility of colloid coagulation and Fe/Al hydroxide precipitation after photo-degradation of DOM-metal complexes (Helms et al., 2013; Kopacek et al., 2005, 2006). Photo-oxidation of DOM in a temperate river produced a decrease in dissolved ($< 0.02 \mu\text{m}$) Fe and a number of TE associated with Fe and organic colloids such as Co, Ni, Cu, Cr, V, Ce, Pb, U (Shiller et al., 2006).

As a working hypothesis, we expect significant vulnerability to sunlight of organic colloids and associated metals from freshly exposed acidic bog waters and much higher stability of already partially processed organic complexes of metal in circum-neutral stream waters. Moreover, the major organic and, presumably, metal pools in boreal waters – organic and organo-mineral colloids (1 kDa – $0.22 \mu\text{m}$) – are likely to be transformed either to coarse particles ($> 0.22 \mu\text{m}$) thus being removed from solution or to low molecular weight LMW_{< 1 kDa} forms, remaining in solution after sunlight exposure. Besides, photo-oxidation of low-molecular-weight DOM may occur which leads to precipitation of the released Fe(III) as additional colloidal FeOOH (Shiller et al., 2006). To test these hypotheses, we exposed sterile-filtered water to sunlight in UV-transparent reactors and we monitored the concentration of DOC and TE during 2 weeks of reaction. In addition, we employed the ultrafiltration through 1 and 10 kDa membranes in the course of experiment to unravel the colloidal size transformation. Specific goals of this study were (*i*) quantify the evolution of DOC, Fe and trace element in the course of sunlight exposure; (*ii*) distinguish the elements linked to organic-rich and Fe-rich colloids depending on DOC/TE and DOC/Fe ratio evolution; (*iii*) characterize the evolution of elementary composition of

colloids (1 kDa – 0.22 µm), and *iv*) verify the appearance of LMW organo-metal complexes in the course of irradiation. We anticipate that, via selecting two highly contrasting water objects for this study – bog water and stream – and taking the advantage of well-studied landscape continuum, we can adequately assess the degree of colloidal transformation in chosen boreal setting and upscale the obtained results to surface waters of the European subarctic.

4.4. Sampling, materials and methods

4.4.1. Environmental setting

The climate, topography, soil and vegetation of Northern Karelia where the sampling was performed are described in previous works of our group (Ilina et al. 2013, 2014, 2016). Within the hydrological continuum created by glacial processes around 8-10 thousand year ago, the water and soluble compounds travel from the peat mire zone to the adjacent small humic lakes and further downstream the river to a large oligotrophic lake. Two contrasting samples were collected in Northern Karelia in July 2015, during summer baseflow period. The Palojoki River of the Pyaozero Lake basin, with a watershed area of 32 km², was sampled in the middle course of the flow (sample KAR-1, described in details in Ilina et al., 2016). This river is fed by a minerotrophic bog with a surface area of 1.2 km². The bedrock composition of the catchment includes granites, gneisses, syenites, and syenite-diorites of the low-Proterozoic and low-Archean, covered by glacial Quaternary deposits. Similar minerotrophic bog adjacent to the western coast of the Tsipringa Lake has 1.19 km² area and underlains by Early-Archean biotite granito-gneisses (sample ZPBL, described in details in Ilina et al., 2013). The studied surface waters are oxygenated and organic- and Fe-rich (pH = 7.1, DOC = 12 mg/L, Fe = 130 µg/L in KAR-1; pH = 5.5, DOC = 40 mg/L, and Fe = 4000 µg/L in ZPBL) and fairly stable in major chemical composition over past 5 years of summer sampling (end of July – beginning of August). The stream contained lower fraction of high molecular weight (HMW) organic colloids (0.4 µm – 10 kDa) compared to the bog (10% and 69%, respectively) as shown in our previous studies in this region (Ilina et al., 2014, 2016). The LMW_{< 1} kDa fraction of DOC was a factor of 2 higher in the stream compared to the bog (77 and 28.5%, respectively).

4.4.2. Experimental setup

The conceptual scheme of experiments is presented in **Fig. 4.1**. The stream and bog waters were collected in large pre-cleaned polypropylene jars and processed on-site, within 2 h after sampling, in the field-constructed clean laboratory (see description in Ilina et al., 2013). Sterile filtration was performed using single-used Sartorius polystyrene vacuum filtration units (0.22 µm, 250 mL volume) in cleaned, detergent-sterilized polyethylene-covered bench in the proximity of alcohol-based open flame. Filtered fluids were transferred into two types of reactors: (*i*) 270-mL sterilized quartz flasks, filled with 10% air headspace and covered by porous sterile stoppers and (*ii*) 35-mL polysterene Petri dishes, covered by sterile 7.5 µm-thick PVC film, permeable to O₂. This film was fully transparent to UV as verified by measurements using a UV-VIS spectrophotometer Analytik Jena - SPECORD® 50. The dark control of both quartz flasks and Petri dishes was identical to the light samples except that the reactors were wrapped in Al foil. Both dark and light reactors were run in duplicates and they were placed on flat surface at the border of the lake (66°17'04.19"N, 30°52'05.02"E) and exposed to direct unshaded sunlight from July 9 to July 20. The temperature of the experimental reactors followed the diurnal cycle and was equal to 18 ± 5°C over 250 h of exposure. The duplicate samples were collected daily from Petri dish (PVC) reactors. The quartz reactors were sampled after 0, 4 and 8 days of exposure of the bog water (ZPBL) and after 0, 5 and 10 days of exposure of the stream (KAR-1). For each sampling, the whole reactor was sacrificed. The samples were immediately filtered through 0.22 µm Sartorius single-used filter into pre-cleaned polypropylene vials for analysis of trace metals (after acidification by bi-distilled HNO₃) or without acidification for DOC, UV_{254 nm}, DIC and anions analyses. The 0.22 µm filtrate from quartz reactors was additionally ultrafiltered through 1 and 10 kDa regenerated cellulose single-used filters using Amicon 8400 frontal Ultrafiltration unit (continuously stirred 400-ml polycarbonate cell maintained under 1.5–2 atm pressure). Details of ultrafiltration procedure in humic boreal waters of N. Karelia and discussion of possible artifacts are presented elsewhere (Vasyukova et al., 2010; Ilina et al., 2013, 2016).

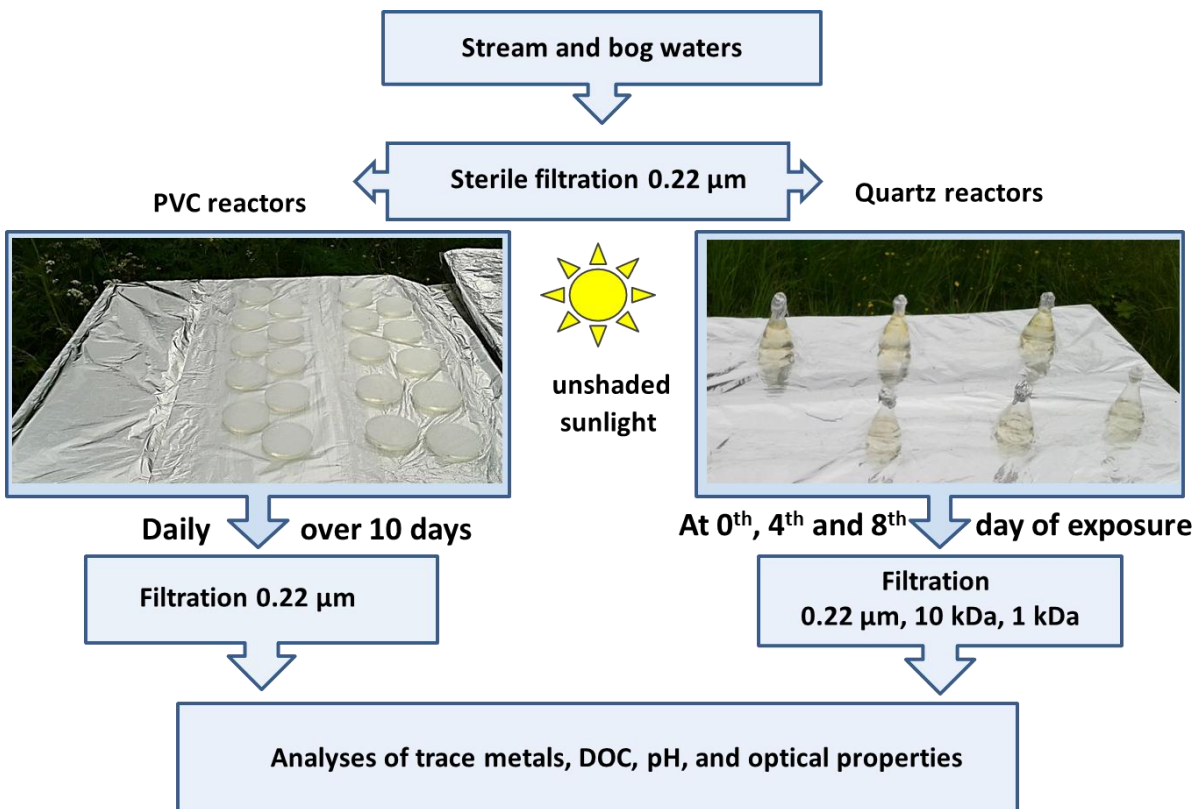


Fig. 4.1. Conceptual scheme of conducted experiments. The stream water was processed only for 0.22 μm and 10 kDa filtration.

4.4.3. Sample analysis

DOC and DIC concentrations were measured by methods routinely used in the Geosciences and Environment Toulouse (GET) laboratory to analyze boreal water samples (Shirokova et al., 2013; Pokrovsky et al., 2012, 2016). Pyrolyzed (2.5 hrs at 550°C) glassware was used for sample collection and storage. DIC was measured via total infrared analysis with a Shimadzu TOC-V_{CSN} (acid addition without combustion), with a detection limit of 0.01 mM and an uncertainty of 5%. The DOC was measured using Shimadzu TOC-V_{CSN} with an uncertainty of 5% and a detection limit of 0.1 mg/L. Good agreement between our replicated measurements and the certified values was obtained (relative difference < 10 %).

The pH was measured using a combination glass electrode calibrated against NIST buffer solutions. Dissolved oxygen was analyzed by a submersible polarographic sonde with Econix-Expert® multimeter (Russia) with an uncertainty of 5%. Major anion concentrations (Cl^- and SO_4^{2-}) were measured by ion chromatography (Dionex 2000i) with an uncertainty of 2%. The internationally

certified water samples (ION-915, MISSISSIPPI-03, RAIN-97, Pérade-20) were used to check the validity and reproducibility of the anion analysis. Major and trace elements, including Fe, were measured by ICP-MS (7500ce, Agilent Technologies) without pre-concentration. Indium and rhenium were used as internal standards. The international geostandard SLRS-5 (Riverine Water Reference Material for Trace Metals certified by the National Research Council of Canada) was used to check the validity and reproducibility of each analysis (see Vasyukova et al. (2010) for analytical details). There was good agreement between our replicated measurements of SLRS-5 and the certified values (relative difference < 15 %) of the elements presented in this work. The test of Fe(II) appearance in sunlight-irradiated samples were performed using conventional ferrozine method (Viollier et al., 2000), employing a standard addition technique, to account for the presence of high humic concentration. The uncertainty of this technique was \pm 10% and the quantification limit of 100 $\mu\text{g/L}$ Fe(II).

The value of the optical wavelength ratio a_{470}/a_{665} and specific UV-absorbency (SUVA₂₅₄) can be used as proxies for aromatic C, molecular weight and the source of DOM (Uyguner and Bekbolet, 2005; Weishaar et al., 2003; Ilina et al., 2014 and references therein). The absorption spectra of filtrates and ultrafiltrates over a range of 200 to 700 nm with 1 nm resolution were measured in the laboratory using 1 cm quartz cuvette. The specific UV-absorbency ($\text{L mg}^{-1} \text{ m}^{-1}$) was measured at 254 nm using a CARY-50 UV-VIS spectrophotometer (Bruker, UK) and normalized to the DOC concentration in the sample.

4.4.4. Thermodynamic modeling and statistical treatment

We used the geochemical program Visual MINTEQ (Gustafsson, 1999), version 3.1 for Windows (October 2014) in conjunction with a database and the NICA-Donnan humic ion binding model (Benedetti et al., 1995; Milne et al., 2003) and Stockholm Humic Model (SHM). Speciation calculations were performed for Ba, Ca, Cd, Co, Cu, K, Mg, Mn, Na, Ni, Pb, Sr, Zn, and Al, Fe³⁺ for bog water and stream at the beginning and at the end of irradiation in both < 0.22 μm and < 1 kDa fractions. The main output parameters of the calculation were saturation indices with respect to possible secondary phases (goethite, ferrihydrite, lepidocrocite, Al(OH)₃ and gibbsite) and the proportion of organic-free metals. The calculations were run at 20°C, which is

typical for surface waters of the region during the period of the study (i.e., Ilina et al., 2014, 2016).

The data of the experimental parameters, including pH, DOC, and major and trace element concentrations, were analyzed with best fit functions based on the Pearson correlation and one-way ANOVA with the STATISTICA version 8 software (StatSoft Inc., Tulsa, OK). Regressions and power functions were used to examine the relationships between DOC and major and trace element concentrations as a function of time. The ANOVA method was used to test the differences between dark control and light experimental reactors taking into account the duplicates, over the full duration of the experiment. Significant difference of DOC and TE concentration between control and experiment evolution with time for a given element is at $p < 0.05$ which is typically $> 10\%$.

The apparent rate of element removal from solution during photodegradation was calculated as the slope of element concentration vs elapsed time within statistically significant ($p < 0.05$) linear range of element – time dependence.

4.5. Results

4.5.1. pH, DOC, SUVA, phosphorus and anions in $<0.22 \mu\text{m}$ fraction

There was no statistically significant variation of pH in the course of experiments, both in Petri dishes and quartz reactors: within the uncertainty of duplicates ($< 0.1\text{--}0.2$ pH unit), the pH in dark control and the light experiment was identical and equal to 7.0 ± 0.2 and 5.3 ± 0.1 in the stream and bog water, respectively. No formation of flocculent material during experiment was visible with the naked eye. The oxygen level in both quartz reactors and PVC-covered Petri dishes remained at $90 \pm 10\%$ saturation over full duration of exposure. The concentration of DOC ($< 0.22 \mu\text{m}$) in stream water decreased by ca. 20% over 120 h of exposure, relative to the dark control in PVC reactors and by 30% over 240 h of exposure in quartz reactors (Fig. 4.2 A, B). The decrease of DOC ($< 0.22 \mu\text{m}$) in the bog water was ca. twice higher in both reactors (50% over 240 h, Fig. 4.2 C, D). The decrease of specific UV_{254 nm} absorbency during sunlight exposure of stream water ranged from 55% to 50% over 240 h in Petri dishes and quartz reactors, respectively (Fig. 4.3 A, B). In the bog water, this decrease was strongly pronounced and ranged between a factor of 10 and 5 over 240 h of exposure in Petri dishes and quartz reactors, respectively (Fig. 4.3 C, D). There was a good correlation between UV_{254 nm} and Fe concentration in bog water (R^2

$= 0.928$) which was absent in the stream water ($R^2 = 0.19$) suggesting that the majority of Fe that is removed from the bog water was bound to aromatic (colored) organic carbon.

Total dissolved P exhibited strong decrease during first 150 h of irradiation of bog water with complete removal of P from solution after 200 h of reaction (Fig. 4.4). There was no change in P concentration in the stream water during the experiment. Consistent with the SUVA results, a decrease of a_{470}/a_{665} absorbance ratio in the course of bog water exposure to the sunlight (Fig. 4.5) indicated on the aromaticity and molecular size decrease. The apparent rates of the DOC, SUVA₂₅₄ and P decrease in 0.22 μm fraction were quite similar for both types of reactors as listed in Table 4.1. Chloride and sulfate exhibited some increase in the course of bog water exposure to sunlight (a factor of 1.2 and 3, respectively, significant at $p < 0.05$) whereas the change of Cl and SO₄ concentration in stream water were within the uncertainties (Fig. 4.6).

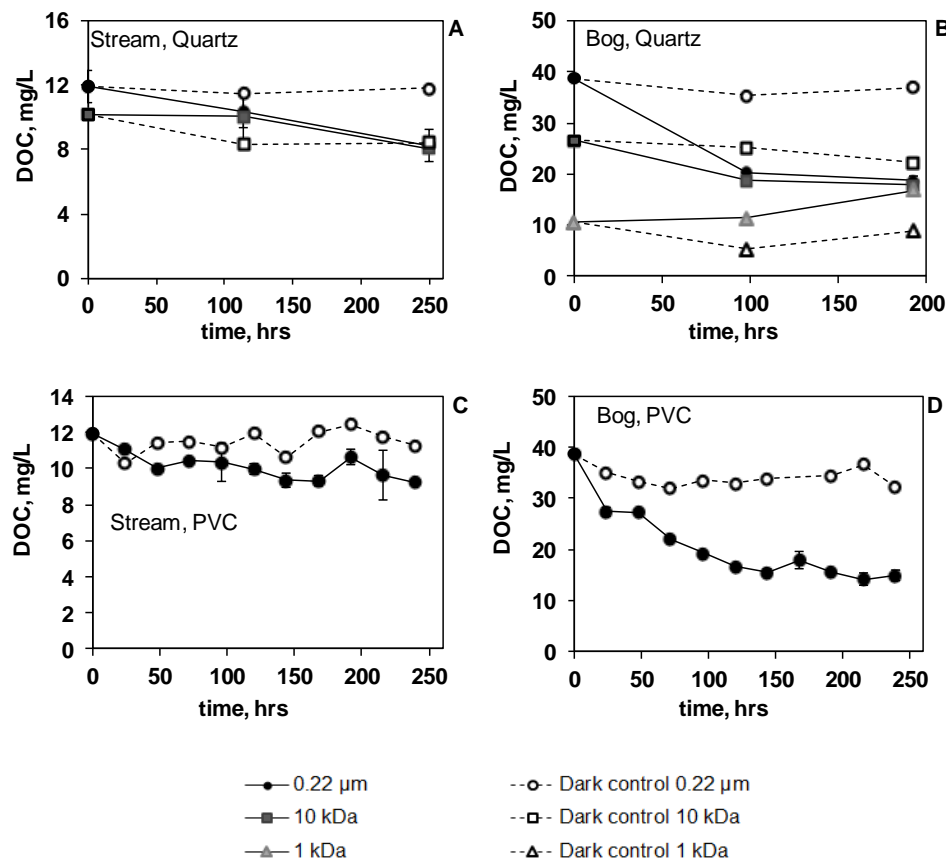


Fig. 4.2. Evolution of DOC during sunlight exposure of stream and bog water in Quartz (A, B) and PVC (C, D) reactors. The error bars represent s.d. of duplicates unless they are smaller than the symbol size. The error bars represent s.d. of duplicates unless they are smaller than the symbol size.

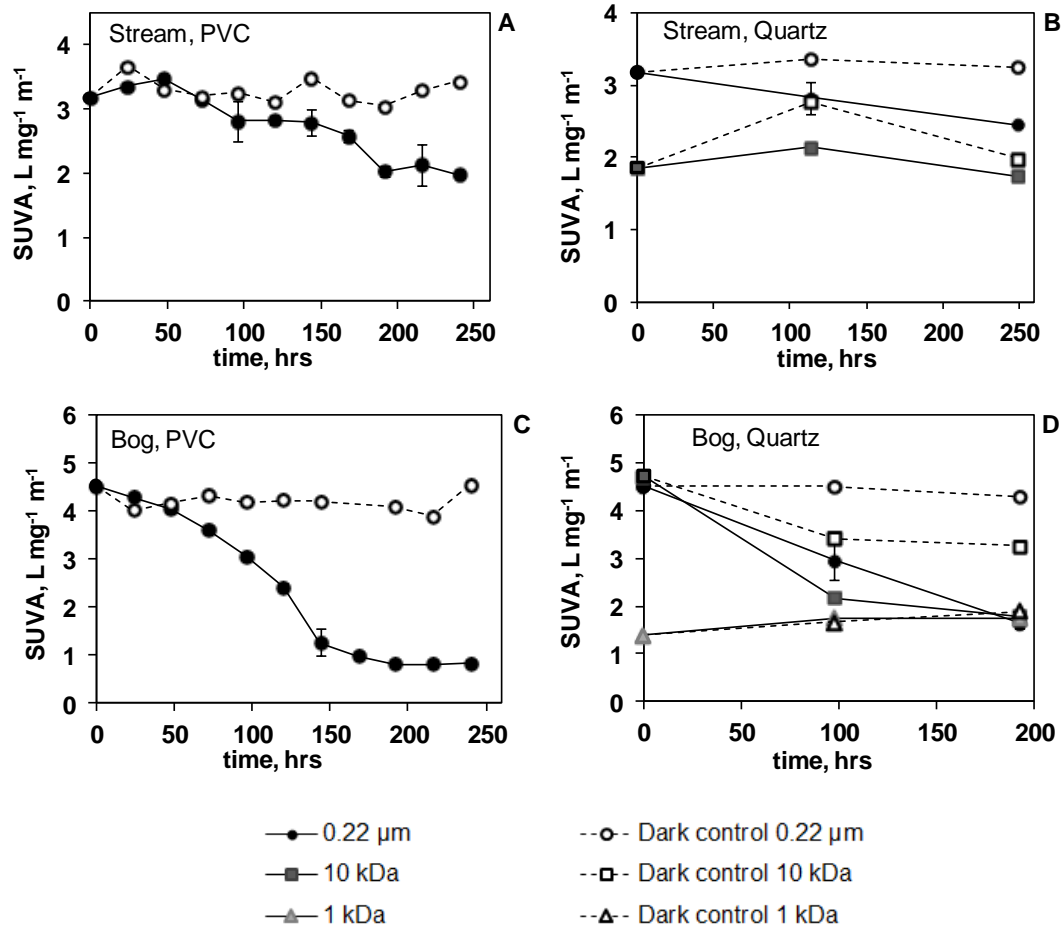


Fig. 4.3. Evolution of SUVA in stream (A, B) and bog (C, D) water in Petri dishes (A, C) and quartz reactors (B, D).

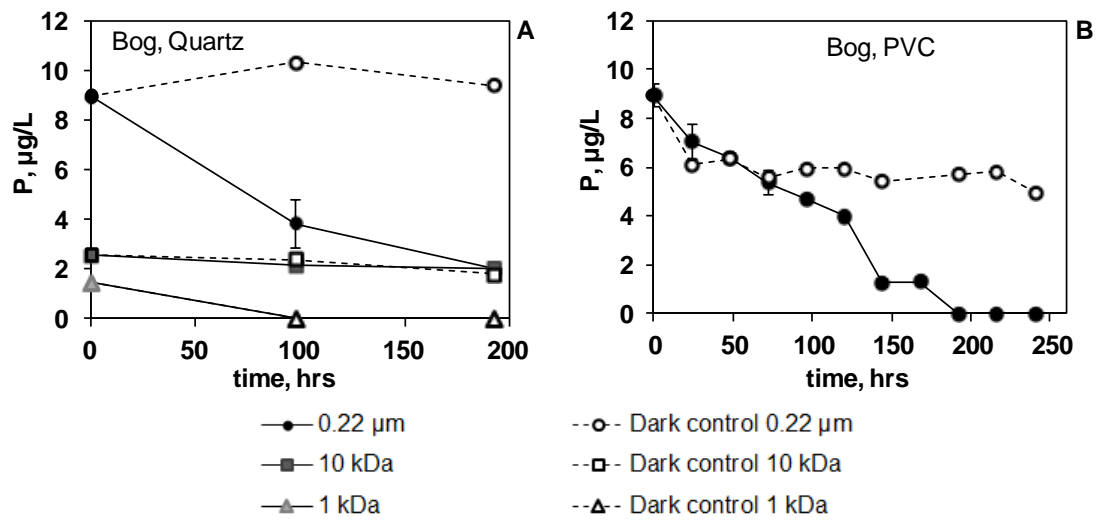


Fig. 4.4. Total phosphorus evolution of sunlight-exposed bog water in quartz reactors (A) and Petri dishes (B). The error bars represent s.d. of duplicates unless they are smaller than the symbol size.

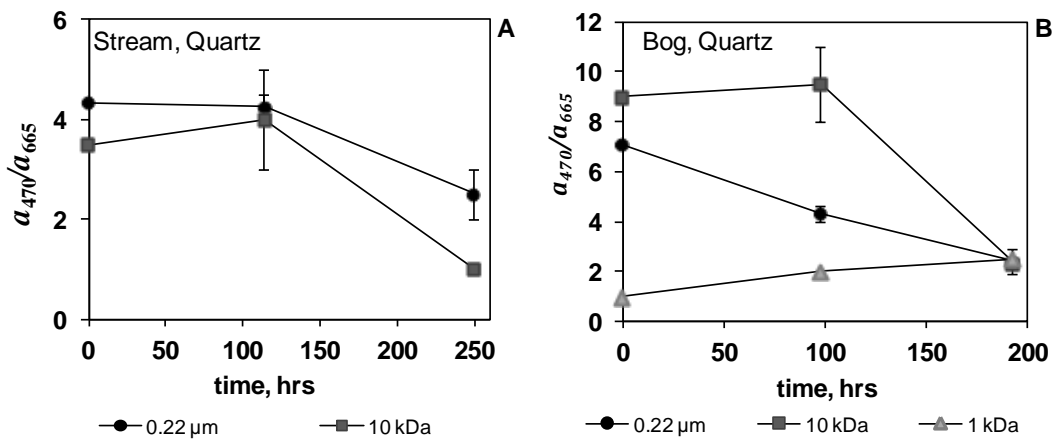


Fig. 4.5. Evolution of optical visual range ratio (a_{470}/a_{665}) in the course of sunlight exposure of stream and bog water in quartz reactors.

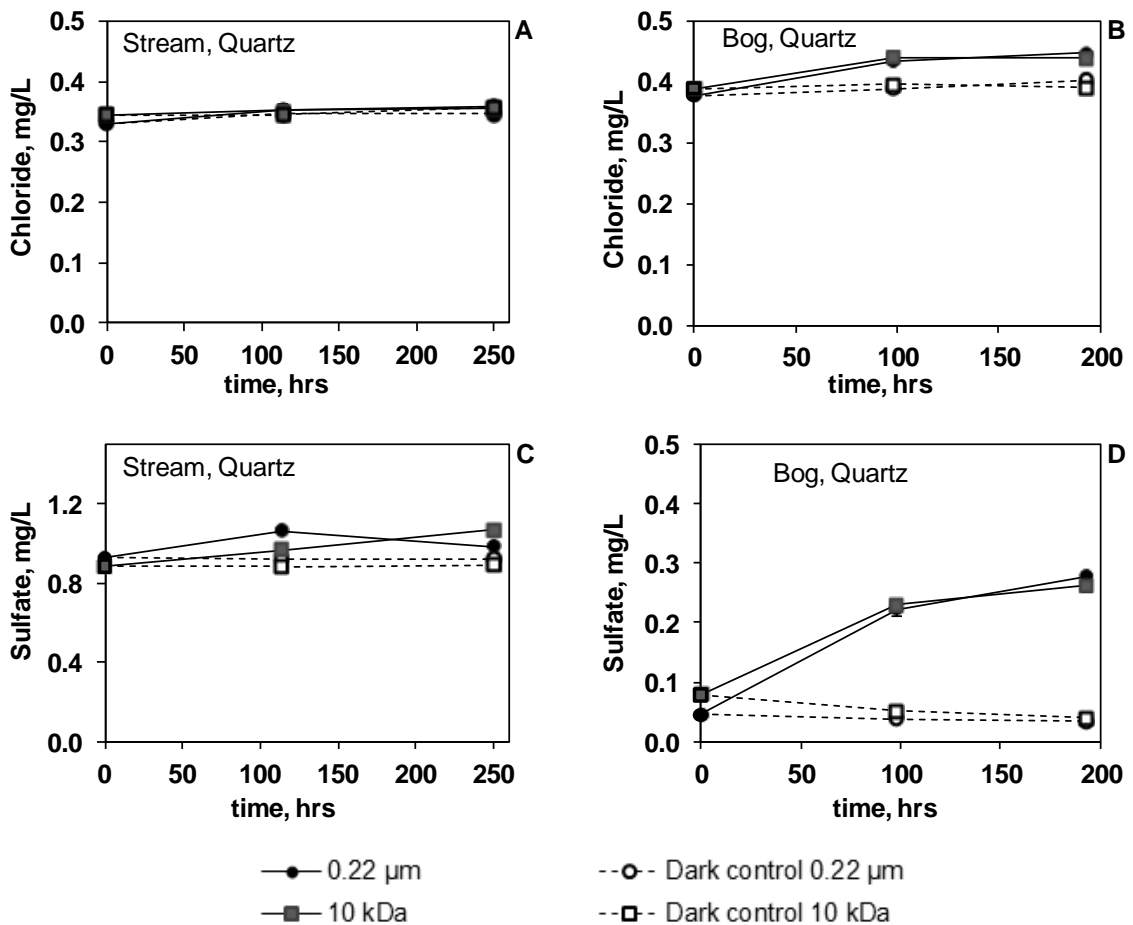


Fig. 4.6. Evolution of Cl and SO₄ concentration in various fractions of stream (A, B) and bog water (C, D) exposure to sunlight in quartz reactors

Table 4.1. Apparent rate of DOC, SUVA₂₅₄ and trace element decrease of 0.22 µm fraction in stream and bog water, over first 200 h of exposure to sunlight in Quartz reactors and Petri dishes. Na, Mg, Si, K, Ca, Mn, Co, Ni, Cu, Zn, Rb, Sr, Cd, Sb, Ba, W, Tl did not exhibit any measurable rates or the rates were within the uncertainty of duplicates (10-20%).

Element	Quartz reactors, µg L ⁻¹ day ⁻¹		Petri dishes, µg L ⁻¹ day ⁻¹	
	Stream water	Bog water	Stream water	Bog water
DOC	350±60	2500±130	250±80	2420±140
SUVA ₂₅₄ *	0.07±0.03	0.36±0.06	0.11±0.02	0.36±0.01
Li	0.0009±0.0005	no effect	0.002±0.001	0.0023±0.0014
Al	no effect	12.7±1.4	no effect	17±1
P	no effect	0.87±0.14	no effect	0.89±0.06
Ti	no effect	0.29±0.03	no effect	0.23±0.03
V	no effect	0.038±0.004	no effect	0.032±0.001
Cr	no effect	0.152±0.016	no effect	0.145±0.004
Fe	no effect	420±50	no effect	407±9
Ga	no effect	0.006±0.0005	no effect	0.0059±0.0001
As	no effect	0.013±0.001	no effect	0.011±0.001
Y	no effect	0.039±0.004	no effect	0.038±0.001
Zr	0.002±0.001	0.053±0.005	no effect	0.044±0.001
Nb	no effect	0.0027±0.0003	no effect	0.0023±0.0005
Mo	no effect	0.0025±0.0003	no effect	0.0022±0.0005
La	no effect	0.046±0.004	no effect	0.045±0.001
Ce	no effect	0.13±0.01	no effect	0.125±0.002
Pr	no effect	0.012±0.001	no effect	0.012±0.001
Nd	no effect	0.044±0.004	no effect	0.045±0.001
Sm	no effect	0.008±0.001	no effect	0.0082±0.0002
Eu	no effect	0.0017±0.0002	no effect	0.0015±0.0001
Tb	no effect	0.0011±0.0001	no effect	0.0011±0.0001
Gd	no effect	0.007±0.001	no effect	0.0073±0.0002
Dy	no effect	0.007±0.001	no effect	0.0064±0.0001
Ho	no effect	0.0014±0.0002	no effect	0.0014±0.0001
Er	no effect	0.004±0.001	no effect	0.0041±0.0001
Tm	no effect	0.0006±0.0001	no effect	0.0006±0.0001
Yb	no effect	0.004±0.001	no effect	0.0041±0.0001
Lu	no effect	0.0006±0.0001	no effect	0.00065±0.00005
Hf	no effect	0.0017±0.0003	no effect	0.0017±0.0001
Pb	no effect	0.013±0.002	no effect	0.010±0.001
Th	0.00033±0.00007	0.013±0.001	0.00032±0.00008	0.012±0.001
U	no effect	0.0023±0.0002	no effect	0.0022±0.0001

SUVA₂₅₄*, L mg⁻¹ m⁻¹

4.5.2. Fe, Al and trace element in 0.22 μm fraction during sunlight exposure

The behaviors of Fe and Al are presented separately of other trace elements because Fe and Al are the major components of organic- and organo-mineral colloids. Relative to the dark control, the stream water Al concentration remained fairly stable over 250 h of sunlight exposure in both reactors (**Fig 4.7 A, B**) but demonstrated a sizeable decrease (by a factor of 1.6 to 2.6) in the bog water (**Fig. 4.7 C, D**). Fe concentration remained generally constant over 250 h of stream water exposure to sunlight (**Fig. 4.8 A-B**), but strongly decreased in bog water in both reactors (**Fig. 4.8 C-D**). There was no difference ($p < 0.05$) in Fe(II) evolution in irradiated and dark (control) reactors (not shown), suggesting that, within the resolution of analysis (100 $\mu\text{g/L}$), no measurable photo-reduction of Fe(III) occurred although it is not excluded that Fe(II) was at steady-state but below the detection limit of our method. Two type of reactors yielded comparable values of Fe and Al apparent removal rates in the bog water (410 and 15 $\mu\text{g L}^{-1} \text{d}^{-1}$, **Table 4.1**).

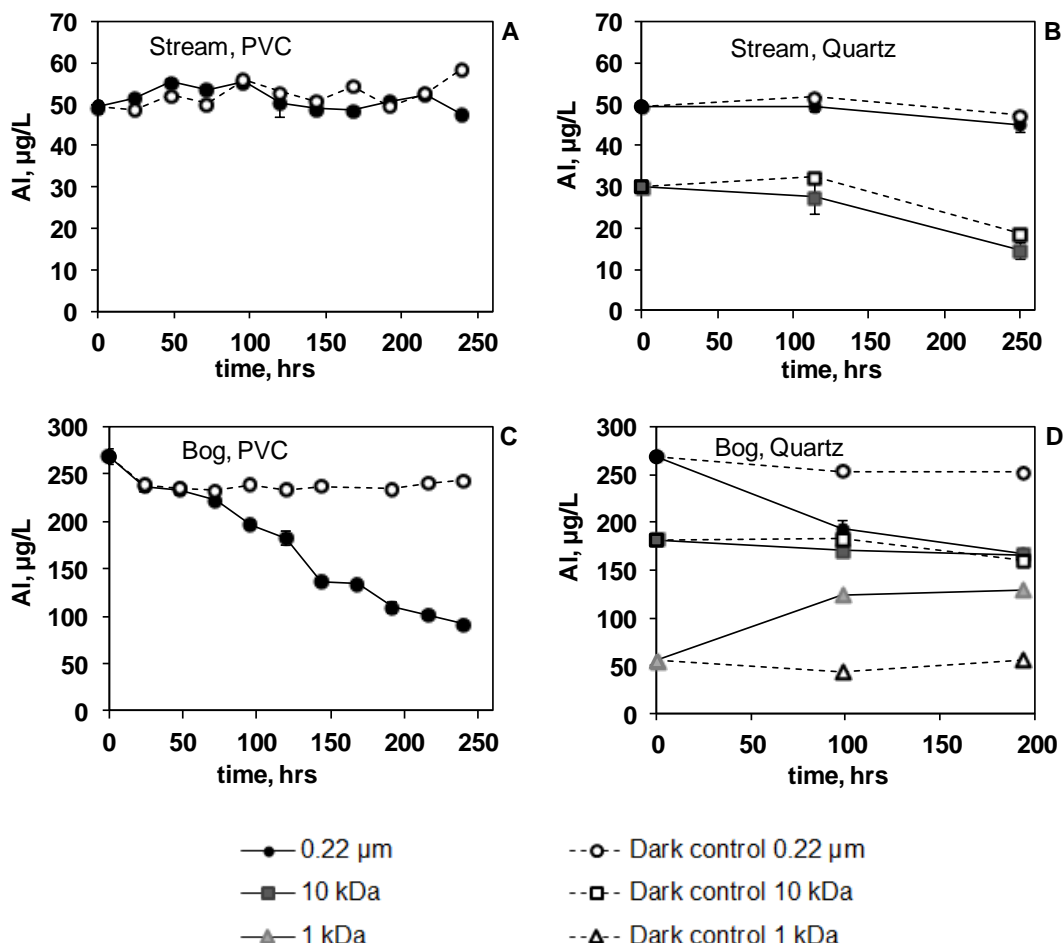


Fig. 4.7. Dissolved Al concentration in stream (A, B) and bog (C, D) water samples exposed to sunlight in PVC (A, C) and quartz (B, D) reactors. The error bars represent s.d. of duplicates unless they are smaller than the symbol size.

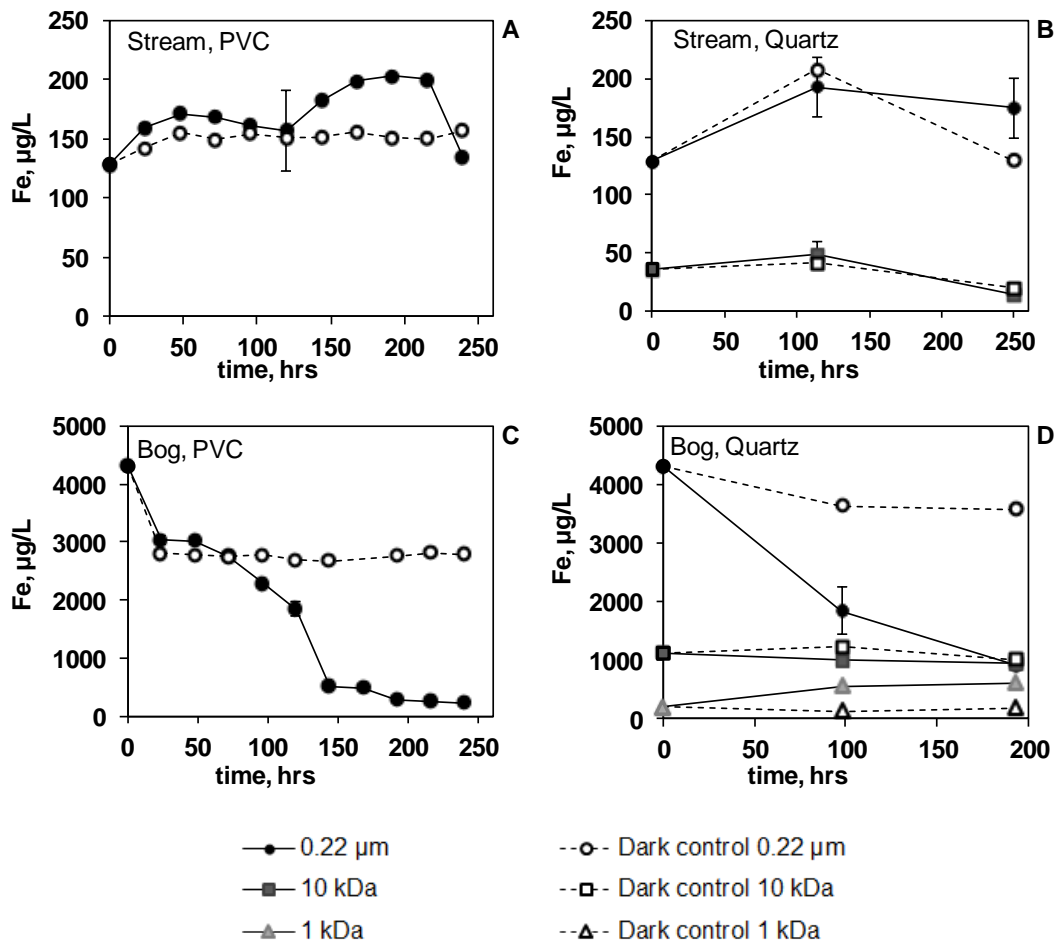


Fig. 4.8. Dissolved Fe concentration in stream (A, B) and bog (C, D) water samples exposed to sunlight in PVC (A, C) and quartz (B, D) reactors. The error bars represent s.d. of duplicates unless they are smaller than the symbol size.

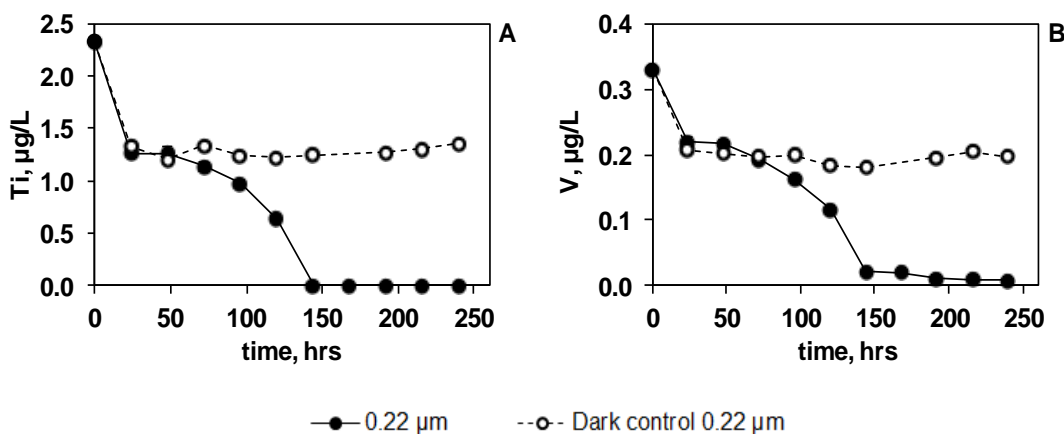


Fig. 4.9. Dissolved (< 0.22 µm) concentration of Ti (A) and V (B) in bog water exposed to sunlight in PVC reactors. The behavior of Cr, As, Y, Zr, Hf and Th was identical to that of Ti and V and thus not shown.

During sunlight exposure, the 0.22 µm fraction of bog water became depleted in Fe as illustrated from the evolution of the molar ratio of DOC/Fe (**Fig. 4.10**). This trend mainly stems from more efficient Fe removal compared to DOC. The change of this ratio in the stream water was within the experimental uncertainty. Two main groups of elements can be distinguished based on their behavior in the course of sunlight exposure:

- (i) Significantly (> 50-100% at $p < 0.01$) decreasing their concentration in bog water sample but remaining statistically stable ($\pm 10\%$ at $p < 0.05$) in stream water sample: P, Al, Fe, Ti, V, Cr, Ga, Y, Zr, Nb, REEs, Hf, Th, Pb and U as illustrated in **Figs 4.4, 4.7, 4.8 and 4.9 (A, B)** for P, Al, Fe, Ti, and V. This group of element also exhibited quite constant ratio Fe/TE over the first 100 h of experiment ($\pm 10\%$ variation, not shown) when the change of TE concentration was maximal, suggesting that these TEs tightly followed the behavior of Fe-rich colloids. The mass balance calculation demonstrate that, in the course of experiments with bog water, $38 \pm 7\%$ of Al and $79 \pm 10\%$ of Fe were precipitated in the form of hydroxides.
- (ii) Conservative, highly stable elements whose concentration in 0.22 µm fraction of bog water did not evolve within $\pm 10\text{--}15\%$ of the control: Cl, Li, B, Na, Mg, Si, K, Rb, Ca, Sr, Ba, Mn, Co, Zn, Cd, Sb, illustrated for Mn, Co, Ni and Cd (**Fig. 4.11 A-D**).

In contrast to the bog water, the stream water yielded a lack of any significant concentration decrease over time, except quite low (ca. $20 \pm 10\%$ relative to control) decrease of Ga, Y, Zr, REEs and Th (not shown).

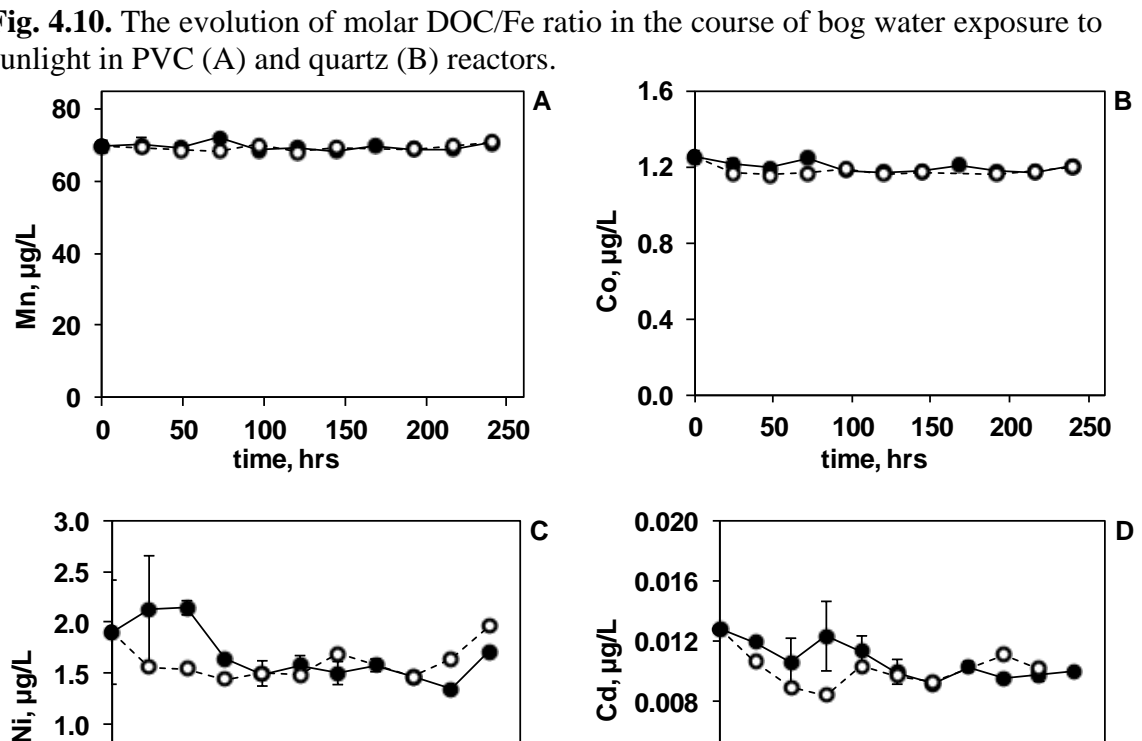
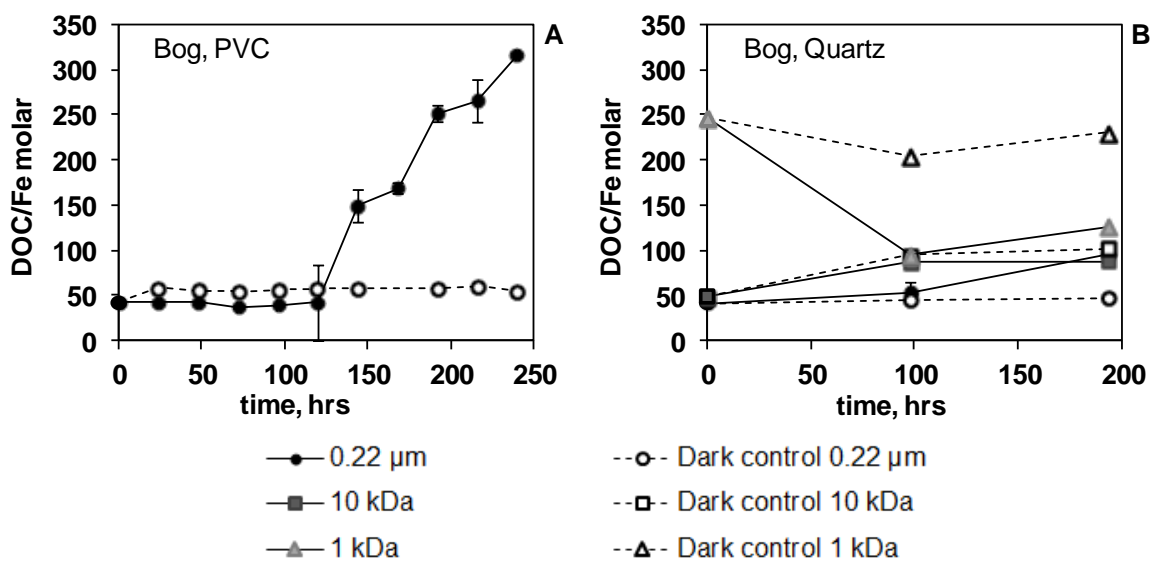


Fig. 4.11. Dissolved (< 0.22 μm) concentration of Mn (A), Co (B), Ni (C), and Cd (D) in bog water exposed to sunlight in PVC reactors.

4.5.3. Elementary composition of colloids, DOC and TE size fractionation change in the course of photo-degradation

The elementary composition of the bog water colloids (1 kDa – 0.22 µm) systematically evolved in the course of photo-degradation, from $C_1Fe_{0.031}Al_{0.0034}P_{0.0001}Ca_{0.014}Mg_{0.016}$ at the beginning of experiment to $C_1Fe_{0.032}Al_{0.0091}P_{0.0004}Ca_{0.045}Mg_{0.032}$ after 200 h of sunlight exposure. The evolution of the molar ratio of organic carbon to element in colloidal, conventionally dissolved (< 0.22 µm) and LMW (< 1 kDa) fractions is listed in **Table 4.2**. The molar ratio of C_{org} to most major and TE (Mg, Ca, P, Al, Mn, Co, Ni, Zn, Sr, Ba, REEs) in colloids exhibited a decrease by a factor of 2 to 5, whereas the ratio of Fe, Zr, and Th to C_{org} remained constant within 10-30%. In the conventionally dissolved fraction (< 0.22 µm), the C_{org}/TE ratio decreased by a factor of 1.3 to 2.0 for Mg, Ca, Sr, Ba, Al, Mn, Co, Ni, Cu, and Zn but increased by a factor of 2 to 5 for Fe, P, Ti, V, Zr, REEs, Th and U. Finally, in low molecular weight fraction (< 1 kDa), the ratio of C_{org} to Mg, Ca, Sr, Ba, Al, Mn, Fe, Co, Ni, and Cu decreased by a factor of 1.2 to 2.8 (**Table 4.2**). This strongly suggests a preferential enrichment of the $LMW_{<1\text{ kDa}}$ fraction in Fe, Al, Ca, Mg and other divalent metals relative to C_{org} .

Table 4.2. Molar ratio of C_{org} to TE at the beginning and at the end of sunlight exposure of bog water, in colloidal and low molecular weight fraction.

	Colloidal (1 kDa - 0.22 µm)		LMW < 1 kDa	
	0 h	193 h	0 h	193 h
DOC/Mg	65	31	81	33
DOC/Al	297	110	430	291
DOC/P	9688	2328	19006	ND
DOC/Ca	71	22	76	39
DOC/Ti	49798	ND	569267	ND
DOC/V	452943	ND	679000	2492000
DOC/Mn	2375	1137	3165	1232
DOC/Fe	32	31	247	126
DOC/Co	134412	42319	231000	82318
DOC/Ni	92542	24933	125000	57800
DOC/Zn	46100	17100	12432	13200
DOC/Sr	36600	12100	53500	20800
DOC/Zr	483000	456000	3166600	8120000
DOC/Ba	74125	16194	140800	50300
DOC/La	786000	428000	2780000	5440000
DOC/Pb	5510000	ND	7460000	21580000
DOC/Th	4983000	4676000	21110000	59850000

A preferential removal of elements of the 1st group (see section 3.2) relative to C_{org} from the dissolved (< 0.22 µm) to the particulate fraction (> 0.22 µm) is illustrated by temporal evolution of DOC/TE ratio for Ti, V, Zr, La and Th (**Fig. 4.12 A-E**). In contrast, the impoverishment of Ca, Mg, Co, Mn and Sr relative to OC in the colloidal pools in the course of experiment (**Fig. 4.13 A-F** of Supplement) is due to the transfer of these elements from colloidal to LMW_{< 1 kDa} fraction. Indeed, there was distinctly different behavior of the LMW_{< 1 kDa} fraction compared to the other colloidal and subcolloidal fractions in bog waters exposed to sunlight (**Table 4.3**). Unlike the < 0.22 µm and < 10 kDa fractions, the < 1 kDa fraction of organic carbon and many TE increased its concentration with time by a factor of 1.5 to 2.0. A large number of major and trace element demonstrated this increase in < 1 kDa fraction relative to dark control, such as Li, Na, K, Rb, Cs, Mg, Ca, Sr, Ba, Al, Mn, Co, Zn, Cd, Fe, illustrated for Al and Fe in **Figs. 4.7 D, 4.8 D** and for Ca, Mn, Co, and Ni in **Fig. 4.14 A, B, C, and D**, respectively. On a percentage scale, this increase was equal or slightly lower than the proportion of colloidal forms of divalent metals in the bog water. In contrast, P and many insoluble heavy elements (Ti, V, Y, Zr, Nb, REEs, Hf, Th) were removed from both < 0.22 µm and < 1 kDa fractions since their concentration in the latter remained constant or decreased in the course of exposure (**Table 4.3**).

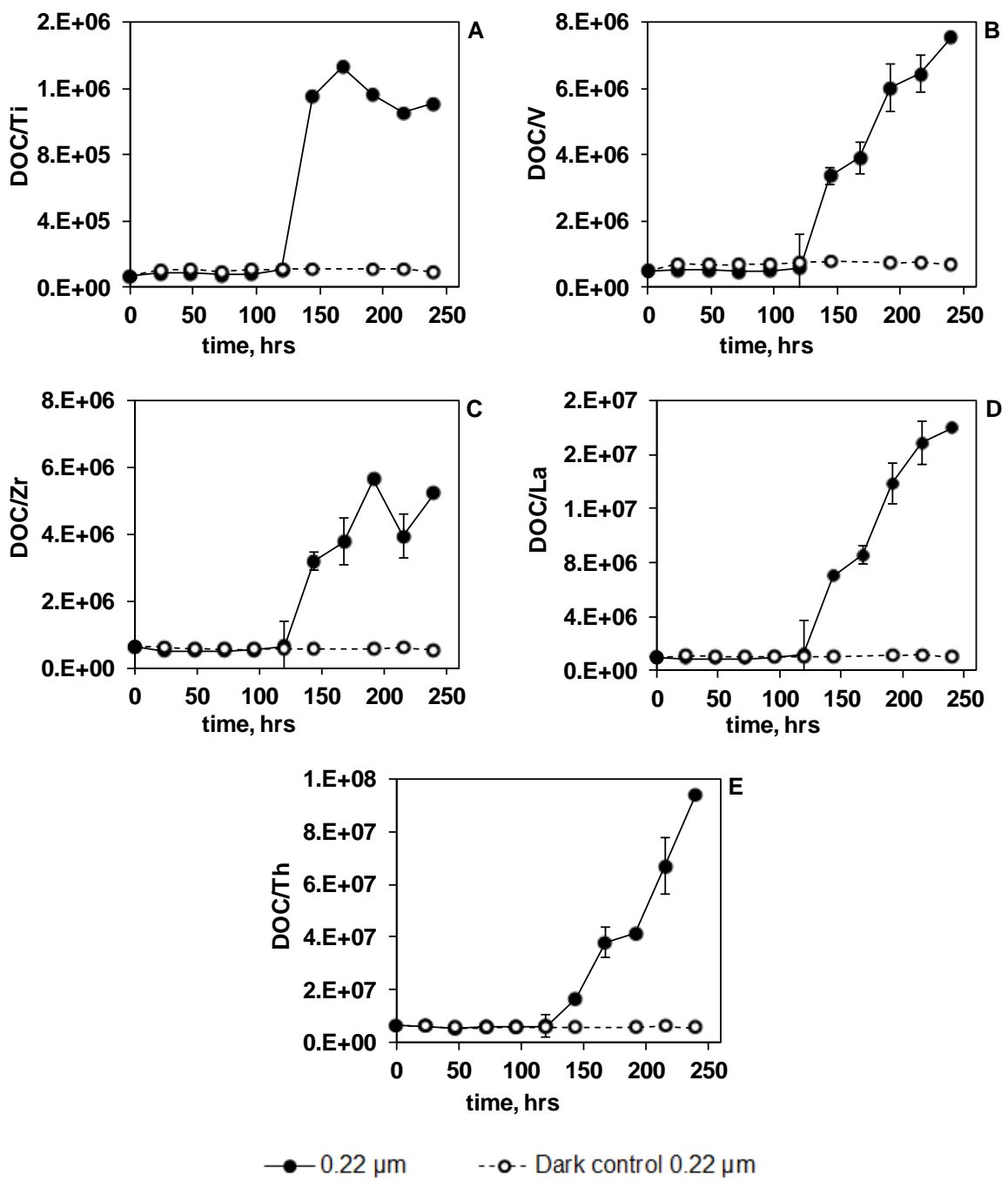


Fig. 4.12. Molar ratio of DOC to TE in dissolved (< 0.22 μm) fraction of bogwater exposed to sunlight in PVC reactors for Ti (A), V (B), Zr (C), La (D), and Th (E).

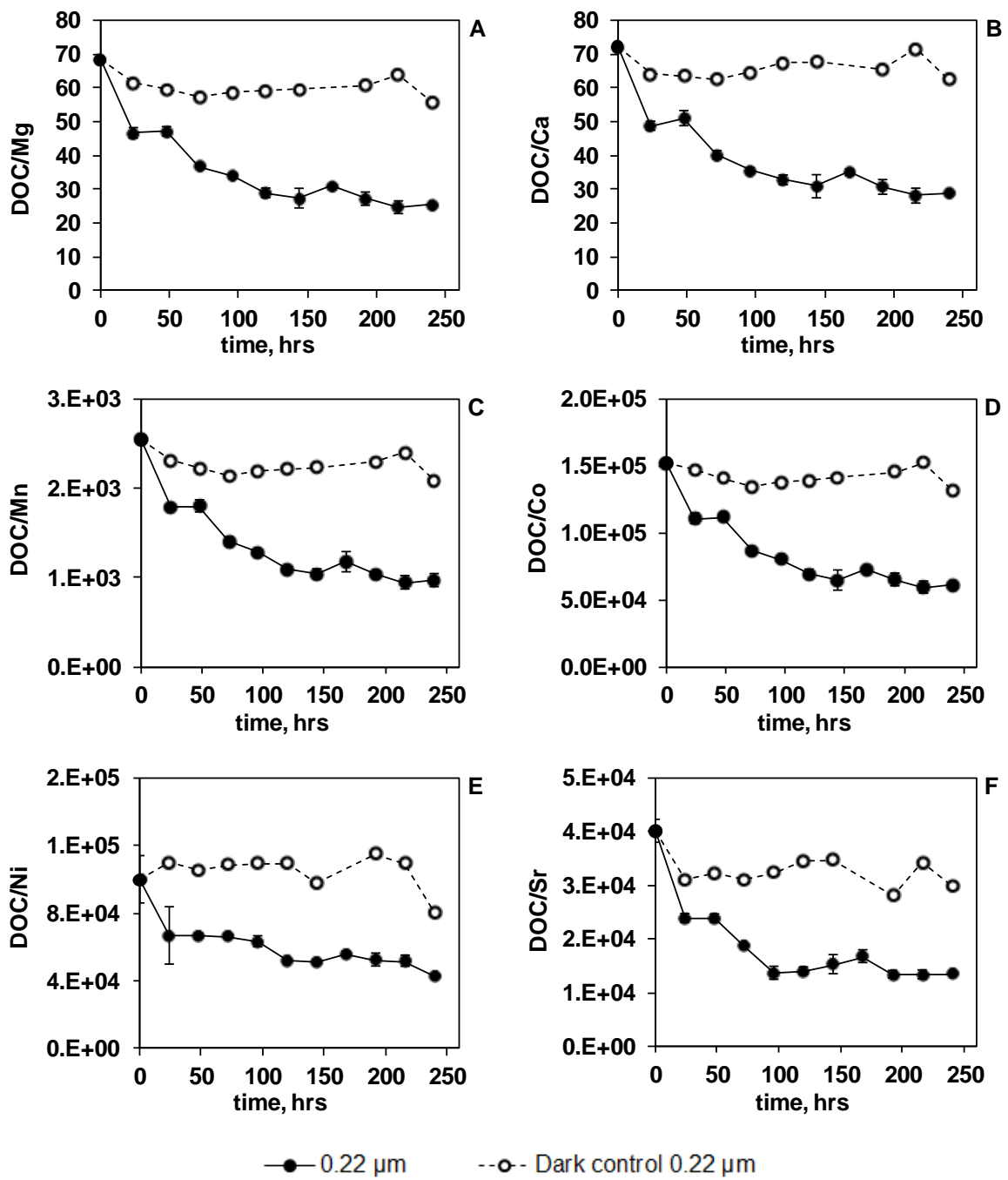


Fig. 4.13. Molar ratio of DOC to TE in dissolved (< 0.22 μm) fraction of bog water exposed to sunlight in PVC reactors for Mg (A), Ca (B), Mn (C), Co (D), Ni (E) and Sr (F).

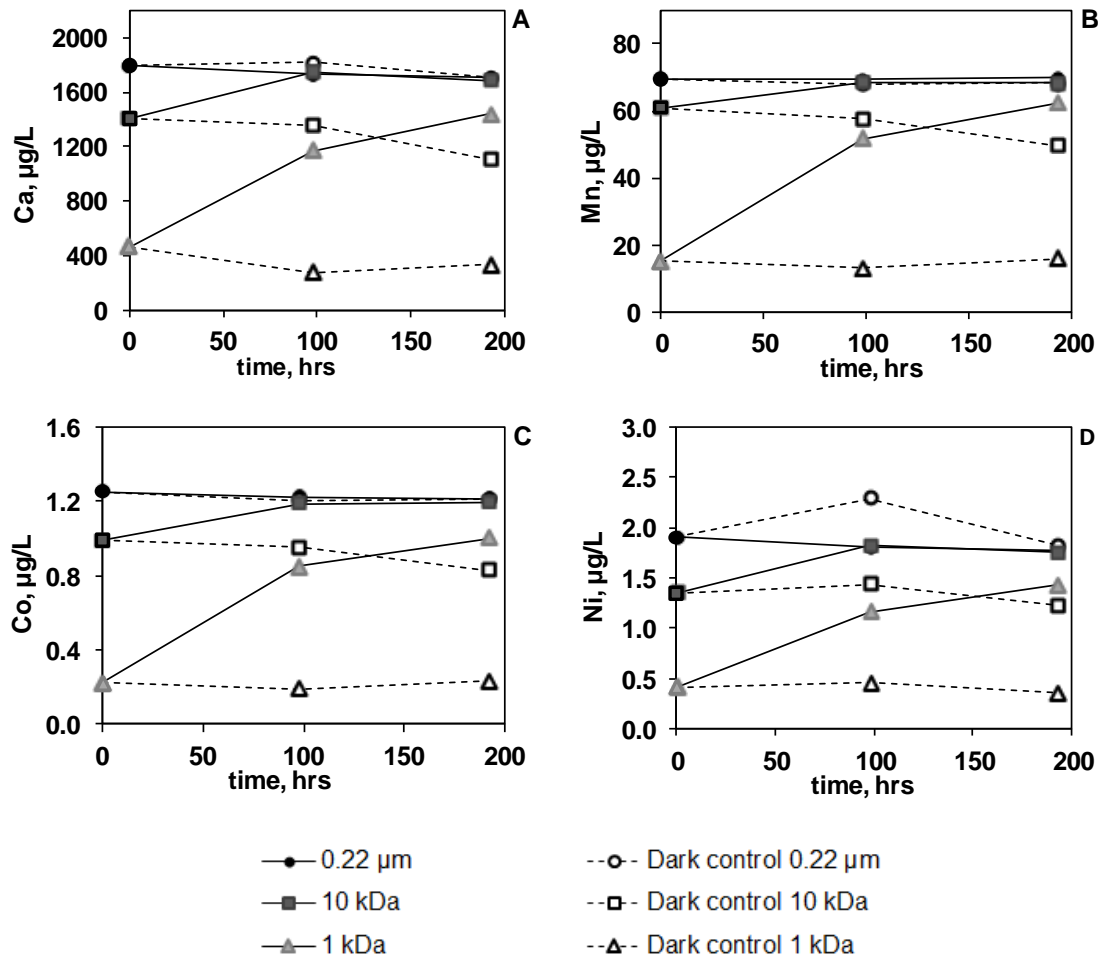


Fig. 4.14. An increase in < 1 kDa fraction (grey triangles) in bog water exposed to sunlight in quartz reactors for Ca (A), Mn (B), Co (C), Ni (D). The behavior of Sr and Ba was identical to that of Ca and thus not shown. The error bars represent s.d. of duplicates unless they are smaller than the symbol size.

Table 4.3. The relative change (% of the starting value) of element concentration in 3 fractions of bog water after 250 h of sunlight exposure in quartz reactors. The sign (-) and (+) stands for relative decrease and increase, respectively. The uncertainty represents s.d. of duplicates. Si, Cu, Zn, Sb and W did not exhibit measurable change in all fractions and thus not shown.

Element	< 0.22 μm	< 10 kDa	< 1 kDa
DOC	(-)52±6	(-)33±5	(+)59±19
Li	no effect	no effect	(+)39±10
Na	no effect	(-)5±3	(+)84±5
Mg	no effect	(+)13±1	(+)290±7
Al	(-)38±7	(-)9±4	(+)135±10
P	(-)78±13	(-)20±5	no effect
K	no effect	no effect	(+)95±3
Ca	no effect	(+)20±1	(+)210±15
Ti	(-)100±10	(-)100±7	(-)99±10

Table 4.3, continued.

Element	< 0.22 µm	< 10 kDa	< 1 kDa
V	(-)92±10	(-)78±4	(-)57±16
Cr	(-)70±7	(-)56±3	(+)50±12
Mn	no effect	(+)12±1	(+)310±5
Fe	(-)79±10	(-)16±9	(+)210±15
Co	no effect	(+)21±2	(+)350±7
Ni	no effect	(+)30±4	(+)245±10
Ga	(-)79±7	(-)74±3	no effect
As	(-)39±6	(-)14±4	(+)10±5
Rb	no effect	no effect	(+)90±6
Sr	no effect	(+)18±2	(+)310±10
Y	(-)80±8	(-)76±5	no effect
Zr	(-)90±8	(-)79±3	no effect
Nb	(-)89±11	(-)78±3	no effect
Mo	(-)80±9	no effect	no effect
Cd	no effect	no effect	(+)110±17
Ba	no effect	(+)28±5	(+)345±8
La	(-)81±8	(-)76±5	no effect
Ce	(-)81±8	(-)75±5	no effect
Pr	(-)78±8	(-)73±6	no effect
Nd	(-)77±7	(-)70±6	no effect
Sm	(-)77±6	(-)70±7	no effect
Eu	(-)77±8	(-)66±6	no effect
Tb	(-)80±7	(-)73±5	no effect
Gd	(-)76±8	(-)69±7	no effect
Dy	(-)81±8	(-)76±5	no effect
Ho	(-)81±8	(-)77±4	no effect
Er	(-)80±8	(-)75±6	no effect
Tm	(-)78±7	(-)76±6	no effect
Yb	(-)77±9	(-)73±4	no effect
Lu	(-)75±7	(-)67±4	no effect
Hf	(-)78±11	(-)65±7	no effect
Tl	no effect	no effect	(+)71±5
Pb	(-)93±11	no effect	no effect
Th	(-)88±7	(-)75±6	no effect
U	(-)72±6	(-)39±7	(+)90±12

4.6. Discussion

We hypothesize several processes responsible for TE removal and redistribution among different colloidal pools in DOM- and Fe-rich bog water under sunlight exposure: (*i*) photochemical oxidation of DOM and Fe coagulation via Fe oxy(hydr)oxide precipitation after removal of complexing organic ligands (i.e., Stolpe et al., 2013a, b); *ii*) agglomeration and coagulation of high molecular weight (10 kDa–0.22 µm) Fe-rich organo-mineral colloids into the particulate (> 0.22 µm) form, which scavenged TE³⁺, TE⁴⁺ hydrolysates, As and U; (*iii*) production of LMW_{< 1 kDa} organic ligands binding Al³⁺ and Fe³⁺; (*iv*) degradation of colloidal DOM and release of alkali and alkaline-earth metals, Co, Ni, Mn, Cd, U(VI), SO₄²⁻ in solution, in the form of LMW_{< 1 kDa} organic complexes or ions. First, we will analyze the DOM and trace metal behavior and then we discuss the production of LMW fraction and provide the natural application of obtained results.

4.6.1. Change of concentration, optical properties and size fractionation of DOC during sunlight exposure

The relative role of photo-degradation versus bio-degradation of DOM in boreal waters is currently recognized to be much higher than previously thought: the photochemical oxidation may account for 70 to 95% of total DOC processed in the water column of arctic lakes and rivers (Cory et al., 2013, 2014; Ward and Cory, 2016). The photo-degradation of DOC is known to produce CO₂(g) and HCO₃⁻(aq) (Mopper et al., 1991; Miller and Zepp, 1995; Granéli et al., 1996; Porcal et al., 2015). Part of colloidal (1 kDa – 0.22 µm) DOC can be converted to low molecular weight carboxylates (Bertelsson and Tranvik, 1998; Xie et al., 2004), carbonyl compounds (Kieber et al., 1990), highly oxidized ligands (Gonsior et al., 2013), alkyl and short aromatic ligands (Helms et al., 2013). The UV-irradiation of humic and fulvic acids and natural humic lake water yielded the appearance of carboxyl and carbonyl atoms with aliphatic character (Corin et al., 1996; Kulovaara et al., 1996). Low molecular weight organic carbon production upon sunlight exposure of surface waters is well known since pioneering works of Zafiriou et al. (1984) and confirmed over past decade in the Arctic waters (Cory et al., 2007, 2014). A photochemically-induced depolymerization and a decrease in molecular weight of natural DOM were reported using size exclusion chromatography (Lou and Xie, 2006; Thomson et al., 2004) and mass spectrometric analysis (Gonsior et al., 2013) and also indirectly inferred from

field studies (Kothawala et al., 2006; Pokrovsky and Shirokova, 2013; Shirokova et al., 2013; Ilina et al., 2016). In our experiments, these photochemically produced organic ligands are < 1 kDa as follows from the increase of LMW_{< 1 kDa} concentration of organic carbon in quartz reactors in the course of sunlight irradiation (**Fig. 4.2 B**). Besides, over 10 days of solar irradiation, the bog water from N. Karelia produced a 2-fold increase in concentration of low molecular aliphatic acids (acetic, formic, oxalic and citric) and benzol-carbonic acids (Drozdova et al., 2017; Oleinikova et al., 2015). This increase (ca. 0.2 mg/L of acids), however, represented less than 10% of overall DOC increase in the LMW_{< 1 kDa} fraction.

The SUVA₂₅₄ was highly sensitive to the irradiation by sunlight. Over 200 h of exposure, this parameter decreased by a factor of 4±1 and 1.5 in bog and stream water, respectively; in both cases this decrease was significantly higher than that of DOC_{< 0.22 μm}. This result is consistent with strong sensitivity of chromophoric DOM (CDOM) to photo-irradiation, leading to the production of optically-transparent organic ligands during sunlight exposure (Cory et al., 2013; Osburn et al., 2009). Studies of both biologically-produced DOM and allochthonous riverine DOM revealed that photodegradation of CDOM and SUVA₂₅₄ were greater than DOC losses (i.e., Spencer et al., 2009; Reche et al., 2000; Vähäntalo and Wetzel, 2004; Bittar et al., 2015). In accord with SUVA_{254 nm} evolution, the optical properties of 0.22 μm fraction suggested a decrease in the aromaticity and the molecular size, reflected in the decrease of a_{470}/a_{665} absorbance ratios.

Large differences in the degree of photo-degradation between the bog water (ZPBL) and the stream (KAR) observed in this study stem from the combination of two main factors controlling the degree of DOM photo-reactivity in natural waters: the bog water is a 1.5 unit of pH lower than the stream (5.3±0.1 and 7.0±0.2, respectively) and a factor of 30 higher in Fe concentration (4000 and 125 μg/L in ZPBL and KAR, respectively). This is in full agreement with previous observations on 1) the positive effect of water acidity on the photolysis of DOM (Voelker and Sulzberger, 1996; Molot and Dillon, 1997; Gao and Zepp, 1998; Anesio and Granéli, 2003; Molot et al., 2005) and 2) the enhancing of DOM photobleaching by elevated Fe concentration via the photo-Fenton effect below pH 6 (Gao and Zepp, 1998; Bertelsson and Tranvik, 2000; Brinkman et al., 2003). Thus, employing the relationship between the photodegradation rate constant (K), pH and [Fe] from small boreal streams (Porcal et al., 2013b), we obtain a factor of 30 higher K in ZPBL relative to KAR. This

difference is in reasonable agreement with a factor of 10 higher apparent rates of DOC photodegradation in the bog water (2500 ± 130 and $2420 \pm 14 \mu\text{g L}^{-1} \text{ day}^{-1}$ in quartz and PVC reactors, respectively), compared to the stream water (350 ± 60 and $250 \pm 80 \mu\text{g L}^{-1} \text{ day}^{-1}$ in quartz and PVC reactors, respectively, see Table 1). Note that these numbers are much higher than the overall oxidation rate in neutral ($\text{pH} = 6.4$) organic- and Fe-poor temperate river ($66 \mu\text{g L}^{-1} \text{ day}^{-1}$, Shiller et al., 2006).

4.6.2. Mechanisms of organo-mineral colloid transformation during irradiation of stream and bog waters

During photolysis of bog waters, the decrease of Fe concentration was a factor of 2 more efficient than that of Al (80 and 40% decrease in $< 0.22 \mu\text{m}$ fractions, respectively). It follows that the Fe hydroxide dominated the bulk chemical composition of formed precipitates ($> 0.22 \mu\text{m}$). At the same time, the chemical composition of colloids demonstrated their 3-fold enrichment in Al and relatively constant C_{org} to Fe ratio (see section 3.3). Given that the molar ratio of DOC to Fe is 50 in bog water and > 300 in the stream, and the molar ratio of DOC to Al is > 300 , it is unlikely that the complexation of Fe and Al with DOC and the removal of dissolved Fe and Al in the form of hydroxides are capable to affect the complexation capacities of DOM and speciation of organic ligands.

The iron redox transformation under sunlight is known to produce Fe(II) in natural waters although this divalent Fe undergoes rapid oxidation with the half-times on the order of minutes (Garg et al., 2013 a, b). The reduction of Fe strongly increases with a decrease of pH below 4 (Garg et al., 2015). Examples of sunlight-induced changes in Fe speciation in low-DOM environment are well known from the experiments with acidic lakes and seawater and involve both the reduction of ferric iron species and the dissolution of colloidal iron(III) oxides (Collienne, 1983; Anderson and Morel, 1982; Waite and Morel, 1984). The present study does not confirm or dismiss the photoproduction of Fe(II) from Fe(III)-rich organo-mineral colloids. Circum-neutral pH (7.0) of the stream water may inhibit the photochemical process, whereas the appearance of small amount of Fe^{2+} in more acidic ($\text{pH} = 5.3$) bog waters cannot be detected at already high level of colloidal Fe^{3+} ($4000 \mu\text{g/L}$). The photo-reduction of Fe(III) is likely to be sensitive to the size of organo-mineral colloids and to the distribution of Fe(III) between Fe oxyhydroxide and Fe organic complexes. In case of the dominance of Fe-organic ligands, photo-degradation of

DOM may bring about the appearance of Fe(II). However, given that Fe(III) is predicted to be 100% complexed with DOM in the course of experiment with both water samples, these effects could not be verified in this study.

We observed that a significant decrease in the proportion of colloidal forms of Fe and Al in the bog water (63 and 57 %, respectively) in the course of sunlight exposure is accompanied by an increase in the proportion of LMW_{< 1 kDa} forms (200 and 135%, respectively, see **Fig. 4.7 D, 4.8 D**). Such an increase in LMW forms is not observed for P and other insoluble metals such as Ti, Zr, Hf, Th, Y, REEs (**Table 4.3**). Analyses of colloid speciation in Northern Karelia waters demonstrated that these hydrolysates are not complexed with organic matter but adsorbed onto or coprecipitated with Fe (Al) oxy(hydr)oxides (Pokrovsky and Schott, 2002; Vasyukova et al., 2010; Ilina et al., 2016). As a result, these elements could be protected from interaction with external solution and sunlight being incorporated inside the colloidal Fe oxy(hydroxides). Thus, after photolysis of colloidal DOM, destabilization of ferric colloids and Fe(III), Al(III) coagulation in the form of amorphous Fe, Al-rich particles, these particles scavenge most of TE³⁺, TE⁴⁺. Such a scavenging may prevent the complexation of these elements with photolytically-produced LMW organic ligands. Another explanation of the lack of TE³⁺, TE⁴⁺ LMW_{< 1 kDa} production during irradiation is competition between Fe³⁺, Al³⁺ and other trivalent and tetravalent metals for LMW organic ligands. As a result, these trace elements remain adsorbed onto or coprecipitated with Fe hydroxide forms and thus removed from solution at the end of experiment. These was slightly more efficient removal of light REEs (LREEs) compared to heavy REE (HREEs) in 0.22 µm fraction (Table 2), consistent with REE adsorption and the affinity to solid phases generally decreasing from LREEs to HREEs (Tang and Johannesson, 2010; Johannesson et al., 2017). Noteworthy that phosphorus did not follow soluble alkali-earth but was totally removed from solution together with Fe (**Fig. 4.4**). It is possible that the organic complexes of phosphorus were oxidized under sunlight and transformed into orthophosphate ions. The PO₄³⁻(aq) thus produced was coprecipitating with Fe hydroxide upon the photodestruction of DOM.

Overall, the impoverishment of colloids in C_{org} relative to most TE is due to an efficient removal of the DOC from the 0.22 µm fraction to both LMW_{< 1 kDa} fraction and CO₂. Based on observed pattern of DOC and trace element behavior in the course of irradiation of bog water, we suggest 4 main processes responsible for TE removal and redistribution among different colloidal pools: formation of particulate Al, Fe

hydroxides; coprecipitation of TE³⁺, TE⁴⁺ with these oxyhydroxides; generation of LMW_{< 1 kDa} organic ligands and organic complexes of Fe³⁺, Al³⁺ and transition metals Me²⁺; liberation of alkaline-earths and divalent transition metals in the form of inorganic complexes and ions. A cartoon of possible processes in organic-and Fe-rich waters subjected to solar irradiation is given in **Figure 4.15**.

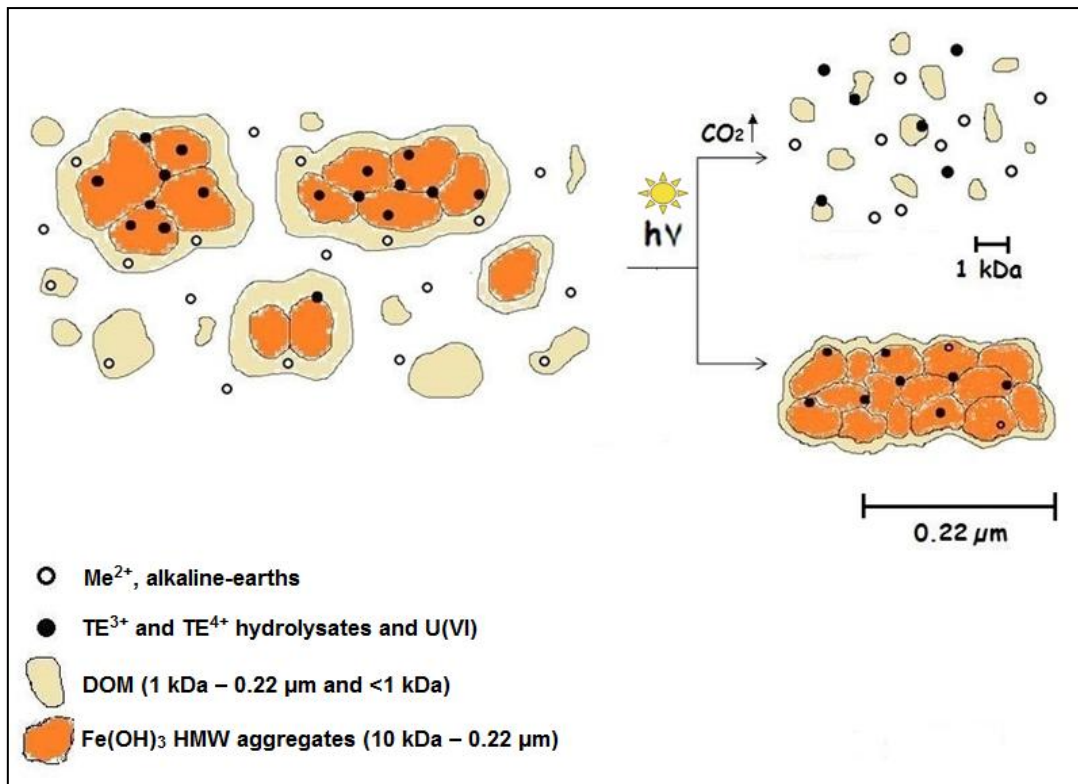


Fig. 4.15. Cartoon of sunlight-induced transformation of organic and organo-mineral colloids, consisting in coagulation of Fe, Al-rich particles and production of LMW organic complexes and ions of Fe, Al and divalent metals.

We hypothesize that the mechanisms identified in this study should operate in all surface waters of the boreal zone, but the effect of solar irradiation is most visible in acidic, humic Fe-rich environments such as bog waters. In these settings, there are two main pools of DOM: (i) metal-poor organic colloids (1 kDa – 0.22 μm) and LMW_{< 1 kDa} fractions, whose behavior does not presumably affect the fate of major and trace elements and (ii) Fe and Al nano-oxy(hydr)oxides stabilized by organic coating or embedded into the organic matrix in the form of large size (10 kDa – 0.22 μm) organo-mineral colloids. These pools are inferred from numerous studies of dissolved (< 0.45 μm) fraction of boreal surface waters conducted using dialysis, ultrafiltration (Vasyukova et al., 2010; Pokrovsky et al., 2010; Ilina et al., 2016), optical spectroscopic measurements (Ilina et al., 2014), and specific size fractionation techniques in temperate (Dia et al., 2000; Pédrot et al., 2008, 2009; Neubauer et al.,

2013a, b, c) and subarctic (Lyvén et al., 2003) region of Europe and Alaska (Stolpe et al., 2013a, b) and also confirmed by in-situ X-ray Absorption Spectroscopy (Sundman et al., 2014). After the light irradiation-induced removal of a part of the DOM that stabilized Fe oxy(hydr)oxides nanoparticles, these colloids are subjected to agglomeration and coagulation into large particulate forms ($> 0.22 \mu\text{m}$), since the initially supersaturated solution ($\Omega_{\text{ferrihydrite}} = 23.4$; $\Omega_{\text{gibbsite}} = 2.7$) becomes undersaturated with respect to secondary hydroxides after 200 h of irradiation ($\Omega_{\text{ferrihydrite}} = 0.06$; $\Omega_{\text{gibbsite}} = 0.45$). The coagulation of Fe and Al hydroxides during irradiation of temperate streams (Porcal et al., 2010, 2013a), acidic lake waters (Kopacek et al., 2005, 2006) and soil fulvates and humates (Porcal et al., 2009b) occurs due to destruction of organically-bound Fe and Al (Kopacek et al., 2006; Porcal et al., 2014) leading to formation of insoluble products (Porcal et al., 2013). In addition, particulate metals can adsorb to DOC, thereby transforming it to particulate organic carbon (Porcal et al., 2004, 2013a, 2014). We believe that nano-particulate Fe oxy(hydr)oxide is stabilized by “allochthonous” humic and fulvic-like substances having high negative charge which is not modified after irradiation (as proven by ion chromatography of studied samples; Drozdova et al., 2017). If the colloidal DOM was “autochthonous” and rich in proteins, then the amount of negatively-charged compounds would decrease. Note that during photo-degradation of temperate organic-rich river, the amount of Fe that was retained by AGMP anion-exchange resin also remained constant (Shiller et al., 2006).

The coagulation of Fe and Al hydroxide may scavenge TE^{3+} , TE^{4+} hydrolysates, As and U^{VI} . A part of colloidal Fe and Al can be transformed into $\text{LMW}_{< 1 \text{ kDa}}$ organic complexes since there was a strong increase of $\text{LMW}_{< 1 \text{ kDa}}$ fraction of Fe and Al upon sunlight exposure of the bog water. It is important to note that the 10 kDa fraction of Fe did not increase in concentration in the course of experiment, which suggests that the HMW Fe-rich organo-mineral colloids (10 kDa – $0.22 \mu\text{m}$) are partially transformed into $\text{LMW}_{< 1 \text{ kDa}}$ fraction rather than into LMW colloids (1 kDa – 10 kDa). Unfortunately, we could not distinguish between Fe(III)- and Fe(II)-OM complexes and Fe(II) ionic forms in this $< 1 \text{ kDa}$ fraction. Overall, our results corroborate the previous finding on boreal stream waters that in summertime, the photoreaction of Fe(III) under the visible range of light and UV may produce labile ($< 100 \text{ Da}$) Fe (Kelton et al., 2007). At the same time, significant photo-degradation of LMW organic matter was reported for temperate river (Shiller et al., 2006). These authors invoked

the release of DOM-complexed Fe(III) during photo-degradation of the LMW organic ligands followed either by *i*) precipitation of colloidal FeOOH or *ii*) formation of HMW ($> 0.02 \mu\text{m}$) Fe(III)-organic complexes. The first scenario was further confirmed by Fe speciation studies using Chelex and AGMP ion exchange resins (Shiller et al., 2005). We suggest that much higher Fe and DOC concentration in Karelian samples and more acidic nature of the bog water studied in the present work may be responsible for the observed difference in $\text{LMW}_{< 1 \text{ kDa}}$ organic matter and metal complexes pattern during photo-degradation of boreal and temperate waters. Another reason may be the difference in the molecular nature of DOM in the Pearl River of Shiller et al. (soil forest humic substances but also autochthonous easily-degradable organics) and essentially allochthonous (refractory) nature of DOM in Karelian surface waters.

The photo degradation of DOM exerted an unexpected impact on the colloidal speciation of alkali, alkaline earths and several important divalent metal micronutrients (Mn, Co, Ni, Cd). Whilst the $< 0.22 \mu\text{m}$ concentration of these elements remained fairly constant (**Fig. 4.11**), the concentration of these elements in the $\text{LMW}_{< 1 \text{ kDa}}$ fraction greatly increased after exposure to sunlight (**Fig. 4.14**). The evolution of DOC to divalent metal ratio in the $\text{LMW}_{< 1 \text{ kDa}}$ fraction (**Table 4.2**) demonstrates that upon the degradation of colloidal DOM, the ionic (organic-free) forms of these metals enrich the $< 1 \text{ kDa}$ fraction in a much stronger degree than the newly-produced low molecular weight OM.

Recently, it was demonstrated that the photolysis of boreal water sample produces low-molecular weight carboxylic ligands: the concentration of acetic, formic, succinic and oxalic acid increased by a factor of 10, 3, 2 and 7 during 10-day irradiation of interstitial soil solution of studied Karelian watershed (Drozdova et al., 2017). These newly produced organic acids however represent a minor fraction of overall DOC (< 10%, see section 4.6.1). The results of vMinteq metal speciation simulation (**Fig. 4.16 and Table 4.4**) suggest that the nature of $\text{LMW}_{< 1 \text{ kDa}}$ fractions of Me^{2+} is inorganic rather than organic. Indeed, according to vMinteq prediction, in the course of sunlight irradiation of $\text{LMW}_{< 1 \text{ kDa}}$ fraction, the proportion of uncomplexed (inorganic) forms of Ca, Mg, Sr, Ba and Mn increases from 60 ± 1 to $77 \pm 2\%$. Significant (by 10 to 20%) increase of inorganic forms is also predicted in $\text{LMW}_{< 1 \text{ kDa}}$ fraction of Cd, Zn, Co and Ni. The decrease of the colloidal fraction of metals and the increase of their $\text{LMW}_{< 1 \text{ kDa}}$

k_{Da} forms at the end of experiment is largely due to 2 to 3 fold decrease of the main complexant of 0.22 μm fraction, the colloidal DOM (**Fig. 4.2 B, D**).

The concentration of carboxylates in $\text{LMW}_{<1 \text{ kDa}}$ fraction after 200 h of sunlight exposure was quite low: 0.05, 0.17, 0.12 and 0.01 mg/L of acetate, formate, oxalate and citrate, respectively, and 14.8 $\mu\text{g}/\text{L}$ of benzoate (Drozdova et al., 2017). Including these acids to the thermodynamic calculation did not appreciably modify the speciation of metals in irradiated samples as illustrated for Ca, Cu, Fe and Al in **Table 4.5**: the majority of metals remain complexed with fulvic acids.

Sulfate can be considered within the group of elements which are liberated from organic colloids upon photodegradation of DOM. The concentration of SO_4^{2-} in bog water measured by HPLC increased more than two-fold over 100-200 h of reaction, both in < 0.22 μm and < 10 kDa fractions. We interpret this increase as either release of sulfate from the colloid-bound complexes or organic sulfur oxidation and transformation to sulfate. This is consistent with several indications in the literature that 1) the dissolved organic sulfur (DOS) may constitute between 20 and 60% of total dissolved sulfur in a forested organic-rich stream (Wang et al., 2012), 2) the DOC and DOS are generally correlated (Homann et al., 1990), and 3) from 10% to 20% of the dissolved sulfur in soil and groundwater could be bound to DOM (Nilsson et al., 2001; Mitchell et al., 1986, 1989).

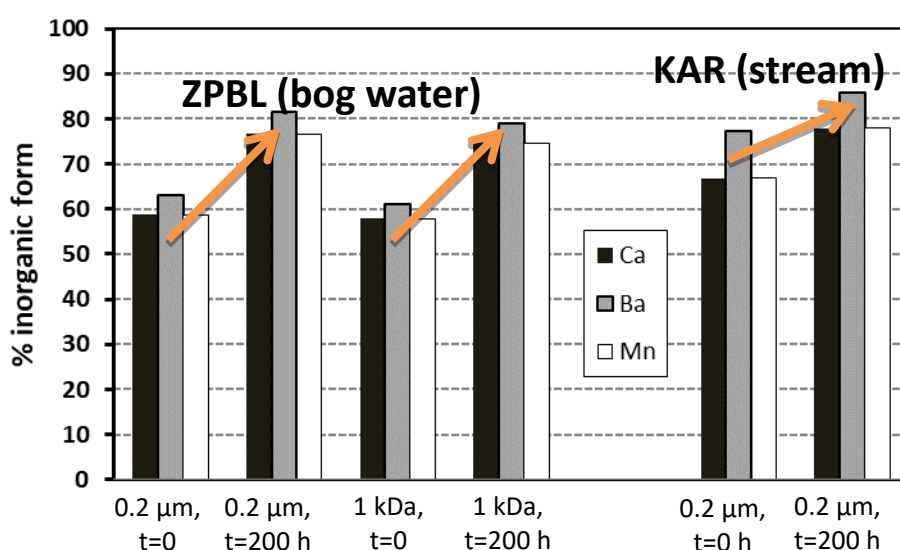


Fig. 4.16. The increase of the proportion of inorganic (DOM-uncomplexed) forms of Ca, Ba and Mn in 0.22 μm and 1 kDa fractions in the course of irradiation reaction of bog water and boreal stream. The arrows indicate the change of speciation between the beginning and the end of sunlight irradiation.

Table 4.4. Visual Minteq-predicted* proportion (% of total concentration) of metal that is not complexed to DOM and saturation indices with respect to main secondary oxy(hydr)oxides at the beginning and at the end of exposure in 0.22 µm and 1 kDa fraction of peat water (ZPBL) and stream water (KAR).

	0.2 µm, t = 0	0.2 µm, t = 200 h	1 kDa, t = 0	1 kDa, t = 200 h	0.2 µm, t = 0	0.2 µm, t = 200 h
	ZPBL	ZPBL	ZPBL	ZPBL	KAR	KAR
Al	0.6	0.27	0.18	0.54	2.0	4.5
Fe	0.5	0.02	0.01	0.2	0.0	0.1
K	99.1	99.6	99.5	99.6	99.6	99.7
Na	99.1	99.6	99.5	99.6	99.6	99.7
Mg	59.7	77.8	58.6	75.6	69.1	79.7
Ca	58.7	76.7	57.9	74.7	66.8	77.9
Sr	62.5	80.9	60.5	78.2	75.6	84.5
Ba	63.2	81.7	61.0	78.9	77.3	85.7
Mn	58.7	76.7	57.9	74.7	66.9	78.0
Ni	23.1	26.2	20.8	33.1	10.9	18.6
Co	46.1	57.4	44.2	61.1	35.1	49.9
Zn	41.8	53.6	41.9	56.6	27.2	41.3
Cu	5.7	2.7	1.8	7.1	0.1	0.3
Cd	41.1	49.2	38.0	55.1	25	39
Pb	5.5	5.9	5.0	8.1	0.5	1.0
Saturation indices ($\log \Omega$)						
Ferrihydrite	1.37	-1.24	-1.81	0.242	-0.11	0.50
Goethite	4.20	1.59	1.02	3.07	2.72	3.32
Lepidocrocite	3.49	0.89	0.323	2.37	2.02	2.62
Al(OH)₃ soil	-0.12	-0.90	-1.37	-0.50	0.403	0.74
Gibbsite	0.43	-0.35	-0.82	0.051	0.953	1.29
Possible precipitated solid phases, mol/L						
Ferrihydrite	4.5×10^{-5}			1.8×10^{-6}		
Goethite	7.5×10^{-5}				2.1×10^{-6}	3.0×10^{-6}
Gibbsite	6.6×10^{-7}				1.15×10^{-6}	9.4×10^{-7}

* According to vMinteq prediction, 4.5×10^{-5} M of ferrihydrite was precipitated from ZPBL waters over 200 h of solar irradiation. This is equivalent to ~2250 µg/L of dissolved Fe concentration decrease, which is comparable to the range encountered in the experiment (ca. 4000 µg/L, see Fig. 5 C). At the same time, vMinteq predicted the supersaturation with respect to ferrihydrite (and thus its possible precipitation in the amount of 2.0×10^{-6} M of goethite which is equivalent to ~100 µg/L Fe) in the stream water, where Fe concentration did not decrease at all during the experiment.

Table 4.5. Speciation of Ca, Cu, Fe and Al in < 1 kDa fraction of bog water after 200 h of sunlight exposure. Two basic scenarios were assumed: the appearance or not of carboxylic acids. The concentration of acetate, formate, oxalate and citrate was equal to 0.05, 0.17, 0.12 and 0.01 mg/L, respectively, that of benzoate was 14.8 µg/L (Drozdova et al., 2017 and in preparation).

Species	% with carboxylates	% w/o carboxylates	Species	% with carboxylates	% w/o carboxylates
Ca+2	69.9	70.0	Fe(OH)2+	0.096	0.096
Ca-Citrate-	0.01		Fe-Citrate (aq)	0.011	
Ca-Oxalate (aq)	0.08		/FA2FeOH(aq)	99.3	99.3
/FA-Ca+2G(aq)	20.9	20.9	/FA2Fe+(aq)	0.564	0.564
/FACa+(aq)	9.06	9.07			
			Al+3	0.028	0.03
Cu+2	3.26	3.31	AlOH+2	0.092	0.101
CuOH+	0.039	0.039	Al(OH)2+	0.132	0.145
Cu-Citrate-	0.30		Al(OH)3 (aq)	0.018	0.02
Cu-(Oxalate)2-2	0.036		Al-Citrate (aq)	0.58	
Cu-Oxalate (aq)	1.27		AlOH-(Oxalate)2-2	0.055	
/FA-Cu+2G(aq)	0.97	0.99	Al(OH)2-Oxalate-	3.63	
/FA2Cu(aq)	46.5	47.2	AlOH-Oxalate	3.48	
/FACu+(aq)	47.5	48.2	Al-(Oxalate)2-	0.39	
/FA2CuOH(aq)	0.177	0.180	Al-Oxalate+	1.02	
			/FA-Al+3G(aq)	0.67	0.74
			/FA-AlOH+2G(aq)	0.027	0.030
			/FA2AlOH(aq)	48.3	53.2
			/FA2Al+(aq)	41.6	45.7

FA stands for Fulvic Acid.

4.6.3. Natural implications

From natural observations in boreal humic lakes, it is known that DOC-to-Fe ratio increases as a function of increasing lake coverage of the catchment because lakes remove Fe more efficiently than DOC (Köhler et al., 2013; Weyhenmeyer et al., 2014 Xiao et al., 2013). The experimental results of sunlight irradiation of humic waters are consistent with these findings and suggest that sunlight can be one of the factors of chemical transformation in the inland waters: the ratio DOC/Fe increased 6-fold between 100 and 250 h of sunlight exposure (Fig. S4 A). The photo-irradiation of DOM in natural waters is known to produce biologically-available organic ligands hence increasing the heterotrophic respiration of DOM (Lindell et al., 1995; Moran and Covert, 2003; Scully et al., 2003; Ruiz-Gonzalez et al., 2013; Porcal et al., 2009b; Cory et al., 2013; Laurion and Mladenov, 2013). To which degree this photo-transformation can modify the fate of micronutrients and toxic metals is still unknown. The obtained results allow the prediction of the fate of insoluble trace elements (Al, Fe, Ti, Ga, Y, Zr, Nb, REEs), toxicants (Al, Cr, As, Pb) and micro-nutrients when the

bog waters are exposed to sunlight at the earth surface via discharge into rivers and lakes. Based on experiments of this study we anticipate significant ($90\pm10\%$) scavenging of P, V, Cr and Fe from the bog water during first week of its exposure to sunlight. At the same time, photo-degradation of organic and organo-mineral colloids is capable releasing a number of metal micronutrients from colloidal (1 kDa – 0.22 μm) into $\text{LMW}_{< 1 \text{ kDa}}$ fraction. Thus, the concentration of K, Rb, Ca, Sr, Mn, Co, Ni, Ba, Cd in this potentially bioavailable fraction may increase by a factor of 2 to 3 for over weekly exposure of surface waters to sunlight. It follows that the residence time of bogwater in shallow surface reservoirs (lakes, rivers) controls the intensity of photo-induced transformation of organic and organo-mineral colloids. Typically, several days of sunlight exposure, which is comparable with water residence time in streams and small lakes of Northern Karelia region studied in this work (i.e., Ilina et al., 2014), might be sufficient to remove significant amount of low-soluble colloidal elements and raise potentially bioavailable concentration of divalent metal micronutrients. It can be hypothesized that, under climate warming scenario, the positive response of sunlight photolytic efficiency to temperature rise (Porcal et al., 2015) is capable to alleviate the on-going browning of boreal surface waters, consisting in the increase of dissolved Fe (Weyhenmeyer et al., 2014; Kritzberg and Ekström, 2012; Kritzberg et al., 2014). An interesting consequence of photolysis of boreal Fe- and organic-rich water for nutrient transport is that rising Fe concentrations could potentially decrease the export of P because P may be immobilized during UV-induced Fe and Al hydroxide coagulation.

4.7. Concluding remarks

The DOM of bogwater was subjected to efficient degradation under sunlight compared to the stream water. In the course of sunlight exposure, colloidal (1 kDa – 0.22 μm) Fe and Al were divided into two pools, $> 0.22 \mu\text{m}$ particles and LMW organic complexes. We observed an increase of C_{org} and constant values of SUVA in $\text{LMW}_{< 1 \text{ kDa}}$ fraction which strongly suggests that the optically-active, but low-aromatic compounds smaller than 1 kDa are highly resistant to sunlight exposure and produced during photo-degradation of HMW organic colloids.

The main results of solar irradiation of bog waters over 10 days of exposure are *i*) the removal of a half of colloidal (1 kDa - 0.22 μm) DOC; *ii*) strong, by a factor of 5, decrease in SUVA_{254} and aromaticity of DOC in 0.22 μm fraction; *iii*) production of

LMW_{< 1 kDa} Fe(III) and Al(III) complexes with DOM; *iv)* degradation of organic colloidal (1 kDa – 0.22 µm) complexes of alkalis, alkaline earths, Mn, Co and Ni and release of free divalent metals in the LMW_{< 1 kDa} presumably inorganic forms, and finally *v)* after DOM degradation, the coagulation and precipitation of colloidal Fe and Al in the form of oxy(hydroxides) which thus scavenge many insoluble trace elements.

The increase of LMW_{< 1 kDa} fraction with time in bog waters was observed only for elements linked to essentially organic components of colloids: these are all alkalis, alkaline earths and some divalent metals such as Mn, Co, Ni. Upon degradation of DOM, these monovalent and divalent metals became largely liberated from their organic complexes. In bog waters, the humic and fulvic complexes of alkali and alkaline-earth metals and divalent metal micronutrients (50-80%) may be completely degraded over a week of sunlight exposure. All other trace elements such as trivalent and tetravalent hydrolysates (TE^{3+} , TE^{4+}) linked to ferric and aluminum colloids did not increase their LMW_{< 1 kDa} concentrations because they could not be detached from their Fe and Al hydroxide carriers. After removal of DOM that stabilized Fe-rich organo-mineral colloids (10 kDa – 0.22 µm), the TE are removed from solution during agglomeration, coagulation and precipitation of particulate Fe hydroxides (> 0.22 µm).

Three major processes of dissolved load transformation under sunlight in natural waters include: *(i)* degradation of organic part of colloidal (1 kDa – 0.22 µm) organic matter and production of low molecular weight (< 1 kDa) organic ligands including carboxylic acids; *(ii)* coagulation and precipitation of Fe and Al-rich oxy(hydroxide) and incorporated trivalent and tetravalent hydrolysates, V, P, Cr and As, after the solar radiation-induced removal of stabilizing dissolved organic matter, and *(iii)* liberation of alkalis, alkaline-earth, Mn, Co, Ni, Zn and SO_4^{2-} from organic complexes. It follows that the sunlight-induced degradation of natural DOM in the boreal zone is capable producing ionic (and thus potentially bioavailable) micro-nutrients such as K, V, Cr, Mn, Co, Ni, Zn, Ba, while scavenging sizeable amount of potentially toxic trace elements but also phosphorus.

4.8. Acknowledgements

We acknowledge support from a RFBR research projects №№ 16-55-150002 CNRS_a, 15-05-05000_a, 14-05-00430_a, 16-05-00542_a and 17-05-00348_a. OP was partially funded by an RSF grant No 15-17-10009 (modeling) and BIO-GEO-CLIM grant No 14.B25.31.0001 of the Russian Ministry of Science and Education (analyses).

Chapitre 5. Conclusion général

L'étude expérimentale de l'impact des bactéries hétérotrophes *Pseudomonas saponiphila* sur la distribution de la taille des colloïdes de carbone organique et des éléments traces métalliques dans les lixiviats de tourbe a permis de distinguer l'adsorption et l'assimilation/coagulation des éléments traces. La composition colloïdale des lixiviats de tourbe est dominée par Fe, qui est 4 fois plus abondant que Al et dont la concentration est de 1 à 2 ordres de grandeur plus élevé que celles des autres éléments traces. Les bactéries hétérotrophes dégradent préférentiellement la fraction de faible poids moléculaire du COD (<3 kDa) ; sa concentration a diminué de $15.8 \pm 0.3\%$ sur 4 jours d'expérience. Le Fe est fortement affecté par l'activité bactérienne, comme en témoigne une augmentation de 40% du rapport COD/Fe dans la fraction colloïdale sur 4 jours d'expérience. V, Ti et Th suivent le comportement de Fe, avec une diminution lente de leurs concentrations au fil du temps. En revanche, les oligo-éléments des métaux divalents (Mn, Ni, Cu) et les toxiques (Cd, Pb) sont uniquement affectés par une adsorption rapide sur les surfaces bactériennes pendant la première heure de réaction avec un impact minimal à long terme sur le métabolisme cellulaire.

Lors d'une expérience d'adsorption rapide (3 h) des constituants des lixiviats de tourbe sur la biomasse de *P. Saponiphila*, une diminution de $30 \pm 20\%$ des concentrations en Al, Fe, Cu, Sr, Y, REE, Th et U a été observée, tandis que le COD et tous les autres ET n'ont pas sensiblement affectés (<5-10% de la quantité initiale). En réponse à l'augmentation du pH de 5 à 7 due au métabolisme microbien, les concentrations en Al, V, Mn, Fe, Ni, Cu, Cd ont diminué de 30-60%, ce qui suggère une certaine adsorption des métaux colloïdaux. Dans l'ensemble l'adsorption rapide sur les surfaces cellulaires s'est révélée plus importante que l'assimilation lente intracellulaire ou que les processus abiotiques comme la coagulation et la coprécipitation. Seuls quelques éléments peu solubles liés aux colloïdes (Al, Ti, Fe, Zr, Nb, Hf, Pb et Th) ont été affectés par une élimination lente (1-93 h d'expérience), probablement par coprécipitation avec des oxydes et hydroxydes de Fe coagulés. Une partie peu importante mais statistiquement significative (5 à 10%) de COD et des ET de diverses fractions de taille a été transférée de la fraction dissoute stricto sensu (poids moléculaire faible) <3 kDa aux fractions colloïdales fine (50 kDa-3 kDa) et grossière (0.45 µm-50 kDa).

En élargissant nos investigations à 7 eaux naturelles du paysage subarctique contenant des MOD essentiellement allochtones, nous avons observés un faible impact de l'activité bactérienne hétérotrophe sur ces MOD. Parmi ces substrats figurent un à nouveau un lixiviat de tourbière, mais également un échantillon d'eau de marais, un échantillon d'eau de ruisseaux, un échantillon de rivière, un échantillon d'eau de lac humique, un échantillon d'eau de lac oligotrophique, et un pluvio-lessivat collecté sous un pin. Seuls 3 types d'eau (lac humique, ruisseaux et marais) ont été caractérisés par une biodégradation significative des MOD après 4 jours de réaction avec la bactérie hétérotrophe de sol *Pseudomonas aureofaciens*. La bactérie hétérotrophe aquatique *Pseudomonas saponiphila* a dégradé environ 5% du COD dans le lixiviat de tourbe, et n'a pas eu d'effet notable sur les COD des autres substrats. Lors de l'interaction entre des bactéries hétérotrophes et divers milieux aquatiques de la zone subarctique, une première phase d'adsorption rapide (0-1 h d'expérience – phase 1) sur les surfaces cellulaires de Al, Fe, Mn, Ni, Co, Cu, Cd, REE, U^{VI} a été identifiée. Son impact est généralement largement dominant par rapport à la diminution lente observée dans la suite des expériences (1-96 h d'expérience – phase 2). Dans quelques cas de figure, les concentrations de certains éléments (COD, Al, Mn, Fe, Co, Ni, Cd et dans une moindre mesure, Ti, Y et REE) diminuent néanmoins sensiblement (10 à 40%) lors cette deuxième phase. Cette diminution lente est probablement liée soit à une assimilation intracellulaire, soit à une précipitation extracellulaire sous forme d'hydroxyde de fer. On observe une telle diminution lente dans les eaux de marais, de lac humique, de ruisseaux et dans le lixiviat de tourbe. Par ailleurs, la diminution totale des éléments Ca, Mg, Y et des REE lors de l'expérience en pluvio-lessivat de pin varient de 30 à 40%.

Pour tous les différents substrats, l'adsorption rapide (phase 1) est une fonction croissante du rapport COD/Fe en solution, ce qui peut être lié à une compétition entre le Fe et les cations métalliques pour les sites d'adsorption anioniques sur les surfaces cellulaires. Aucune corrélation significative n'a pu être mise en évidence entre la diminution lente (phase 2) et le pH et les valeurs absolues des concentrations en COD et en Fe. Cependant, un lien a été observé entre la diminution lente de la phase 2 et le degré initial de sursaturation par rapport aux phases secondaires principales (oxydes et hydroxydes de fer et d'aluminium).

Le taux de minéralisation de COD à long terme dans l'expérience (de 0 à 4,3 mg.C.I⁻¹.jour⁻¹ selon les substrats) était comparable ou inférieur à celui observé dans les

eaux naturelles des tourbières, malgré la concentration de bactéries vivantes de plusieurs ordres de grandeur plus élevés que celles qu'on rencontre en milieux naturels. Ce fait confirme la très faible dégradabilité de la MOD boréal allochtone par les bactéries hétérotrophes étudiées. L'élimination préférentielle du Fe par rapport au COD des fractions dissoute et colloïdale par le métabolisme des bactéries hétérotrophes peut être un mécanisme possible de rétroaction négative par rapport aux « brunissement » des eaux boréales en réponse au réchauffement de l'eau et du sol.

La matière organique allochtone, qui est donc assez stable vis-à-vis de la dégradation par des bactéries hétérotrophes, peut être néanmoins être transformée sous l'action de la lumière du soleil. La MOD d'eau de marais est photo-dégradée plus efficacement que celle de l'eau de la rivière. Au cours de l'exposition à la lumière du soleil, la majeur partie du Fe colloïdal et de l'Al colloïdal (1 kDa – 0.22 µm) a été transformée en deux types de substances : (i) des particules > 0.22 µm et (ii) des complexes organiques de fraction dissoute de poids moléculaire faible < 1 kDa. Nous avons observé lors de ce processus une augmentation de COD et des valeurs constantes d'absorbance spécifique UV ($SUVA_{254}$) dans la fraction <1 kDa, ce qui suggère fortement que dans cette fraction des composés optiquement actifs mais peu aromatiques et hautement résistants à l'action de la lumière solaire sont produits lors de la photodégradation des colloïdes organiques (tailles : 1 kDa – 0.22 µm).

Les principaux résultats de l'irradiation solaire des eaux de marais sur 10 jours d'exposition sont: i) l'élimination de la moitié du COD colloïdal (1 kDa – 0.22 µm); ii) une forte diminution (d'un facteur 5) du $SUVA_{254}$ et de l'aromaticité du COD dans une fraction de tailles inférieures à 0.22 µm; iii) la production de complexes de poids moléculaire faible < 1 kDa des Fe (III) et Al (III) avec la MOD; iv) la dégradation des complexes organiques colloïdaux (1 kDa – 0.22 µm) d'éléments alcalins, alcalino-terreux, Mn, Co et Ni et la libération de métaux divalents libres sous formes de tailles inférieures à 1 kDa (probablement inorganiques) et, finalement, après la dégradation de la MOD, v) la coagulation et la précipitation de Fe et Al colloïdaux sous forme d'oxydes et d'hydroxydes qui piègent ainsi de nombreux éléments traces.

L'augmentation au cours du temps d'expérience des concentrations dans la fraction dissoute de poids moléculaire faible <1 kDa dans l'eau de marais n'a été observée que pour les éléments liés aux composants essentiellement organiques des colloïdes: il s'agit de tous les alcalins, des alcalino-terreux et de certains métaux divalents tels que Mn, Co, Ni. Lors de la dégradation de la MOD, ces métaux

monovalents et divalents sont en grande partie libérés de leurs complexes organiques. Dans l'eau de marais, 50 à 80 % des complexes humiques et fulviques des métaux alcalins et alcalino-terreux et des éléments traces métalliques divalents peuvent être dégradés au cours d'une semaine d'exposition au soleil. Pour tous les autres éléments traces tels que les hydrolysats trivalents et tétravalents (TE^{3+} , TE^{4+}) liés aux colloïdes ferriques et aluminiques, les concentrations n'augmentent pas dans la fraction dissoute de poids moléculaire faible <1 kDa car ils ne peuvent pas fortement associé aux hydroxydes de Fe et Al. Après élimination de la MOD qui stabilise les colloïdes organo-minéraux riches en Fe (10 kDa – 0.22 µm), les ET sont éliminés de la solution pendant la coagulation et la précipitation des hydroxydes de Fe particulières (> 0.22 µm).

Les trois principaux processus responsables de l'élimination et de la redistribution des éléments et de la MOD sous l'effet de la lumière du soleil dans les eaux naturelles sont : (i) la dégradation de la partie organique de la matière colloïdale (1 kDa – 0.22 µm) et la production des ligands organiques de faible masse moléculaire (1 kDa) incluant les acides carboxyliques; (ii) la coagulation et la précipitation des oxydes et des hydroxydes riche en Fe et en Al et des hydrolysats trivalents et tétravalents incorporés, V, P, Cr et As, après élimination de la matière organique dissoute par le rayonnement solaire, et (iii) la libération des éléments alcalins, alcalino-terreux, Mn, Co, Ni, Zn et SO_4^{2-} des complexes organiques. Il s'ensuit que la dégradation de la MOD naturelle induite par la lumière du soleil en zone boréale est capable de produire des ET ioniques (et donc potentiellement biodisponibles) tels que K, V, Cr, Mn, Co, Ni, Zn, Ba, tout en piégeant des ET potentiellement toxiques mais aussi du phosphore.

D'après les observations naturelles dans les lacs humiques boréaux, on sait que le rapport COD/Fe augmente en fonction de l'augmentation de la couverture lacustre du bassin versant parce que les lacs éliminent le Fe plus efficacement que le COD (Köhler et al., 2013, Weyhenmeyer et al. 2014 Xiao et al., 2013). Les résultats expérimentaux de l'irradiation solaire des eaux humiques concordent avec ces résultats et suggèrent que la lumière du soleil peut être un des facteurs de transformation chimique dans les eaux des surfaces continentales : ainsi le rapport COD/Fe augmente d'un facteur 6 entre 100 et 250 h d'exposition au soleil. La photo-irradiation de la MOD dans les eaux naturelles est connue pour produire des ligands organiques biologiquement disponibles augmentant ainsi la respiration hétérotrophique de la

MOD (Lindell et al., 1995, Scully et al., 2003, Ruiz-Gonzalez et al. al., 2013, Porcal et al., 2009b, Cory et al., 2013, Laurion et Mladenov, 2013).

Sur la base des expériences de cette étude, nous prévoyons un piégeage important ($90 \pm 10\%$) de P, V, Cr et Fe de l'eau de tourbière durant la première semaine de son exposition au soleil. Dans le même temps, la photodégradation des colloïdes organiques et organo-minéraux est capable de libérer un certain nombre de micronutriments métalliques de la fraction colloïdale (1 kDa – 0.22 μm) vers la fraction poids moléculaire faible <1 kDa. Ainsi, la concentration de K, Rb, Ca, Sr, Mn, Co, Ni, Ba, Cd dans cette fraction potentiellement biodisponible peut augmenter de 2 à 3 fois pour une exposition solaire hebdomadaire des eaux de surface. Il s'ensuit que le temps de séjour des eaux de tourbières dans les réservoirs de surface peu profonds (lacs, rivières) contrôle l'intensité de la transformation photo-induite des colloïdes organiques et organo-minéraux.

On peut supposer que, dans un scénario de réchauffement climatique, la réponse positive de l'efficacité photolytique à l'élévation de la température (Porcal et al., 2015) est capable d'atténuer «le brunissement» continu des eaux de surface boréales. (Weyhenmeyer et al., 2014, Kritzberg et Ekström, 2012, Kritzberg et al., 2014).

Bibliographie

- Ågren A.M., Buffam I., Cooper D.M., Tiwari T., Evans C.D., Laudon H. (2014) Can the heterogeneity in stream dissolved organic carbon be explained by contributing landscape elements? *Biogeosciences* 11, 1199–1213.
- Amon R.M.W., Benner R. (1996) Bacterial utilization of different size classes of dissolved organic matter. *Limnol. Oceanogr.* 41, 41-51.
- Anderson M.A. and Morel F.M.M. (1982) The influence of aqueous iron chemistry on the uptake of iron by the coastal diatom *Thalassiosira weissflogii*. *Limnol. Oceanogr.* 27, 789-813.
- Andersson K., Dahlqvist R., Turner D., Stolpe B., Larsson T., Ingri J., Andersson P. (2006) Colloidal rare earth elements in a boreal river: Changing sources and distributions during the spring flood. *Geochim. Cosmochim. Acta* 70(13), 3261-3274.
- Andersson P.S., Dahlqvist R., Ingri J., Gustafsson O. (2001) The isotopic composition of Nd in a boreal river: a reflection of selective weathering and colloidal transport. *Geochim Cosmochim Acta* 65(4), 521-527.
- Anesio A.M. and Granéli W. (2003) Increased photoreactivity of DOC by acidification: Implications for the carbon cycle in humic lakes. *Limnol. Oceanogr.* 48, 735–744.
- Arvola L., Kankaala P., Tulonen T., Ojala A. (1996) Effects of phosphorus and allochthonous humic matter enrichment on the metabolic processes and community structure of plankton in a boreal lake (Lake Paajarvi). *Can. J. Fish. Aquat. Sci.*, 53(7), 1646–1662.
- Ask J., Karlsson J., Persson L., Ask P., Byström P., Jansson M. (2008) Whole-lake estimates of carbon flux through algae and bacteria in benthic and pelagic habitats of clear-water lakes. *Ecology* 90, 1923–32.
- Asmala E., Autio R., Kaartokallio H., Stedmon C.A., Thomas D.N. (2014a) Processing of humic-rich riverine dissolved organic matter by estuarine bacteria: effects of photodegradation and inorganic nutrients. *Aquat. Sci.* 76(3), 451-463.
- Audry S., Pokrovsky O. S., Shirokova L. S., Kirpotin S. N., Dupré B. (2011) Organic matter mineralization and trace element post-depositional redistribution in Western Siberia thermokarst lake sediments. *Biogeosciences* 8, 3341-3358.

- Bagard M.L, Chabaux F., Pokrovsky O.S, Prokushkin A.S., Viers J., Dupré B. and Stille P. (2011) Seasonal variability of element fluxes in two Central Siberian rivers draining high latitude permafrost dominated areas. *Geochim. Cosmochim. Acta*, 75, 3335–3357.
- Bailey R., Clark H., Ferris J., Krause S., Strong R. (2002) Chemistry of the Environment (2nd Edition). *Academic Press*, 835.
- Battin T. J., Luyssaert S., Kaplan L. A., Aufdenkampe A. K., Richter A., Tranvik L. J. (2009) The boundless carbon cycle. *Nat. Geosci.* 2, 598-600.
- Benedetti M. F., Milne C., Kinniburgh D., Van Riemsdijk W. H., Koopal L. K. (1995) Metal ion binding to humic substances: Application of the non ideal competitive adsorption model. *Environ. Sci. Technol.* 29, 446-457.
- Berggren M., Lapierre J. F., Del Giorgio P. A. (2012) Magnitude and regulation of bacterioplankton respiratory quotient across freshwater environmental gradients. *The ISME Journal* 6, 984-993.
- Berggren M., Laudon H., Haei M., Ström L., Jansson M. (2010) Efficient aquatic bacterial metabolism of dissolved low-molecular-weight compounds from terrestrial sources. *The ISME Journal* 4, 408-416.
- Berggren M., Laudon H., Jansson M. (2007) Landscape regulation of bacterial growth efficiency in boreal freshwaters. *Global. Biogeochem. Cy.* 21, GB4002, doi: 10.1029/2006GB002844.
- Berggren M., Laudon H., Jansson M. (2009) Hydrological control of organic carbon support for bacterial growth in boreal headwater streams. *Microbial Ecol.* 57, 170-178.
- Bertilsson S. and Tranvik, L.J. (2000) Photochemical transformation of dissolved organic matter in lakes. *Limnol. Oceanogr.* 45, 753–762.
- Bertilsson, S. and Tranvik, L.J. (1998) Photochemically produced carboxylic acids as substrates for freshwater bacterioplankton. *Limnol. Oceanogr.* 43, 885-895.
- Bittar T.B., Vieira A.A.H., Stubbins A. and Mopper K. (2015) Competition between photochemical and biological degradation of dissolved organic matter from the cyanobacteria *Microcystis aeruginosa*. *Limnol. Oceanogr.* 60, 1172-1194.
- Blazevic A., Orlowska E., Kandioller W., Jirsa F., Keppler B.K., Tafili-Krueziu M., Linert W., Krachler R.F., Krachler R. and Rompel A. (2016) Photoreduction of

- terrigenous Fe-humic substances leads to bioavailable iron in oceans. *Angew. Chem. Int. Ed.* 55, 6417-6422.
- Bonneville S., Behrends T., Van Cappellen P., Hyacinthe C., Röling W.F.M. (2006) Reduction of Fe(III) colloids by *Shewanella putrefaciens*: A kinetic model. *Geochim Cosmochim Acta*, 70(23), 5842-5854
- Bosch J., Fritzsche A., Totsche K. U., Meckenstock R.U. (2010) Nanosized ferrihydrite colloids facilitate microbial iron reduction under flow conditions. *Geomicrobiol. J.* 27(2), 123-129.
- Brinkmann T., Sartorius D. and Frimmel F.H. (2003) Photobleaching of humic rich dissolved organic matter. *Aquat. Sci.* 65, 415–424.
- Bushaw K.L. et al. (1996) Photochemical release of biologically available nitrogen from aquatic dissolved organic matter. *Nature* 381, 404-407.
- Cabaniss S.E., Madey G., Leff L., Maurice P.A., Wetzel R. (2005) A stochastic model for the synthesis and degradation of natural organic matter. Part I. Data structures and reaction kinetics. *Biogeochemistry* 76, 319–47.
- Carpita N., Sabulars, D., Montezinos D., Delmer D. (1979) Determination of the pore size of cell walls of living plant cells. *Science* 205, 1144–1147.
- Catrouillet C., Davranche M., Dia A., Bouhnik-Le Coz M., Demangeat E. et Gruau G. (2016) Does As(III) interact with Fe(II), Fe(III) and organic matter through ternary complexes? *J. Colloid Interf. Sci.* 470, 153-161.
- Chan C.S., Fakra S.C., Edwards D.C., Emerson D., Banfield J.F. (2009) Iron oxyhydroxide mineralization on microbial extracellular polysaccharides. *Geochim. Cosmochim. Acta* 73 (13), 3807-3818.
- Châtellier X., Fortin D. (2004) Adsorption of ferrous ions onto *Bacillus subtilis* cells. *Chem. Geol.* 212 (3), 209-228.
- Chen M., Wang W.-X. (2001) Bioavailability of natural colloid-bound iron to marine plankton: Influences of colloidal size and aging. *Limnol. Oceanogr.*, 46(8), 1956-1967.
- Chupakov A.V., Ershova A., Moreva O.Yu, Shirokova L.S., Zabelina S.A., Vorobieva T.Y., Klimov S.I. et al. (2017) Allochthonous and autochthonous carbon in deep organic-rich and organic-poor lakes of the European Russian subarctic. *Boreal Environ. Res.*, 22, 213-230.
- Cole J., Prairie Y.T., Caraco N., McDowell W.H., Tranvik L., Striegl R.G., Duarte C.M., Kortelainen P., Downing J.A., Middelburg J.J., Melack J. (2007) Plumbing

- the global carbon cycle: Integrating inland waters into the terrestrial carbon budget. *Ecosystems* 10, 171–184.
- Collienne R.J. (1983) Photoreduction of iron in the epilimnion of acidic lakes. *Limnol. Oceanogr.* 28, 83-100.
- Corin N., Backlund P., Kulovaara M. (1996) Degradation products formed during UV-irradiation of humic waters. *Chemosphere* 33(2), 245-255, DOI: 10.1016/0045-6535(96)00167-1.
- Cory R.M., Crump B.C., Dobkowski J.A. and Kling G.W. (2013) Surface exposure to sunlight stimulates CO₂ release from permafrost soil carbon in the Arctic. *P. Natl. Acad. Sci. USA*, 110(9), 3429-3434.
- Cory R.M., Harrold K.H., Neilson B.T. and Kling G.W. (2015) Controls on dissolved organic matter (DOM) degradation in a headwater stream: the influence of photochemical and hydrological conditions in determining light-limitation or substrate-limitation of photo-degradation. *Biogeosciences* 12, 6669–6685.
- Cory R.M., McKnight D., Chin Y.P., Miller P. and Jaros C.L. (2007) Chemical characteristics of fulvic acids from Arctic surface waters: Microbial contributions and photochemical transformations. *J. Geophys. Res.* 112, G04S51, DOI:10.1029/2006JG000343.
- Cory R.M., Ward C.P., Crump B.C. and Kling G.W. (2014) Sunlight controls water column processing of carbon in arctic fresh waters. *Science* 345, 925-928.
- Cotner J.B. and Heath R.T. (1990) Iron redox effects on photosensitive phosphorus release from dissolved humic materials. *Limnol. Oceanogr.* 35, 1175-1181.
- Dahlqvist R., Andersson K., Ingri J., Larsson T., Stolpe B., Turner D. (2007) Temporal variations of colloidal carrier phases and associated trace elements in a boreal river. *Geochim. Cosmochim. Acta* 71(22), 5339-5354.
- Dahlqvist R., Benedetti M.F., Andersson K., Turner D., Larsson T., Stolpe B., Ingri J. (2004) Association of calcium with colloidal particles and speciation of calcium in the Kalix and Amazon rivers. *Geochim. Cosmochim. Acta* 68(20), 4059-4075.
- De Haan H. (1993) Solar UV-light penetration and photodegradation of humic substances in peaty lake water. *Limnol. Oceanogr.* 38, 1072-1076.
- Dean W.E., Gorham E. (1998) Magnitude and significance of carbon burial in lakes, reservoirs, and peatlands. *Geology* 26, 535–538.
- Dia A., Gruau G., Olivié-Lauquet G., Riou C., Molénat J. and Curmi P. (2000) The distribution of rare earth elements in groundwaters: assessing the role of source-

- rock composition, redox changes and colloidal particles. *Geochim. Cosmochim. Acta* 64(24), 4131-4151.
- Drake T.W., Wickland K.P., Spencer R.G.M., McKnight D.M., Striegl R.G. (2015) Ancient low-molecular-weight organic acids in permafrost fuel rapid carbon dioxide production upon thaw. *PNAS* 112(45), 13946-13951.
- Drozdova O.Yu., Pokrovsky O.S., Lapitskiy S.A., Shirokova L.S., Gonzalez A.G., Demin V.V. (2014) Decrease in Zn adsorption on soil in the presence of EPS-rich and EPS-poor *Pseudomonas aureofaciens*. *J. Colloid Interf. Sci.* 435, 59-66.
- Drozdova O.Yu., Shirokova L.S., Carrein A., Lapitskiy S.A., Pokrovsky O.S. (2015) Impact of heterotrophic bacterium *Pseudomonas aureofaciens* on the release of major and trace elements from podzol soil into aqueous solution. *Chem. Geol.* 410, 174–187.
- Drozdova, O.Yu., Ilina, S.M., Lapitskiy, S.A. (2017) Transformation of dissolved organic matter in the continuum soil water – bog – stream and terminal lake of a boreal watershed (Northern Karelia). In: Pokrovsky, O.S., Shirokova, L.S., Eds. Dissolved Organic Matter (DOM): Properties, Applications and Behavior, Nova Publishers, Hauppauge, NY, USA, In press.
- Emnova E.E., Varbanets L.D., Vasiliev V.N., Ciocarlan A.G., Brovarskaia O.S., Caunova N.J., Ganea O.G., Toma S.I. (2007) Properties of exopolysaccharides from rhizospheric fluorescent bacteria of *Pseudomonas* genus. Bulletin of Moldovan Academy of Sciences, Life Sciences 1(310), 14-20.
- Fakih M., Châtellier X., Davranche M., Dia A. (2008) *Bacillus subtilis* bacteria hinder the oxidation and hydrolysis of Fe²⁺ ions. *Environ. Sci. Technol.* 42 (9), 3194–3200.
- Fein J. B., Martin A. M., Wightman P. G. (2001) Metal adsorption onto bacterial surfaces: development of a predictive approach. *Geochim. Cosmochim. Acta* 65, 4267–4273.
- Fein J.B., Daughney C.J., Yee N., Davis T.A. (1997) A chemical equilibrium model for metal adsorption onto bacterial surfaces. *Geochim. Cosmochim. Acta* 61, 3319–3328.
- Feng M., Ngwenya B.T., Wang L., Li W., Olive V., Ellam R.M. (2011) Bacterial dissolution of fluorapatite as a possible source of elevated dissolved phosphate in the environment. *Geochim. Cosmochim. Acta*, 75(19), 5785-5796, DOI: 10.1016/j.gca.2011.07.019.

- Ferrarello C.N., Fernández de la Campa M.R., Sanz-Medel A. (2002) Multielement trace-element speciation in metal-biomolecules by chromatography coupled with ICP-MS. *Anal Bioanal Chem.* 373(6), 412-421.
- Finlay K., Leavitt P., Wissel B., Prairie Y.T. (2009) Regulation of spatial and temporal variability of carbon flux in six hard-water lakes of the northern Great Plains. *Limnol. Oceanogr.* 54, 2553–2564.
- Florence T.M., Morrison G.M., Stauber J.L. (1992) Determination of trace element speciation and the role of speciation in aquatic toxicity. *Sci. Total Environ.*, 125, 1–13.
- Florence, T.M. (1983) Trace element speciation and aquatic toxicology. *Trends in Analytical Chemistry*, 2(7), 162–166.
- Förstner U. and Wittmann G. T. W. (1983) Metal pollution in the aquatic environment (2nd edition). *Springer Verlag, Berlin, Heidelberg et New York*, 486.
- Fritzsche A., Bosch J., Rennert T., Heister K., Braunschweig J., Meckenstock R.U., Totsche K.U. (2012) Fast microbial reduction of ferrihydrite colloids from a soil effluent. *Geochim. Cosmochim. Acta*, 77, 444-456.
- Gao H. and Zepp R. G. (1998) Factors influencing photoreactions of dissolved organic matter in a coastal river of the southeastern United States. *Environ. Sci. Technol.* 32, 2940–2946.
- Garg S., Ito H., Rose A.L. and Waite T.D. (2013a) Mechanism and kinetics of dark iron redox transformations in acidic natural organic matter solutions. *Environ. Sci. Technol.* 47, 1861-1867.
- Garg S., Jiang C. and Waite D.T. (2015) Mechanistic insights into iron redox transformations in the presence of natural organic matter: Impact of pH and light. *Geochim. Cosmochim. Acta* 165, 14-34.
- Garg S., Jiang C., Miller C.J., Rose A.L. and Waite T.D. (2013b) Iron redox transformations in continuously photolyzed acidic solutions containing natural organic matter: kinetic and mechanistic insights. *Environ. Sci. Technol.* 47, 9190-9197.
- Gérard E., Moreira D., Philippot P., Van Kranendonk M. J., Lopez-Garcia P. (2009) Modern subsurface bacteria in pristine 2.7 Ga-old fossil stromatolite drillcore samples from the Fortescue Group, Western Australia. *PLoS ONE* 4(4), e5298, doi:10.1371/journal.pone.0005298.

- Gonsior M., Schmitt-Kopplin P. and Bastviken D. (2013) Depth-dependent molecular composition and photo-reactivity of dissolved organic matter in a boreal lake under winter and summer conditions. *Biogeosciences* 10, 6945-6956.
- Gonzalez A., Pokrovsky O. S. (2014a) Metal adsorption on mosses: towards a universal adsorption model. *J. Colloid Interf. Sci.* 415, 169–178.
- Gonzalez A., Shirokova L.S., Pokrovsky O. S., Emnova E. E., Santana-Casiano J. M., Gonzalez-Davila M., Pokrovski G. S. (2010) Adsorption of copper on *Pseudomonas aureofaciens*: protective role of surface exopolysaccharides. *J. Colloid Interf. Sci.* 350, 305-314.
- Gonzalez A.G., Pokrovsky O.S., Jimenez-Villacorta F., Shirokova L.S., Santana-Casiano J.M., Gonzalez-Davila M., Emnova E.E. (2014b) Iron adsorption onto soil and aquatic bacteria: XAS structural study. *Chem. Geol.* 372, 32-45.
- Gonzalez A.G., Santana-Casiano J.M., González-Dávila M., Pérez N. (2012) Effect of organic exudates of *Phaeodactylum tricornutum* on the Fe(II) oxidation rate constant. *Ciencias Marinas* 38(1B), 245–261.
- Granéli W., Lindell M. and Tranvik L. (1996) Photo-oxidative production of dissolved inorganic carbon in lakes of different humic content. *Limnol. Oceanogr.* 41, 698-706.
- Groenveld M., Tranvik L., Natchimuthu S., Koehler B. (2016) Photochemical mineralisation in a boreal brown water lake: considerable temporal variability and minor contribution to carbon dioxide production. *Biogeoscience*, 13, 3931-3943.
- Guo L., Santschi P. H. (2007) Ultrafiltration and its applications to sampling and characterization of aquatic colloids. In *Environmental Colloids and Particles: Behaviour, Separation and Characterisation*, chapter 4 (eds. K. Wilkinson end J. Lead). John Wiley & Sons Ltd, Chichester. pp 159-221.
- Gustafsson J. (2011) Visual MINTEQ ver. 3.0, <http://www2.lwr.kth.se/English/OurSoftware/Vminteq/>
- Gustafsson, J.: Visual MINTEQ ver. 3.1. <http://vminteq.lwr.kth.se>, 2014, assessed 8.10.2016.
- Haukka K., Heikkinen E., Kairesalo T., Karjalainen H., Sivonen K. (2005) Effect of humic material on the bacterioplankton community composition in boreal lakes and mesocosms. *Environ. Microbiol.* 7(5), 620-630.

- Hedges J.I., Clark W.A., Quay P. D., Richey J.E., Devol A.H., Santos U.d.M. (1986) Compositions and fluxes of particulate organic material in the Amazon River. *Limnol. Oceanogr.* 31, 717–738.
- Helms J.R., Mao J., Schmidt-Rohr K., Abdulla H. and Mopper K. (2013) Photochemical flocculation of terrestrial dissolved organic matter and iron. *Geochim. Cosmochim. Acta* 121, 398–413.
- Hessen D.O. and Tranvik L.J., (1998) Aquatic Humic Substances. Ecology and Biogeochemistry. Springer, Berlin.
- Holmes R.M., McClelland J.W., Raymond P.A., Frazer B.B., Peterson B.J., and Stieglitz M. (2008) Lability of DOC transported by Alaskan rivers to the Arctic Ocean. *Geophys. Res. Lett.*, 35, L03402, doi:10.1029/2007GL032837.
- Homann P.S., Mitchell M.J., van Miegroet H. and Cole D.W. (1990) Organic sulfur in throughfall, stem flow, and soil solutions from temperate forests. *Can. J. Forest. Res.* 20(9), 1535–1539.
- Huang Q., Chen W., Xu L. (2005) Adsorption of copper and cadmium by Cu- and Cd-resistant bacteria and their composites with soil colloids and kaolinite. *Geomicrobiol. J.* 22(5), 227-236.
- Hulatt C.J., Kaartokallio H., Asmala E., Autio R., Stedmon C.A., Sonninen E., Oinonen M., Thomas D.N. (2014) Bioavailability and radiocarbon age of fluvial dissolved organic matter (DOM) from a northern peatland-dominated catchment: effect of land-use change. *Aquat Sci* 76(3), 393-404.
- Huser B.J., Köhler S J., Wilander A., Johansson K., Fölster, J. (2011) Temporal and spatial trends for trace metals in streams and rivers across Sweden (1996–2009). *Biogeosciences*, 8, 1813-1823.
- Ilina S. M., Lapitsky S. A., Alekhin Yu.V., Viers J., Benedetti M., Pokrovsky O.S. (2016) Speciation, size fractionation and transport of trace element in the continuum soil water – mire – lake – river – large oligotrophic lake of a subarctic watershed. *Aquat. Geochem.* 22(1), 65-95.
- Ilina S.M., Drozdova O.Yu., Lapitsky S.A., Alekhin Yu.V., Demin V.V., Zavgorodnaya Yu.A., Shirokova L.S., Viers J., Pokrovsky O.S. (2014) Size fractionation and optical properties of dissolved organic matter in the continuum soil solution-bog-river and terminal lake of a boreal watershed. *Org. Geochem.* 66, 14–24.
- Ilina S.M., Lapitsky S.A., Alekhin Y.V., Viers J., Benedetti M. and Pokrovsky O.S. (2016) Speciation, size fractionation and transport of trace element in the

- continuum soil water – mire – lake – river – large oligotrophic lake of a subarctic watershed. *Aquat. Geochem.* 22(1), 65-95.
- Ilina S.M., Poitrasson F., Lapitskiy S.A., Alekhin Yu.V., Viers J. and Pokrovsky O.S. (2013) Extreme iron isotope fractionation between colloids and particles of boreal and temperate organic-rich waters. *Geochim. Cosmochim. Acta* 101, 96-111.
- Ingri J., Widerlund A., Land M., Gustafsson O., Andersson P., Ohlander B. (2000) Temporal variations in the fractionation of the rare earth elements in a boreal river; the role of colloidal particles. *Chem. Geol.* 166, 23-45.
- Jackson T.A., West M., Leppard G.G. (2011) Accumulation and partitioning of heavy metals by bacterial cells and associated colloidal minerals, with alteration, neoformation, and selective adsorption of minerals by bacteria, in metal-polluted lake sediment. *Geomicrobiol. J.* 28(1), 23-55.
- Jansson M., Bergström A.K., Blomqvist P., Drakare S. (2000) Allochthonous organic carbon and phytoplankton/bacterioplankton production relationship in lakes. *Ecology* 81, 3250–3255.
- Jansson M., Hickler T., Jonsson A., Karlsson J. (2008) Links between terrestrial primary production and bacterial production and respiration in lakes in a climate gradient in subarctic Sweden. *Ecosystems* 11, 367–376.
- Jansson M., Persson L., De Roos A. M., Jones R. I., Tranvik L. J. (2007) Terrestrial carbon and intraspecific size-variation shape lake ecosystems. *Trends Ecol. Evol.* 22, 316–322.
- Johannesson K.H., Palmore, C.D., Frackell J., Prouty N.G., Swarzenski P.W., Chevis D. A., Telfeyan K., White C.D., and Burdige D.J. (2017) Rare earth element behavior during groundwater - seawater mixing along the Kona Coast of Hawaii. *Geochim. Cosmocim. Acta* 198, 229-258.
- Jones S.E., Newton R.J. McMahon K.D. (2009) Evidence for structuring of bacterial community composition by organic carbon source in temperate lakes. *Environ. Microbiol.* 11(9), 2463-2472.
- Karlsson T., Persson P., Skyllberg U., Mört C.M., Giesler R. (2008) Characterization of iron (III) in organic soils using extended X-ray absorption fine structure spectroscopy. *Environ. Sci. Technol.* 42 (15), 5449–5454.
- Kellerman A.M., Kothawala D.N., Dittmar T., Tranvik L.J. (2015) Persistence of dissolved organic matter in lakes related to its molecular characteristics. *Nature Geosci.*, 8, 454-457.

- Kelton N., Molot L.A. and Dillon P.J. (2007) Effect of ultraviolet and visible radiation on iron lability in boreal and artificial waters. *Aquat. Sci.* 69, 86–95.
- Kieber R.J., Zhou Z. and Mopper K. (1990) Formation of carbonyl compounds from UV-induced photodegradation of humic substances in natural waters: Fate of riverine carbon in the sea. *Limnol. Oceanogr.* 35, 1503–1515.
- Köhler S., Buffam I., Jonsson A. and Bishop K. (2002) Photochemical and microbial processing of stream and soil water dissolved organic matter in a boreal forested catchment in northern Sweden. *Aquat. Sci.* 64, 269– 281.
- Köhler S.J., Kothawala D., Futter M.N., Liungman O., Tranvik L. (2013) In-lake processes offset increased terrestrial inputs of dissolved organic carbon and color to lakes. *PLoS One* 8(8), e70598, <http://dx.doi.org/10.1371/journal.pone.0070598>.
- Kopácek J., Hejzlar J., Kana J., Porcal P. and Klementová A. (2003) Photochemical, chemical, and biological transformations of dissolved organic carbon and its effect on alkalinity production in acidified lakes. *Limnol. Oceanogr.* 48(1), 106-117.
- Kopáček J., Hejzlar J., Norton S. A. (2008) Proton production by transformations of aluminium and iron in lakes. *Water. Res.* 42, 1220–1228.
- Kopacek J., Klementova S. and Norton S.A. (2005) Photochemical production of ionic and particulate aluminum and iron in lakes. *Environ. Sci. Technol.* 39, 3656–3662.
- Kopáček J., Marešov M., Norton S.A., Porcal P., Veselý J. (2006) Photochemical source of metals for sediments. *Environ. Sci. Technol.* 40, 4455-4459.
- Kothawala D.N., Evans R.D. and Dillon P. J. (2006) Changes in the molecular weight distribution of dissolved organic carbon within a Precambrian shield stream. *Water Resour. Res.* 42, W05401, DOI:10.1029/2005WR004441.
- Krinner G. (2003) Impact of lakes and wetlands on boreal climate. *J. Geophys. Res. Atmos.* 108, 4520, doi: 10.1029/2002JD002597.
- Kritzberg E. S. and Ekstrom S. M. (2012) Increasing iron concentrations in surface waters - a factor behind brownification? *Biogeosciences* 9, 1465–1478.
- Kritzberg E.S., Cole J.J., Pace M.L., Granéli W., Bade D.L. (2004) Autochthonous versus allochthonous carbon sources of bacteria: results from whole-lake ^{13}C addition experiments. *Limnol. Oceanogr.* 49(2), 588–596.
- Kritzberg E.S., Villanueva A.B., Jung M. and Reader H.E. (2014) Importance of boreal rivers in providing iron to marine waters. *PLoS ONE* 9, e107500. DOI: 10.1371/journal.pone.0107500.

- Kulovaara, M., Corin, N., Backlund, P., and Tervo, J. (1996) Impact of UV₂₅₄-radiation on aquatic humic substances. *Chemosphere*, 33(5), 783-790, DOI: 10.1016/0045-6535(96)00233-0.
- Lapierre J.-F. and del Giorgio P.A. (2014) Partial coupling and differential regulation of biologically and photochemically labile dissolved organic carbon across boreal aquatic networks. *Biogeosciences* 11, 5969-5985.
- Larouche J.R., Abbott B.W., Bowden W.B., Jones J.B. (2015) The role of watershed characteristics, permafrost thaw, and wildfire on dissolved organic carbon biodegradability and water chemistry in Arctic headwater streams. *Biogeosciences*, 12, 4221-4233.
- Laudon H., Berggren M., Agren A., Buffam I., Bishop K., Grabs T., Jansson M. and Khöler S. (2011) Patterns and dynamics of dissolved organic carbon (DOC) in boreal streams: the role of processes, connectivity, and scaling. *Ecosystems* 14, 880–893.
- Laurion I. and Mladenov N. (2013) Dissolved organic matter photolysis in Canadian Arctic thaw ponds. *Environ. Res. Lett.* 8, 035026, DOI:10.1088/1748-9326/8/3/035026.
- Lidman F., Kohler S.J., Morth C.-M., Laudon H. (2014) Metal transport in the boreal landscape – the role of wetlands and the affinity for organic matter. *Environ. Sci. Technol.*, 48, 3783-3790.
- Lidman F., Morth C.M., and Laudon H. (2012) Landscape control of uranium and thorium in boreal streams – spatiotemporal variability and the role of wetlands. *Biogeosciences*, 9, 4773-4785.
- Lindell M. J., Granéli H.W. and Bertilsson S. (2000) Seasonal photoreactivity of dissolved organic matter from lakes with contrasting humic content. *Can. J. Fish. Aquat. Sci.* 57, 875–885.
- Lindell M.J., Granéli H.W. and Tranvik L.J. (1995) Enhanced bacterial growth in response to photochemical transformation of dissolved organic matter. *Limnol. Oceanogr.* 40, 195–199.
- Linnik P.M. (2000a) Heavy metals in surface waters of Ukraine: their content and forms of migration. *Hydrobiol. J.*, 36(3), 31–54.
- Linnik P.M. (2000b) Zinc, lead and cadmium speciation in Dnieper water-bodies. *Lakes and Reservoirs: Research and Management*, 5, 261–270.

- Linnik P.N., Vasilchuk T.A., Linnik R.P., Ignatenko I.I.. (2007) The coexisting forms of heavy metals in surface waters of Ukraine and the role of organic matter in their migration. *Metody i obyekty khimicheskogo analiza*, 2(2), 130-145.
- Linnik R.P., Linnik P.N., Zaporozhets O.A. (2006) Methods for studying coexisting forms of metals in natural waters (Review). *Metody i obyekty khimicheskogo analiza*, 1 (1), 4-26.
- Liu Z. D., Hong Z.N., Li J.Y., Jiang J., Xu R.K. (2015) Interactions between Escherchia coli and the colloids of three variable charge soils and their effects on soil surface charge properties. *Geomicrobiol. J.* 32, 511-520.
- Lloyd C.E.M, Michaelides K., Chadwick D.R., Dungait J.A.J., Evershed R.P. Tracing the flow-driven vertical transport of livestock-derived organic matter through soil using biomarkers. *Org Geochem.* 2012;43:56–66. doi: 10.1016/j.orggeochem.2011.11.001.
- Logue J.B., Stedmon C.A., Kellerman A.M., Nielsen N.J., Andersson A.F., Laudon H., Lindström E.S., Kritzberg E.S. (2016) Experimental insights into the importance of aquatic bacterial community composition to the degradation of dissolved organic matter. *The ISME J.* 10, 533–545.
- Lou T., Xie H. (2006) Photochemical alteration of the molecular weight of dissolved organic matter. *Chemosphere* 65, 2333-2342.
- Lyvén B., Hassellöv M., Turner D.R., Haraldsson C. and Andersson K. (2003) Competition between iron- and carbon-based colloidal carriers for trace metals in a freshwater assessed using flow field-flow fractionation coupled to ICPMS. *Geochim. Cosmochim. Acta*, 67, 3791–3802.
- Manasypov R.M., Vorobyev S.N., Loiko S.V., Krivtzov I.V., Shirokova L.S., Shevchenko V.P., Kirpotin S.N., Kulizhsky S.P., Kolesnichenko L.G., Zemtsov V.A., Sinkinov V.V., Pokrovsky O.S. (2015) Seasonal dynamics of thermokarst lake chemical composition in discontinuous permafrost zone of Western Siberia. *Biogeosciences* 12, 3009–3028.
- Mann P.J., Eglinton T.I., McIntyre C.P., Zimov N., Davydova A., Vonk J.E., Holmes R.M., Spencer R.G.M. (2015) Utilization of ancient permafrost carbon in headwaters of Arctic fluvial networks. *Nat. Commun.* 6, doi: 10.1038/ncomms8856.
- Mann P.J., Sobczak W.V., LaRue M.M., Bulygina E., Davydova A., Vonk J.E., Schade J., Davydov S., Zimov N., Holmes R.M., Spencer R.G.M. (2014)

- Evidence for key enzymatic controls on metabolism of Arctic river organic matter. *Global Change Biol.* 20(4), 1089-1100.
- Miller W.L. and Zepp R.G. (1995) Photochemical production of dissolved inorganic carbon from terrestrial organic matter: significance to the oceanic organic carbon cycle. *Geophys. Res. Lett.* 22, 417-420.
- Milne C.J., Kinniburgh D.G., van Riemsdijk W.H., Tipping E. (2003) Generic NICA-donnan model parameters for metal-ion binding by humic substances. *Environ. Sci. Technol.* 37(5), 958-971.
- Mitchell M.J., David M.B., Maynard D.G. and Telang S.A. (1986) Sulfur constituents in soils and streams of a watershed in the rocky mountains of Alberta. *Can. J. Forest. Res.* 16(2), 315–320.
- Mitchell M.J., Driscoll C.T., Fuller R.D., David M.B. and Likens G.E. (1989) Effect of whole-tree harvesting on the sulfur dynamics of a forest soil. *Soil Sci. Soc. Amer. J.* 53(3), 933–940.
- Molot L.A. and Dillon P. J. (1997) Photolytic regulation of dissolved organic carbon in northern lakes. *Global Biogeochem. Cy.* 11, 351–365.
- Molot L.A., Hudson J.J., Dillon P.J. and Miller S.A. (2005) Effect of pH on photo-oxidation of dissolved organic carbon by hydroxyl radicals in a coloured, softwater stream. *Aquat. Sci.* 67, 189–195.
- Mopper K., Zhou X., Kieber R.J., Kieber D.J., Sikorski R.J., Jones R.D. (1991) Photochemical degradation of dissolved organic carbon and its impact on the oceanic carbon cycle. *Nature* 353, 60-62.
- Moran M.A. and Covert J.S. (2003) Photochemically mediated linkages between dissolved organic matter and bacterioplankton. In Aquatic Ecosystems. interactivity of Dissolved Organic matter (eds. S.E.G. Findlay and R.L. Sinsabaugh). Academic Press, Elsevier. pp. 244-262.
- Moran M.A. and Zepp R.G. (1997) Role of photoreactions in the formation of biologically labile compounds from dissolved organic matter. *Limnol. Oceanogr.* 42, 1307–1316.
- Neubauer E., Kohler S.J., Von Der Kammer F., Laudon H., Hofmann T. (2013a) Effect of pH and stream order on iron and arsenic speciation in boreal catchments. *Environ. Sci. Technol.* 47(13), 7120-7128.

- Neubauer E., von der Kammer F. and Hofmann T. (2013c) Using FLOWFFF and HPSEC to determine trace metal – colloid associations in wetland runoff. *Water Res.* 47, 2757-2769.
- Neubauer E., von der Kammer F., Knorr K.-H., Peiffer S., Reichert M. and Hofmann T. (2013b) Colloid-associated export of arsenic in stream water during stormflow events. *Chem. Geol.* 352, 81-91.
- Nguyen H.V., Hur J. (2011) Tracing the sources of refractory dissolved organic matter in a large artificial lake using multiple analytical tools. *Chemosphere* 85, 782-789.
- Nilsson S.I., Andersson S., Valeur I., Persson T., Bergholm J. and Wiren A. (2001) Influence of dolomite lime on leaching and storage of C, N and S in a spodosol under Norway spruce (*Picea abies* (L.) Karst.). *Forest Ecol. Manag.* 146(1-3), 55–73.
- Oleinikova O.V., Drozdova O.Yu., Lapitskiy S.A., Bychkov A.Yu. (2015) Experimental study of the processes of photodegradation of organometallic compounds in natural waters. All-Russian Annual Seminar on Experimental Mineralogy, Petrology and Geochemistry (VESEMPG-2015), 21-22 April 2015, Moscow, Vernadsky Institute RAN (GEOKHI), p. 72.
- Oleinikova O.V., Shirokova L.S., Gérard E., Drozdova O.Yu, Lapitskiy S.A., Bychkov A.Yu, Pokrovsky O.S. (2017) Transformation of organo-ferric peat colloids by a heterotrophic bacterium. *Geochim. Cosmochim. Acta* 205, 313-330.
- Osburn C.L., Retamal L. and Vincent W.F. (2009) Photoreactivity of chromophoric dissolved organic matter transported by the Mackenzie River to the Beaufort Sea. *Mar. Chem.* 115, 10-20.
- Pédrot M., Dia A. and Davranche M. (2009) Double pH control on humic substance-borne trace elements distribution in soil waters as inferred from ultrafiltration. *J Colloid Interface Sci.* 339, 390–403.
- Pédrot M., Dia A., Davranche M., Coz M.B.-L, Henin O. and Gruau G. (2008) Insights into colloid-mediated trace element release at the soil / water interface. *J. Colloid. Interf. Sci.* 325, 187–197.
- Pokrovsky O. S., Pokrovski G.S., Shirokova L. S., Emnova E.E., Gonzalez A., Feurtet-Mazel A. (2012) Chemical and structural status of copper associated with oxygenic and anoxygenic phototrophs and heterotrophs: possible evolutionary consequences. *Geobiology* 10, 130-149.

- Pokrovsky O.S. and Schott J. (2002) Iron colloids/organic matter associated transport of major and trace elements in small boreal rivers and their estuaries (NW Russia). *Chem. Geol.* 190, 141–179.
- Pokrovsky O.S., Dupré B., Schott J. (2005) Fe-Al-organic colloids control of trace elements in peat soil solutions: results of ultrafiltration and dialysis. *Aquatic Geochemistry* 11, 241-278.
- Pokrovsky O.S., Manasypov R.M., Loiko S.V., Shirokova L.S. (2016b) Organic and organo-mineral colloids of discontinuous permafrost zone. *Geochim Cosmochim Acta*, 188, 1-20.
- Pokrovsky O.S., Martinez R., Kompantzeva E.I., Shirokova L.S. (2013b) Interaction of metals and protons with anoxygenic phototrophic bacterium *Rhodobacter blasticus*. *Chem. Geol.* 335, 75-86.
- Pokrovsky O.S., Shirokova L.S. (2013) Diurnal variations of dissolved and colloidal organic carbon and trace metals in a boreal lake during summer bloom. *Water. Res.* 47(2), 922–932.
- Pokrovsky O.S., Shirokova L.S., Kirpotin S.N., Kulizhsky S.P., Vorobiev S.N. (2013a) Impact of Western Siberia heat wave 2012 on greenhouse gases and trace metal concentration in thaw lakes of discontinuous permafrost zone. *Biogeosciences*, 10, 5349–5365.
- Pokrovsky O.S., Shirokova L.S., Zabelina S.A, Vorobieva T.Y., Moreva O.Y., Klimov S.I., Chupakov A.V., Shorina N.V., Kokryatskaya N.M., Audry S., Viers J., Zoutien C. and Freydier R. (2012) Size fractionation of trace elements in a seasonally stratified boreal lakes: Control of organic matter and iron colloids. *Aquat. Geochem.* 18, 115–139.
- Pokrovsky O.S., Viers J., Shirokova L.S., Shevchenko V.P., Filipov A.S. and Dupré B. (2010) Dissolved, suspended, and colloidal fluxes of organic carbon, major and trace elements in the Severnaya Dvina River and its tributary. *Chem. Geol.* 273(1-2), 136-149.
- Pokrovsky, O.S., Manasypov, R.M., Loiko, S., Krickov I.A., Kopysov S.G., Kolesnichenko L. G., Vorobyev S.N., Kirpotin S.N. (2016a) Trace element transport in western Siberia rivers across a permafrost gradient. *Biogeosciences*, 13, 1877–1900.

- Porcal P., Amirbahman A., Kopacek J. and Norton S.A. (2010) Experimental photochemical release of organically-bound aluminum and iron in three streams in Maine, USA. *Environ Monit. Assess.* 171(1-4), 71-81.
- Porcal P., Amirbahman A., Kopacek J., Novak F. and Norton S.A. (2009a) Photochemical release of humic and fulvic acid-bound metals from simulated soil and streamwater. *J. Environ. Monit.* 11, 1064–1071.
- Porcal P., Dillon P.J. and Molot L.A. (2013a) Photochemical production and decomposition of particulate organic carbon in a freshwater stream. *Aquat. Sci.* 75, 469–482.
- Porcal P., Dillon P.J. and Molot L.A. (2013b) Seasonal changes in photochemical properties of dissolved organic matter in small boreal streams. *Biogeosciences* 10, 5553-5543.
- Porcal P., Dillon P.J. and Molot L.A. (2014) Interaction of extrinsic chemical factors affecting photodegradation of dissolved organic matter in aquatic ecosystems. *Photochem. Photobiol. Sci.* 13, 799-812.
- Porcal P., Dillon P.J. and Molot L.A. (2015) Temperature dependence of photodegradation of dissolved organic matter to dissolved inorganic carbon and particulate organic carbon. *Plos ONE* 10(6), e0128884, DOI:10.1371/journal.pone.0128884.
- Porcal P., Hejzlar J. and Kopacek J. (2004) Seasonal and photochemical changes of DOM in an acidified forest lake and its tributaries. *Aquat. Sci.* 66, 211–222.
- Porcal P., Koprivnjak J.F., Molot L.A. and Dillon P.J. (2009b) Humic substances-part 7: the biogeochemistry of dissolved organic carbon and its interactions with climate change. *Environ. Sci. Pollut. Res.* 16(6), 714-726.
- Reche I., Pace M.L. and Cole J.J. (2000) Modeled effects of dissolved organic carbon and solar spectra on photobleaching in lake ecosystems. *Ecosystems* 3, 419-432.
- Roehm C.L., Giesler R., Karlsson J. (2009) Bioavailability of terrestrial organic carbon to lake bacteria: The case of a degrading subarctic permafrost mire complex. *J. Geophys. Res.* 114, G03006, doi: 10.1029/2008JG000863.
- Ruiz-Gonzalez C., Simo R., Sommaruga R. and Gasol J.M. (2013) Away from darkness: a review on the effects of solar radiation on heterotrophic bacterioplankton activity. *Front. Microbiol.* 4, 1–24.
- Salomons W. and Förstner U. (1984) Metals in the Hydrocycle. Berlin, Heidelberg: Springer Verlag, 349.

- Salonen K. and Vähätalo A. (1994) Photochemical mineralization of dissolved organic matter in Lake Skervatjern. *Environ. Internat.* 20, 307-312.
- Samanidou V., Papadoyannis I., Vasilikiotis G. (1991) Mobilization of heavy metals from river sediments of Northern Greece, by humic substances. *J. Environ. Sci. and Health A*, 26(7), 1055-1068.
- Sarkkola S., Nieminen M., Koivusalo H., Laurén A., Kortelainen P., Mattsson T., Palviainen M., Piirainen S., Starr M., Finér L. (2013) Iron concentrations are increasing in surface waters from forested headwater catchments in eastern Finland. *Sci. Total. Environ.* 463-464, 683-689.
- Sayre A. (1994). *Taiga*, New York: Twenty-First Century Books.
- Scheibe A, Gleixner G. (2014) Influence of litter diversity on dissolved organic matter release and soil carbon formation in a mixed beech forest. *PLoS One* 8; 9(12):e114040. doi: 10.1371/journal.pone.0114040.
- Scully N.M., Cooper W.J. and Tranvik, L.J. (2003) Photochemical effects on microbial activity in natural waters: the interaction of reactive oxygen species and dissolved organic matter. *FEMS Microbiol. Ecol.* 46, 353-357.
- Shiller A.M. (2003) Syringe filtration methods for examining dissolved and colloidal trace element distribution in remote field locations. *Environ. Sci. Technol.*, 37, 3953-3957.
- Shiller A.M., Duan S., van Erp P. and Bianchi T.S. (2006) Photo-oxidation of dissolved organic matter in river water and its effect on trace element speciation. *Limnol. Oceanogr.*, 51(4), 1716-1728.
- Shirokova L. S., Pokrovsky O. S., Kirpotin S. N., Desmukh C., Pokrovsky B. G., Audry S., Viers J. (2013a) Biogeochemistry of organic carbon, CO₂, CH₄, and trace elements in thermokarst water bodies in discontinuous permafrost zones of Western Siberia. *Biogeochemistry* 113, 573-593.
- Shirokova L., Vorobyeva T., Zabelina S., Klimov S., Moreva O. et al. (2016) Small boreal lake ecosystem evolution under the influence of natural and anthropogenic factors: Results of multidisciplinary long-term study. *Water*, 8, 316, doi:10.3390/w8080316.
- Shirokova L.S., Bredoire R., Rolls J.L., Pokrovsky O.S. (2017a) Moss and peat leachate degradability by heterotrophic bacteria: fate of organic carbon and trace metals. *Geomicrobiol. J.* 34(8), 641-655, DOI: 10.1080/01490451.2015.1111470.

- Shirokova L.S., Kunhel L., Rols J.L., Pokrovsky O.S. (2015) Experimental modeling of cyanobacterial bloom in a thermokarst lake: Fate of organic carbon, trace metal, and carbon sequestration potential. *Aquat. Geochem.*, 21(6), 487-511.
- Shirokova L.S., Labouret J., Gurge M., Gérard E., Zabelina S.A., Ivanova I.S., Pokrovsky O.S. (2017b) Impact of cyanobacterial associate and heterotrophic bacteria on dissolved organic carbon and metal in moss and peat leachate: application to permafrost thaw in aquatic environments. *Aquatic Geochem.*, submitted.
- Shirokova L.S., Pokrovsky O.S., Moreva O.Y., Chupakov A.V., Zabelina S.A. et al. (2013b) Decrease of concentration and colloidal fraction of organic carbon and trace elements in response to the anomalously hot summer 2010 in a humic boreal lake. *Sci. Total Environ.*, 463–464, 78–90.
- Shirokova, L.S., Pokrovsky O.S., Bénézeth, P., Gérard E., Ménez B., Alfredsson, H.A. (2012) Experimental study of the effect of heterotrophic bacterium (*Pseudomonas reactans*) on olivine dissolution kinetics in the context of CO₂ storage in basalts. *Geochimica Cosmochimica Acta*, 80, 30-50.
- Sivan O., Adler M., Pearson A., Gelman F., Bar-Or I. , John S.G. and Eckert W. (2011) Geochemical evidence for iron-mediated anaerobic oxidation of methane. *Limnol. Oceanogr.* 56, 1536-1544.
- Sivan O., Antler G., Turchyn A.V., Marlow J.J., and Orphan V.J. (2014) Iron oxides stimulate sulfate driven anaerobic methane oxidation in seeps. *PNAS* 111(40), 4139-4147.
- Sivan O., Antler G., Turchyn A.V., Marlow J.J., and Orphan V.J. (2014) Iron oxides stimulate sulfate driven anaerobic methane oxidation in seeps. *PNAS* 111(40), 4139-4147.
- Sivan O., Erel Y., Mandler D. and Nishri A. (1998) The dynamic redox of iron in the epilimnion of Lake Kinneret (Sea of Galilee). *Geochim. Cosmochim. Acta*, 62, 565-576.
- Sleighter R.L., Cory R.M., Kaplan L.A., Abdulla H.A.N., Hatcher P.G. (2014) A coupled geochemical and biogeochemical approach to characterize the bioreactivity of dissolved organic matter from a headwater stream. *J. Geophys. Res.-Biogeo.* 119, 1520-1537.
- Smiejan A., Wilkinson K.J., Rossier C. (2003) Cd bioaccumulation by a freshwater bacterium, *Rhodospirillum rubrum*. *Environ Sci Technol.*, 37(4), 701-706.

- Spencer R.G.M., Mann P. J., Dittmar T., Eglinton T.I., McIntyre C., Holmes R.M., Zimov N., Stubbins A. (2015) Detecting the signature of permafrost thaw in Arctic rivers. *Geophys. Res. Lett.* 42, 2830-2835.
- Spencer R.G.M., Stubbins A., Hernes P.J., Baker A., Mopper K., Aufdenkampe A.K., Dyda R.Y., Mwamba V.L., Mangangu A.M., Wabakanghanzi J.N. and Six J. (2009) Photochemical degradation of dissolved organic matter and dissolved lignin phenols from the Congo River. *J. Geophys. Res.* 114, G03010, DOI: 10.1029/2009JG000968.
- Stedmon, C. A., Markager S. (2005) Tracing the production and degradation of autochthonous fractions of dissolved organic matter by fluorescence analysis. *Limnol. Oceanogr.* 50, 1415–1426.
- Stets E.G., Striegl R.G., Aiken G.R., Rosenberry D.O., Winter T.C. (2009) Hydrologic support of carbon dioxide flux revealed by whole-lake carbon budgets. *J. Geophys. Res. Biogeosci.* 114, G01008, doi: 10.1029/2008JG000783.
- Stockmann G.J., Shirokova L.S., Pokrovsky O.S., Bénézeth P., Bovet N., Gislason S.R., Oelkers E. H. (2012) Does the presence of heterotrophic bacteria *Pseudomonas reactans* affect basaltic glass dissolution rates? *Chem. Geol.* 296-297, 1 –18.
- Stolpe B., Hassellöv M., Andersson K., Turner D.R. (2005) High resolution ICPMS as an on-line detector for flow field-flow fractionation; multi-element determination of colloidal size distributions in a natural water sample. *Anal. Chim. Acta* 535(1-2),109-121.
- Stolpe B., Guo L. and Shiller A. (2013b) Binding and transport of rare earth elements by organic and iron-rich nanocolloids in Alaskan rivers, as revealed by field-flow fractionation and ICP-MS. *Geochim. Cosmochim. Acta*, 106, 446-462.
- Stolpe B., Guo L., Shiller A.M. and Aiken G.R. (2013a) Abundance, size distributions and trace-element binding of organic and iron-rich nanocolloids in Alaskan rivers, as revealed by field-flow fractionation and ICP-MS. *Geochim. Cosmochim. Acta* 105, 221-239.
- Stubbins A., Mann P., Powers L., Bittar T.B., Dittmar T., McIntyre C., Eglinton T., Zimov N. and Spencer R.G.M. (2016) Ancient permafrost carbon resists degradation by sunlight. *Science*, submitted.
- Stubbins A., Spencer R.G.M., Chen H., Hatcher P.G., Mopper K., Hernes P.J., Mwamba V.L., Mangangu A.M., Wabakanghanzi J.N. and Six J. (2010)

- Illuminated darkness: Molecular signatures of Congo River dissolved organic matter and its photochemical alteration as revealed by ultrahigh precision mass spectrometry. *Limnol. Oceanogr.* 55(4), 1467–1477.
- Stumm W (1992) Chemistry of the Solid-Water Interface. John Wiley & Sons, New York, 428 pp.
- Stutter M.I., Richards S., Dawson J.J.C. (2013) Biodegradability of natural dissolved organic matter collected from a UK moorland stream. *Water Res.* 47(3), 1169–1180
- Suhett A.L., Amado A.M., Enrich-Prast A., de Assis, E.F. and Farjalla V.F. (2007) Seasonal changes of dissolved organic carbon photo-oxidation rates in a tropical humic lagoon: the role of rainfall as a major regulator. *Can . J. Fish. Aquat. Sci.* 64, 1266-1272.
- Sundman A., Karlsson T., Laudon H. and Persson P. (2014) XAS study of iron speciation in soils and waters from a boreal catchment. *Chem. Geol.* 364, 93–102.
- Tang J. and Johannesson K.H. (2010) Rare earth elements adsorption onto Carrizo sand: Influence of strong solution complexation. *Chem. Geol.* 279, 120-133.
- Tarr M.A., Wang W., Bianchi T.S., Engelhaupt E. (2001) Mechanisms of ammonia and amino acid photoproduction from aquatic humic and colloidal matter. *Water Res.* 35, 3688-3696.
- Thomson J., Parkinson A. and Roddick F.A. (2004) Depolymerization of chromophoric natural organic matter. *Environ. Sci. Technol.* 38, 3360-3369.
- Tourney J., Ngwenya, B.T. (2014) The role of bacterial extracellular polymeric substances in geomicrobiology. *Chem.l Geol.* 386, 115-132. DOI: 10.1016/j.chemgeo.2014.08.011.
- Tranvik L. (1998b) Availability of dissolved organic carbon for planktonic bacteria in oligotrophic lakes of differing humic content. *Microbiol. Ecol.* 16, 311–22.
- Tranvik L. J., Downing J. A., Cotner J. B., Loiselle S. A., Striegl R. G. and others. (2009) Lakes and reservoirs as regulators of carbon cycling and climate. *Limnol. Oceanogr.* 54, 2298-2314.
- Tranvik L.J. (1998a) Degradation of dissolved organic matter in humic waters by bacteria. In *Aquatic Humic Substances, Ecology and Biogeochemistry* (eds. L. J. Tranvik and D. O. Hessen). Springer-Verlag, Berlin. pp. 259-283.
- Tranvik L.J. and Bertilsson, S. (2001) Contrasting effects of solar UV radiation on dissolved organic sources for bacterial growth. *Ecol. Lett.* 4, 458-463.

- Tranvik L.J., Jorgensen N.O.G. (1995) Colloidal and dissolved organic matter in lake water: carbohydrate and amino acid composition, and ability to support bacterial growth. *Biogeochemistry* 30, 77–97.
- Tranvik, L. J., Downing, J. A., Cotner, J. B., Loiselle, S. A., Striegl, R. G., Ballatore, T. J., ... Weyhenmeyer, G. A. (2009). Lakes and reservoirs as regulators of carbon cycling and climate. *Limnol. Oceanogr.*, 54(6 PART 2), 2298-2314.
- Trias J., Jarlier V., Benz R. (1992) Porins in the cell wall of mycobacteria. *Science* 258, 1479–1481.
- Uyguner C., Bekbolet M. (2005) Implementation of spectroscopic parameters for practical monitoring of natural organic matter. *Desalination* 176, 47–55.
- Vähäalto A.V. and Wetzel R.G. (2004) Photochemical and microbial decomposition of chromophoric dissolved organic matter during long (months-years) exposures. *Mar. Chem.* 89, 313-326.
- Vähäalto A.V., Salonen K., Münster U., Järvinen M. and Wetzel R.G. (2003) Photochemical transformation of allochthonous organic matter provides bioavailable nutrients in a humic lake. *Acta Hydrobiol.* 156, 287-314.
- Van Hees P.A.W., Jones D. L., Finlay R., Godbold D.L., Lundstrom U.S. (2005) The carbon we do not see—the impact of low molecular weight compounds on carbon dynamics and respiration in forest soils: a review. *Soil Biol. Biochem.* 37, 1–13.
- Vasyukova E., Pokrovsky O.S., Viers J., Dupré B. (2012) New operational method of testing colloid complexation with metals in natural waters. *Appl. Geochem.* 27, 1226–1237.
- Vasyukova E., Pokrovsky O.S., Viers J., Oliva P., Dupré B., Martin F., Candaudap F. (2010) Trace elements in organic- and iron-rich surficial fluids of boreal zone: Assessing colloidal forms via dialysis and ultrafiltration. *Geochim. Cosmochim. Acta* 74, 449-468.
- Vidal L.O., Granéli W., Daniel C.B., Heiberg L., Roland F. (2011) Carbon and phosphorus regulating bacterial metabolism in oligotrophic boreal lakes. *J. Plankton Res.* 33(11), 1747–1756.
- Viollier E., Inglett P.W., Hunter K., Roychoudhury A.N. and Van Cappellen P. (2000) The ferrozine method revisited: Fe(II)/Fe(III) determination in natural waters. *Appl. Geochem.* 15(6), 785–790.
- Voelker B.M. and Sulzberger B. (1996) Effects of fulvic acid on Fe(II) oxidation by hydrogen peroxide. *Environ. Sci. Technol.* 30, 1106-1114.

- Vonk J.E., Tank S.E., Bowden W.B., Laurion I., Vincent W.F., Alekseychik P., Amyot M., Billet M. F., Canário J., Cory R.M., Deshpande B.N., Helbig M., Jammet M., Karlsson J., Larouche J., MacMillan G., Rautio M., Walter Anthony K.M., Wickland K. P. (2015a) Reviews and syntheses: Effects of permafrost thaw on Arctic aquatic ecosystems. *Biogeosciences* 12, 7129-7167.
- Vonk J.E., Tank S.E., Mann P.J., Spencer R.G.M., Treat C.C., Striegl R.G., Abbott B.W. and Wickland K.P. (2015b) Biodegradability of dissolved organic carbon in permafrost soils and waterways: a meta-analysis. *Biogeosciences* 12, 6915-6930.
- Waite D.T. and Morel F.M.M. (1984) Photoreductive dissolution of colloidal iron oxides in natural waters. *Environ. Sci. Technol.* 18, 860-868.
- Wang Z., Zhang X., Wang Z., Zhang Y., Li B. and Vogt R. (2012) Dissolved organic sulfur in streams draining forested catchments in southern China. *J. Environ. Sci. (China)* 24(4), 704-710.
- Ward C.P. and Cory R.M. (2016) Complete and partial photo-oxidation of dissolved organic matter draining permafrost soils. *Environ. Sci. Technol.* 50(7), 3545–3553.
- Ward C.P. and Cory R.M. (2015) Chemical composition of dissolved organic matter draining permafrost soils. *Geochim. Cosmochim. Acta* 167, 63-79.
- Weishaar J.L., Aiken G.R., Bergamaschi B.A., Fram M.S., Fujii R., Mopper K. (2003) Evaluation of specific ultraviolet absorbance as an indicator of the chemical composition and reactivity of dissolved organic carbon. *Env. Sci. Technol.*, 37, 4702–4708.
- Wetzel R.G., Hatcher P.G. and Bianci T.S. (1995) Natural photolysis by ultraviolet irradiance of recalcitrant dissolved organic matter to simple substrates for rapid bacterial metabolism. *Limnol. Oceanogr.* 40, 1369-1380.
- Weyhenmeyer G.A., Prairie Y.T. and Tranvik L.J. (2014) Browning of boreal freshwaters coupled to carbon-iron interactions along the aquatic continuum. *PLoS ONE* 9, e88104, doi:10.1371/journal.pone.0088104.
- Wickland K.P., Aiken G.R., Butler K., Dornblaser M.M., Spencer R.G.M., Striegl R.G. (2012) Biodegradability of dissolved organic carbon in the Yukon River and its tributaries: seasonality and importance of inorganic nitrogen. *Glob Biogeochem Cycle* 26:2012gb004342.
- Wilkinson G. M., Pace M. L., Cole J. J. (2013) Terrestrial dominance of organic matter in north temperate lakes. *Global. Biogeochem. Cy.* 27, 43-51.

- Wu H., Chen W., Rong X., Cai P., Dai K., Huang Q. (2014) Soil colloids and minerals modulate metabolic activity of *Pseudomonas putida* measured using microcalorimetry. *Geomicrobiol. J.* 31(7), 590-596.
- Wu L., Jacobson A.D. and Hausner M. (2008) Characterization of elemental release during microbe-granite interactions at T = 28°C. *Geochim Cosmochim Acta* 72, 1076-1095.
- Wu L., Jacobson A.D., Chen H.-C. and Hausner M. (2007) Characterization of elemental release during microbe-basalt interactions at T = 28°C. *Geochim. Cosmochim. Acta* 71, 2224-2239.
- Xiao Y.-H., Hoikkala L., Kasurinen V., Tirola M., Kortelainen P., Vähäalto A.V. (2016) The effect of iron on the biodegradation of natural dissolved organic matter. *J. Geophys. Res. Biogeosci.*, 121, 2544–2561, doi:10.1002/2016JG003394.
- Xiao Y.-H., Raike A., Hartikainen H., Vähäalto A.V. (2015) Iron as a source of color in river waters. *Sci. Total Environ.* 536, 914–923, doi:10.1016/j.scitotenv.2015.06.092.
- Xie H., Zafiriou O.C., Cai W.-J., Zepp R.G. and Wang Y. (2004) Photooxidation and its effects on the carboxyl content of dissolved organic matter in two coastal rivers in the southeastern United States. *Environ. Sci. Technol.* 38, 4113–4119.
- Xu H. and Jiang H. (2013) UV-induced photochemical heterogeneity of dissolved and attached organic matter associated with cyanobacterial blooms in a eutrophic freshwater lake. *Water Res.* 47, 6506-6515.
- Yang Z., Wullschleger S.D., Liang L., Graham D.E., Gu B. (2016) Effects of warming on the degradation and production of low-molecular-weight labile organic carbon in an Arctic tundra soil. *Soil Biol. Biochem.*, 95, 202-211. doi:10.1016/j.soilbio.2015.12.022.
- Yeghicheyan D., Bossy C., Bouhnik Le Coz M., Douchet C., Granier G., Heimbürger A., Lacan F., Lanzanova A., Rousseau T. C. C., Seidel J. L., Tharaud M., Candaudap F., Chmeleff J., Cloquet C., Delpoux S., Labatut M., Losno R., Pradoux C., Sivry Y., Sonke J. E. (2014) A Compilation of silicon, rare earth element and twenty-one other trace element concentrations in the natural river water reference material SLRS-5 (NRC-CNRC). *Geostand. Geoanal. Res.* 37, 449-467.

- Zafiriou O.C., Joussot-Dubien J., Zepp R.G. and Zika R.G. (1984) Photochemistry of natural waters. *Environ. Sci. Technol.* 18(12), 358A–371A.
- Zepp R.G., Callaghan T.V. and Erickon D.J. (1998) Effects of enhanced solar ultraviolet radiation on biogeochemical cycles. *J. Photoch. Photobio. B* 46, 69-82.
- Zobkova M.V., Efremova T.A., Lozovik P.A., Sabyrina A.V. (2015) Organic substance and its components in surface waters of the humid zone. *Uspekhi sovremennoego yestestvoznaniya* 12, 115-120.